



Year: 2011

## Development of novel bissulfoxide and phosphine-olefin ligands for transition metal catalysis

Drinkel, Emma

**Abstract:** Die Bindungseigenschaften von Sulfoxiden mit Übergangsmetallen sind gut bekannt und viele Beispielen von Sulfoxidkomplexen existieren. Trotzdem, werden diese Komplexe für die Katalyse, besonders für die Enantioselektivekatalyse, nicht viel benutzt. Durch die Verwendung von chiralen Sulfoxiden sollten chirale Phosphinliganden ersetzt werden können. Im zweiten Kapitel wird die Synthese einer neuen Klasse chiraler Bissulfoxide beschrieben. Diese neue Liganden sind C1-symmetrisch hetero-Bissulfoxiden (fig. 1). O O R' = p-Tol 1. n-BuLi, THF, -78°C X = H, OMe 4-MeO-Ph X S or X S 4-t-Bu-Ph R Mg, THF, 0°C R R = t-Bu, 1-Me-cyclohexyl cyclohexyl o-Tol 2. sulfinate R' 4-F-Ph -78°C ! RT S 4-Cl-Ph 2-MeO-1-naphthyl X X O 3,5-di-(t-Bu)-4-MeO-Ph X = H, OMe R = t-Bu, 1-Me-cyclohexyl Fig. 1 C1-symmetrisch hetero-Bissulfoxiden Ihre Bindung mit Iridium wird im dritte Kapitel beschrieben. Diese Komplexe werden als Präkatalysatoren bei der Iridium-katalysierten intramolekularen Hydroamination mit vielversprechenden Ergebnissen angewendet. Ph Ph [Ir(L\*)Cl]2 N Ph N Ph ! H toluene 70°C Ph Ph Ausbeute bis 98% bis 40% e.e. Fig. 2 Iridium-katalysierten intramolekularen hydroamination Das vierter Kapitel beschäftigt sich mit der Synthese, Charakterisierung, Koordination und dem katalytischem Verhalten des Bissulfoxidliganden Binaso mit Palladium und Platin. Die Beschaffenheit der anderen Ligands im Komplex wurde beobachtet, um für leistungsfähige Schwergängigkeit des bissulfoxide Ligand wichtig zu sein. n+ O M = Pd, Pt p-Tol n = 0,1, 2 S X X = Cl, I, Me, TFA, Binaso M CH3CN, acac, COD X S acac = acetylacetonate p-Tol COD = cyclooctadiene O Fig. 3 Palladium und platin Komplexen mit Binaso Schliesslich, werden neue Rhodium und Kupfer Komplexe mit Phosphin-olefinliganden präsentiert. Sie erwiesen sich als exzellente Präkatalysatoren für die 1,4-Addition von Borsäuren und AlEt3 an zyklische und azyklische Ketone. O O O 1.5 mol% [Rh(L\*)][BF4] KOH (50 mol%) N P + 1.5 Ph-B(OH)2 Dioxane/H2O (10/1) O 40°C, 1 h ! Ph Ausbeute 93% 92% e.e. L\* Fig. 4 Rhodium-katalysierten 1,4-addition an cyclohexenone The binding properties of sulfoxides to transition metals are well known and many examples of metal-sulfoxide complexes exist. However their use in transition metal catalysis, particularly enantioselective catalysis, is rather less well developed. Due to the chiral nature of sulfoxides, they should be viable replacements for chiral phosphine ligands in enantioselective catalysis. This thesis investigates the use of sulfoxide and P-alkene ligands in transition metal catalysis. In the second chapter, the synthesis of a new class of chiral sulfoxides is described. These are C1-symmetric hetero-bissulfoxide ligands. O O R' = p-Tol 1. n-BuLi, THF, -78°C X = H, OMe 4-MeO-Ph X S or X S 4-t-Bu-Ph R Mg, THF, 0°C R R = t-Bu, 1-Me-cyclohexyl cyclohexyl o-Tol 2. sulfinate R' 4-F-Ph -78°C ! RT S 4-Cl-Ph 2-MeO-1-naphthyl X X O 3,5-di-(t-Bu)-4-MeO-Ph X = H, OMe R = t-Bu, 1-Me-cyclohexyl Fig. 1 C1-symmetrisch hetero-Bissulfoxiden The complexation of these ligands with iridium is discussed in chapter 3. The resulting complexes were then used as precatalysts in iridium-catalysed hydroamination reactions with some success. Ph Ph [Ir(L\*)Cl]2 N Ph N Ph ! H toluene 70°C Ph Ph Ausbeute bis 98% bis 40% e.e. Fig. 2 Iridium-katalysierten intramolekularen hydroamination The fourth chapter details the synthesis, characterisation, complexation and catalytic properties of the bissulfoxide ligand, binaso, with palladium and platinum. The nature of other ligands in the complex was observed to be important in determining the stability of the bissulfoxide-metal complex. n+ O M = Pd, Pt p-Tol n = 0,1, 2 S X X = Cl, I, Me, TFA, Binaso M CH3CN, acac, COD X S acac = acetylacetonate p-Tol COD = cyclooctadiene O Fig. 3 Palladium und platin Komplexen mit Binaso Finally, in chapter 5 novel copper and rhodium complexes

with phosphine-olefin ligands are presented. These complexes proved to be excellent precatalysts for the 1,4-addition of arylboronic acids and AlEt<sub>3</sub> to cyclic and acyclic enones. O O O 1.5 mol% [Rh(L\*)][BF<sub>4</sub>] KOH (50 mol%) N P + 1.5 Ph-B(OH)<sub>2</sub> Dioxane/H<sub>2</sub>O (10/1) O 40°C, 1 h ! Ph Ausbeute 93% 92% e.e. L\* Fig. 4 Rhodium-katalysierten 1,4-addition an cyclohexenone

Posted at the Zurich Open Repository and Archive, University of Zurich

ZORA URL: <https://doi.org/10.5167/uzh-164069>

Dissertation

Published Version

Originally published at:

Drinkel, Emma. Development of novel bissulfoxide and phosphine-olefin ligands for transition metal catalysis. 2011, University of Zurich, Faculty of Science.

# **Development of Novel Bissulfoxide and Phosphine-Olefin Ligands for Transition Metal Catalysis**

**Dissertation**

zur

Erlangung der naturwissenschaftlichen Doktorwürde  
**(Dr. sc. nat.)**

vorgelegt der

**Mathematisch-naturwissenschaftlichen Fakultät**

der

**Universität Zürich**

von

**Emma Drinkel**

aus

England

Promotionskomitee

Prof. Dr. Reto Dorta (Vorsitz und Leitung der Dissertation)

Prof. Dr. Roger Alberto

Prof. Dr. Cristina Nevado

Zürich 2011





## Acknowledgements

First of all I would like to thank Prof. Dr. Reto Dorta for giving me the opportunity to carry out my thesis in his laboratory, and for all his support and guidance.

I would also like to thank Prof. Dr. Romano Dorta for the chance to collaborate with his research.

For all the helpful discussions and for their friendship, I would like to thank my co-workers in the laboratory Dr. Ronaldo Mariz, Dr. Xinjun Luan, Dr. Michele Gatti, Linglin Wu, Justus Bürgi, Dr. Ludovic Vieille-Petit, Samanta Capolicchio and Fiona Gaggia.

I would like to thank PD Dr. Anthony Linden and Sascha Blumentritt for all the crystal structure determinations and the NMR team for help whenever needed. Additionally, thanks go to PD Dr. Laurent Bigler and his team for mass spectra measurements and the mikrolabor at ETH for elemental analyses.

To Prof. Dr. Roger Alberto and Prof. Dr. Cristina Nevado I would like to express my gratitude for being part of my Promotionskomitee.

I would like to thank all my family and friends for their support and belief throughout my studies.

Finally, I would like to thank the University of Zürich and the Roche Research Foundation for financial support



## Zusammenfassung

Die Bindungseigenschaften von Sulfoxiden mit Übergangsmetallen sind gut bekannt und viele Beispielen von Sulfoxidkomplexen existieren. Trotzdem, werden diese Komplexe für die Katalyse, besonderes für die Enantioselektivekatalyse, nicht viel benutzt. Durch die Verwendung von chiralen Sulfoxiden sollten chirale Phosphinliganden ersetzt werden können. Im zweiten Kapitel wird die Synthese einer neuen Klasse chiraler Bissulfoxide beschrieben. Diese neue Liganden sind  $C_1$ -symmetrisch hetero-Bissulfoxiden (fig. 1).

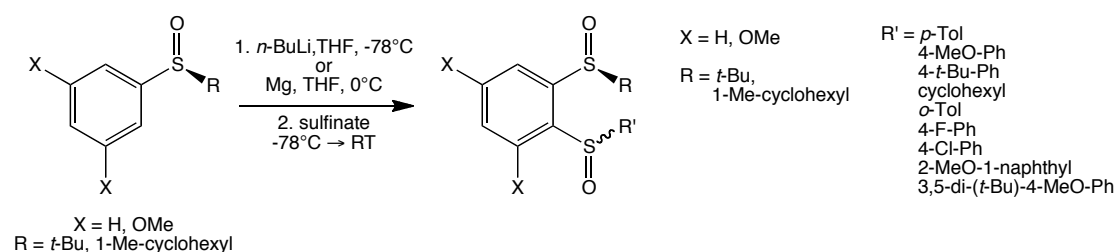


**Fig. 1**  $C_1$ -symmetrisch hetero-Bissulfoxiden

Ihre Bindung mit Iridium wird im dritte Kapitel beschrieben. Diese Komplexe werden als Präkatalysatoren bei der Iridium-katalysierten intramolekularen Hydroamination mit vielversprechenden Ergebnissen angewendet.

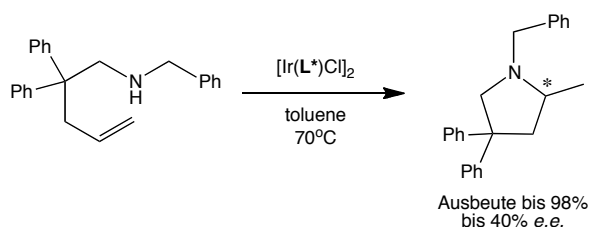


**Fig. 2** Iridium-katalysierten intramolekularen hydroamination

Das vierter Kapitel beschäftigt sich mit der Synthese, Charakterisierung, Koordination und dem katalytischem Verhalten des Bissulfoxidliganden Binaso mit Palladium und Platin. Die Beschaffenheit der anderen Ligands im Komplex wurde beobachtet, um für leistungsfähige Schwergängigkeit des bissulfoxide Ligand wichtig zu sein.

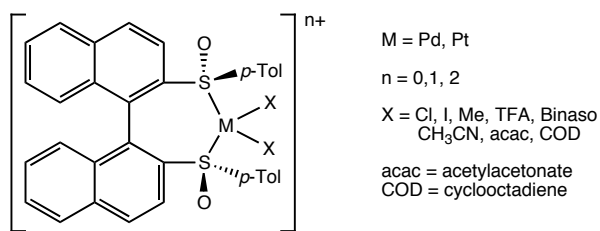


**Fig. 3** Palladium und platin Komplexen mit Binaso

Schliesslich, werden neue Rhodium und Kupfer Komplexe mit Phosphin-olefinliganden präsentiert. Sie erwiesen sich als exzellente Präkatalysatoren für die 1,4-Addition von Borsäuren und  $\text{AlEt}_3$  an zyklische und azyklische Ketone.

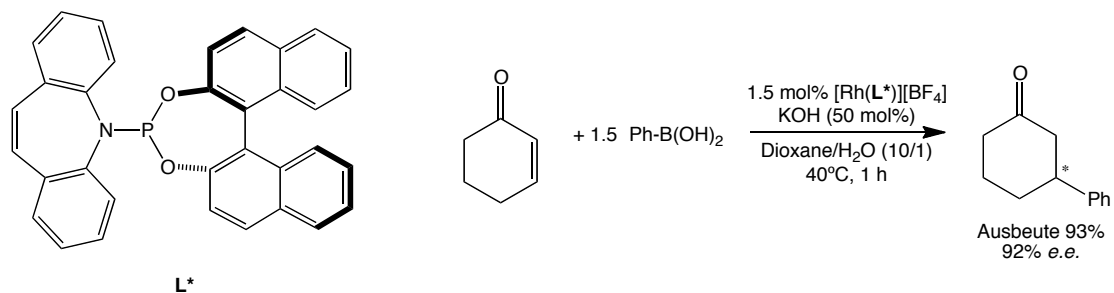


**Fig. 4** Rhodium-katalysierten 1,4-addition an cyclohexenone

## Abstract

The binding properties of sulfoxides to transition metals are well known and many examples of metal-sulfoxide complexes exist. However their use in transition metal catalysis, particularly enantioselective catalysis, is rather less well developed. Due to the chiral nature of sulfoxides, they should be viable replacements for chiral phosphine ligands in enantioselective catalysis. This thesis investigates the use of sulfoxide and P-alkene ligands in transition metal catalysis. In the second chapter, the synthesis of a new class of chiral sulfoxides is described. These are  $C_1$ -symmetric hetero-bissulfoxide ligands.

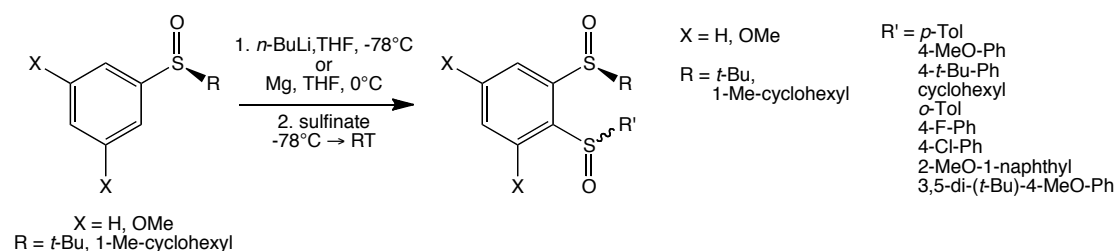


**Fig. 1**  $C_1$ -symmetrisch hetero-Bissulfoxiden

The complexation of these ligands with iridium is discussed in chapter 3. The resulting complexes were then used as precatalysts in iridium-catalysed hydroamination reactions with some success.

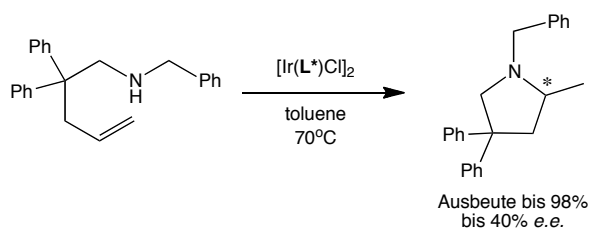


**Fig. 2** Iridium-katalysierten intramolekularen hydroamination

The fourth chapter details the synthesis, characterisation, complexation and catalytic properties of the bissulfoxide ligand, binaso, with palladium and platinum. The nature of other ligands in the complex was observed to be important in determining the stability of the bissulfoxide-metal complex.

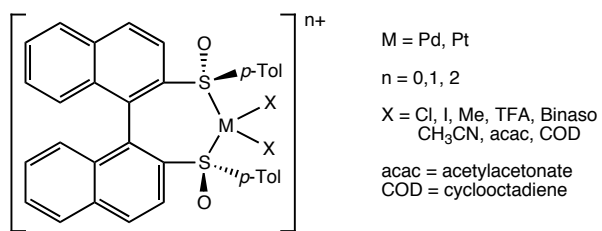


**Fig. 3** Palladium und platin Komplexen mit Binaso

Finally, in chapter 5 novel copper and rhodium complexes with phosphine-olefin ligands are presented. These complexes proved to be excellent precatalysts for the 1,4-addition of arylboronic acids and  $\text{AlEt}_3$  to cyclic and acyclic enones.

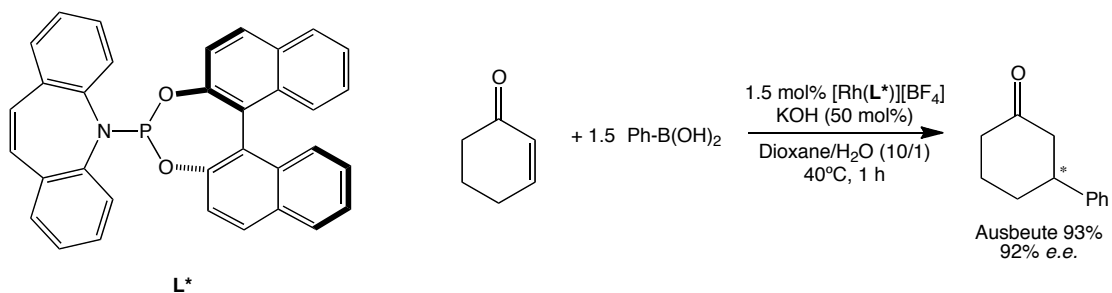


**Fig. 4** Rhodium-katalysierten 1,4-addition an cyclohexenone

# Table of Contents

<b>Chapter 1</b> .....	<b>1</b>
The Emergence of Sulfoxides as Efficient Ligands in Transition Metal Catalysis	
<b>Chapter 2</b> .....	<b>43</b>
The Synthesis of Novel Sulfoxide Ligands	
<b>Chapter 3</b> .....	<b>69</b>
Iridium Catalysed Hydroamination	
<b>Chapter 4</b> .....	<b>95</b>
Synthesis, Structure and Catalytic Studies of Novel Palladium and Platinum Bissulfoxide Complexes	
<b>Chapter 5</b> .....	<b>127</b>
Hemilabile P-Alkene Ligands in Chiral Rh and Cu Complexes: Catalytic Asymmetric 1,4 Additions to Enones, Part 2	
<b>Chapter 6</b> .....	<b>159</b>
Conclusions	





# Chapter 1

## The Emergence of Sulfoxides as Efficient Ligands in Transition Metal Catalysis

### 1.1. Introduction to Sulfoxides

Since the middle of the last century there has been an academic interest regarding the stereochemical properties of sulfoxides, their synthesis and their stability. However, the past thirty years have seen an increase in focus on sulfoxides as a chiral species, stimulated by their use as chiral auxiliaries in organic reactions.<sup>1</sup> The chirality in sulfoxides arises from their approximately pyramidal structure<sup>2</sup> (Figure 1). When the R groups are different from each other two possible enantiomers exist.

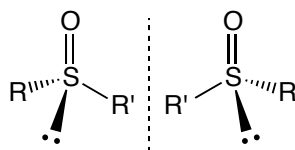


**Figure 1** Two enantiomers of the same sulfoxide

In the 1960's, enantiopure sulfoxides were made readily available when Andersen adapted a reaction first observed by Gilman,<sup>3</sup> by reacting menthyl *p*-toluene sulfinate, which is commercially available, with organometallic reagents.<sup>4</sup> Alternatively, enantiopure sulfoxides can be obtained either by:

1. Resolution techniques; these involve making a salt, which is only possible if there is an acid or basic group in the sulfoxide.<sup>5</sup>
2. Or by enantioselective oxidation of sulfides.<sup>6</sup> Although methods to enantioselectively oxidise sulfides have improved considerably since the 1960's, they are not so well developed.<sup>7</sup>

Andersen's method is still the preferred method when generating sulfoxides, because it is a relatively straightforward reaction that can be used to generate either enantiomer. The procedure was later improved by Solladié to make the reaction more suitable for large-scale applications.<sup>8</sup>

Andersen's method was later adapted by Kagan to make a wide variety of chiral sulfoxides from chiral sulfites.<sup>9</sup> Cyclic sulfites were prepared with chirality at S, and one chiral –OR group. These could be reacted with an organometallic species,  $R^1M$ , to enantioselectively give a sulfinate. Reaction of the sulfinate with a second organometallic species,  $R^2M$ , gave the enantiopure, chiral sulfoxide, as shown in figure 2.

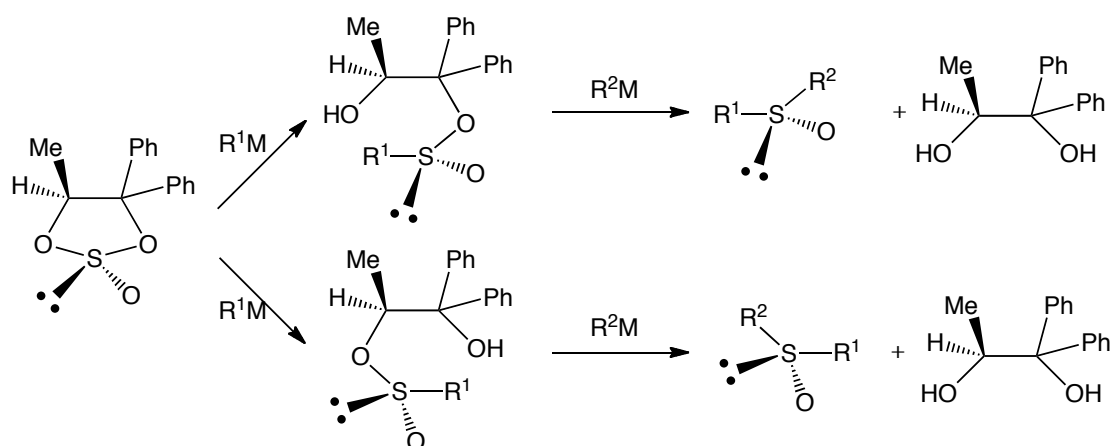


**Figure 2** Kagan's method to synthesise enantiopure sulfoxides

Khier *et al.* later extended the variety of sulfoxides obtainable by making new enantiomerically pure sulfonates with Diacetone-D-glucose as the –OR group.<sup>10</sup>

An advantage of using sulfoxides as chiral species in enantioselective organic transformations is their high optical stability. For the majority of sulfoxides, racemisation only occurs in appreciable amounts at around 200°C.<sup>11</sup> Exceptions to these being allyl and benzyl sulfoxides, where rearrangement reactions occur before pyramidal inversion at temperatures of 50-70°C and 130-150°C respectively.<sup>12</sup> Also, sulfoxides with a proton in the  $\beta$  position may undergo elimination to generate olefins at temperatures of around 80°C.<sup>13</sup>

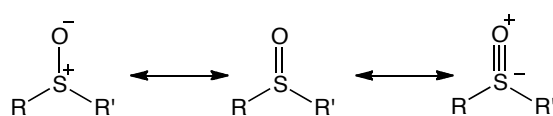


**Figure 3** Canonical forms of sulfoxides

The S-O bond of a free sulfoxide molecule is polarised and can be thought of as existing in three canonical forms (Figure 3), with the first two being the main components. Owing to the polarised nature of the S-O bond, with a net positive

charge on sulfur, sulfoxides are able to interact with both Lewis acids and transition metals.<sup>14</sup> The coordination of sulfoxides to metals has been comparatively well studied and many metal-sulfoxide complexes are known. The use of these complexes in catalysis is, however, rather less well established.

## 1.2. Metal Sulfoxide Complexes

Sulfoxides are able to bind to metals in two ways, either through the sulfur or through the oxygen. The 'hardness' or 'softness' of the metal centre determines how the sulfoxide will bind to it, with hard metal centres preferentially binding through O, and soft metal centres binding through S. An analysis by Calligaris<sup>14</sup> of all the X-ray crystal structures of sulfoxide complexes known to that date across the periodic table showed that there is a preference for O-bound complexes. However, groups 8-10 of the periodic table show a preference for S-bound sulfoxide complexes. Sometimes the same metal can bind through S or O, depending on the oxidation state of the metal and the other ligands around. There can even be S- and O-bound sulfoxides within the same complex.<sup>15</sup> To determine whether a sulfoxide is S- or O-bound, an X-ray crystal structure is the surest way, but IR data can also be useful. It is widely accepted that binding of a sulfoxide through S causes a decrease in the S-O bond length, whereas binding through O leads to an increase.<sup>15</sup> These changes in bond length can be seen as a change in stretching frequency in the IR spectra, making IR spectrometry a useful tool in determining the nature of ligation in metal-sulfoxide complexes.

In the following sections, some metal complexes with DMSO (dimethylsulfoxide) and other larger sulfoxides will be discussed, along with some applications of these metal complexes. The metal complexes with DMSO and other small sulfoxides have been studied since the 1960's,<sup>16</sup> and a great many structures are known with various metal centres. There are already several exhaustive review articles on the subject,<sup>14,17,18</sup> so here these types of complexes will be only covered briefly, concentrating on Ru, Rh, Ir, Pd and Pt complexes. These complexes are often used as precursors to make other coordination compounds. DMSO-metal complexes were also of interest for their potential activity in homogeneous catalysis.<sup>19,20</sup> Many studies on these structures have been concerned with the nature of the binding within the complex, and on *cis/trans* effects of sulfoxide ligands.

### 1.2.1. Ruthenium DMSO complexes

The first reported complex of ruthenium with DMSO was dichlorotetrakis(dimethylsulphoxide)ruthenium(II) **1**, synthesised in 1971 by James *et al.*<sup>21</sup> This was achieved by refluxing hydrated ruthenium trichloride in DMSO under an atmosphere of hydrogen. Wilkinson later showed that the hydrogen atmosphere was unnecessary,<sup>22</sup> and suggested that the complex contained both S- and O-bound sulfoxides. This theory was confirmed by an X-ray crystal structure of the complex. The complex has one O-bound ( $OS(CH_3)_2$ ) and three S-bound ( $SO(CH_3)_2$ ) DMSO ligands, with the chlorides in a *cis* arrangement (Figure 4).<sup>23</sup>

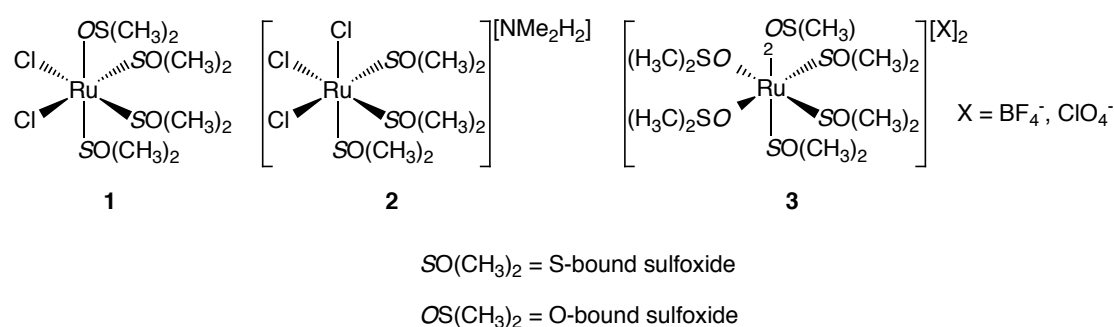


**Figure 4** Ru(II) DMSO complexes

Interestingly, the analogous bromo complex of **1** contains the bromides in a *trans* arrangement. The *cis*-chloro complex can be converted to the *trans*-chloro complex by photoisomerisation at room temperature in DMSO.<sup>24</sup> A method to obtain the *trans*-isomer directly from  $RuCl_3 \cdot 3H_2O$  was later discovered by James.<sup>25</sup>

It is also possible to synthesise complex **2**, where the O-bound DMSO ligand in **1** is replaced by a chloride (figure 4)<sup>26</sup> by refluxing ruthenium trichloride hydrate with a stoichiometric amount of DMSO in N,N-dimethylacetamide. Wilkinson and Trotter observed that dissolving complexes **1** and **2** in an aqueous solution of silver nitrate abstracted the chlorides and replaced them in the complex by  $H_2O$  ligands.<sup>22,26</sup> Abstraction of the chloride ligands using silver salts was also the method used to synthesise complex **3** from complex **1** in a solution of DMSO,<sup>22,27</sup> this complex has three S-bound and three O-bound DMSO ligands, with each S-bound ligand *trans* to an O-bound ligand.

It was not until the early 1990's that a Ru(III) DMSO complex was unequivocally made.<sup>28</sup> The isomer made and characterised was the *mer*-isomer, **4**, with two S-bound DMSOs and one O-bound DMSO.

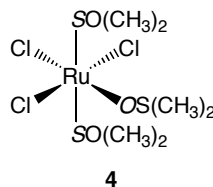


**Figure 5** Ru(III) DMSO complex

The development of ruthenium sulfoxide complexes continued with the discovery of bridging S,O-bidentate sulfoxide ligands, **5** and **6**.<sup>29,30</sup> The length of the S-O bond of the bridging sulfoxide is between the lengths of the S-O bonds in the solely S-bound and solely O-bound sulfoxides.

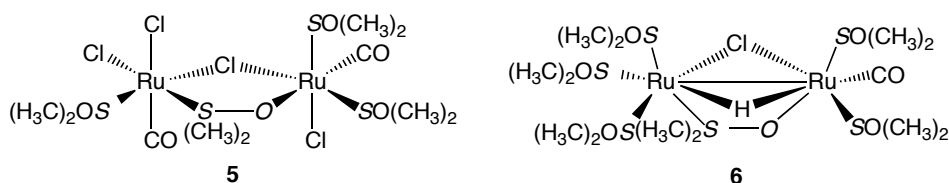


**Figure 6** Bridged ruthenium DMSO complexes

### 1.2.2. Rhodium and Iridium DMSO complexes

The first Rh(I) and Ir(I) complexes containing only DMSO as a dative ligand were reported in 2002 by Milstein *et al.* (Figure 7).<sup>31,32,33</sup> RhCl(DMSO)<sub>3</sub> (**6**) and IrCl(DMSO)<sub>3</sub> (**7**) were synthesised by treating a toluene slurry of [M(COE)<sub>2</sub>Cl]<sub>2</sub> (M = Rh, Ir; COE = cyclooctene) with an excess of DMSO. When the same reaction is repeated in the Rh case with only 2-4 equivalents of DMSO, **8** with a bridging DMSO ligand is the result.

Addition of diethyl ether to a CH<sub>2</sub>Cl<sub>2</sub> solution of complex **7** gives [Ir(DMSO)<sub>2</sub>Cl]<sub>2</sub> (**9**). Treating **7** or **9** in acetone with H<sub>2</sub>O led to complex **10** by oxidative addition of a water molecule to iridium.

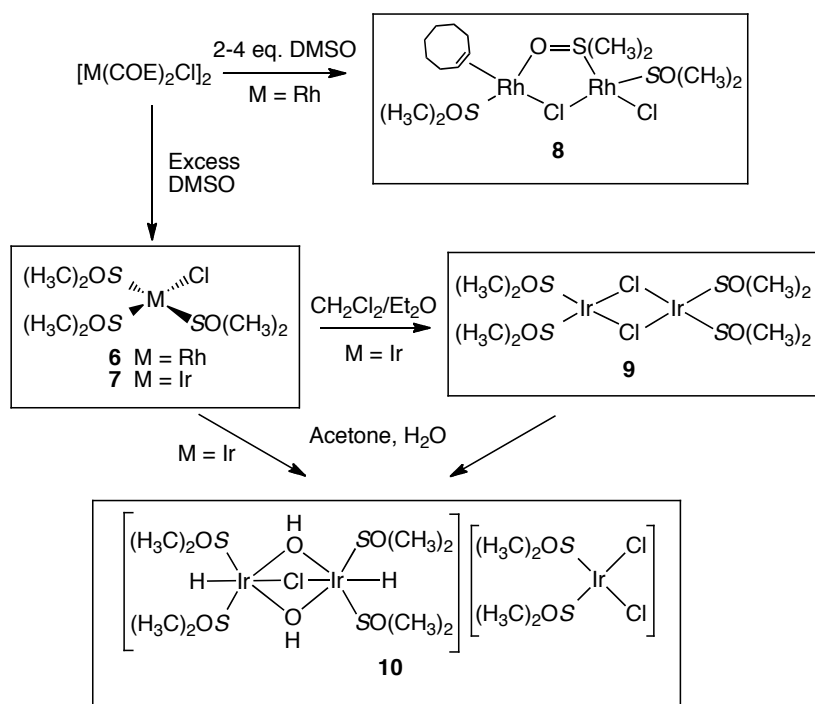


**Figure 7** Rh(I) and Ir(I) DMSO complexes

**11** was synthesised by treating  $[M(\text{COE})_2\text{Cl}]_2$  (where M = Rh, Ir) with  $\text{AgPF}_6$ , to abstract the chlorides, in acetone. The acetone and COE ligands could then be displaced by 4 equivalents of DMSO, to give **12** and **13**, with 2 S-bound and 2 O-bound. The Rh-complex **12** could be isolated and an X-ray crystallographic analysis was performed to confirm the structure. However, the Ir-complex **13** was not isolated, but was believed to be the structure shown in figure 8 and was used *in situ* to form other isolable complexes. For example,  $\text{H}_2\text{O}$  could be oxidatively added to form **14**, of which an X-ray crystal structure could be obtained.

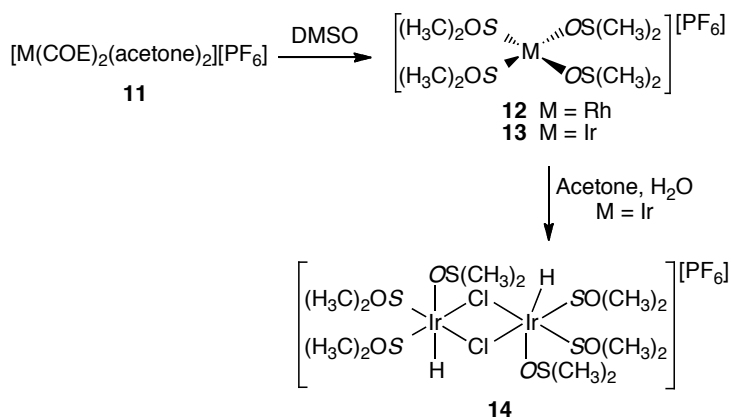


**Figure 8** Rh(I) and Ir(I) DMSO complexes

It can be seen in the complexes that when the complex is neutral and the metal centre is ‘softer’, the DMSO is always S-bound. On the other hand, when the complex is cationic, and the metal centre is ‘harder’, it is possible to have O-bound DMSO ligands.

More recently rhodium(III) complexes have been reported with 5 and 6 bound DMSO ligands,  $[\text{Rh}(\text{OS}(\text{CH}_3)_2)_5(\text{SO}(\text{CH}_3)_2)](\text{CF}_3\text{SO}_3)_3$  and  $[\text{Rh}(\text{OS}(\text{CH}_3)_2)_3(\text{SO}(\text{CH}_3)_2)_2\text{Cl}](\text{CF}_3\text{SO}_3)_2$ .<sup>34</sup>

### 1.2.3. Platinum and Palladium DMSO complexes

Platinum and palladium complexes with DMSO of the type  $\text{M}(\text{DMSO})_2\text{Cl}_2$  were synthesised and characterised in the 1970s. Both DMSO ligands were found to bind through sulfur.<sup>35</sup> Crystal structures of these compounds revealed that in the platinum case, the DMSO ligands were *cis* to one another,<sup>36</sup> but in the palladium case they were *trans*.<sup>37</sup> Subsequently, dicationic Pd and Pt complexes with four bound DMSO ligands were prepared.<sup>35b</sup> These complexes were postulated to comprise of two S-bound and two O-bound DMSO ligands from analysis by IR spectroscopy. This was later confirmed by X-ray crystallography of the palladium complex,<sup>38</sup> and the platinum complex.<sup>39</sup> In both complexes the similarly bound ligands were *cis* to each other.

### 1.2.4 Non-DMSO Metal Complexes

Methods of making bissulfoxide compounds have been known for a long time. Bissulfoxides with a methylene bridge, **15** (figure 9), were first made in 1912<sup>40</sup> and those with an ethylene bridge, **16**, were first made in 1927.<sup>41</sup> The *meso* (*R,S*) form of **15a** was not separated from the racemate (*R,R* and *S,S*), and was not characterised until much later.<sup>42</sup> The crystal structure of *meso* **16a** was reported in 1976.<sup>43</sup>

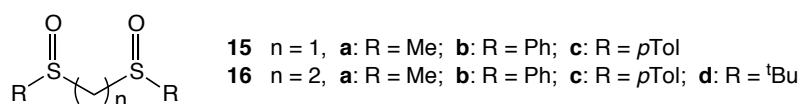


**Figure 9** Methylene and ethane bridged bissulfoxides

A similar enantiomerically pure bissulfoxide, **17**, was prepared shortly after this by reacting methylsulfinylcarbanion (made by treating DMSO with a strong base e.g. NaH) with (-)-menthyl-(*S*)-*p*-toluene sulfinate (Figure 10).

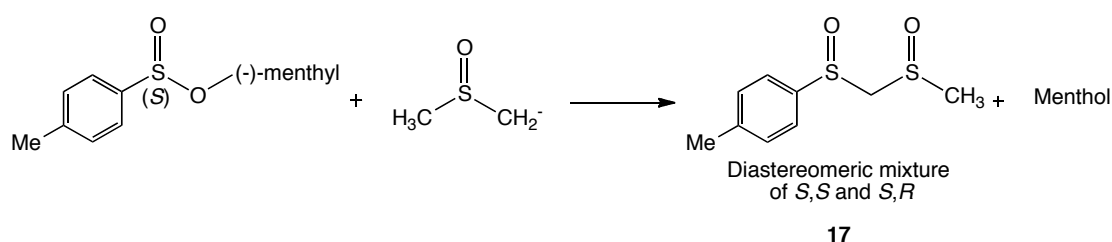


**Figure 10** Preparation of **17** from methylsulfinylcarbanion and (-)-menthyl-(*S*)-tolyl sulfinate

A mixture of the *meso* form and the enantiomerically pure bissulfoxide was obtained, which could be separated by crystallisation.<sup>44</sup> This method was extended to produce other bissulfoxides by varying the substituents on the sulfinylcarbanion and sulfinate.<sup>45</sup>

The sulfinylcarbanion was also generated in the synthesis of **16c**. Two equivalents of the optically pure *p*-tolyl-sulfinylcarbanion were then joined by CuCl<sub>2</sub> oxidative coupling to give the bissulfoxide (Figure 11).<sup>46</sup>

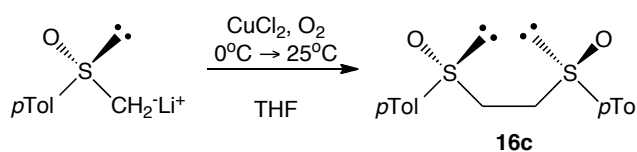


**Figure 11** Oxidative coupling method affording bissulfoxides

Ligand **16a** was used in complexation studies with several transition metals.<sup>47</sup> It was found that with the first row metals and Cd<sup>2+</sup>, complexes with the formula (M(ligand)<sub>3</sub>)<sup>2+</sup> are formed, where M = Mn<sup>2+</sup>, Fe<sup>2+</sup>, Co<sup>2+</sup>, Ni<sup>2+</sup>, Cu<sup>2+</sup>, Zn<sup>2+</sup> and Cd<sup>2+</sup>. The IR spectra were indicative of binding through oxygen. However, with Pd<sup>2+</sup> and Pt<sup>2+</sup>, the complex obtained had the formula M(ligand)Cl<sub>2</sub>, and only S-bound sulfoxides were observed by IR spectroscopy.



A platinum complex was also made with **16b** and a crystal structure of this compound was obtained.<sup>48</sup> In this case, it was clear to see that the ligand was bound through sulfur, and had the formula M(ligand)Cl<sub>2</sub>.

The complexation of **16c** was studied with several late transition metals, namely Pd<sup>2+</sup>, Pt<sup>2+</sup>, Rh<sup>+</sup> and Ir<sup>+</sup> by Evans.<sup>49</sup> The authors noted that these complexes were sterically and electronically dissymmetric. For example, in [Ir(COD)**16c**]BF<sub>4</sub> (COD = cyclooctadiene) the Ir-C bonds *syn* to the *p*-tolyl groups were considerably longer than those *anti* to the *p*-tolyl groups. Bissulfoxide ligands can have an impact on the steric environment of the metal, demonstrating that they should potentially be useful in enantioselective catalysis.

Evans also made Rh- and Ir-dimers with this ligand of the form [Ir(μ-Cl)**16c**]<sub>2</sub>. Analogous structures to these were synthesised with **16d** by Milstein, and reactivity studies made with these complexes.<sup>50</sup> Some interesting complexes were made by stoichiometric addition of pyridine derivatives to the Rh- and Ir-dimers to give monomeric structures (figure 12).

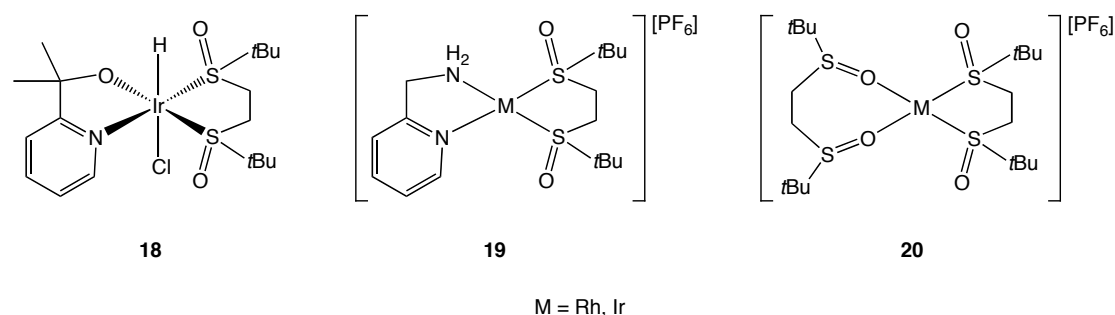


**Figure 12** Monomeric Ir(I) bissulfoxide complexes made with **16d**

In most cases, pyridine derivatives with substituents in the 2-position (–CH<sub>3</sub>, –CH<sub>2</sub>NH<sub>2</sub>, –CH<sub>2</sub>OH) simply cleaved the chloro bridge, binding to the metal through the nitrogen in the ring only. When a sterically demanding alcohol was in the 2-position, oxidative addition of the O-H bond was observed and complex **18** was the result. The pyridine derivatives could also be made to chelate the metal by the addition of AgPF<sub>6</sub> into the reaction mixture to abstract the chloride and give cationic complexes such as **19**. It was mentioned earlier<sup>33</sup> that [M(DMSO)<sub>4</sub>]PF<sub>6</sub> (where M = Rh, Ir) contains two S-bound and two O-bound sulfoxide ligands, the analogous structures can be made with chelating sulfoxides, see complex **20**.

Recently, platinum(II) dichloride complexes were reported of the methylene bridged bissulfoxides with substituents on the bridge.<sup>51</sup> Ligand **21** was first synthesised by Khier and was used in asymmetric Diels-Alder reactions.<sup>52</sup> The syntheses of **22** and **23**, by Malacria *et al.*, were inspired by the work of Aggarwal and Khier.<sup>9,10,53</sup>

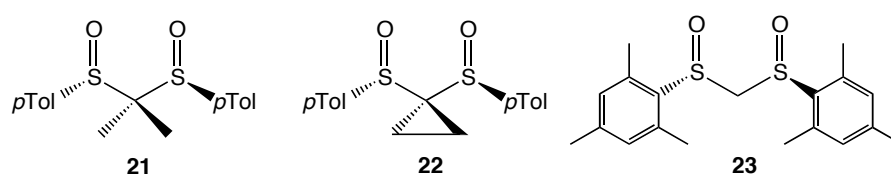


**Figure 13** Methylene bridged bissulfoxide ligands

The formation of platinum complexes with ligands **15a** (figure 9), **21**, **22** and **23** were attempted, but the only isolated complexes were those with **21** and **22**. The *gem*-substituents are apparently very important for forcing the correct orientation of the sulfoxides, so that they coordinate with platinum in 4-membered S-bound metallocycles.

Ethylene-bridged bissulfoxide ligands were also made with ethyl substituents on the backbone, **24**.<sup>54</sup> This was achieved by the same oxidative coupling method shown in figure 11, using the lithiated derivative of *n*-propyl *p*-tolyl sulfoxide. This gave a diastereomeric mixture of bissulfoxide ligands, which could be separated by column chromatography.

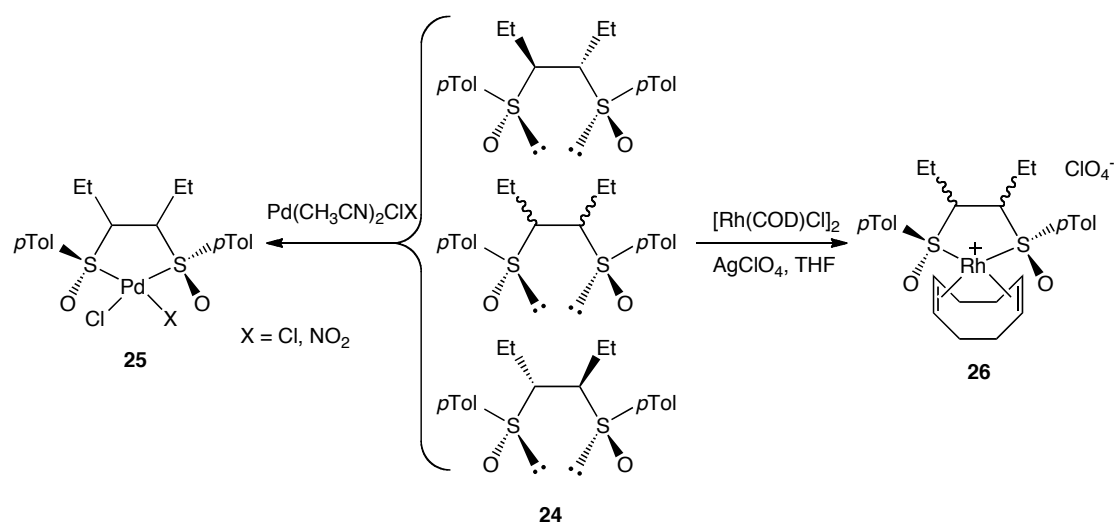


**Figure 14** Diastereoisomers of **24** and their Pt and Rh complexes

The three diastereomers shown in figure 14 were then reacted with  $\text{Pd(II)(CH}_3\text{CN)}_2\text{ClX}$  (where  $\text{X} = \text{Cl}$  or  $\text{NO}_2$ ). In all cases the acetonitrile was

displaced by the ligand to provide **25** in good yield. The cationic rhodium complex, **26**, could also be obtained with the *meso* ligand by abstracting the chlorides with silver salt in a solution of the ligand. X-ray and IR analysis confirmed that the ligands were S-bound to both Rh and Pd.

A more complex bissulfoxide ligand reported by Poli *et al.* was generated from two units of benzothiophene, which were oxidised to give the bissulfoxide.<sup>55</sup> The synthesis of the ligand produced a mixture of diastereoisomers, but only one of them had the correct geometry to bind to a metal through sulfur. When PdCl<sub>2</sub> was reacted with the mixture of ligands, just one enantiomerically pure palladium complex, **27**, was isolated.

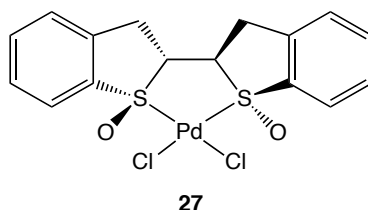


**Figure 15** PdCl<sub>2</sub> complex isolated with only one diastereoisomer of the ligand

No crystal structure was obtained of this complex, but IR spectroscopy indicated that the ligand was S-bound.

Another interesting bissulfoxide-pincer ligand was studied through its complex with palladium, **28**.<sup>56</sup>

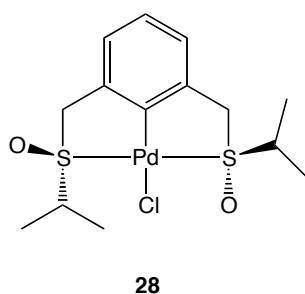


**Figure 16** Monomeric Pd complexes with pincer ligand

The complex was found to be S-bound and very stable. ESI-MS analyses of this complex in methanol revealed that the major cationic species present had a mass corresponding to [2,6-(*i*-PrS(O)CH<sub>2</sub>))<sub>2</sub>C<sub>6</sub>H<sub>3</sub>Pd]<sub>2</sub>-μ<sup>2</sup>-Cl<sup>+</sup>. As was previously observed with Pd(NCN) pincer complexes,<sup>57</sup> it seems that dimerisation is possible with bissulfoxide-pincer palladium complexes.

In the last twenty years there have been sporadic examples of bissulfoxide ligands with  $C_2$ -symmetry and aromatic backbones, the first example being (*S,S*)-1,2-bis(*p*-tolylsulfinyl)benzene (BTSB), **29**.<sup>58</sup> The ligand was successfully used to make compounds with Ru(II), **30**, Rh(I), **31**, and Pd(II), **32**, (Figure 17). A crystal structure of the palladium complex, **32**, revealed the ligand to be S-bound.

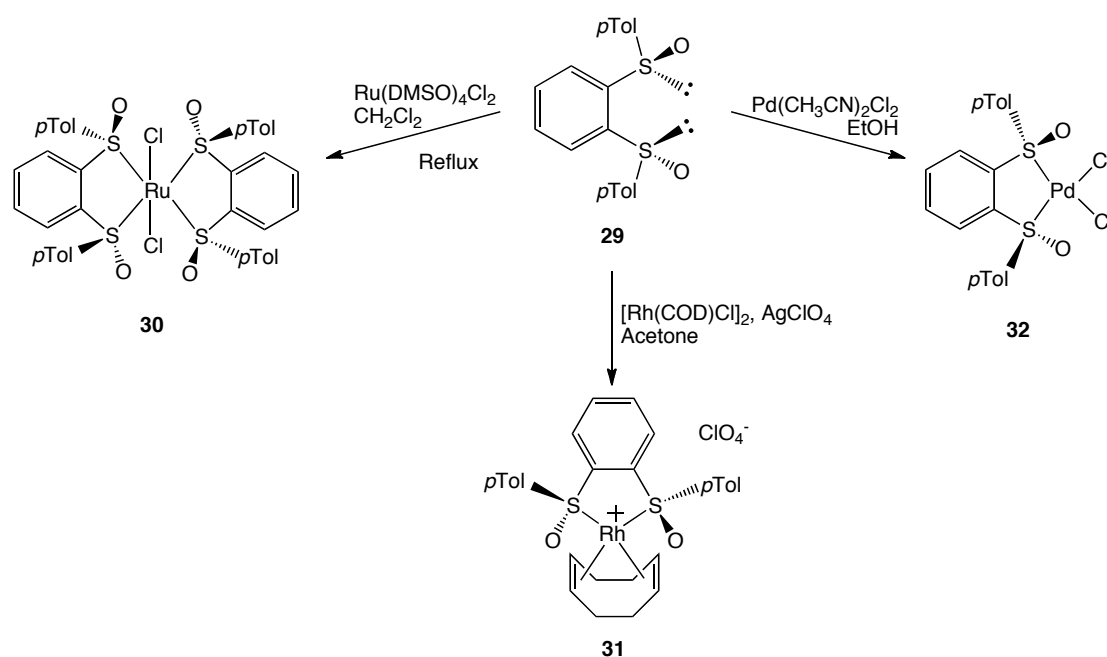


**Figure 17** Complexes made with BTSB, **29**

The palladium complex with BTSB will be discussed later as a catalyst for allylic alkylation reactions.

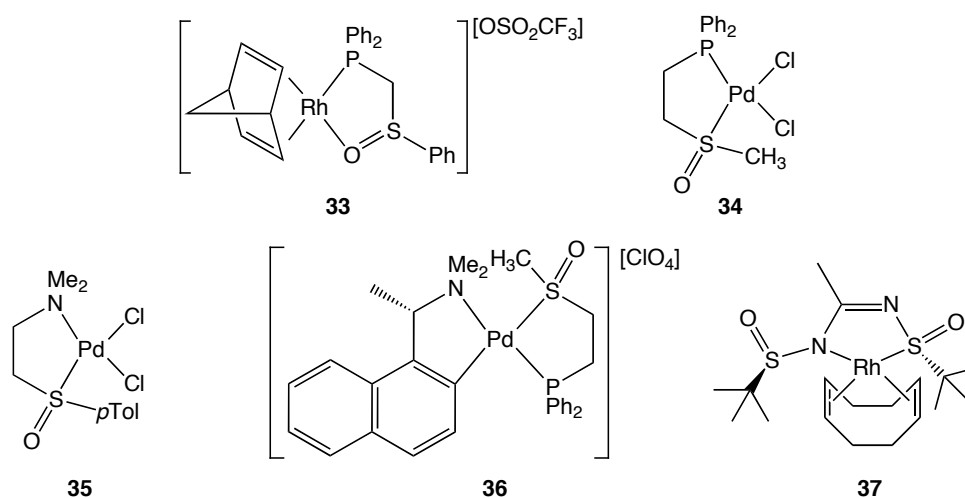


**Figure 18** Examples of complexes with ligands chelating through a sulfoxide and another heteroatom

Metal catalysis using ligands chelating through a sulfoxide and through another heteroatom have produced variable results, which will be discussed below. As well as using these ligands for catalysis, there have been several studies into the binding of these types of ligands. The structures of a few of these, **33**,<sup>59</sup> **34**,<sup>60</sup> **35**,<sup>54</sup> **36**,<sup>61</sup> and **37**,<sup>62</sup> are shown in figure 18.

#### 1.4. Non-enantioselective Catalysis with Bissulfoxide Ligands

Iridium complexes with DMSO ligands first became of interest when Henbest and co-workers demonstrated their catalytic activity in the reduction of cyclohexenones to alcohols (Figure 19).<sup>63</sup> Most systems performing the same transformation known until that time gave predominantly the equatorial alcohol, but the iridium DMSO catalysts gave mostly the axial alcohol.

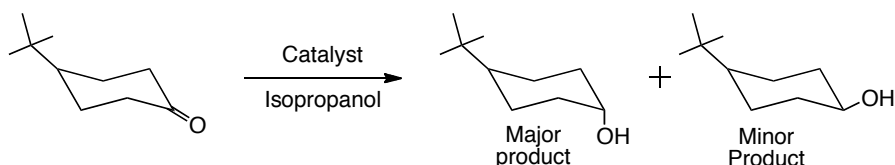


**Figure 19** Reduction of cyclohexenones by Ru DMSO complexes

The Ir complexes used for this reaction were Ir(III)(DMSO)<sub>3</sub>Cl<sub>3</sub> and the iridium acid [HDMSO<sub>2</sub>][Cl<sub>4</sub>Ir(III)(DMSO)<sub>2</sub>], giving an axial:equatorial ratio of 78:22 for the above reaction. The mechanism of the reaction was investigated, but it appeared to be quite complex.<sup>64,65</sup> An iridium hydride intermediate, HIr(III)(DMSO)<sub>3</sub>Cl<sub>2</sub> was isolated and an X-ray crystal analysis performed.<sup>66</sup> This revealed that the DMSO *trans* to the hydride is weakly bound and labile, suggesting it could dissociate during catalysis.

Following this, James reported that the same system can be used to selectively reduce the carbonyl bond of an  $\alpha,\beta$ -unsaturated aldehyde, with very little, if any, reduction of the olefin.<sup>67</sup> This success was, however, limited to aldehydes, in the case of  $\alpha,\beta$ -unsaturated ketones, reduction of both the carbonyl and the olefin was observed.

Ruthenium DMSO complexes have been shown to be successful catalysts for the molecular oxidation of sulfides to sulfoxides.<sup>68,69</sup> *cis*-Ru(II)Cl<sub>2</sub>(DMSO)<sub>4</sub>, *trans*-

$\text{Ru(II)Cl}_2(\text{DMSO})_4$  and *mer*- $\text{Ru(III)Cl}_3(\text{DMSO})_3$  all displayed good activity, and no over-oxidation to the sulfone was detected in the reaction shown in Figure 20.

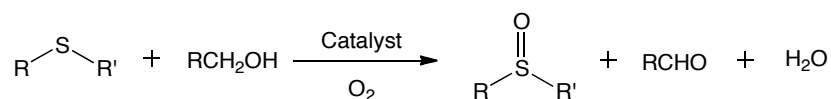


**Figure 20** Oxidation of sulfides to sulfoxides catalysed by ruthenium DMSO complexes

$\text{Ru(II)Cl}_2(\text{DMSO})_3(\text{DMSO})$  has more recently been used as a catalyst in the Ring Opening Metathesis Polymerization of norbornene, giving yields of up to 90% at room temperature.<sup>70</sup>

It was noticed by Bäckvall and co-workers that the use of catalytic amounts of sulfoxide in combination with  $\text{Pd}(\text{OAc})_2$  in the 1,4-diacetoxylation of 1,3-dienes improved both the conversion and regioselectivity of the reaction.<sup>71</sup> The group first attempted the reaction with a sulfinylbenzoquinone, **38**, (benzoquinone is normally employed in the reaction as an oxidant), but they later observed that DMSO gave the same selectivity (figure 21). It was reasoned that binding of a sulfoxide to palladium encourages formation of a ( $\sigma$ -allyl)-palladium complex with the 1,3-diene, which facilitates internal migration of the acetate. Speckamp and co-workers later used a similar catalytic system of  $\text{Pd}(\text{OAc})_2$ , DMSO and  $\text{Cu}(\text{OAc})_2$  to carry out oxidative cyclisations, in good yield and excellent selectivity for the 5-exo cyclisation product.<sup>72</sup>

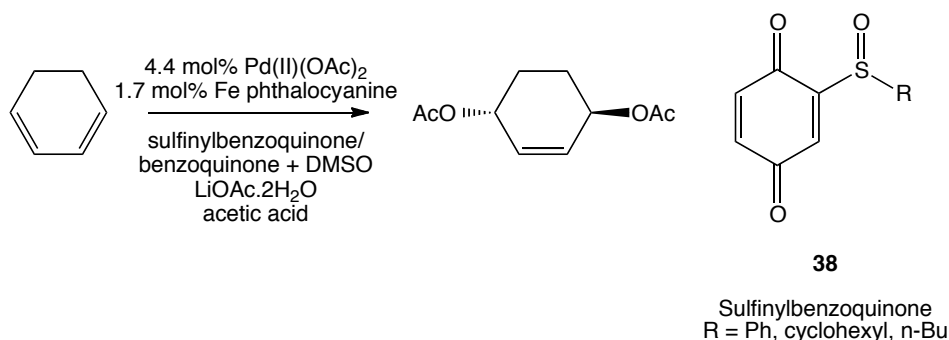


**Figure 21** Palladium catalysed 1,4-diacetoxylation of 1,3-dienes with sulfoxides as co-catalysts

The reactions mentioned above require the use of iron phthalocyanine or  $\text{Cu}(\text{OAc})_2$  as an external oxidant to recycle the palladium catalyst by reoxidising it from  $\text{Pd(0)}$  to  $\text{Pd(II)}$ . Speckamp subsequently discovered that the metal co-oxidant could be replaced by an atmosphere of molecular oxygen, if DMSO was used as the solvent. These conditions provide the added advantages of requiring less catalyst and giving

higher yields in shorter reaction times for the palladium-catalysed oxidative cyclisation of allylic amines.<sup>73</sup> Bäckvall and Larock further explored the scope of this catalytic system, finding it could be successfully applied to other oxidative cyclisations<sup>74</sup> and the conversion of enol silanes to enones and enals.<sup>75</sup> However, the reason this catalytic system was so successful was still unclear, although it had been speculated that Pd clusters were responsible for the catalysis. To investigate this theory, Speckamp and co-workers performed TEM imaging on typical reaction solutions and observed that Pd clusters were present.<sup>76</sup> They proposed that these clusters enable catalysis and reoxidation of Pd(0) to Pd(II) by molecular oxygen, and they are stabilised by ligation of DMSO to palladium.

Later Stahl and co-workers explored the mechanistics of the Pd(OAc)<sub>2</sub>/DMSO catalytic system in aerobic alcohol oxidation and found the turnover-limiting step to be the aerobic oxidation of Pd(0) to Pd(II).<sup>77</sup> However further studies revealed that this is due to the low solubility of molecular oxygen in DMSO.<sup>78</sup> For similar reactions in other solvents, the Pd(II)-mediated oxidation of the alcohol was shown to be the turnover-limiting step in the catalytic cycle. The same group later used a Pd(TFA)<sub>2</sub>/DMSO (TFA = trifluoroacetate) catalyst system for the aerobic oxidative cyclisation of allylic sulfamides, the products of which could easily be converted to diamines.<sup>79</sup>

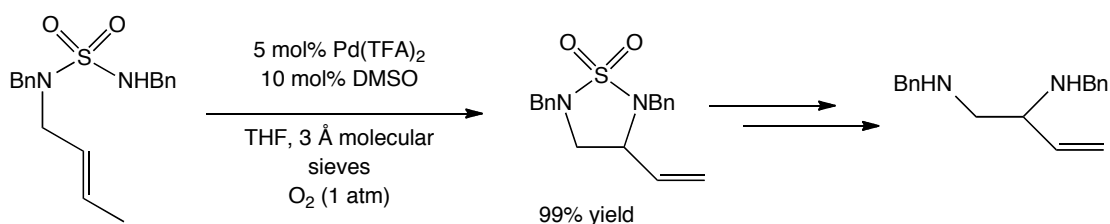


**Figure 22** Aerobic oxidation of allylic sulfamides using Pd(TFA)<sub>2</sub>/DMSO catalyst system

The Pd(TFA)<sub>2</sub>/DMSO system was later used in the dehydrogenation of substituted cyclohexanones to yield phenols.<sup>80</sup> However, in this example DMSO was used as the solvent rather than in catalytic amounts and the addition of 6 mol% 2-(*N,N*-dimethylamino)pyridine and 12 mol% *p*-toluenesulfonic acid were also required to achieve the product in good yield. Stahl *et al.* subsequently discovered that a slightly different catalyst system of Pd(TFA)<sub>2</sub> and DMSO in only 10 mol% efficiently dehydrogenated the same substrate, but gave the cyclic enone rather than the phenol as the product (figure 23).<sup>81</sup>

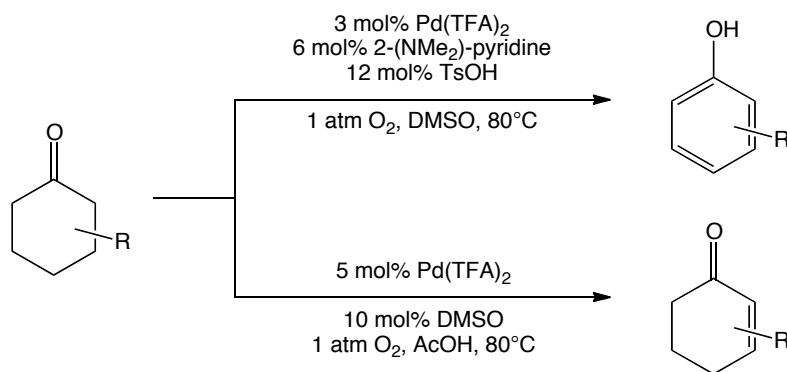


**Figure 23** The different uses of DMSO in the Pd-catalysed aerobic dehydrogenation of cyclohexanones

A similar combination of Pd(OAc)<sub>2</sub> and DMSO in trifluoroacetic acid was also used by Buchwald et al. to catalyse the ortho-arylation of anilides in aerobic conditions.<sup>82</sup>

Pd-DMSO complexes were also claimed by White and co-workers to be responsible for selectively catalysing an allylic C-H oxidation reaction (Figure 24), when a monosubstituted olefin is subjected to a catalytic system of Pd(OAc)<sub>2</sub>, DMSO and benzoquinone.<sup>83</sup> The reaction without DMSO leads to a mixture of addition products, but when DMSO is present, it is highly selective for the linear-(*E*)-allylic acetate. The authors propose that the ligation of DMSO to the Pd leads to the selectivity of the reaction, but there is no mention as to the mode of binding. This route to allylic acetates is a useful, concise way of generating intermediates in natural product syntheses.<sup>84</sup> The same group also used ethylene-bridged bissulfoxides with Pd(OAc)<sub>2</sub> (**39**) in similar reactions. Whereas DMSO gave the linear product, the bissulfoxide gave the branched product (figure 24).

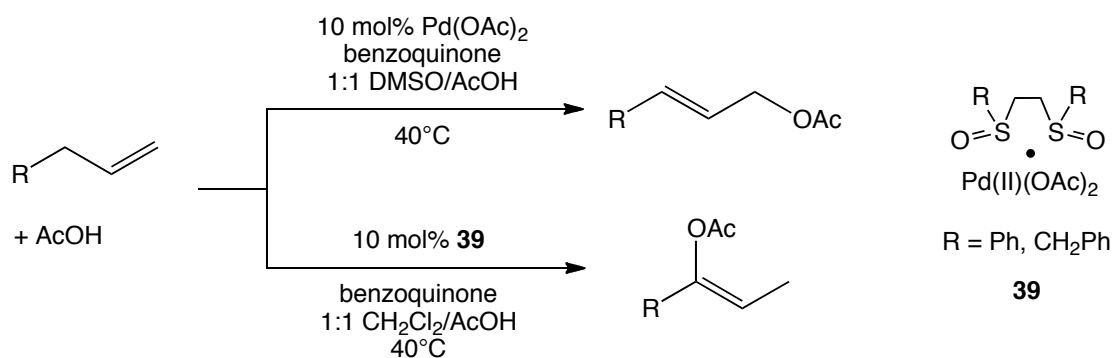


**Figure 24** Different selectivity of Pd(II) DMSO complex and Pd(II) bissulfoxide complex in allylic alkylation reactions

Carboxylic acids other than acetic acid were used in the reaction,<sup>85</sup> and the system was applied to the synthesis of macrolides.<sup>86</sup> Large rings (14 to 19 membered), with a



range of different functionalities, were made in moderate yields. Most notably, the aglycone precursor to erythromycin antibiotics, 6-deoxyerythronolide B (6-dEB), could be made by this methodology.<sup>87</sup> Subsequently, it was discovered by White *et al.* that the cyclic acetal protecting groups, previously thought to be necessary for efficient lactonisation, could be replaced by methoxy protecting groups. The reaction proceeded in 36% yield with the same reaction conditions, compared to 34% yield obtained in the reaction shown in figure 25.<sup>88</sup>

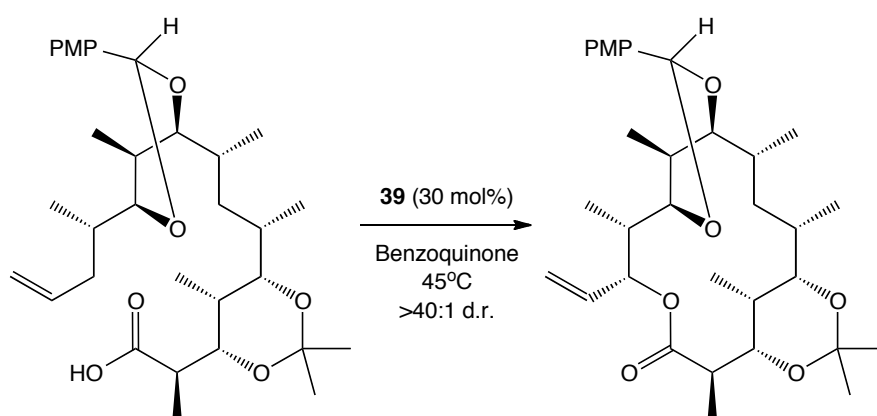


**Figure 25** Pd(OAc)<sub>2</sub>/bissulfoxide catalysed allylic C-H oxidation to give precursor to 6-dEB

Allylic C-H aminations, where the carboxylic acid is replaced by a carbamate, also worked in good yield with this system, to give 5- and 6-membered rings.<sup>89</sup> Products from these reactions could then be used in the preparation of *syn*-1,3-amino alcohol motifs, which are commonly present in pharmaceutically active molecules and natural products (figure 26).

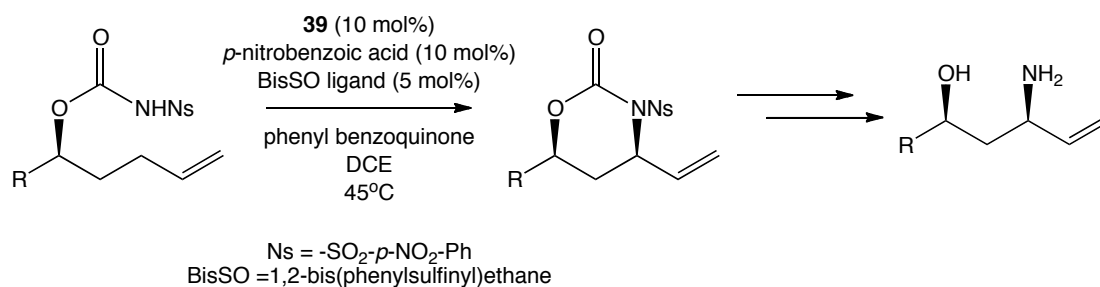


**Figure 26** Allylic C-H amination used in the preparation of *syn*-1,3-amino alcohol motifs

This methodology was also applied to other vinylic C-H arylation,<sup>90</sup> allylic C-H alkylation<sup>91</sup> and allylic C-H esterification<sup>92</sup> reactions. More recently, the allylic C-H alkylation of unactivated, as well as activated alkenes was realised using **39**. It was

discovered that the bissulfoxide competes with DMSO and benzoylacetone, also used in the reaction, to bind to palladium.<sup>93</sup>

The bissulfoxide-Pd complex **39** is represented, as shown in figure 24, without proper bonds between the sulfoxide and the Pd because the nature of the binding is unclear. It seems complexation does occur, there is a colour change when the bissulfoxide is added to the Pd(OAc)<sub>2</sub> and the elemental analysis fits. However, when the <sup>1</sup>H NMR of the free ligand and the ‘complex’ are compared, there is very little, if any, difference in the shifts. This suggests that the ligand interacts very weakly with the Pd. The role of the bissulfoxide in the catalytic reactions is not completely apparent, and it is unknown whether it is chelated to palladium throughout the catalytic cycle. This is perhaps why when the reaction was attempted with chiral sulfoxides, no enantioselectivity was observed. However, the reaction could be made asymmetric by the use of chiral Cr(III)salen complexes as co-catalysts.<sup>94</sup>

### 1.5. Enantioselective Catalysis with Sulfoxide Ligands

The first ever example of enantioselective transition-metal catalysis with a chiral sulfoxide ligand (figure 27) was reported by James.<sup>95</sup> The ligand, **40**, was tested in the ruthenium-catalysed hydrogenation of olefins.

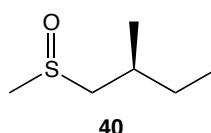


**Figure 27** First sulfoxide ligand used in enantioselective catalysis

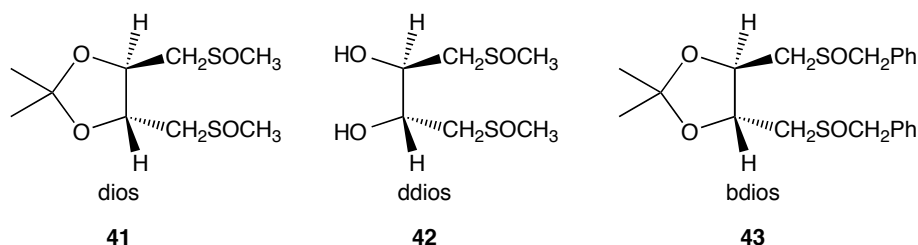


**Figure 28** Bissulfoxide ligands based on the phosphine ligand, diop

The enantioselectivity, however, was quite low, ~12% *e.e.*, and in an attempt to increase it, attention was turned to chelating, chiral bissulfoxides as ligands. A series

of bissulfoxides based on the known phosphine ligand diop, (-)-2,3-O-Isopropylidene-2,3-dihydroxy-1,4-bis(diphenylphosphino)butane, were synthesised (figure 28) and tested in the same catalytic reaction.<sup>96</sup> Using  $\text{Ru(II)Cl}_2(\text{dios})(\text{ddios})$ , the enantioselectivity of the reaction was increased to 25% *e.e.* Following the pioneering work of James there has been a steady increase in the number of bissulfoxide ligands developed and used in catalysis, both enantioselective and non-enantioselective. In the rest of this section, the developments in this field will be explored.

A decade later, rhodium-catalysed transfer hydrogenation of aryl-alkyl ketones was attempted using *N*-acetyl-(*S*)-methionine (*R,S*)-sulfoxide (AMSO, **44**).<sup>97</sup> The ligand was synthesised by non-stereoselective oxidation of methionine, hence a mixture of the (*R<sub>S</sub>*)- and (*S<sub>S</sub>*)- diastereomers were obtained, and used as such in catalysis. AMSO was used in combination with  $[\text{Rh}(\text{hd})\text{Cl}]_2$  (hd = 1,5-hexadiene), in a 1:2 ratio of Rh/ligand. Only moderate yields were achieved, but in the hydrogenation of 4-methylacetophenone, an *e.e.* of 75% was achieved (figure 29), despite the use of a mixture of diastereomers. The reaction was only effective for the hydrogenation of aryl-alkyl ketones, alkyl-alkyl ketones could not be reduced by this system. It was thought that the ligand binds to rhodium through the acyl group and through the sulfoxide, although there were no studies to confirm this.

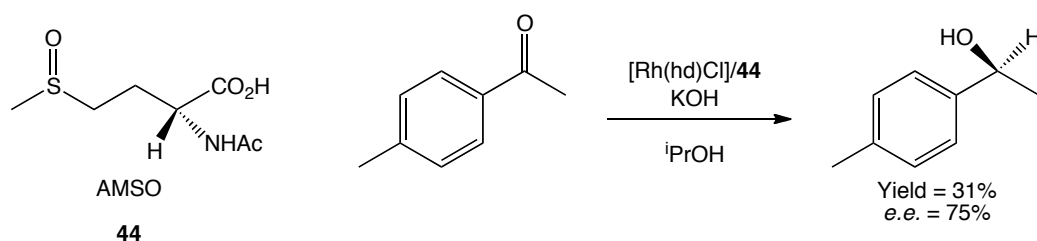


**Figure 29** AMSO and rhodium catalysed transfer hydrogenation

Aminosulfoxides were later also used in iridium-catalysed asymmetric transfer hydrogenation,<sup>98</sup> using formic acid as the hydrogen donor, instead of 2-propanol. The side product of this reaction is  $\text{CO}_2$ , which will leave as a gas and so the reaction will be irreversible. In this class of ligands, it is believed that binding to the iridium is through S and N.

The ligand could be obtained enantiomerically pure by crystallisation, but it was first used in catalysis as a mixture. The mixture gave 35% *e.e.* of the (*S*)- product,

however when they were used separately, (*S*<sub>S</sub>)-**45** gave the (*S*)- product in 65% *e.e.* and (*R*<sub>S</sub>)-**45** gave the (*R*)- product in 27% *e.e.*

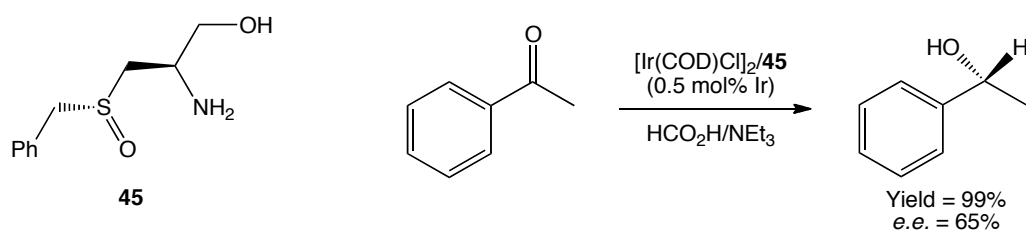


**Figure 30** *S*-benzyl-(*R*)-cysteinol-(*S*<sub>S</sub>)-sulfoxide, **45**, and iridium catalysed transfer hydrogenation of acetophenone

The 1,2-addition of diethyl zinc to benzaldehyde to give 1-phenyl-propanol is a reaction that has been extensively studied with different catalytic systems. Enantiomerically pure  $\beta$ -hydroxysulfoxides, such as **46** (figure 31), were tested in this reaction.<sup>99</sup> The  $\beta$ -hydroxysulfoxides were believed to co-ordinate to the zinc in a bidentate fashion. The results obtained were moderate; with those ligands containing a tertiary alcohol, rather than a secondary one, giving the highest enantioselectivities (up to 45% *e.e.* with **46**, compared to 23% *e.e.* with the best secondary alcohol). The addition reaction was in competition with another side reaction, namely the reduction of benzaldehyde to give benzyl alcohol. It was observed that as the enantioselectivity increased, the extent of the side reaction also increased.

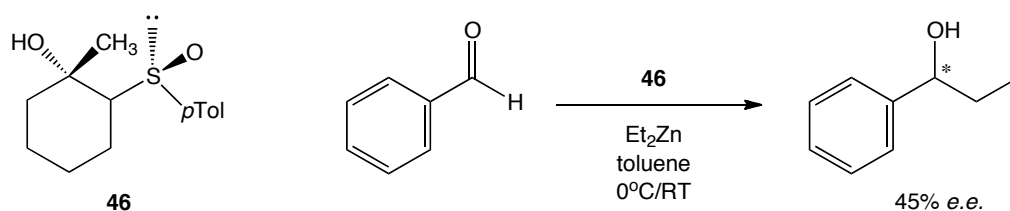


**Figure 31**  $\beta$ -hydroxysulfoxide ligand, **46**, and 1,2-addition reaction of  $\text{Et}_2\text{Zn}$  to benzaldehyde

Carretero achieved more success with 2-amino-1-*tert*-butylsulfinyl ferrocene ligands, **47** (figure 32).<sup>100</sup> Good yields and enantioselectivities of up to 88% *e.e.* were observed for the 1,2-addition of diethyl zinc to benzaldehyde. When the *tert*-butyl group was replaced by a *p*-tolyl, the *e.e.* decreased dramatically to 32%. This indicates that steric bulk around the sulfoxide is important for high *e.e.*

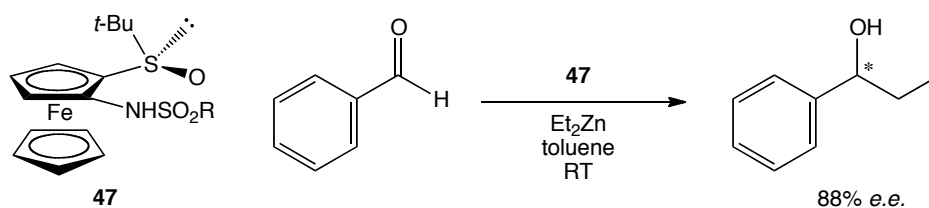


**Figure 32** 1,2-Addition of  $\text{Et}_2\text{Zn}$  to benzaldehyde with 2-amino-1-*tert*-butylsulfinyl ferrocene, **47**

Interestingly, when the sulfoxide was reduced to a sulfide, or oxidised to a sulfone, and used in the same reaction, almost the same *e.e.* was reached. This demonstrates that the planar chirality of the ferrocene plays a major role.

As mentioned before, ligands **15a** and **21** were used in asymmetric Diels-Alder reactions.<sup>52</sup>  $\text{FeI}_3$  was mixed with the ligand and the resulting complex was used to catalyse the reaction shown below. The two ligands were both almost completely selective for the *endo* product (figure 33) and displayed moderate enantioselectivity.

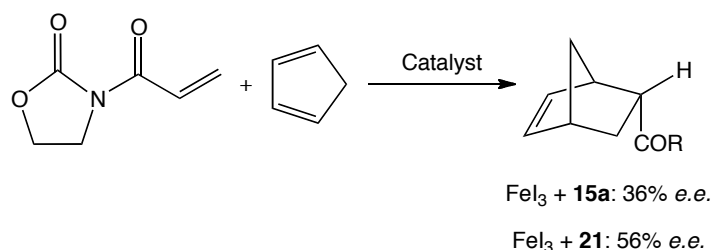


**Figure 33** Iron catalysed Diels-Alder reaction with bissulfoxide ligands

Sulfinamide ligands, **48**, **49**, and **50**, inspired by bis-oxazoline ligands, which were previously found to be highly reactive and selective in various Lewis Acid-catalysed reactions,<sup>101</sup> were synthesised by Ellman.<sup>102</sup> They were then tested in a copper catalysed Diels-Alder reaction, initially using  $\text{Cu}(\text{OTf})_2$  as the copper source in 10 mol% and the ligands in 11 mol%. **48** displayed excellent reactivity, but almost no selectivity; **49** and **50** provided moderate selectivity and reactivity (figure 34).

Changing the copper source to  $\text{Cu}(\text{SbF}_6)_2$  and using ligand **50** gave complete conversion and an excellent enantioselectivity of 98% *e.e.* for the reaction shown. The authors originally thought that the ligands would bind through N, but an X-ray crystal structure of ligand **50** bound to Cu revealed that it actually bound through the oxygens of the sulfoxides, in a  $\text{M}_2\text{L}_4$  quadruple stranded helicate. The authors investigated the scope of this catalytic system, and found that it also provided good results with less reactive acyclic diene substrates (up to 96% yield and 92% *e.e.*).<sup>103</sup> This was not the case when bis-oxazolines were used as ligands, where poor selectivities were

measured. However, lower selectivities were obtained when acyclic substrates with terminal substituents were used.

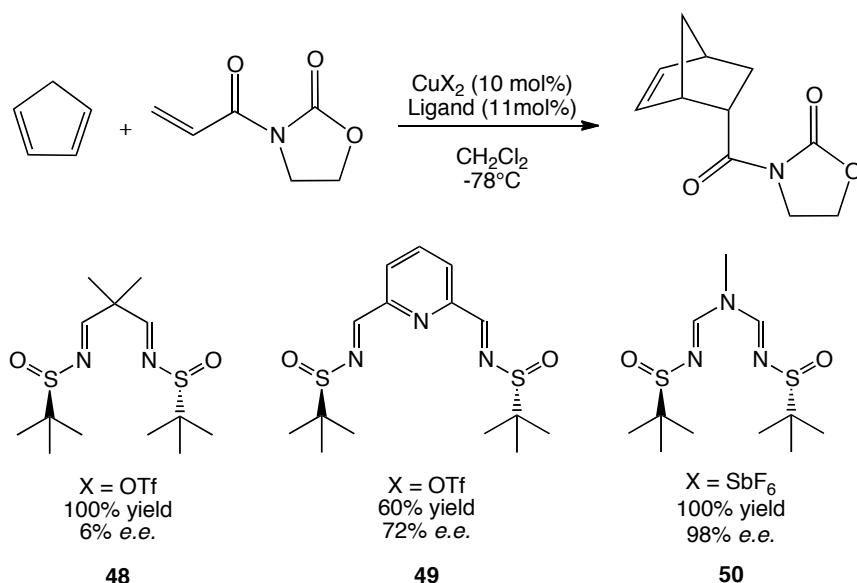


**Figure 34** Sulfonamide ligands used in copper catalysed Diels-Alder reactions

Williams demonstrated that S,N ligands could be successfully applied in palladium-catalysed allylic alkylation reactions.<sup>104,105</sup> The ligand presented, **51** (figure 35), contained a chiral sulfoxide and a chiral oxazoline moiety, and provided enantioselectivities of up to 88% *e.e.*

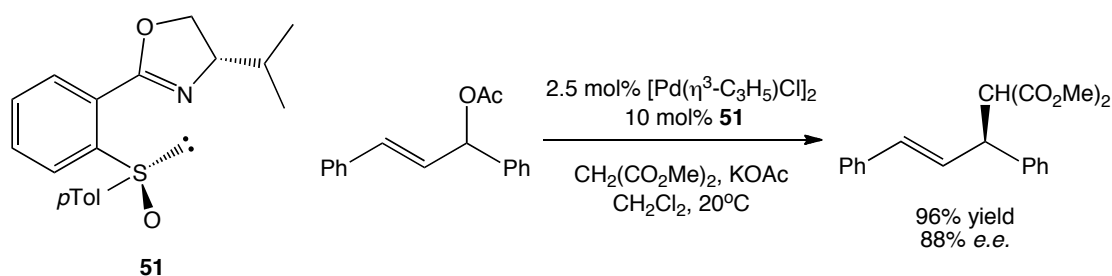


**Figure 35** Palladium catalysed allylic alkylation reaction with **51** as ligand

The ligand was also synthesised without a chiral centre on the oxazoline moiety, the *i*-Pr was replaced by two Hs, causing the enantioselectivity to drop to 56% *e.e.* When two methyl groups replaced the *i*-Pr, it dropped even further to 49% *e.e.* The combination of the chirality on the sulfoxide and the oxazoline is important to achieve high enantioselectivity.

A few years later, Hiroi began to investigate the palladium-catalysed allylic alkylation reaction with  $\beta$ -amino sulfoxides.<sup>106,107</sup> First attempts were carried out with

ligand **52** (figure 36), however low yields and enantiomeric excesses of only 39% *e.e.* were obtained. Additionally, a ligand/metal ratio of 4:1 had to be employed. In an effort to increase the enantioselectivity of the reaction, the authors rigidified the backbone of the ligand by introducing a phenyl ring. Ligand **53**, when applied in the same catalysis, gave low yields, but the enantioselectivity was increased to 50% *e.e.* Another modification made to the ligand was to add an extra carbon between the phenyl group and the amino group. Ligand **54** would then form a 6-membered, rather than a 5-membered ring with palladium. Generally these ligands gave lower enantioselectivity than the ones without the extra carbon. This was explained by looking at models of the bound ligand. It could be seen that a 5-membered metallocycle provided more steric hindrance around the metal, and thus would be expected to provide better selectivity.

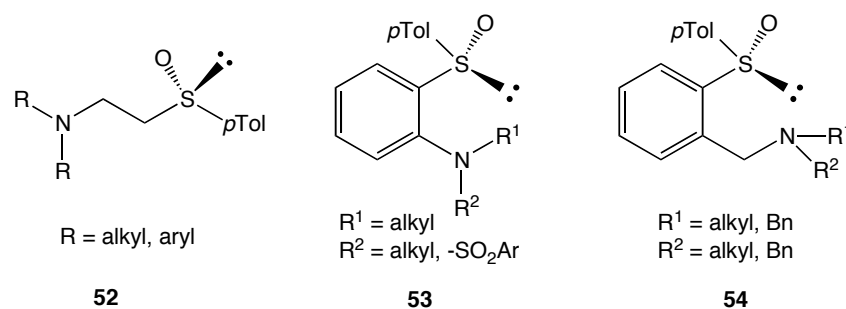


**Figure 36** Amino sulfoxide ligands used in palladium catalysed allylic alkylation reaction

The same group later had more success with phosphino sulfoxide and phosphinoamido sulfoxide ligands. The amino group of ligand **53** could be replaced by a phosphine, to give ligand **55** that was stable at room temperature.<sup>108</sup> The ligand could also be synthesised with 2-methoxy-naphthalene on the sulfoxide, instead of *p*-tolyl, the idea being that a larger aryl group would create more steric hindrance around the metal centre, and lead to better selectivity. This new ligand was tested in the palladium-catalysed addition of sodium malonate to diphenylallyl acetate, and yields up to 75% were achieved.

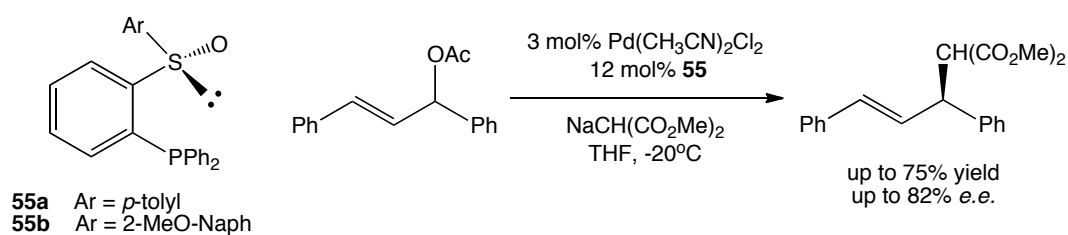


**Figure 37** Palladium catalysed allylic alkylation with **55**

Changing the palladium source from  $[\text{Pd}(\eta\text{-C}_3\text{H}_5)\text{Cl}]_2$  to  $\text{Pd}(\text{CH}_3\text{CN})_2\text{Cl}_2$  was found to be favourable for selectivity. Also, the change of the aryl group on the sulfoxide from *p*-tolyl to 2-methoxynaphthalene made a big difference in terms of selectivity. Ligand **55a** provided the product in only 46% *e.e.* (*R*), whereas ligand **55b** gave the product in 82% *e.e.* (*S*).<sup>109</sup> Substitutions (alkyl and alkoxy groups) were also made on the phenyl backbone of the ligand, but these were found to have no effect on the selectivity of the reaction.

Hiroi and co-workers then developed phosphinoamido sulfoxide ligands (Figure 38), by inserting a nitrogen atom between the phenyl and the phosphine.<sup>110</sup> Again, the 2-methoxy-naphthalene sulfoxide derivative, **56**, was the best ligand achieving an excellent enantioselectivity of 97% *e.e.*, when the ratio of ligand to  $[\text{Pd}(\eta\text{-C}_3\text{H}_5)\text{Cl}]_2$  was 8:1. However the isolated yield was only moderate.

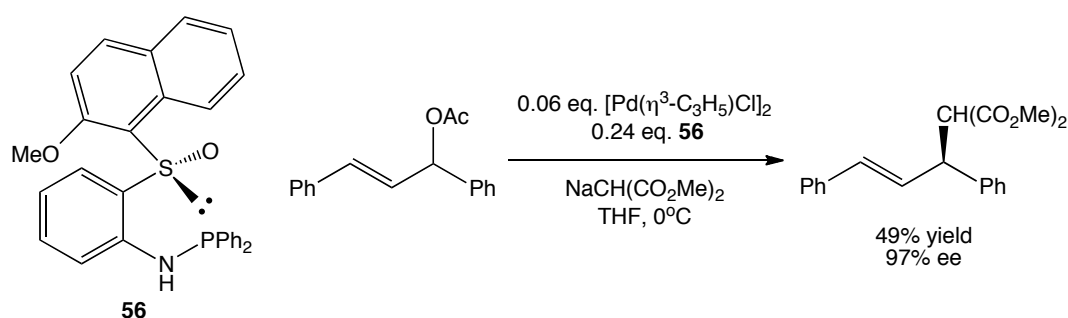


**Figure 38** Palladium catalysed allylic alkylation with **56**

The choice of solvent was found to be crucial for high selectivity, with THF giving the best results. In DMSO an enantioselectivity of only 11% *e.e.* was reached.

Hiroi presented a further class of *N*-phosphinosulfinyl ligands, *N*-phosphanopyrrolyl aryl sulfoxides, **57**, and *N*-phosphinoindolyl aryl sulfoxides, **58** and **59** (Figure 39).<sup>111</sup> These ligands were also successfully employed in the same allylic alkylation reaction shown above (figure 38).

Both the *N*-phosphanopyrrol and the *N*-phosphanoindolyl ligands were made with *p*-tolyl-, 1-naphthyl-, and 2-methoxy-1-naphthyl sulfoxide substituents. In all examples the latter displayed the best enantioselectivity, giving 93% *e.e.* in the case of **58**, when the reaction was carried out at  $-78^\circ\text{C}$ . It was suggested that repulsions between the methoxy on the naphthyl ring and the S-O bond fix a configuration, which leads to the high selectivity by blocking access to the metal centre on one side.



In addition, substituting electron-donating groups onto the pyrrol or indole ring improved the reactivity considerably.

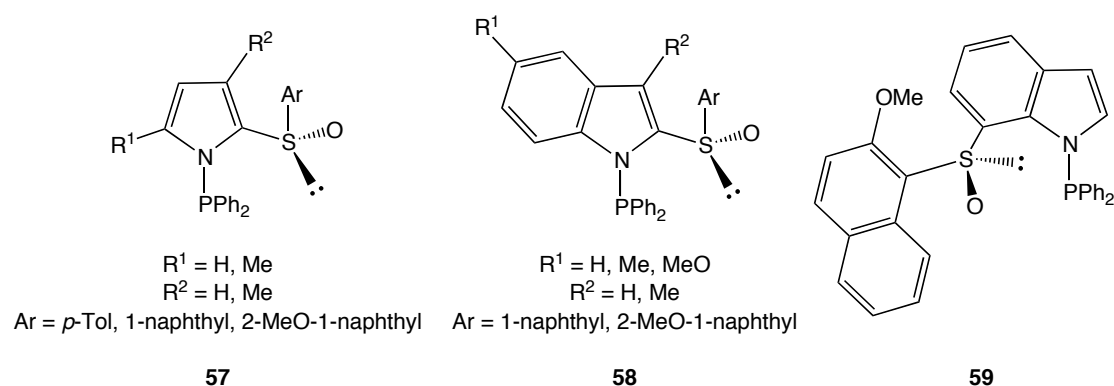


**Figure 39** N-phosphanopyrrol and N-phosphanoindolyl aryl sulfoxides

The first promising results in terms of enantioselectivity, employing a bissulfoxide ligand were achieved by Shibasaki with the previously mentioned ligand BTSB, **29**.<sup>58</sup> The ligand was tested in the palladium-catalysed allylic alkylation reaction (figure 40), using 5 mol% Pd and 20 mol% ligand, where it gave moderate results (70% yield, 62% *e.e.*). At the time this was the best enantioselectivity known in transition metal catalysis with chiral bissulfoxide ligands.

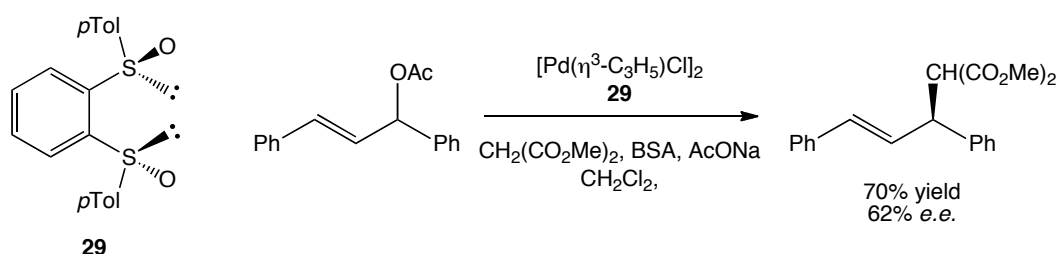


**Figure 40** Palladium-catalysed allylic alkylation with **29**

It wasn't until 2008 when the next asymmetric catalysis with a chiral bissulfoxide ligand was reported by Dorta *et al.*<sup>112</sup> The ligand reported, named *p*-tolyl-binaso (1,1'-binaphthalene-2,2'-diyl-bis-(*p*-tolylsulfoxide)), was the bissulfoxide analogue of the well-known phosphine ligand, binap (binaphthalene-2,2'-diyl-bis-diphenylphosphine), developed by Noyori in 1980<sup>113</sup>. The ligand was readily synthesised from commercially available starting materials. This ligand was of interest because as well as the chirality on the sulfur, it also contains axial chirality in the backbone. When enantiomerically pure sulfinate, *S*- or *R*-, was used in the synthesis of the ligand, two diastereomers of the ligand were obtained, which could be

separated by column chromatography. The (*M,S<sub>S</sub>,S<sub>S</sub>*)- and the (*P,R<sub>S</sub>,R<sub>S</sub>*)- diastereoisomers of *p*-tolyl-binaso formed a Rh(I) dimer, **60**, when reacted with [Rh(C<sub>2</sub>H<sub>4</sub>)<sub>2</sub>Cl]<sub>2</sub>. However, the (*M,R<sub>S</sub>,R<sub>S</sub>*)- and the (*P,S<sub>S</sub>,S<sub>S</sub>*)- diastereoisomers did not bind to Rh.

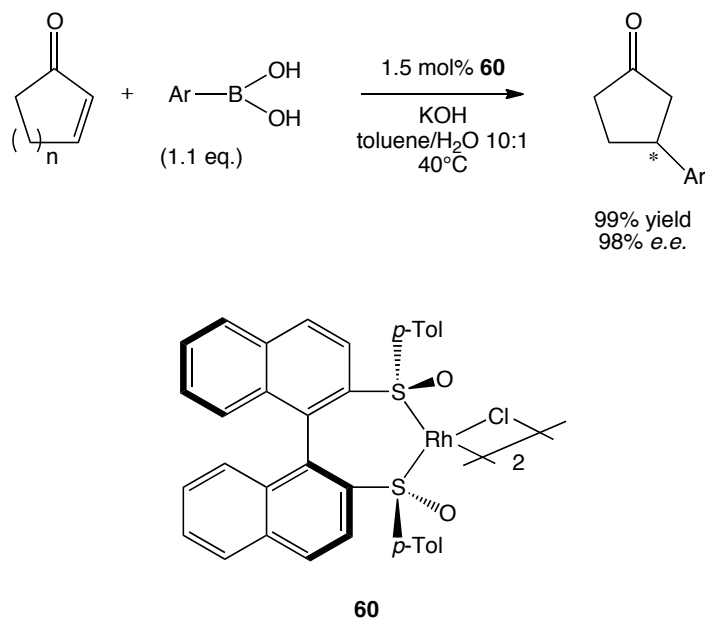


**Figure 41** Rhodium catalysed 1,4-addition of phenylboronic acid to cyclohexenone

The Rh complex, [ $\{(P,R_S,R_S)\text{-}p\text{-tolyl-binaso}\}\text{RhCl}]_2$  **60**, was tested in the 1,4-addition of aryl-boronic acids to cyclic enones (Figure 41) with toluene as the solvent, and found to give excellent yields and enantioselectivities, without the need for high excesses of expensive boronic acid.

Even better results were obtained with another bisulfonate ligand based on the previously known phosphine ligand, biphemp (dimethylbiphenyl-2,2'-diyl-bis(diphenylphosphine)). As in the case of binaso, this ligand, *p*-tolyl-Me-bipheso, contains axial chirality.<sup>114</sup>

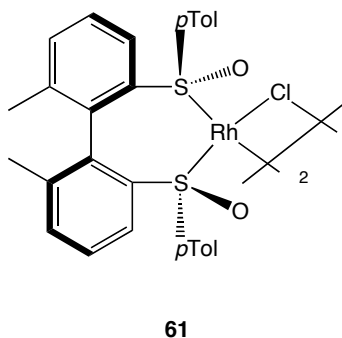


**Figure 42** Rh complex of (*M,S<sub>S</sub>,S<sub>S</sub>*)-*p*-tolyl-bipheso, **61**

[{(M,S<sub>S</sub>,S<sub>S</sub>)-*p*-tolyl-bipheso}RhCl]<sub>2</sub>, **61**, was made and tested in the same 1,4-addition reaction (figure 42). A lower catalyst loading of only 0.5 mol%, and a shorter reaction time of 30 minutes, was required. With these conditions, yields up to 98% and enantioselectivities of >99% *e.e.* were recorded.

A whole family of bissulfoxide ligands based on *p*-tolyl-binaso was later synthesised by making modifications to the original ligand (figure 43).<sup>115</sup> The *p*-tolyl group was replaced by other aromatic rings, or cyclohexyl, **62**; and in one case, the binaphthyl backbone was partially hydrogenated, **63**. The rhodium complex of the binaso derivative with the partially hydrogenated backbone was comparable as a precatalyst in the 1,4-addition reaction to that of (M,S<sub>S</sub>,S<sub>S</sub>)-*p*-tolyl-bipheso. This suggests that the greater the steric bulk on the backbone of the ligand, the better the precatalyst for this reaction. The other binaso ligands, **63**, with the exception of the 4-F-Ph derivative were, however, less active and less selective.

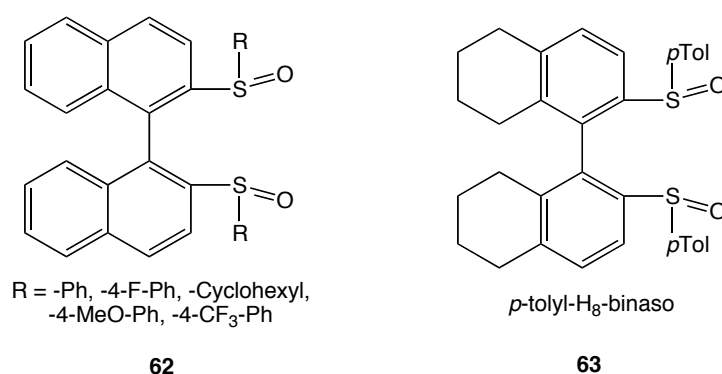


**Figure 43** Other ligands in the binaso family

The electron-donating properties of the binaso family of ligands, bipheso, binap and biphemp to rhodium were estimated from the IR stretching frequencies of the CO ligands in the respective [Rh(ligand)(CO)<sub>2</sub>][BF<sub>4</sub>] complexes.<sup>114,115</sup> Converse to what was expected, the bissulfoxide ligands presented were more electron-donating to rhodium than their diphosphine counterparts.

X-ray crystal structures of the rhodium complexes, **60** and **61**, demonstrated that the ligands do not provide a lot of steric bulk around the metal centre. The *p*-tolyl substituents are pointed away from the metal, and parallel to the backbone. The only moieties creating any steric hindrance around the metal are the sulfoxide oxygens. This observation prompted studies into the origin of the enantioselectivity of the reaction. In-depth DFT studies were carried out with **61** to investigate how the nature

of the transition state affected the enantioselectivity of the reaction.<sup>115,116</sup> These revealed that co-ordination of the enone to the metal centre was not the enantio-discriminating step. The enantioselective step of the reaction is the formation of the C-C bond between the 3-position of the enone and the phenyl group. As can be seen in figure 44, there are two possible transition states leading to the product. Transition state **A** leads to the *R* product, whereas transition state **B** leads to the *S* product. In transition state **A**, the phenyl and the C=O of the substrates are pointed towards the *p*-tolyl groups of the ligand, where there is an open space, and minimum interaction with the sulfoxide oxygens. In transition state **B**, the phenyl group and the C=O of the substrates form unfavourable steric and electronic interactions with the sulfoxide groups. Hence, **B** is higher in energy by 4.4 kcal mol<sup>-1</sup> and is disfavoured, this explains the very high selectivity for the *R* product.

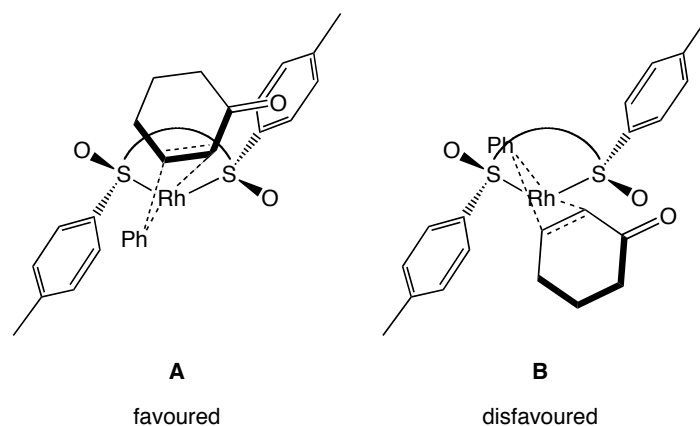


**Figure 44** Transition states for the formation of the C-C bond in the 1,4-addition reaction

Computational studies were also performed to investigate the nature of the interaction between the substrates in the 1,4-addition (cyclohexenone and phenyl) and the Rh complex in the C-C bond formation step, with the ligands bipheso and biphemp.<sup>116</sup> This revealed that the enantioselective control with the biphemp complex was almost entirely due to the steric hindrance from the phenyl groups of the ligand, whereas the selectivity with the bipheso complex is mostly controlled by electrostatic interactions.

Liao recently presented promising results with a new ligand, (*R<sub>s</sub>*,*R<sub>s</sub>*)-1,2-bis(*tert*-butylsulfinyl)benzene **64**, which was readily prepared in a two-step synthesis from bromobenzene and *tert*-butyl thiosulfinate.<sup>117</sup>

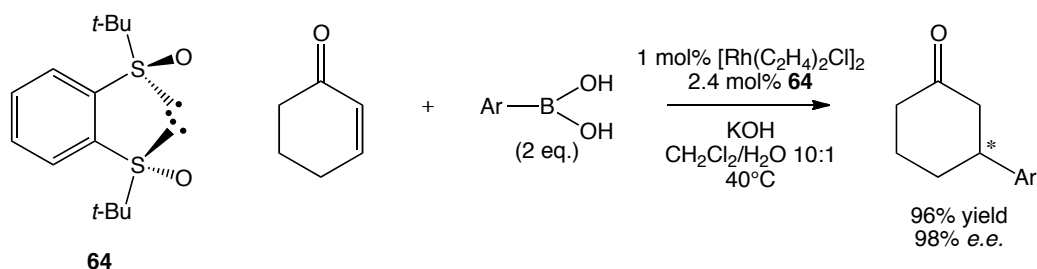


**Figure 45** Rhodium-catalysed 1,4-addition of phenylboronic acid to cyclohexenone with **64**

This ligand in combination with  $[\text{Rh}(\text{C}_2\text{H}_4)_2\text{Cl}]_2$  (2 mol% Rh) catalysed the 1,4-addition of phenyl boronic acid to cyclohexenone in excellent yield and enantioselectivity (figure 45). The only difference between the conditions used for the reaction with this ligand and with *p*-tolyl-binaso was the use of  $\text{CH}_2\text{Cl}_2$  instead of toluene as solvent. These excellent results demonstrated that chirality in the backbone of the ligand was not necessary to achieve high enantioselectivity.

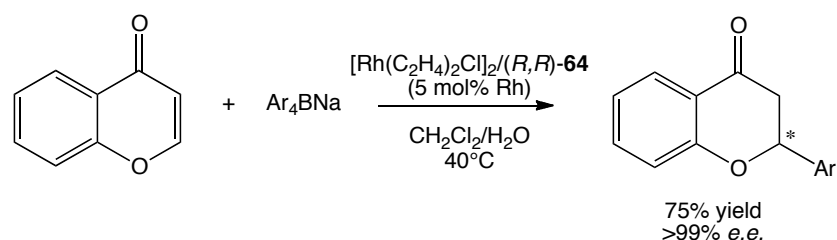


**Figure 46** Rhodium-catalysed 1,4-addition of sodium tetraaryl borates to chromenone

The authors were also able to carry out a transformation previously not achieved by late transition-metal catalysis. **64** and  $[\text{Rh}(\text{C}_2\text{H}_4)_2\text{Cl}]_2$  were used to catalyse the 1,4-addition of sodium tetraaryl borates to chromenones, in moderate to good yields and excellent enantioselectivities (figure 46). This is a challenging reaction due to the more electron-rich nature of the double bond in chromenone compared to enones.

Another transformation recently achieved by the same group, this time with the isolated  $[\text{Rh}(\textbf{64})\text{Cl}]_2$  complex, was the 1,4-addition of boronic acids to  $\gamma$ -phthalimidocrotonates (figure 47).<sup>118</sup> The same reaction conditions were used as for the previously mentioned 1,4-addition with the same ligand (figure 45). The products of the catalysis are synthetic precursors to pharmaceutically active molecules. Enantioselectivities of up to 96% *e.e.* were reached with this system, and so it could potentially be used as the key step in preparing enantiopure pharmaceuticals.

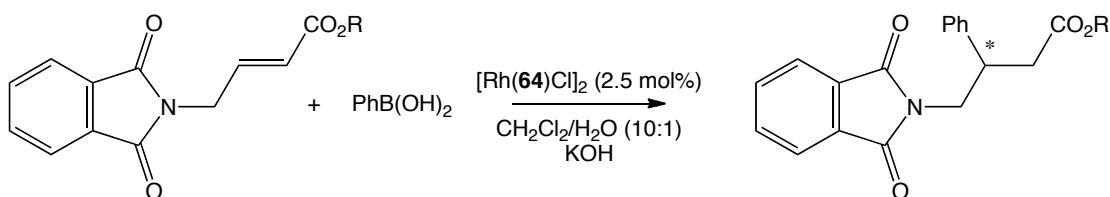


**Figure 47** Rhodium catalysed 1,4-addition of sodium tetraaryl borates to  $\gamma$ -phthalimidocrotonates

The mono-sulfoxide, *tert*-butylsulfinylbenzene, could be reacted with different sulfinates to generate a new class of heterobissulfoxide ligands. These were then applied to catalysis, and it was found that it was possible to carry out the 1,4-addition of phenylboronic acids to chromenones. This is much more convenient than using tetraarylborates, which are not so readily available and generally produce toxic side-products.<sup>119</sup> The best ligand was discovered to be 1-((*R*)-*tert*-butylsulfinyl)-2-((*S*)-mesitylsulfinyl)benzene, **65**, which gave a good yield of 67%, with excellent enantioselectivity.

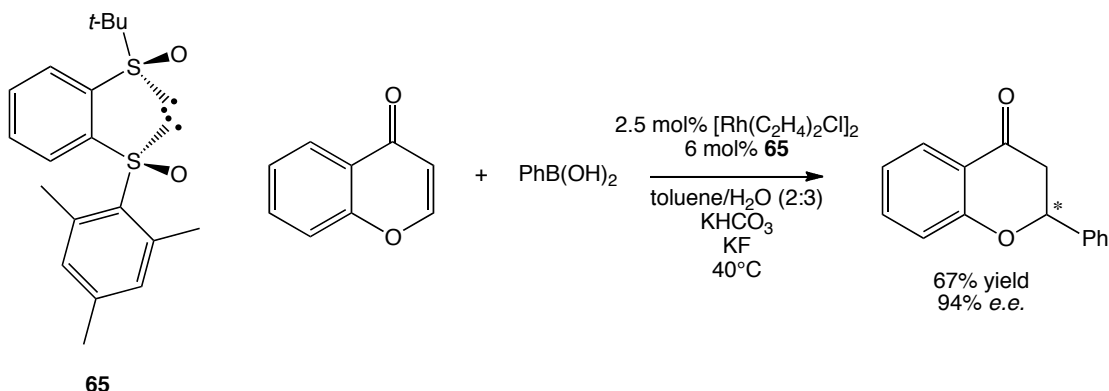


**Figure 48** Rhodium-catalysed 1,4-addition of phenylboronic acid to chromenone with **65**

Prior to the bissulfoxide ligand, **64**, Liao and co-workers developed sulfinyl phosphine ligands, **66**, which they then used in asymmetric transition-metal catalysis. Firstly, an asymmetric addition of diethylzinc to diphenylphosphonyl imines (figure 49) was attempted.<sup>120</sup> **66** was used in combination with  $\text{Cu}(\text{CO}_2\text{CF}_3)_2 \cdot x\text{H}_2\text{O}$ , in a 1:2 ratio, with toluene as the solvent.

It was apparent that an alkoxy group *ortho* to the phosphine was important to achieve high reactivity and high enantioselectivity. When R was a methoxy the best results were obtained, 89% isolated yield and 92% *e.e.* for the reaction shown above. The ligand where R =  $\text{OCH}_2\text{OCH}_3$  proved to be successful in palladium allylic alkylation and allylic amination reactions, giving excellent yields and moderate to good

enantioselectivities.<sup>121</sup> This class of *tert*-butylsulfinylphosphines were also tested in the rhodium-catalysed 1,4-addition shown in figure 50.<sup>122</sup>

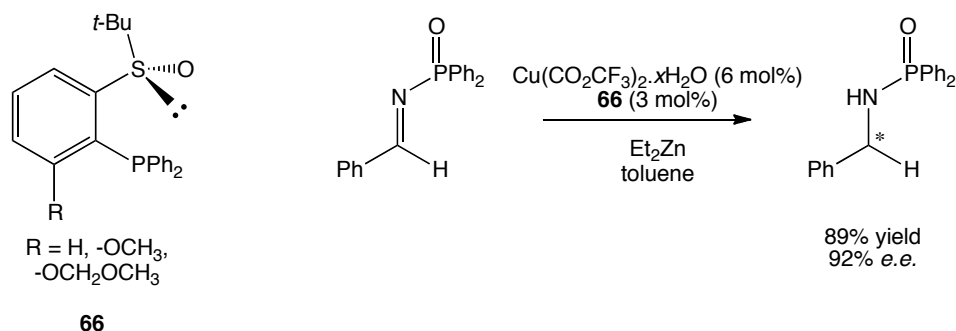


**Figure 49** Sulfinylphosphine ligand, **66**, and copper catalysed addition of diethyl zinc to diphenylphosphonyl imine

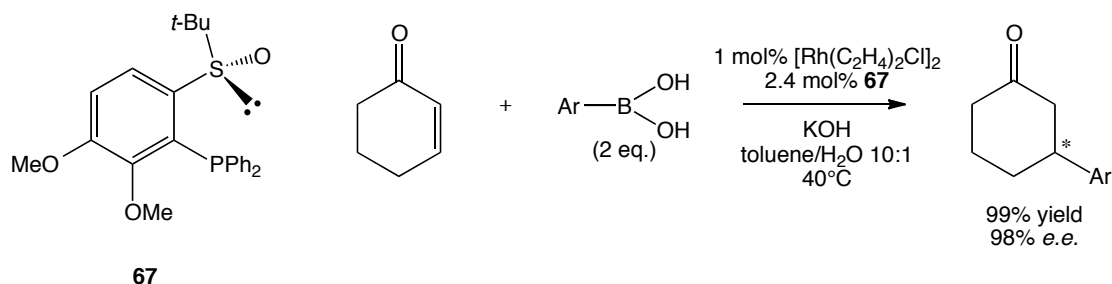


**Figure 50** Rh-catalysed 1,4-addition reaction of phenylboronic acid to cyclohexenone with **67**

The reaction is a unique example of a sulfinylphosphine ligand being used in rhodium catalysis and the results were promising. The scope of this reaction was expanded to include 1,4-addition reactions to 2-nitrostyrenes (figure 51).<sup>123</sup> This was the first time nitrostyrenes could be used in this type of reaction.

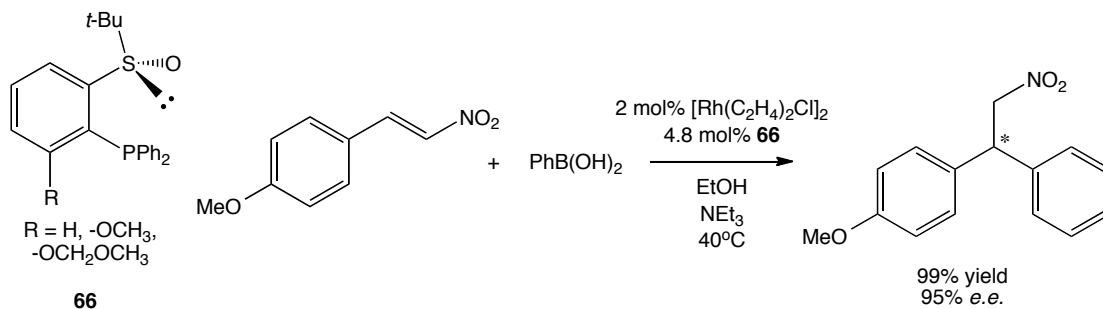


**Figure 51** Rhodium catalysed 1,4-addition reaction of phenylboronic acid to 4-MeO-2-nitrostyrene with **66**

The sulfinylphosphine ligand where R = -OCH<sub>2</sub>OCH<sub>3</sub> was the best for this reaction, enabling yields as high as 99% and enantioselectivities of up to 95% *e.e.* The

methodology was applied to the synthesis of the pharmaceutically active natural product (*R*)-cheryline, giving highly enantio-enriched product.

The latest contributions to the area have seen the introduction of novel sulfoxide-alkene<sup>124</sup> and sulfinamide-alkene<sup>125</sup> ligands, both of which were applied to Rh-catalysis. These types of ligands are inspired by the chiral dienes of Hayashi and Carreira,<sup>126</sup> and P/N-olefin ligands<sup>127</sup>. Knochel and co-workers synthesised two diastereoisomers of a sulfoxide-alkene ligand, **68** and **69** (figure 52). The chirality on both ligands was the same at sulfur, but different with regards to the alkene. Both ligands were tested in the rhodium-catalysed 1,4-addition of arylboronic acids to enones, and were both found to give the product in equally high enantioselectivities, but opposite configuration. This points to the conclusion that it is the chiral environment around the alkene that determines the enantioselectivity of the reaction.

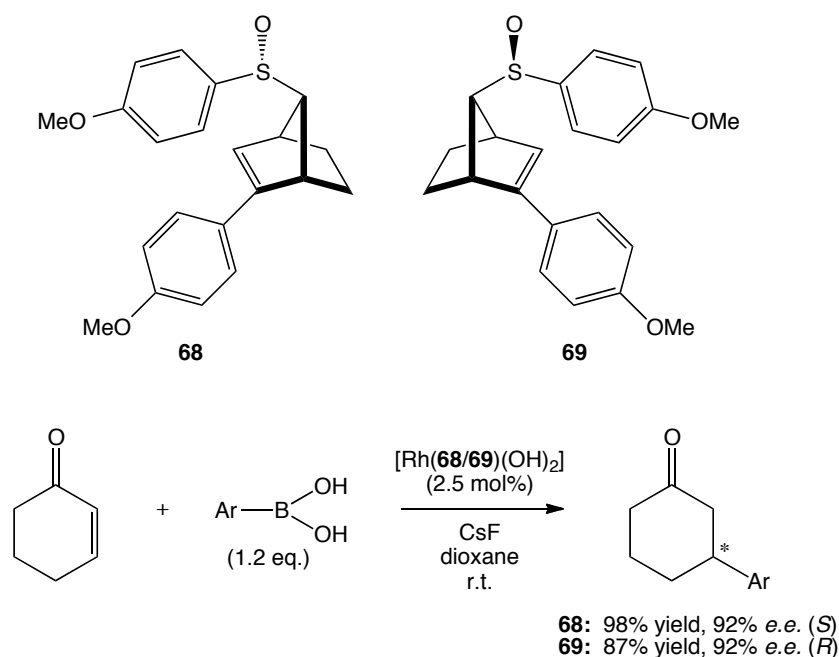


**Figure 52** Rh catalysed 1,4-addition of phenylboronic acid to cyclohexenone with **68** and **69**

Xu presented a family of sulfoxide-alkene ligands, **70**, based on the bissulfoxide mentioned earlier from Liao **64**, with one sulfoxide replaced by an olefin.<sup>128</sup> These ligands were highly active for the 1,4-addition of arylboronic acid to cyclic enones, (figure 53). It was observed that exchanging the *tert*-butyl on the sulfoxide with *p*-tolyl dramatically reduced the selectivity of the system. Substituting methoxy groups onto the backbone of the ligand increased the activity and selectivity of the catalyst. The best ligand was when  $R_1 = \text{OMe}$  and  $R_2 = \text{Ph}$ , giving 99% yield and 95% *e.e.* for



the reaction shown.

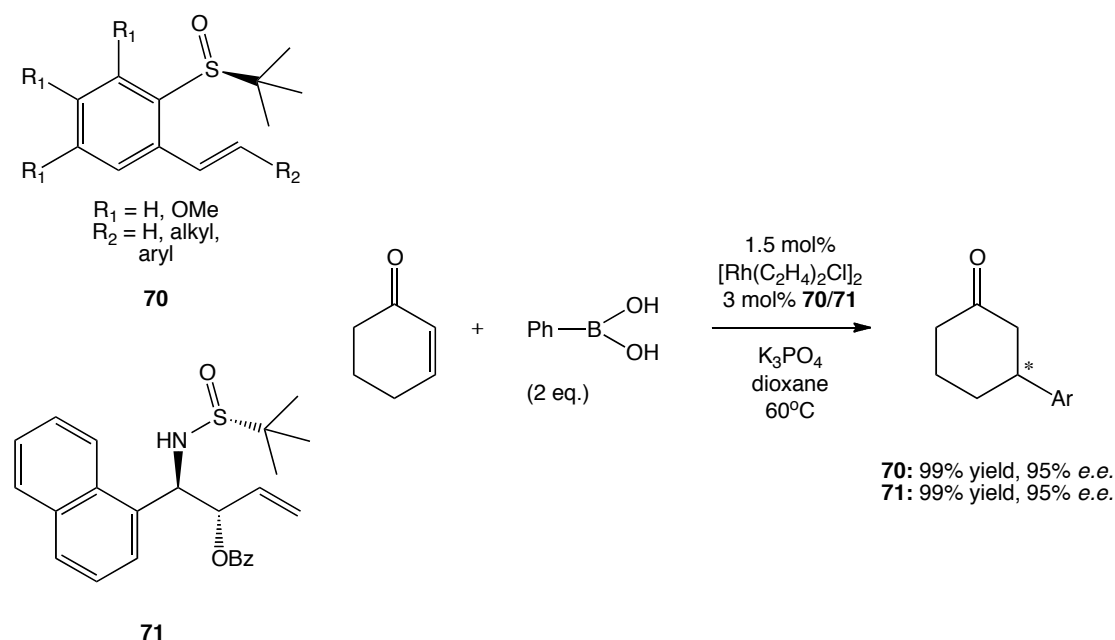


**Figure 53** Rhodium-catalysed 1,4 addition of phenylboronic acid to cyclohexenone with **70** and **71**

Xu also synthesised **71**, a sulfonamide-olefin ligand which enabled high yields and enantioselectivities to be reached in the 1,4-addition reaction shown in figure 53.<sup>128</sup> Interestingly, changing the chirality at the C-1 and C-2 positions of the ligand had no effect on the selectivity of the reaction, indicating that it is controlled solely by the *tert*-butyl-sulfonamide moiety.

A class of sulfonamide-olefin ligands similar to **71** was developed by Du and co-workers, **72**.<sup>129</sup> In this report, it was established that the olefin and the sulfoxide are bound to rhodium during catalysis. **72a** and **72b** were used in the reaction shown in figure 54, giving good yields and excellent selectivities. **72b** also proved to be a good ligand for the addition of aryl boronic acids to *tert*-butyl cinnamate. This is important as often rhodium-catalysed 1,4-addition reactions to acyclic substrates are difficult to achieve, even with systems that show excellent activity in the reactions with cyclic substrates.

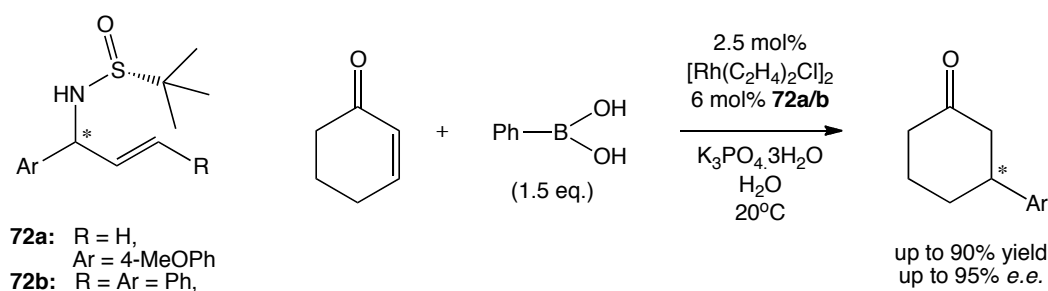


**Figure 54** Rhodium catalysed 1,4-addition of phenylboronic acid to cyclohexenone with **72**

## 1.7 Phosphine-Olefin Ligands

Alkene ligands have been thoroughly studied, and their complexation with transition metals is well understood. Complexes of these types of ligands are often used as precursors to other metal complexes. Compared to other ligands, *e.g.* phosphines, they are relatively labile. Examples of these complexes are shown in figure 55.

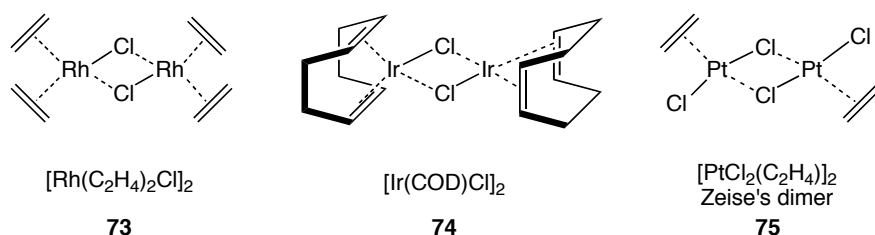


**Figure 55** Examples of well known transition metal olefin complexes

Chiral versions of these ligands have been developed and used in asymmetric transition metal catalysis.<sup>130</sup> Pioneering work in this area was carried out by Hayashi and Carreira. Hayashi developed ligands based on norbornadiene (nbd), **76**,<sup>126a,131</sup> and bicyclo[2,2,2]octadiene, **77**,<sup>132</sup> whereas Carreira developed Carvone derived ligands, **78**<sup>126b</sup> and **79**<sup>133</sup> (figure 56).

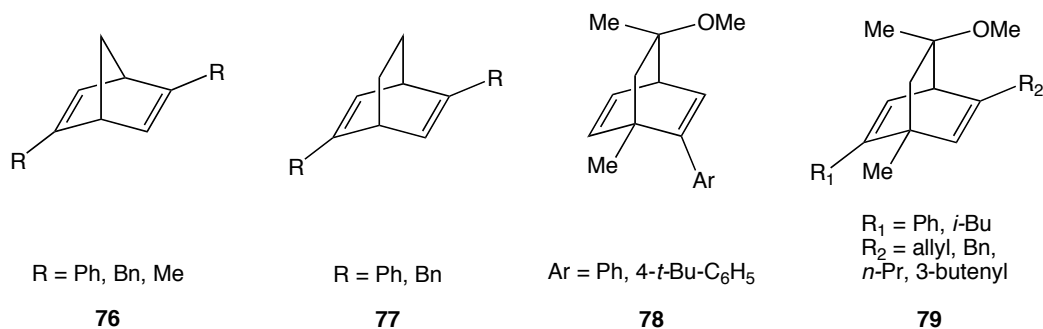


**Figure 56** Diene ligands developed by Hayashi and Carreira

These ligands were shown to induce high levels of selectivity in rhodium-catalysed 1,4-addition reactions, achieving up to 99% *e.e.* In some cases better results were obtained with diene ligands than with phosphine ligands. However, their greater lability in metal complexes, compared to phosphine ligands, is a drawback. In order to attempt to overcome these problems, ligands were developed incorporating both a phosphine and an olefin. The first example of this type of ligand was presented by Grützmacher.<sup>127a</sup> This ligand was used to make rhodium and iridium complexes, **80**,

which were then employed as catalysts for iridium-catalysed hydrogenation reactions and rhodium-catalysed conjugate addition reactions (figure 57).<sup>134</sup>

Soon after this, Hayashi described the preparation of another type of phosphine-olefin ligand, **81**.<sup>127b</sup> This was then used in rhodium-catalysed 1,4-addition of aryl boronic acids to maleimides, giving excellent results, better than with diene ligand, **76**. Widhalm and co-workers introduced **82**,<sup>135</sup> which was attractive compared to other diene and phosphine-olefin ligands because of its straightforward synthesis. Good results were also obtained in rhodium-catalysed 1,4-addition reactions with this ligand.

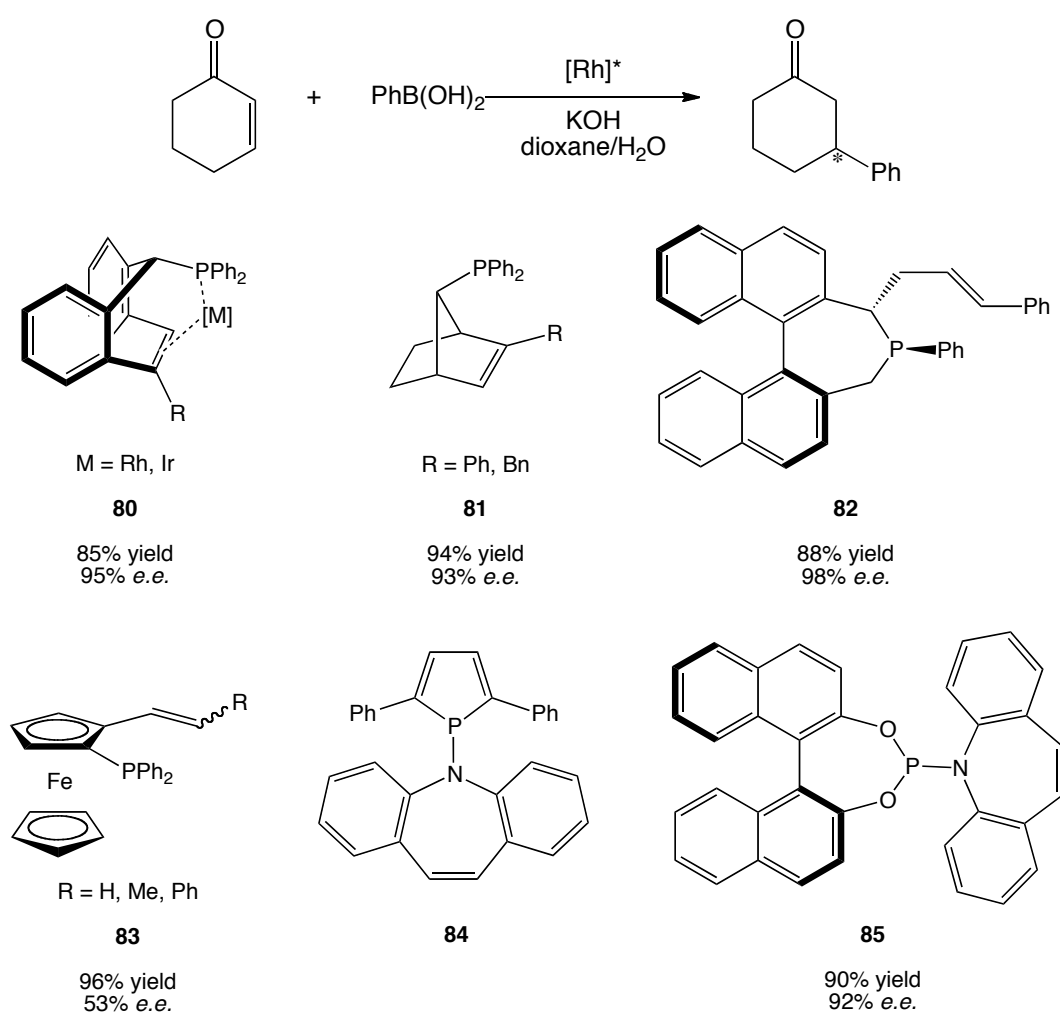


**Figure 57** Phosphine-olefin ligands and their activity in the rhodium catalysed 1,4-addition reaction of phenyl boronic acid to cyclohexenone

Phosphine-olefin ligands with a ferrocene backbone, similar to **83**, were synthesised and shown to bind to transition-metals, Pd and W, through phosphorus and the olefin by Stepnicka and co-workers.<sup>136</sup> Although no application of these ligands was presented by Stepnicka, Bolm and co-workers later employed ligands of this type in

rhodium-catalysed 1,4-addition reactions, with moderate success.<sup>137</sup> The aminophosphole-olefin ligand, **84**, was developed by Le Floch and co-workers.<sup>138</sup> This ligand was produced in a one-pot synthesis and then used to make rhodium complexes, which proved to be good catalysts for the hydroformylation of olefins, showing good reactivity and regioselectivity. Inspired by a combination of Grützmacher's P-olefin ligand, **80**, and Feringa's phosphoramidite ligands,<sup>139</sup> **85** was prepared by Carreira and co-workers. This ligand was tested in iridium-catalysed synthesis of allylic amines from allylic alcohols and displayed good yields and enantioselectivity.<sup>140</sup> This ligand was also tested in rhodium-catalysed 1,4-addition reactions with great success, along with a series of other phosphoramidite olefin ligands, by Dorta and co-workers.<sup>141</sup>

## 1.8. Summary

Sulfoxides and methods of making them have been known for many years now. Even enantiopure syntheses of sulfoxides are now quite well developed. Metal complexes with sulfoxides, especially DMSO, have also been well studied, and their binding methods are understood. Despite this, examples of enantioselective metal catalysis with sulfoxide ligands have been sporadic over the last forty years. Recent reports of chiral sulfoxide ligands employed in asymmetric catalysis have shown outstanding activity and enantioselectivity. Sulfoxide ligands have now proven their potential as excellent chiral ligands, but there is still a lot of scope for the development of new ligands, and their application in new catalytic reactions.

In this thesis, the syntheses of new sulfoxide ligands will be described and their activity in iridium-catalysed intramolecular hydroamination reactions will be presented. Novel palladium and platinum complexes with the known bisulfonide ligand, *p*-tolyl-binaso **58**, will be presented. Through X-ray crystallographic analysis of the resulting complexes, the nature of ligation will be discussed in detail, and some catalytic results will be shown.

Phosphine-olefin ligands have also emerged as promising ligands. They have already proven to form excellent precatalysts with rhodium for 1,4-addition reactions to enones. In the final chapter of this thesis, new complexes with phosphoramidite-

olefin ligands will be presented, along with their activity in rhodium-catalysed 1,4-addition of arylboronic acids to cyclic and acyclic enones.

---

## 1.9. References

- <sup>1</sup> Solladié, G. *Synthesis* **1981**, 185
- <sup>2</sup> Eriks, K.; Shoemaker, C.B.; Thomas, R. *Acta Crystallogr.* **1966**, 21, 12
- <sup>3</sup> Gilman, H.; Robinson, J.; Beaber, N.J. *J. Am. Chem. Soc.* **1926**, 48, 2715
- <sup>4</sup> (a) Andersen, K.K. *Tetrahedron Lett.* **1962**, 3, 93; (b) Andersen, K.K.; Gaffield, W.; Papaninikolaou, N.E.; Foley, J.W.; Perkins, R.I. *J. Am. Chem. Soc.* **1964**, 86, 5637
- <sup>5</sup> Harrison, P.W.B.; Kenyon, J.; Phillips, H. *J. Chem. Soc.* **1926**, 2079
- <sup>6</sup> Maccioni, R.; Montanari, M.; Secci, M.; Tramontini, M. *Tetrahedron Lett.* **1961**, 2, 607
- <sup>7</sup> (a) Pitchen, P.; Dunach, E.; Deshmukh, M.N.; Kagan, H.B. *J. Am. Chem. Soc.* **1984**, 106, 8188; (b) Zhao, S.H.; Samuel, O.; Kagan, H.B. *Tetrahedron* **1987**, 43, 5135; (c) Di Furia, F.; Modena, G.; Seraglia, R. *Synthesis* **1984**, 325; (d) Fernandez, I.; Khiar, N. *Chem. Rev.* **2003**, 103, 3651; (e) Legros, J.; Dehli, J.R.; Bolm, C. *Adv. Synth. Catal.* **2005**, 347, 19
- <sup>8</sup> Solladié, G.; Hutt, J.; Girardin, A. *Synthesis* **1987**, 173
- <sup>9</sup> Rebiere, F.; Samuel, O.; Ricard, L.; Kagan, H.B.; *J. Org. Chem.* **1991**, 56, 5991
- <sup>10</sup> Fernandez, I.; Khiar, N.; Llera, J.M.; Alcudia, F. *J. Org. Chem.* **1992**, 57, 6789
- <sup>11</sup> Rayner, D.R.; Gordon, A.J.; Mislow, K. *J. Am. Chem. Soc.* **1968**, 90, 4854
- <sup>12</sup> (a) Miller, E.G.; Rayner, D.R.; Thomas, H.T.; Mislow, K. *J. Am. Chem. Soc.* **1968**, 90, 4861; (b) Bickart, B.; Carson, F.W.; Jacobus, J.; Miller, E.G.; Mislow, K. *J. Am. Chem. Soc.* **1968**, 90, 4869
- <sup>13</sup> Kingsbury, C.A.; Cram, D.J. *J. Am. Chem. Soc.* **1960**, 82, 1810
- <sup>14</sup> (a) Calligaris, M. *Coord. Chem. Rev.* **1996**, 153, 83; (b) Calligaris, M. *Coord. Chem. Rev.* **2004**, 248, 351
- <sup>15</sup> Davies, A.R.; Einstein, F.W.B.; Farrell, N.P.; James, B.R.; McMillan, R.S. *Inorg. Chem.* **1978**, 17, 1965
- <sup>16</sup> (a) Lindqvist, I.; Einarsson, P. *Acta. Chem. Scand.* **1959**, 13, 420; (b) Cotton, F.A.; Francis, R. *J. Am. Chem. Soc.* **1960**, 82, 2986
- <sup>17</sup> Davies, J.A. *Adv. Inorg. Chem. Radiochem.* **1981**, 24, 11
- <sup>18</sup> Alessio, E. *Chem. Rev.* **2004**, 104, 4203
- <sup>19</sup> McPartlin, M.; Mason, R. *J. Chem. Soc. (A)* **1970**, 2206
- <sup>20</sup> (a) Haddad, Y.M.Y.; Henbest, H.B.; Trocha-Grimshaw, J. *J. Chem. Soc., Perkin Trans. I* **1974**, 592; (b) Haddad, Y.M.Y.; Henbest, H.B.; Husbands, J.; Mitchell, T.R.B.; Trocha-Grimshaw, J. *J. Chem. Soc., Perkin Trans. I* **1974**, 596
- <sup>21</sup> James, B.R.; Ochiai, E.; Rempel, G.I. *Inorg. Nuclear Chem. Lett.* **1971**, 7, 781
- <sup>22</sup> Evans, I.P.; Spencer, A.; Wilkinson, G. *J. Chem. Soc. Dalton Trans.* **1973**, 204
- <sup>23</sup> Mercer, A.; Trotter, J. *J. Chem. Soc. Dalton Trans.* **1975**, 2480
- <sup>24</sup> Alessio, E.; Mestroni, G.; Nardin, G.; Attia, W.M.; Calligaris, M.; Sava, G.; Zorzet, S. *Inorg. Chem.* **1988**, 27, 4099
- <sup>25</sup> Jaswal, J.S.; Rettig, S.J.; James, B.R. *Can. J. Chem.* **1990**, 68, 1808
- <sup>26</sup> McMillan, R.S.; Mercer, A.; James, B.R.; Trotter, J. *J. Chem. Soc. Dalton Trans.* **1975**, 1006
- <sup>27</sup> Davies, A.R.; Einstein, F.W.B.; Farrell, N.P.; James, B.R. *Inorg. Chem.* **1978**, 17, 1965
- <sup>28</sup> Alessio, E.; Balducci, G.; Calligaris, M.; Costa, G.; Attia, W.M. *Inorg. Chem.* **1991**, 30, 609

- 
- <sup>29</sup> Tanase, T.; Aiko, T.; Yamamoto, Y. *Chem. Commun.* **1996**, 2341
- <sup>30</sup> Geremia, S.; Mestroni, S.; Alessio, E. *J. Chem. Soc., Dalton Trans.* **1998**, 2447
- <sup>31</sup> Dorta, R.; Rozenberg, H.; Shimon, L.J.W.; Milstein, D. *J. Am. Chem. Soc.* **2002**, *124*, 188
- <sup>32</sup> Dorta, R.; Rozenberg, H.; Milstein, D. *Chem. Commun.* **2002**, 710
- <sup>33</sup> Dorta, R.; Rozenberg, H.; Shimon, L.J.W.; Milstein, D. *Chem. Eur. J.* **2003**, *9*, 5237
- <sup>34</sup> Abbasi, A.; Skripkin, M.Y.; Eriksson, L.; Torapava, N. *Dalton Trans.* **2011**, *40*, 1111
- <sup>35</sup> (a) Kitching, W.; Moore, C.J.; Doddrell, D. *Inorg. Chem.* **1970**, *9*, 541; (b) Price, J.H.; Williamson, A.N.; Schramm, R.F.; Wayland, B.B. *Inorg. Chem.* **1972**, *11*, 1280
- <sup>36</sup> Melanson, R.; Rochon, F. *Can. J. Chem.* **1975**, *53*, 2371
- <sup>37</sup> Bennett, M.J.; Cotton, F.A.; Weaver, D.L.; Williams, R.J.; Watson, W.H. *Acta. Cryst.* **1967**, *23*, 788
- <sup>38</sup> Johnson, B.F.G.; Puga, J.; Raithby, P.R. *Acta Crystallogr., Sect. B: Struct. Sci.* **1981**, *37*, 953
- <sup>39</sup> Elding, L.I.; Oskarsson, A. *Inorg. Chem. Acta* **1987**, *130*, 209
- <sup>40</sup> Hinsberg, O. *J. Prakt. Chem.* **1912**, *85*, 344
- <sup>41</sup> Bell, E.V.; Bennett, G.M. *J. Chem. Soc.* **1927**, 1798
- <sup>42</sup> Greene Jr., J.L.; Shevlin, P.B. *J. Chem. Soc. D, Chem. Commun.* **1971**, 1092
- <sup>43</sup> Svinning, T.; Mo, F.; Bruun, T. *Acta Cryst., Sect. B: Struct. Sci.* **1976**, *32*, 759
- <sup>44</sup> Kuneida, N.; Nokami, J.; Kinoshita, M. *Chem. Lett.* **1973**, 871
- <sup>45</sup> Kuneida, N.; Nokami, J.; Kinoshita, M. *Bull. Chem. Soc. Jpn.* **1976**, *49*, 256
- <sup>46</sup> Maryanof, C.; Maryanof, B.; Tang, R.; Mislow, K. *J. Am. Chem. Soc.* **1973**, *95*, 5839
- <sup>47</sup> Madan, S.K.; Hull, C.M.; Herman, L.J. *Inorg. Chem.* **1968**, *7*, 491
- <sup>48</sup> Cattalini, L.; Michelon, G.; Marangoni, G.; Pelizzi, G. *J. Chem. Soc., Dalton Trans.* **1979**, 96
- <sup>49</sup> Evans, D.R.; Huang, M.; Seganish, W.M.; Fettingner, J.C.; Williams, T.L. *Inorg. Chem. Commun.* **2003**, *6*, 462
- <sup>50</sup> Schaub, T.; Diskin-Poser, Y.; Radius, U.; Milstein, D. *Inorg. Chem.* **2008**, *47*, 6502
- <sup>51</sup> Mallorquin, R.M.; Chelli, S.; Brebion, F.; Fensterbank, L.; Goddard, J-P.; Malacria, M. *Tetrahedron: Asymmetry* **2010**, *21*, 1695
- <sup>52</sup> Khiar, N.; Fernandez, I.; Alcudia, F. *Tetrahedron Lett.* **1993**, *34*, 123
- <sup>53</sup> Aggarwal, V.K.; Drabowicz, J.; Grainger, R.S.; Gültekin, Z.; Lightowler, M.; Spargo, P.L. *J. Org. Chem.* **1995**, *60*, 4962
- <sup>54</sup> Pettinari, C.; Pelli, M.; Cavicchio, G.; Crucianelli, M.; Panzeri, W.; Colapietro, M.; Cassetta, A. *Organometallics* **1999**, *18*, 555
- <sup>55</sup> Madec, D.; Mingoia, F.; Macovei, C.; Maitro, G.; Giambastiani, G.; Poli, G. *Eur. J. Org. Chem.* **2005**, 552
- <sup>56</sup> Evans, D.R.; Huang, M.; Seganish, W.M.; Fettingner, J.C.; Williams, T.L. *Organometallics*, **2002**, *21*, 893
- <sup>57</sup> Grove, D.M.; van Koten, G.; Ubbels, H.J.C. *J. Am. Chem. Soc.* **1982**, *104*, 4285
- <sup>58</sup> Tokunoh, R.; Sodeoka, M.; Aoe, K.; Shibasaki, M. *Tetrahedron Lett.* **1995**, *36*, 8035
- <sup>59</sup> Alcock, N.W.; Brown, J.M.; Evans, P.L. *J. Organomet. Chem.* **1988**, 356, 233
- <sup>60</sup> Chooi, S.Y.M.; Leung, P.H.; Mok, K.F. *Inorg. Chim. Acta.* **1993**, *205*, 245

- <sup>61</sup> (a) Chooi, S.Y.M.; Siah, S.Y.; Leung, P.H.; Mok, K.F. *Inorg. Chem.* **1993**, *32*, 4812; (b) Chooi, S.Y.M.; Ranford, J.D.; Leung, P.H.; Mok, K.F. *Tetrahedron: Asymmetry* **1994**, *5*, 1805
- <sup>62</sup> Souers, A.J.; Owens, T.D.; Oliver, A.G.; Hollander, F.J.; Ellman, J.A. *Inorg. Chem.* **2001**, *40*, 5299
- <sup>63</sup> (a) Haddad, Y.M.Y.; Henbest, H.B.; Husbands, J.; Mitchell, T.R.B. *Proc. Chem. Soc.* **1964**, 361; (b) Trocha-Grimshaw, J.; Henbest, H.B. *Chem. Commun.* **1967**, 544
- <sup>64</sup> Gullotti, M.; Ugo, R. *J. Chem. Soc. (C)* **1971**, 2652
- <sup>65</sup> (a) Haddad, Y.M.Y.; Henbest, H.B.; Trocha-Grimshaw, J. *J. Chem. Soc., Perkins Trans.* **1974**, 592; (b) Haddad, Y.M.Y.; Henbest, H.B.; Husbands, J.; Mitchell, T.R.B.; Trocha-Grimshaw, J. *J. Chem. Soc., Perkins Trans.* **1974**, 596
- <sup>66</sup> McPartlin, M.; Mason, R. *J. Chem. Soc. (A)* **1970**, 2206
- <sup>67</sup> James, B.R.; Morris, R.H. *J. Chem. Soc., Chem. Commun.* **1978**, 929
- <sup>68</sup> Riley, D.P. *Inorg. Chem.* **1983**, *22*, 1965
- <sup>69</sup> Srivastava, R.S.; Milani, B.; Alessio, E.; Mestoni, G. *Inorg. Chim. Acta* **1992**, *191*, 15
- <sup>70</sup> Santana, S.A.A.; Carvalho Jr., V.P.; Lima-Neto, B.S. *J. Braz. Chem. Soc.* **2010**, *21*, 279
- <sup>71</sup> Grennberg, H.; Gogoll, A.; Bäckvall, J.E. *J. Org. Chem.* **1991**, *56*, 5808
- <sup>72</sup> van Benthem, R.A.T.M.; Hiemstra, H.; Speckamp, W.N. *J. Org. Chem.* **1992**, *57*, 6083
- <sup>73</sup> van Benthem, R.A.T.M.; Hiemstra, H.; Michels, J.J.; Speckamp, W.N. *J. Chem. Soc., Chem. Commun.* **1994**, 357
- <sup>74</sup> (a) Rönn, M.; Bäckvall, J.E.; Andersson, P.G. *Tetrahedron Lett.* **1995**, *36*, 7749; (b) Rönn, M.; Andersson, P.G.; Bäckvall, J.E. *Acta Chem. Scan.* **1997**, *51*, 773; (c) Larock, R.C.; Hightower, T.R. *J. Org. Chem.* **1993**, *58*, 5298; (d) Larock, R.C.; Hightower, T.R.; Hasvold, L.A.; Peterson, K.P. *J. Org. Chem.* **1996**, *61*, 3584
- <sup>75</sup> Larock, R.C.; Hightower, T.R.; Kraus, G.A.; Hahn, P.; Zheng, D. *Tetrahedron Lett.* **1995**, *36*, 2423
- <sup>76</sup> van Benthem, R.A.T.M.; Hiemstra, H.; van Leeuwen, P.W.N.M.; Geus, J.W.; Speckamp, W.N. *Angew. Chem. Int. Ed.* **1995**, *34*, 457
- <sup>77</sup> B.A. Steinhoff, S.R. Fix, S.S. Stahl, *J. Am. Chem. Soc.*, 2002, **124**, 766
- <sup>78</sup> B. A. Steinhoff, S.S. Stahl, *J. Am. Chem. Soc.*, 2006, **128**, 4348
- <sup>79</sup> R.I. McDonald, S.S. Stahl, *Angew. Chem. Int. Ed.*, 2010, **49**, 5529
- <sup>80</sup> Y. Izawa, D. Pun, S.S. Stahl, *Science*, 2011, **333**, 209
- <sup>81</sup> T. Diao, S.S. Stahl, *J. Am. Chem. Soc.*, 2011, **133**, 14566
- <sup>82</sup> G. Brasche, J. Garcia-Fortanet, S.L. Buchwald, *Org. Lett.*, 2008, **10**, 2207
- <sup>83</sup> Chen, M.S.; White, M.C. *J. Am. Chem. Soc.* **2004**, *126*, 1346
- <sup>84</sup> (a) Fraunhoffer, K.J.; Bachovchin, D.A.; White, M.C. *Org. Lett.* **2005**, *7*, 223; (b) Covell, D.J.; Vermeulen, N.A.; Labenz, N.A.; White, M.C. *Angew. Chem. Int. Ed.* **2006**, *45*, 8217
- <sup>85</sup> Chen, M.S.; Prabakaran, N.; Labenz, N.A.; White, M.C. *J. Am. Chem. Soc.* **2005**, *127*, 6970
- <sup>86</sup> Fraunhoffer, K.J.; Prabakaran, N.; Sirois, L.E.; White, M.C. *J. Am. Chem. Soc.* **2006**, *128*, 9032
- <sup>87</sup> Stang, E.M.; White, M.C. *Nature Chemistry* **2009**, *1*, 547
- <sup>88</sup> Stang, E.M.; White, M.C. *Angew. Chem. Int. Ed.* **2011**, *50*, 2094



- <sup>89</sup> (a) Fraunhoffer, K.J.; White, M.C. *J. Am. Chem. Soc.* **2007**, *129*, 7274; (b) Reed, S.A.; Mazzoti, A.R.; White, M.C. *J. Am. Chem. Soc.* **2009**, *131*, 11701; (c) Qi, X.; Rice, G.T.; Lall, M.S.; Plummer, M.S.; White, M.C. *Tetrahedron* **2010**, *66*, 4816
- <sup>90</sup> (a) Delcamp, J.H.; White, M.C. *J. Am. Chem. Soc.* **2006**, *128*, 15076; (b) Delcamp, J.H.; Brucks, A.P.; White, M.C. *J. Am. Chem. Soc.* **2008**, *130*, 11270
- <sup>91</sup> Young, A.J.; White, M.C. *J. Am. Chem. Soc.* **2008**, *130*, 14090
- <sup>92</sup> Vermeulen, N.A.; Delcamp, J.H.; White, C.M. *J. Am. Chem. Soc.* **2010**, *132*, 11323
- <sup>93</sup> Young, A.J.; White, M.C. *Angew. Chem. Int. Ed.* **2011**, *50*, 6824
- <sup>94</sup> Covell, D.J.; White, M.C. *Angew. Chem. Int. Ed.* **2008**, *47*, 6448
- <sup>95</sup> James, B.R.; McMillan, R.S.; Reimer, K.J. *J. Mol. Cat.* **1975**, *6*, 1, 439
- <sup>96</sup> James, B.R.; McMillan, R.S. *Can. J. Chem.* **1977**, *55*, 3927
- <sup>97</sup> Kvintovics, P.; James, B.R.; Heil, B. *J. Chem. Soc., Chem. Commun.* **1986**, 1810
- <sup>98</sup> Petra, D.G.I.; Kamer, P.C.J.; Spek, A.L.; Schoemaker, H.E.; van Leeuwen, P.W.N.M. *J. Org. Chem.* **2000**, *65*, 3010
- <sup>99</sup> Carmen Carreno, M.; Garcia Ruano, J.L.; Carmen Maestro, M.; Martin Cabrejas, L.M. *Tetrahedron: Asymmetry* **1993**, *4*, 727
- <sup>100</sup> Priego, J.; Mancheno, O.G.; Cabrera, S.; Carretero, J.C. *J. Org. Chem.* **2002**, *67*, 1346
- <sup>101</sup> Johnson, J.S.; Evans, D.A. *Acc. Chem. Res.* **2000**, *35*, 325
- <sup>102</sup> Owens, T.D.; Hollander, F.J.; Oliver, A.G.; Ellman, J.A. *J. Am. Chem. Soc.* **2001**, *123*, 1539
- <sup>103</sup> Owens, T.D.; Souers, A.J.; Ellman, J.A. *J. Org. Chem.* **2003**, *68*, 3
- <sup>104</sup> Allen, J.V.; Bower, J.F.; Williams, J.M.J. *Tetrahedron: Asymmetry* **1994**, *5*, 1895
- <sup>105</sup> Williams, J.M.J. *Synlett* **1996**, 705
- <sup>106</sup> Hiroi, K.; Suzuki, Y. *Heterocycles* **1997**, *46*, 77
- <sup>107</sup> Hiroi, K.; Suzuki, Y.; Ikuko, A.; Hasegawa, Y.; Suzuki, K. *Tetrahedron: Asymmetry* **1998**, *9*, 3797
- <sup>108</sup> Hiroi, K.; Suzuki, Y.; Kawagishi, R. *Tetrahedron Lett.* **1999**, *40*, 715
- <sup>109</sup> Hiroi, K.; Suzuki, Y.; Abe, I.; Kawagishi, R. *Tetrahedron* **2000**, *56*, 4701
- <sup>110</sup> Hiroi, K.; Suzuki, Y. *Tetrahedron Lett.* **1998**, *39*, 6499
- <sup>111</sup> Hiroi, K.; Izawa, I.; Takizawa, T.; Kawai, K. *Tetrahedron* **2004**, *60*, 2155
- <sup>112</sup> Mariz, R.; Luan, X.; Gatti, M.; Linden, A.; Dorta, R. *J. Am. Chem. Soc.* **2008**, *130*, 2172
- <sup>113</sup> Miashita, A.; Yasuda, A.; Takaya, H.; Toriumi, K.; Ito, T.; Souchi, T.; Noyori, R. *J. Am. Chem. Soc.* **1980**, *102*, 7933
- <sup>114</sup> Bürgi, J.J.; Mariz, R.; Gatti, M.; Drinkel, E.; Luan, X.; Blumentritt, S.; Linden, A.; Dorta, R. *Angew. Chem. Int. Ed.* **2009**, *48*, 2768
- <sup>115</sup> Mariz, R.; Poater, A.; Gatti, M.; Drinkel, E.; Bürgi, J.J.; Luan, X.; Blumentritt, S.; Linden, A.; Cavallo, L.; Dorta, R. *Chem. Eur. J.* **2010**, *16*, 14335
- <sup>116</sup> Poater, A.; Ragone, F.; Mariz, R.; Dorta, R.; Cavallo, L. *Chem. Eur. J.* **2010**, *16*, 14348
- <sup>117</sup> Chen, J.; Chen, J.; Lang, F.; Zhang, X.; Cun, L.; Zhu, J.; Deng, J.; Liao, J. *J. Am. Chem. Soc.* **2010**, *132*, 4552
- <sup>118</sup> Han, F.; Chen, J.; Zhang, X.; Liu, J.; Cun, L.; Zhu, J.; Deng, J.; Liao, J. *Tetrahedron Lett.* **2011**, *52*, 830
- <sup>119</sup> Han, F.; Chen, G.; Zhang, X.; Liao, J. *Eur. J. Org. Chem.*, **2011**, 2928
- <sup>120</sup> Chen, J.; Li, D.; Ma, H.; Cun, L.; Zhu, J.; Deng, J.; Liao, J. *Tetrahedron Lett.* **2008**, *49*, 6921

- 
- <sup>121</sup> Chen, J.; Lang, F.; Li, D.; Cun, L.; Zhu, J.; Deng, J.; Liao, J. *Tetrahedron: Asymmetry* **2009**, *20*, 1953
- <sup>122</sup> Lang, F.; Li, D.; Chen, J.; Chen, J.; Li, L.; Cun, L.; Zhu, J.; Deng, J.; Liao, J. *Adv. Synth. Catal.* **2010**, *352*, 843
- <sup>123</sup> Lang, F.; Chen, G.; Li, L.; Xing, J.; Han, F.; Cun, L.; Liao, J. *Chem. Eur. J.* **2011**, *17*, 5242
- <sup>124</sup> Thaler, T.; Guo, L.; Steib, A.K.; Raducan, M.; Karaghiosoff, K.; Mayer, P.; Knochel, P. *Org. Lett.* **2011**, *13*, 3182
- <sup>125</sup> Jin, S.S.; Wang, H.; Xu, M.H. *Chem. Commun.* **2011**, *47*, 7230
- <sup>126</sup> (a) Hayashi, T.; Ueyama, K.; Tokunaga, N.; Yoshida, K. *J. Am. Chem. Soc.* **2003**, *125*, 11508; (b) Fischer, C.; Defieber, C.; Suzuki, T.; Carreira, E.M. *J. Am. Chem. Soc.* **2004**, *126*, 1628
- <sup>127</sup> (a) Maire, P.; Deblon, S.; Breher, F.; Geier, J.; Böhrer, C.; Rüegger, H.; Schönberg, H.; Grützmacher, H. *Chem. Eur. J.* **2004**, *10*, 4198; (b) Shintani, R.; Duan, W.L.; Nagano, T.; Okada, A.; Hayashi, T. *Angew. Chem. Int. Ed.* **2005**, *44*, 4611; (c) Defieber, C.; Ariger, M.A.; Moriel, P.; Carreira, E.M. *Angew. Chem. Int. Ed.* **2007**, *46*, 3139
- <sup>128</sup> Qi, W.-Y.; Zhu, T.-S.; Xu, M.-H. *Org. Lett.* **2011**, *13*, 3410
- <sup>129</sup> Feng, X.; Wang, Y.; Wei, B.; Yang, J.; Du, H. *Org. Lett.* **2011**, *13*, 3300
- <sup>130</sup> Defieber, C.; Grützmacher, H.; Carreira, E.M. *Angew. Chem. Int. Ed.* **2008**, *47*, 4482
- <sup>131</sup> Berthon-Gelloz, G.; Hayashi, T. *J. Org. Chem.* **2006**, *71*, 8957
- <sup>132</sup> (a) Tokunaga, N.; Otomaru, Y.; Okamoto, K.; Ueyama, K.; Shintani, R.; Hayashi, T. *J. Am. Chem. Soc.* **2004**, *126*, 13584; (b) Otomaru, Y.; Okamoto, K.; Shintani, R.; Hayashi, T. *J. Org. Chem.* **2005**, *70*, 2503
- <sup>133</sup> Defieber, C.; Paquin, J.F.; Serna, S.; Carreira, E.M. *Org. Lett.* **2004**, *6*, 3873
- <sup>134</sup> Piras, E.; Läng, F.; Rüegger, H.; Stein, D.; Wörle, M.; Grützmacher, H. *Chem. Eur. J.* **2006**, *12*, 5849
- <sup>135</sup> Kasak, P.; Arion, V.B.; Widhalm, M. *Tetrahedron: Asymmetry* **2006**, *17*, 3084
- <sup>136</sup> Stepnicka, P.; Cisarova, I. *Inorg. Chem.* **2006**, *45*, 8785
- <sup>137</sup> Stemmler, R.T.; Bolm, C. *Synlett* **2007**, *9*, 1365
- <sup>138</sup> Mora, G.; van Zutphen, S.; Thoumazet, C.; Le Goff, X.F.; Ricard, L.; Grützmacher, H.; Le Floch, P. *Organometallics* **2006**, *25*, 5528
- <sup>139</sup> Feringa, B.L. *Acc. Chem. Res.* **2000**, *33*, 346
- <sup>140</sup> Defieber, C.; Ariger, M.A.; Moriel, P.; Carreira, E.M. *Angew. Chem. Int. Ed.* **2007**, *46*, 3139
- <sup>141</sup> Mariz, R.; Briceño, A.; Dorta, R.; Dorta, R. *Organometallics* **2008**, *27*, 6605

## Chapter 2

### The Synthesis of Novel Sulfoxide Ligands

#### 2.1. Introduction to Synthesis of Sulfoxides

Sulfoxide ligands have been sporadically used in catalysis since the middle of the last century. Simple sulfoxides, such as DMSO (dimethyl sulfoxide) have been well studied with respect to their complexation with metals,<sup>1</sup> and have also been used as ligands in catalysis.<sup>2</sup> Bissulfoxide ligands with backbones consisting of a one or two carbon chain, shown in figure 1, are well known. These types of ligands have been studied as complexes with metals,<sup>3</sup> and as ligands in catalysis.<sup>4</sup>

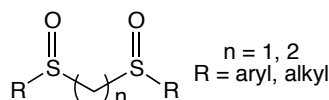


**Figure 1** Bissulfoxide ligands with 1 or 2 carbon backbone

Sulfoxides are an interesting chemical species with regards to their complexation with metals. They can bind either through S or O, depending on the steric and electronic environment. When they are dissymmetrically substituted, they are chiral due to an electron lone pair, which gives them a tetrahedral configuration. These properties make sulfoxides good candidates for the design of novel chiral ligands for asymmetric catalysis. In addition, they are optically stable up to temperatures of 200°C in most cases.

Methods to make chiral sulfoxides have been well developed;<sup>5</sup> these include selective oxidation of sulfides and reacting enantiopure sulfinates with organometallic species. Techniques to make sulfoxides by enantioselective oxidation are regarded as the most straightforward routes, but these reactions often do not have a very broad scope. Nevertheless, considerable advances have been made in this area.<sup>6</sup>

The nucleophilic attack of an organometallic species on a sulfinates is probably the most commonly used way of making chiral sulfoxides. It was Andersen who first

discovered this synthesis in the 1960s,<sup>7</sup> by adapting observations earlier made by Gilman (figure 2).<sup>8</sup>

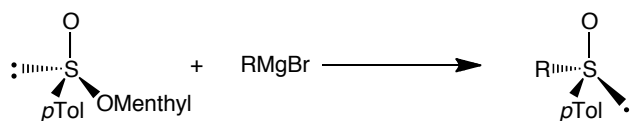


**Figure 2** Anderson method for the synthesis of enantiopure sulfoxides

The attack of the Grignard reagent occurs with inversion of configuration at the sulfur.<sup>9</sup> This method was made more favourable after Solladié improved the synthesis, making it suitable for large-scale applications.<sup>10</sup> The limitation of this method of making enantiopure sulfoxides is the availability of the enantiopure sulfinate. Aryl menthyl sulfinates can be crystallised to obtain only the less soluble diastereoisomer. The yield of the crystallisation can be improved by acidifying the solution with a few drops of concentrated HCl, this racemises the sulfinate in solution.<sup>11</sup> Acquiring alkyl menthyl sulfinates enantiomerically pure is less simple, as they tend to be oils and not crystalline. However since the 1960's, methods of making enantiopure sulfinates have been enhanced greatly, with many different alkyl and aryl groups, made with menthol<sup>12</sup> and with other alcohols.<sup>13</sup>

Another route to enantiopure sulfinates was developed by Fernandez *et al.* and named the 'DAG-methodology' by the authors.<sup>14</sup> DAG (diacetone-D-glucose), a cheap and readily available chiral alcohol, was reacted with various aryl and alkyl sulfinyl chlorides in the presence of a base to give sulfinates in a highly selective fashion. It was observed that the nature of the base was very important in determining the diastereomer of the sulfinate obtained. When Hunig's base ( $i\text{-PrNEt}_2$ ) in toluene was used, the ( $S_S$ ) configuration was predominantly obtained at sulfur. On the other hand, when pyridine was used as the base and THF as the solvent, the preferred configuration at sulfur was ( $R_S$ ). The diastereomers could, in most cases, then be separated by column chromatography or crystallisation. However, despite the wealth of knowledge on the synthesis of sulfoxides and their coordination properties with metals, very little has been attempted towards the synthesis of chelating bissulfoxide ligands, which can then be used in metal catalysis. Herein will be described the synthesis and development of bissulfoxide ligands that has taken place in our group.

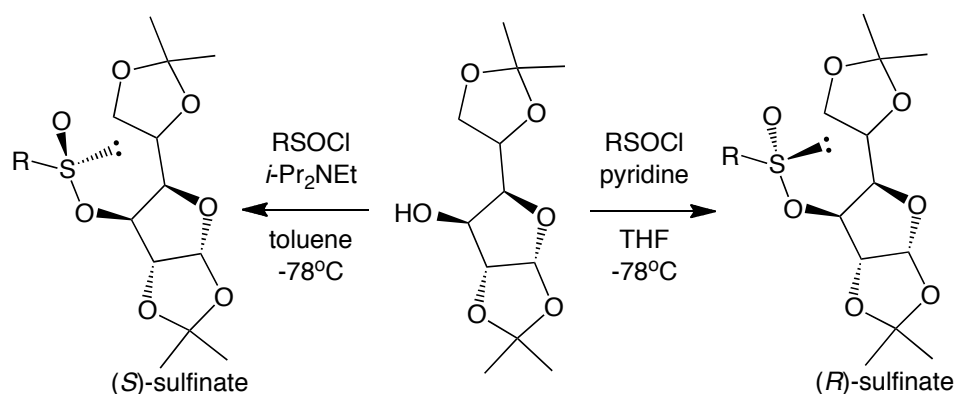


**Figure 3** Enantioselective syntheses of sulfonates *via* the DAG-methodology

In our laboratory, synthesis of bissulfoxide ligands began with *p*-tolyl-binaso (1,1'-binaphthalene-2,2'-diyl-bis(*p*-tolylsulfoxide)),<sup>15</sup> based on the well known ligand, binap (1,1'-binaphthalene-2,2'-diyl-diphenylphosphine) developed by Noyori *et al.*<sup>16</sup> This was synthesised from commercially available 2,2'-dibromo-1,1'-binaphthalene, by lithium-halogen exchange of both bromines by *n*-BuLi, and subsequent quenching with menthyl-*p*-tolyl sulfinate. This gave two diastereomers when enantiopure sulfinate was used, which could be separated by column chromatography.

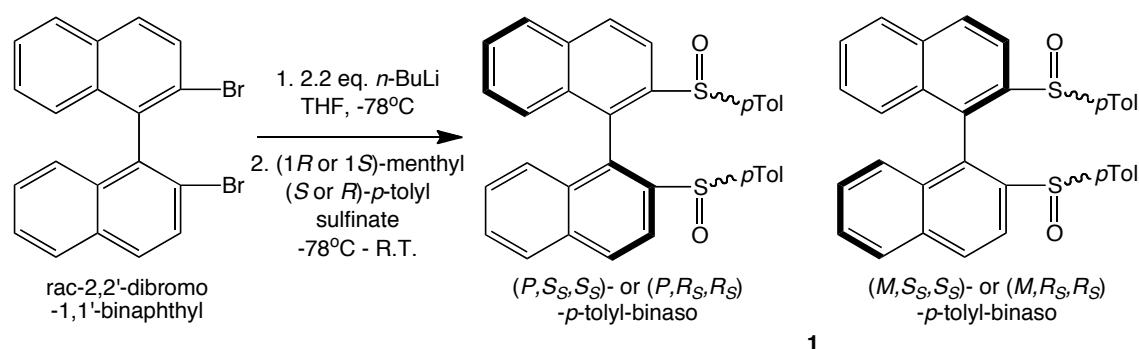


**Figure 4** Synthesis of *p*-tolyl-binaso

It was found that this ligand could coordinate to Rh when treated with  $[\text{Rh}(\text{C}_2\text{H}_4)_2\text{Cl}]_2$  and this complex was an excellent precatalyst for the asymmetric 1,4-addition of aryl boronic acids to electron deficient enones (figure 5).<sup>15</sup>

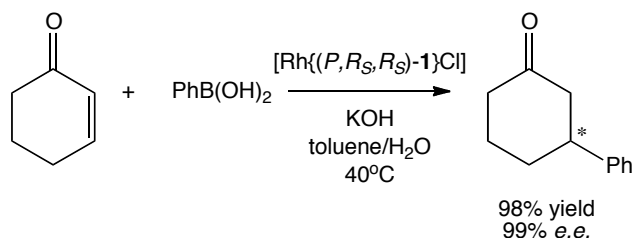


**Figure 5** Rhodium-catalysed 1,4-addition of phenylboronic acid to cyclohexenone

This work was extended by developing a family of ligands based on the same structure as *p*-tolyl-binaso. The binaphthyl backbone as well as the substituent on sulfur can be modified to give new ligands with different electronic and steric properties.<sup>17</sup> These ligands are shown in figure 6.

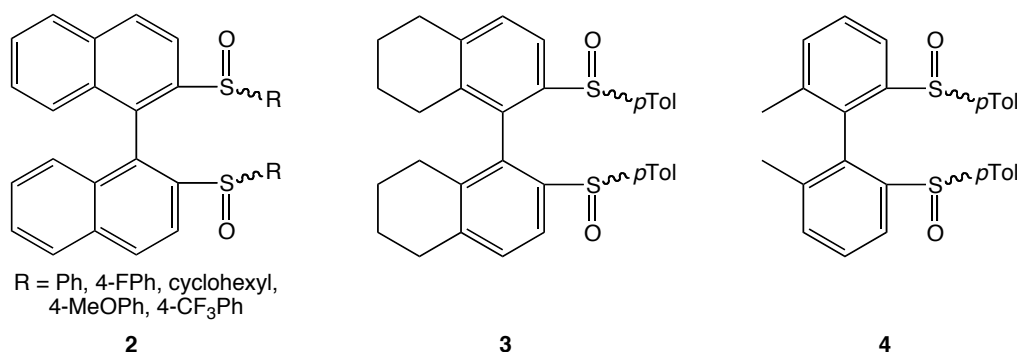


**Figure 6** Bissulfonate ligands developed previously in our lab

These ligands were used to make rhodium precatalysts for the same 1,4-addition reaction (figure 5). It was observed that the electronic nature of the ligand was important in determining the binding strength of the ligand to rhodium, as well as the success in catalysis.

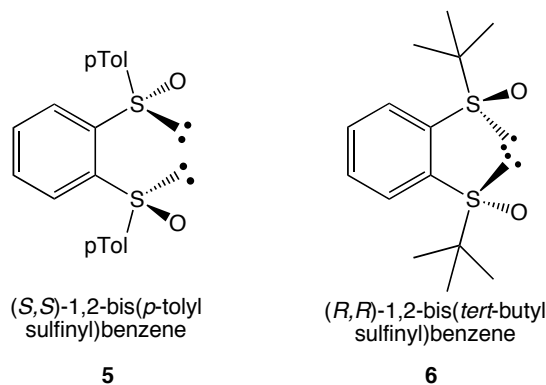


**Figure 7**  $C_2$ -symmetric bisulfonate ligands with a phenyl backbone

Recently, bisulfonate ligands based on a phenyl backbone have also demonstrated excellent activity in rhodium-catalysed 1,4-addition reactions. This implies that a chiral backbone is not necessary in order to achieve high enantioselectivity in catalysis. Ligands of this type have previously been reported with  $C_2$ -symmetry as shown in figure 7.<sup>18</sup> The new family of ligands presented in this chapter are  $C_1$ -symmetric hetero-bissulfonates.

The synthesis of **5** involves first generating a sulfide with a bromine in the ortho position from 2-bromoaniline. The bromo species is then lithiated and quenched with

(-)-menthyl-(*S*)-*p*-tolyl sulfinate. In the last step, *m*-CPBA (*meta*-chloroperbenzoic acid) is used to oxidise the sulfide, giving a mixture of (*S,S*)-bissulfoxide, (*S,R*)-bissulfoxide and the over-oxidised sulfone, which can all be separated by column chromatography (figure 8).

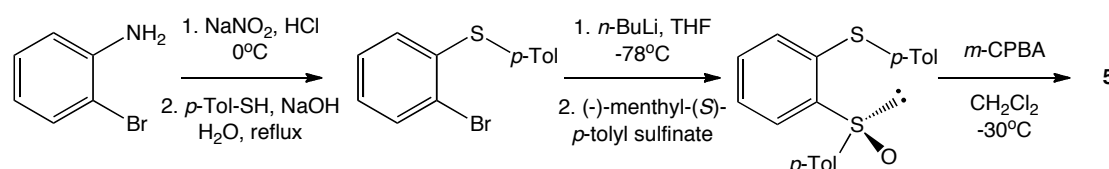


**Figure 8** Synthesis of (*S,S*)-1,2-bis(*p*-tolylsulfinyl)benzene, **5**, according to Shibasaki

The synthesis of **6** is much more facile. Firstly bromobenzene is lithiated by lithium-halogen exchange, and then quenched with one equivalent of (*S*)-*tert*-butyl *tert*-butanethiosulfinate, which is easily prepared enantiomerically pure.<sup>13g,19</sup> The monosulfoxide is then lithiated once more, the position next to the sulfoxide is activated, and quenched with another equivalent of (*S*)-*tert*-butyl *tert*-butanethiosulfinate to give the bissulfoxide (figure 9).

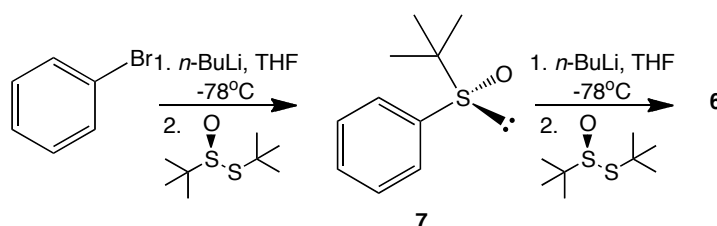


**Figure 9** Synthesis of (*R,R*)-1,2-bis(*tert*-butylsulfinyl)benzene, **6**, according to Liao

This is the method we chose to use to generate a new family of hetero-bissulfoxide ligands.

## 2.2. Results and Discussion

For the synthesis of new bissulfoxide ligands, we began with the same monosulfoxide first reported by Liao *et al.*<sup>20</sup> It is necessary to have an alkyl sulfoxide, with no hydrogen  $\alpha$  to the sulfoxide, so that only the aromatic hydrogen in the  $\alpha$ -position is exchanged with lithium in the second step. In the case where a bisaryl

sulfoxide was used, a complicated mixture of products was obtained. The lithiated monosulfoxide was then quenched with a range of enantiopure sulfinates to give new hetero-bissulfoxides. The synthesis of these ligands is shown in figure 10 below.

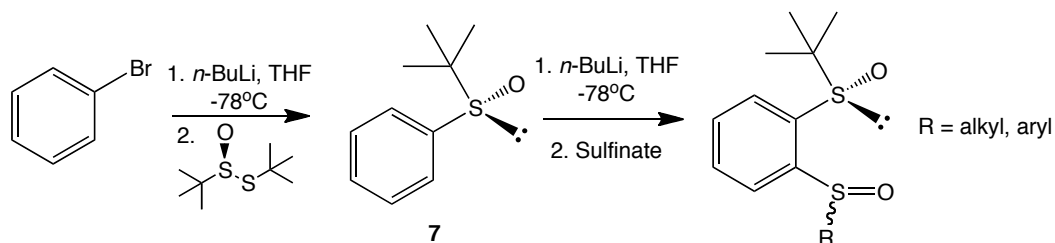


**Figure 10** Synthesis of hetero-bissulfoxides

It was possible to make bissulfoxides where the second moiety added had an alkyl or an aryl group attached to the sulfoxide. The ligands made by this method are shown in figure 11.

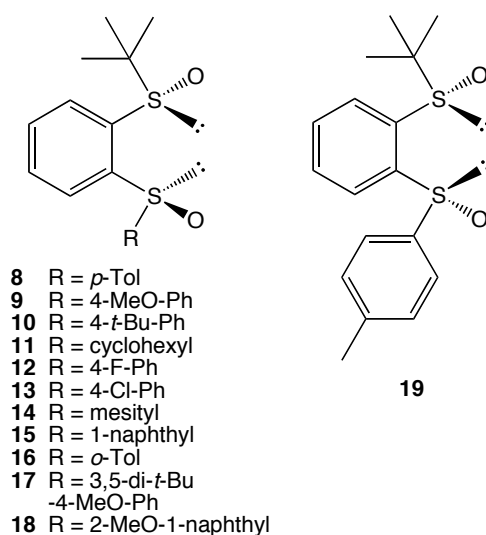
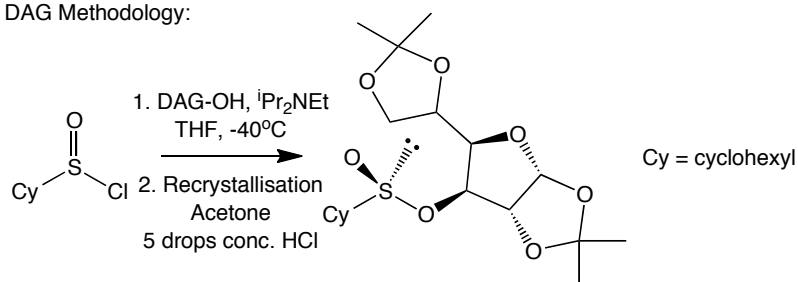


**Figure 11** Hetero-bissulfoxide ligands

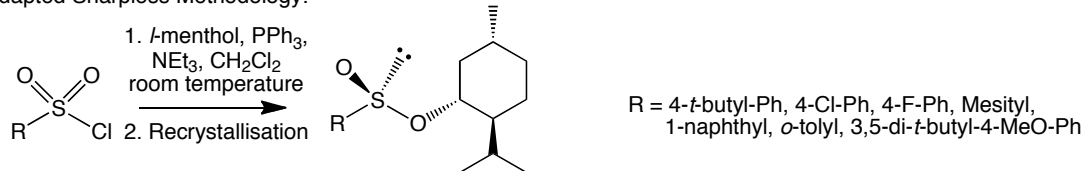
Most of the sulfinates required to make **8-19** were either commercially available ((*S*)- and (*R*)-menthyl *p*-tolylsulfinates), known in our lab<sup>17b</sup> or known in the literature.<sup>12</sup> The (*S*)-DAG cyclohexylsulfinates were made by the DAG-methodology (figure 8), previously mentioned, and the aryl sulfinates were made by the adapted Sharpless method of Watanabe *et al.*<sup>12c</sup> The (*S*)-menthyl 2-methoxy-1-naphthalenesulfinate was made according to Pyne *et al.*<sup>12b</sup> These methods are shown below (figure 12).



DAG Methodology:



Adapted Sharpless Methodology:



(*S*)-menthyl 2-methoxy-1-naphthalenesulfinate Synthesis:

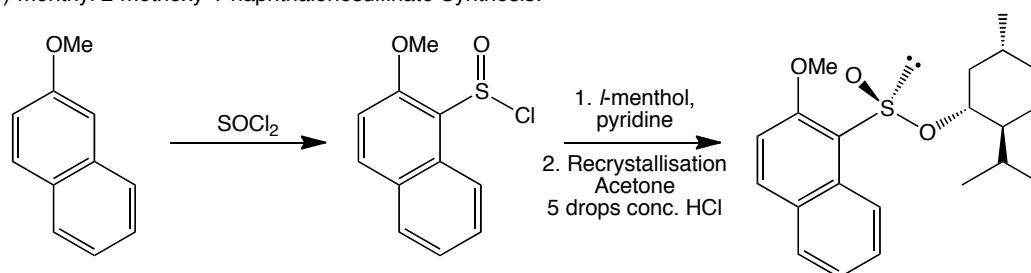


**Figure 12** Syntheses of sulfates

All of the described sulfates could be obtained pure, with (*S*)-configuration at sulfur, except the menthyl mesitylsulfate. This was used as a mixture of diastereoisomers in the sulfoxide formation. The major product was the (*S,S*)-bissulfoxide, with a small amount of the (*S,R*)-bissulfoxide, which could be easily removed by column chromatography. In the case of the menthyl 3,5-di-*tert*-butyl-4-methoxyphenyl sulfinate, the diastereomer crystallising was the (*R*)-sulfinate. The mother liquor after crystallisation was therefore enriched with the (*S*)-sulfinate, with small amounts of the (*R*)-sulfinate remaining. When this almost pure sulfinate was used to produce the bissulfoxide, only the (*S,S*)-bissulfoxide was formed.

As an extension to this family of bissulfoxide ligands, we also tried to vary the alkyl group on the first sulfoxide. We first attempted to put a cyclohexyl in this position. However, lithiating bromobenzene with *n*-BuLi and quenching with sulfinate did not work well in this case. Fortunately, the phenyl-Grignard nucleophile did react with the DAG-(*S*)-cyclohexylsulfinate to give the monosulfoxide in good yield.

Reaction with a second sulfinate was carried out by the usual method, but as previously mentioned, an inseparable mixture of products was obtained due to the  $\alpha$ -

H of the alkyl group, which could also be removed by *n*-BuLi. To solve this problem, the cyclohexyl phenyl monosulfoxide, **20**, can be lithiated selectively at the  $\alpha$ -hydrogen of the alkyl group, using LDA (lithium diisopropylamine), and then quenched with MeI (figure 13). Instead of a hydrogen  $\alpha$  to the sulfoxide, there is now a methyl and this monosulfoxide can then be reacted with *n*-BuLi and quenched with sulfinate to give only one product. As 1-((*S*)-*tert*-butylsulfinyl)-2-((*S*)-4-*tert*-butylphenylsulfinyl)benzene gave the best results in catalysis out of all the ligands shown in figure 7 (see chapter 3 of this thesis), the methyl-cyclohexyl analogue of this ligand was made, **23**.

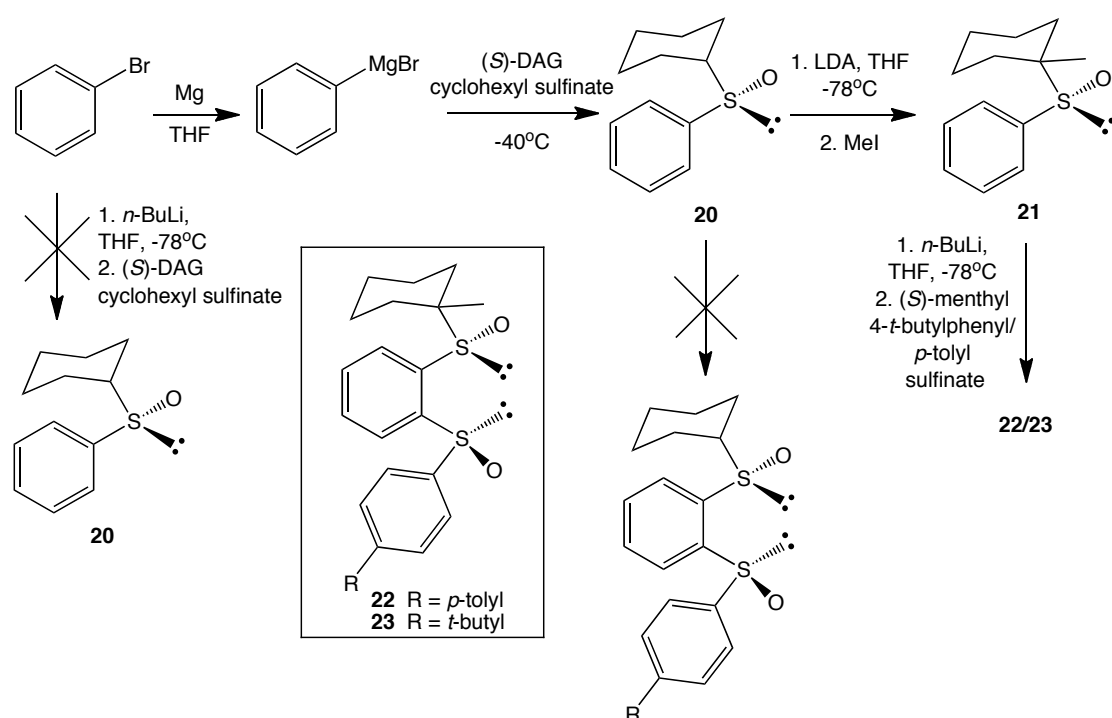


**Figure 13** Synthesis of **22** and **23**

The *p*-tolyl analogue, **22** was also made to better compare the effect of a bulkier aryl substituent in catalysis.

Another variation made on the first ligands was to introduce substituents on the backbone. Methoxy groups were chosen, in the hope that they would make the ligand more electron-rich, and in turn coordinate more favourably to metals. The synthesis was carried out in a similar fashion to that of **8-19**, the only difference being that 3,5-dimethoxybromobenzene, which is commercially available, was used as the starting material (figure 14).

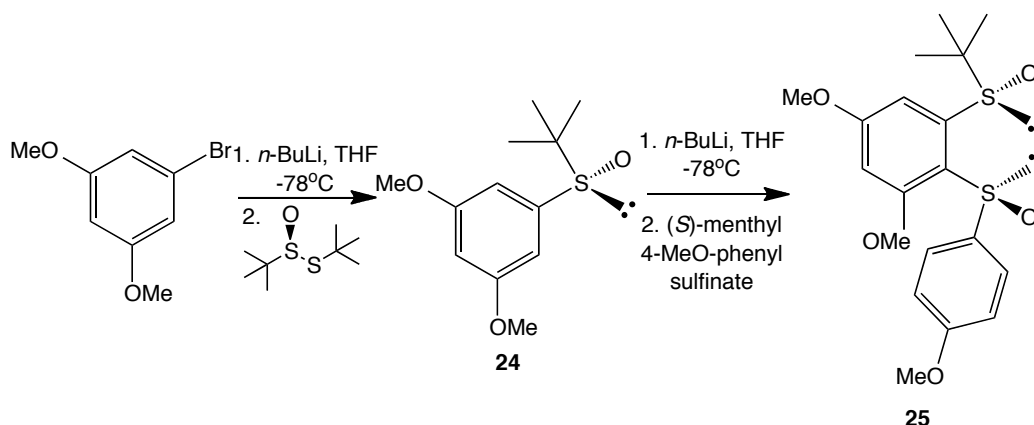


Figure 14 Synthesis of **25**

The 4-methoxyphenyl substituent was chosen as the second sulfoxide to attempt to make this ligand as electron-rich as possible.

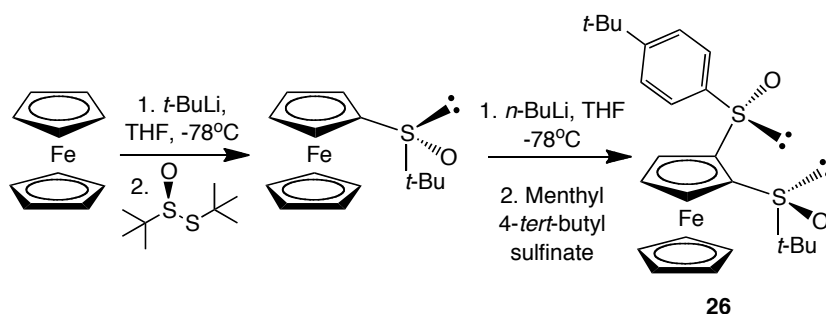
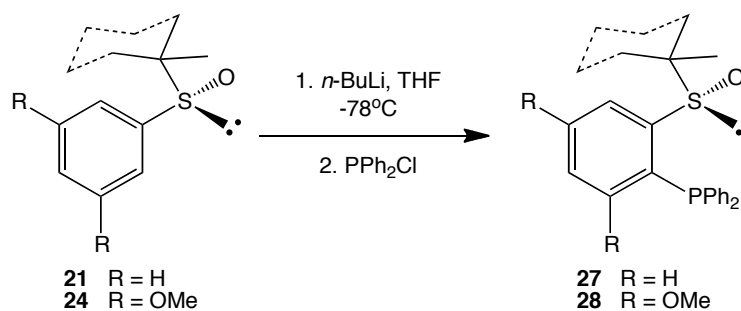


Figure 15 Synthesis of **26**

In order to create a ligand with a different bite angle and different electronic properties, ferrocene was also used as the backbone. This could be lithiated and quenched with (*S*)-*tert*-butyl *tert*-butanethiosulfinate, to give the monosulfoxide as reported by Carretero.<sup>21</sup> The monosulfoxide was then lithiated, and quenched with (-)-menthyl-(*S*)-4-*tert*-butylphenyl sulfinate, to give the bisulfoxide **26** (figure 15).

Finally, a couple of sulfinylphosphine ligands were synthesised to analyse the effect of the presence of a phosphine on the metal binding properties and reactivity of the ligand. Sulfinylphosphines are already known from the groups of Hiroi<sup>22</sup> and Liao,<sup>20,23</sup> and have been successfully used in transition-metal catalysis. The monosulfoxides, **21** and **24**, were used to make new sulfinyl phosphines, **27** and **28**, by first lithiating and then quenching with PPh<sub>2</sub>Cl (figure 16).



**Figure 16** Synthesis of **27** and **28**

Once isolated, **27** and **28** were stable, and when stored at -20°C no transfer of the oxygen atom from the sulfur to the phosphine was observed.

### 2.3. Conclusions

A family of bissulfoxide ligands could be easily prepared using commercially available bromobenzene and derivatives, in conjunction with sulfinates that were prepared *via* reported methods. Novel sulfinyl phosphines were also synthesised to evaluate the effect of the presence of a phosphine.

It is envisioned that these ligands will be able to form complexes with metals, particularly late-transition metals. The binding properties of these ligands will be investigated, and the complexes formed will be tested in catalysis. Given the promising results of sulfoxide-containing ligands similar to these, it is hoped that these structures will provide good reactivity and selectivity in catalytic reactions.

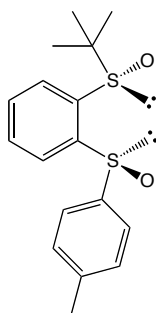
Considering the different structural and electronic variations in each of these ligands, it is expected that something can be learnt about the structure-activity relationship in enantioselective catalysis. This will then help with the design of new ligands to further improve their performance in catalysis.

### 2.4. Experimental Section

All reactions were carried out using standard Schlenk or glovebox (Mecaplex or Innovative Technology) techniques under nitrogen. NMR spectra were collected on an AV2 400 MHz Bruker spectrometer. HR-MS was acquired on a *Finnigan MAT 95* (*Finnigan MAT95*, San Jose, CA; USA) double-focusing magnetic sector mass

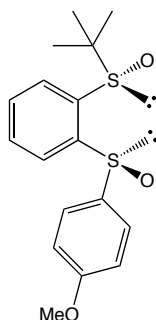
spectrometer (geometry BE). Solvents were purchased in the best quality available, degassed by purging thoroughly with nitrogen and dried over activated molecular sieves of appropriate size. Alternatively, they were purged with argon and passed through alumina columns in a solvent purification system (Innovative Technology). Bromobenzene, 3,5-dimethoxybromobenzene, *n*-BuLi, *t*-BuLi, (1*S*,2*R*,5*S*)-(+)-Menthyl-(*R*)-*p*-toluenesulfinate, ferrocene, iodomethane and *P*-chlorodiphenylphosphine were purchased from Aldrich, Acros or Fluka and used as received. Solvents for NMR spectroscopy were degassed with nitrogen and dried over molecular sieves (4Å). Sulfonates were prepared following literature procedures.<sup>12-14</sup>

**General procedure for the synthesis of bissulfoxides 8-19:** A 100 ml Schlenk flask was charged with 500mg (2.74 mmol) ((*S*)-*tert*-butylsulfinyl)benzene as a solution in 15ml dry THF. The solution was cooled to -78°C and 1.2ml (3 mmol) of a 2.5M solution of *n*-BuLi in hexanes was added dropwise *via* syringe, with stirring. After 1 hour a purple solution was formed, to this was added, dropwise, *via* a dropping funnel, at -78°C, a solution of the sulfinate (3 mmol) in 15ml dry THF. After the addition was complete, the reaction was stirred at -78°C for another 30 minutes, and then allowed to warm to room temperature over 1 hour. The reaction was quenched with 15ml H<sub>2</sub>O and 5 ml acetone, and extracted with CH<sub>2</sub>Cl<sub>2</sub> (3 x 20ml). The combined organic phases were dried over MgSO<sub>4</sub> and volatiles were removed *in vacuo*. The residue was purified by column chromatography using either a mixture of CH<sub>2</sub>Cl<sub>2</sub>/ethyl acetate, or hexane/ethyl acetate.

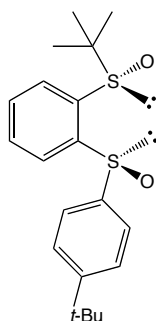


**1-((*S*)-*tert*-butylsulfinyl)-2-((*S*)-*p*-tolylsulfinyl)benzene (8):** Eluted with hexane/ethyl acetate 2:1. White solid, yield 76%. <sup>1</sup>H NMR (400 MHz, CDCl<sub>3</sub>): δ = 1.31 (s, 9H), 2.32 (s, 3H), 7.21-7.23 (d, *J* = 8.0 Hz, 2H), 7.54-7.56 (d, *J* = 8.1 Hz, 2H), 7.58-7.67 (m, 2H), 7.87-7.89 (d, *J* = 7.7 Hz, 1H), 8.08-8.10 (d, *J* = 7.6, 1H) ppm. <sup>13</sup>C

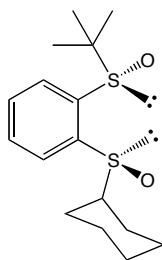
NMR (400 MHz, CDCl<sub>3</sub>):  $\delta$  = 21.63 (s), 23.37 (s), 59.10 (s), 123.86 (s), 125.45 (s), 126.82 (s), 130.49 (s), 131.55 (s), 132.93 (s), 138.56 (s), 141.43 (s), 142.45 (s), 146.76 (s) ppm. HRMS: Calculated for C<sub>17</sub>H<sub>20</sub>O<sub>2</sub>S<sub>2</sub>+Na: 343.0797, found: 343.0797.



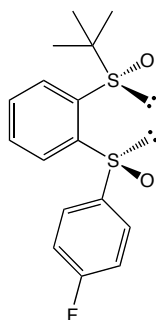
**1-((*S*)-*tert*-butylsulfinyl)-2-((*S*)-*p*-methoxy-phenylsulfinyl)benzene (9):** Eluted with CH<sub>2</sub>Cl<sub>2</sub>/ethyl acetate 9:1. White solid, yield 61%. <sup>1</sup>H NMR (400 MHz, CDCl<sub>3</sub>):  $\delta$  = 1.31 (s, 9H), 3.78 (s, 3H), 6.90-6.92 (d, *J* = 7.6 Hz, 2H), 7.57-7.70 (m, 4H), 7.86-7.88 (d, *J* = 7.8 Hz, 1H), 8.14-8.16 (d, *J* = 7.6 Hz, 1H) ppm. <sup>13</sup>C NMR (400 MHz, CDCl<sub>3</sub>):  $\delta$  = 23.42 (s), 55.78 (s), 59.12 (s), 115.37 (s), 123.62 (s), 126.93 (s), 127.81 (s), 131.51 (s), 132.91 (s), 135.54 (s), 138.41 (s), 146.84 (s) ppm. HRMS: Calculated for C<sub>17</sub>H<sub>20</sub>O<sub>3</sub>S<sub>2</sub>+Na: 359.0460, found: 359.0461.



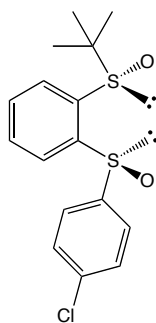
**1-((*S*)-*tert*-butylsulfinyl)-2-((*S*)-4-*tert*-butyl-phenylsulfinyl)benzene (10):** Eluted with CH<sub>2</sub>Cl<sub>2</sub>/ethyl acetate 9:1. White solid, yield 70%. <sup>1</sup>H NMR (300 MHz, CDCl<sub>3</sub>):  $\delta$  = 1.25 (s, 9H), 1.32 (s, 9H), 7.40-7.44 (dt, *J* = 7.8 Hz, *J* = 1.8 Hz, 2H), 7.56-7.70 (m, 4H), 7.86-7.89 (dd, *J* = 7.5 Hz, *J* = 1.5 Hz, 1H), 8.12-8.15 (dd, *J* = 7.4 Hz, *J* = 1.6 Hz, 1H) ppm. <sup>13</sup>C NMR (300 MHz, CDCl<sub>3</sub>):  $\delta$  = 23.42 (s), 31.35 (s), 35.28 (s), 59.19 (s), 123.89 (s), 125.45 (s), 126.85 (s), 126.96 (s), 131.60 (s), 132.99 (s), 138.58 (s), 141.26 (s), 146.61 (s), 155.58 (s) ppm. HRMS: Calculated for C<sub>20</sub>H<sub>26</sub>O<sub>2</sub>S<sub>2</sub>+Na: 385.1266, found 385.1265.



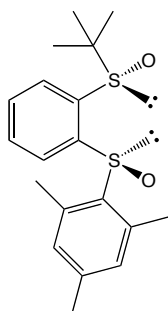
**1-((*S*)-*tert*-butylsulfinyl)-2-((*S*)-cyclohexylsulfinyl)benzene (11):** Eluted with hexane/ethyl acetate 4:1. White solid, yield 72%.  $^1\text{H}$  NMR (400 MHz,  $\text{CDCl}_3$ ):  $\delta$  = 1.27 (s, 9H), 1.15-1.98 (m, 10H), 2.82-2.89 (m, 1H), 7.66-7.73 (m, 2H), 7.95-8.01 (m, 2H) ppm.  $^{13}\text{C}$  NMR (400 MHz,  $\text{CDCl}_3$ ):  $\delta$  = 23.23 (s), 23.33 (s), 25.34 (s), 25.45 (s), 25.95 (s), 27.26 (s), 59.22 (s), 62.79 (s), 124.98 (s), 126.57 (s), 131.47 (s), 132.32 (s), 139.10 (s), 143.09 (s) ppm. HRMS: Calculated for  $\text{C}_{16}\text{H}_{24}\text{O}_2\text{S}_2+\text{Na}$ : 335.1115, found: 335.1113.



**1-((*S*)-*tert*-butylsulfinyl)-2-((*S*)-*p*-F-phenylsulfinyl)benzene (12):** Eluted with  $\text{CH}_2\text{Cl}_2$ /ethyl acetate 9:1. White solid, yield 24%.  $^1\text{H}$  NMR (400 MHz,  $\text{CDCl}_3$ ):  $\delta$  = 1.31 (s, 9H), 7.09-7.13 (t,  $J$  = 8.5 Hz, 2H), 7.60-7.69 (m, 4H), 7.88-7.90 (d,  $J$  = 7.5 Hz, 1H), 8.06-8.08 (d,  $J$  = 7.6 Hz, 1H) ppm.  $^{13}\text{C}$  NMR (400 MHz,  $\text{CDCl}_3$ ):  $\delta$  = 23.55 (s), 59.23 (s), 117.06 (s), 117.28 (s), 123.71 (s), 126.99 (s), 127.69 (s), 127.78 (s), 131.83 (s), 133.09 (s), 138.60 (s) ppm.  $^{19}\text{F}$  NMR (400 MHz,  $\text{CDCl}_3$ ):  $\delta$  = -107.16--107.09 (m, 1F) ppm. HRMS: Calculated for  $\text{C}_{16}\text{H}_{17}\text{FO}_2\text{S}_2+\text{Na}$ : 347.0546, found: 347.0546.

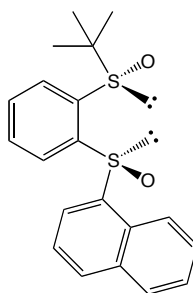


**1-((*S*)-*tert*-butylsulfinyl)-2-((*S*)-*p*-Cl-phenylsulfinyl)benzene (13):** Eluted with CH<sub>2</sub>Cl<sub>2</sub>/ethyl acetate 9:1. White solid, yield 40%. <sup>1</sup>H NMR (400 MHz, CDCl<sub>3</sub>):  $\delta$  = 1.32 (s, 9H), 7.39-7.41 (d,  $J$  = 8.4 Hz, 2H), 7.61-7.68 (m, 4H), 7.89-7.91 (d,  $J$  = 7.9 Hz, 1H), 8.02-8.04 (d,  $J$  = 8.0 Hz, 1H) ppm. <sup>13</sup>C NMR (400 MHz, CDCl<sub>3</sub>):  $\delta$  = 23.37 (s), 59.36 (s), 123.95 (s), 126.62 (s), 127.09 (s), 130.18 (s), 132.00 (s), 133.23 (s), 138.15 (s), 138.80 (s), 143.31 (s), 146.33 (s) ppm. HRMS: Calculated for C<sub>16</sub>H<sub>17</sub>ClO<sub>2</sub>S<sub>2</sub>+Na: 363.0251, found: 363.0249.

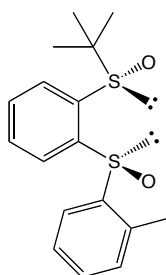


**1-((*S*)-*tert*-butylsulfinyl)-2-((*S*)-2,4,6-trimethyl-phenylsulfinyl)benzene (14):** Eluted with hexane/ethyl acetate 2:1. White solid, yield 53%. <sup>1</sup>H NMR (400 MHz, CDCl<sub>3</sub>):  $\delta$  = 1.20 (s, 9H), 2.23 (s, 3H), 2.36 (s, 6H), 6.80 (s, 2H), 7.59-7.63 (t,  $J$  = 7.5 Hz, 1H), 7.67-7.71 (t,  $J$  = 7.6 Hz, 1H), 7.88-7.90 (d,  $J$  = 7.7 Hz, 1H), 8.24-8.26 (d,  $J$  = 7.8 Hz, 1H) ppm. <sup>13</sup>C NMR (400 MHz, CDCl<sub>3</sub>):  $\delta$  = 19.73 (s), 21.35 (s), 23.14 (s), 58.65 (s), 126.93 (s), 127.00 (s), 130.46 (s), 131.51 (s), 131.59 (s), 135.43 (s), 138.04 (s), 140.08 (s), 143.19 (s), 144.13 (s) ppm. HRMS: Calculated for C<sub>19</sub>H<sub>24</sub>O<sub>2</sub>S<sub>2</sub>+ Na: 371.1115, found: 371.1113.

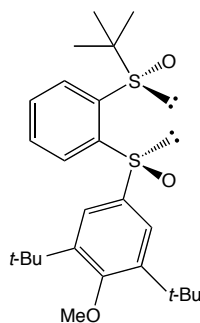




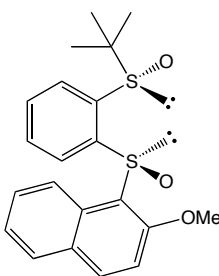
**1-((*S*)-*tert*-butylsulfinyl)-2-((*S*)-1-naphthylsulfinyl)benzene (15):** Eluted with hexane/ethyl acetate 2:1. White solid, yield, 67%.  $^1\text{H}$  NMR (400 MHz,  $\text{CDCl}_3$ ):  $\delta$  = 1.37 (s, 9H), 7.49-7.64 (m, 5H), 7.86-7.97 (m, 4H), 8.08-8.10 (d,  $J$  = 7.3 Hz, 1H), 8.19-8.22 (d,  $J$  = 8.4 Hz, 1H) ppm.  $^{13}\text{C}$  NMR (400 MHz,  $\text{CDCl}_3$ ):  $\delta$  = 23.52 (s), 58.97 (s), 122.52 (s), 124.44 (s), 125.73 (s), 126.27 (s), 126.84 (s), 127.20 (s), 128.23 (s), 129.14 (s), 129.43 (s), 131.85 (s), 132.52 (s), 132.84 (s), 133.88 (s), 139.96 (s), 140.46 (s), 145.26 (s) ppm. HRMS: Calculated for  $\text{C}_{20}\text{H}_{20}\text{O}_2\text{S}_2+\text{Na}$ : 379.0797, found: 379.0795.



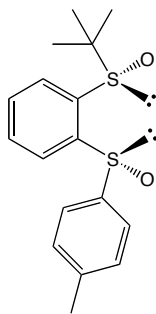
**1-((*S*)-*tert*-butylsulfinyl)-2-((*S*)-*o*-tolylsulfinyl)benzene (16):** Eluted with hexane/ethyl acetate 2:1. White solid, yield 72%.  $^1\text{H}$  NMR (400 MHz,  $\text{CDCl}_3$ ):  $\delta$  = 1.31 (s, 9H), 2.46 (s, 3H), 7.15-7.17 (m, 1 H), 7.32-7.34 (m, 2H), 7.62-7.69 (m, 3H), 7.89-7.92 (m, 2H) ppm.  $^{13}\text{C}$  NMR (400 MHz,  $\text{CDCl}_3$ ):  $\delta$  = 19.25 (s), 23.40 (s), 58.72 (s), 125.31 (s), 126.09 (s), 126.71 (s), 127.59 (s), 131.36 (s), 131.66 (s), 131.82 (s), 132.86 (s), 136.63 (s), 139.65 (s), 142.73 (s), 144.83 (s) ppm. HRMS: Calculated for  $\text{C}_{17}\text{H}_{20}\text{O}_2\text{S}_2+\text{Na}$ : 343.0797, found: 343.0796.



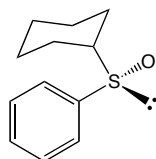
**1-((*S*)-*tert*-butylsulfinyl)-2-((*S*)-3,5-di-*tert*-butyl-4-methoxyphenylsulfinyl)benzene (17):** Eluted with hexane/ethyl acetate 1:1. Colourless oil, yield 28%.  $^1\text{H}$  NMR (400 MHz,  $\text{CDCl}_3$ ):  $\delta$  = 1.15 (s, 9H), 1.35 (s, 18H), 3.64 (s, 3H), 7.54-7.58 (m, 1H), 7.60 (s, 2H), 7.66-7.70 (m, 2H), 8.10-8.12 (d,  $J$  = 7.8 Hz, 1H) ppm.  $^{13}\text{C}$  NMR (400 MHz,  $\text{CDCl}_3$ ):  $\delta$  = 23.69 (s), 32.01 (s), 36.46 (s), 58.69 (s), 64.74 (s), 125.15 (s), 126.45 (s), 127.75 (s), 130.93 (s), 132.63 (s), 138.15 (s), 140.00 (s), 145.56 (s), 148.09 (s), 162.31 (s) ppm. HRMS: Calculated for  $\text{C}_{25}\text{H}_{36}\text{O}_3\text{S}_2+\text{Na}$ : 471.1998, found: 471.1996.



**1-((*S*)-*tert*-butylsulfinyl)-2-((*S*)-2-methoxy-1-naphthylsulfinyl)benzene (18):** Eluted with  $\text{CH}_2\text{Cl}_2$ /ethyl acetate 4:1. White solid, yield 58%.  $^1\text{H}$  NMR (400 MHz,  $\text{CDCl}_3$ ):  $\delta$  = 1.23 (s, 9H), 3.78 (s, 3H), 7.13-7.16 (d,  $J$  = 9.1 Hz, 1H), 7.34-7.38 (t,  $J$  = 7.5 Hz, 1H), 7.50-7.58 (m, 2H), 7.67-7.71 (t,  $J$  = 7.6 Hz, 1H), 7.74-7.76 (d,  $J$  = 8.2 Hz, 1H), 7.81-7.83 (d,  $J$  = 7.8 Hz, 1H), 7.92-7.94 (d,  $J$  = 9.1 Hz, 1H), 8.41-8.43 (d,  $J$  = 7.9 Hz, 1H), 8.66-8.68 (d, 8.7 Hz, 1H) ppm.  $^{13}\text{C}$  NMR (400 MHz,  $\text{CDCl}_3$ ):  $\delta$  = 23.19 (s), 56.40 (s), 58.35 (s), 113.33 (s), 121.73 (s), 122.43 (s), 124.66 (s), 126.33 (s), 126.90 (s), 128.58 (s), 129.09 (s), 129.45 (s), 130.36 (s), 131.37 (s), 132.65 (s), 135.95 (s), 137.98 (s), 145.09 (s), 157.66 (s) ppm. HRMS: Calculated for  $\text{C}_{21}\text{H}_{22}\text{O}_3\text{S}_2+\text{Na}$ : 409.0908, found: 409.0906.

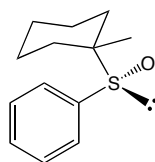


**1-((*S*)-*tert*-butylsulfinyl)-2-((*R*)-*p*-tolylsulfinyl)benzene (19):** Eluted with CH<sub>2</sub>Cl<sub>2</sub>/ethyl acetate 4:1. Foam, yield 82 %. <sup>1</sup>H NMR (400 MHz, CDCl<sub>3</sub>):  $\delta$  = 1.26 (s, 9H), 2.31 (s, 3H), 7.19-7.21 (d, *J* = 8.1 Hz, 2H), 7.47-7.51 (m, 2H), 7.58-7.61 (m, 1H), 7.63-7.65 (d, *J* = 8.0 Hz, 2H), 8.12-8.14 (d, *J* = 8.0 Hz, 2H) ppm. <sup>13</sup>C NMR (400 MHz, CDCl<sub>3</sub>):  $\delta$  = 21.50 (s), 23.75 (s), 58.67 (s), 125.98 (s), 126.64 (s), 127.91 (s), 129.95 (s), 130.63 (s), 132.52 (s), 139.28 (s), 141.38 (s), 142.43 (s), 148.73 (s) ppm. HRMS: Calculated for C<sub>17</sub>H<sub>20</sub>O<sub>2</sub>S<sub>2</sub>+Na: 343.0797, found: 343.0800.



**Synthesis of ((*S*)-cyclohexylsulfinyl)benzene (20):** A 500ml Schlenk flask was charged with a suspension of 851mg (35 mmol) Mg in 50ml dry THF. 3.4ml (31.8 mmol) bromobenzene was added dropwise to this, with stirring, *via* syringe at 0°C. The reaction was left at this temperature for another 30 minutes and then allowed to warm to room temperature and react for another hour. Once the magnesium was practically all consumed, the flask was cooled to -40°C and a solution of 13.68g (35 mmol) (*S*)-DAG cyclohexyl sulfinate in 50ml dry THF was added, dropwise, *via* dropping funnel. After the addition, the reaction was kept at this temperature for another 30 minutes, and then allowed to warm to room temperature. After another hour, the reaction was quenched with 50ml 2M HCl, and extracted with three portions of CH<sub>2</sub>Cl<sub>2</sub> (50ml each). The combined organic phases were then washed first with 20ml saturated NaHCO<sub>3</sub> solution and finally with 40ml brine. The organic phase was dried over MgSO<sub>4</sub>, and volatiles removed *in vacuo*. The residue was redissolved in 100ml CH<sub>3</sub>CN, 40ml distilled water and 4ml triflic acid were added and the mixture was left stirring overnight. The reaction was quenched with 40ml saturated NaHCO<sub>3</sub>.

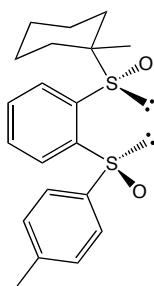
solution and diluted with 50ml diethyl ether. The aqueous and organic phases were separated and the organic phase was washed with four portions of water (50ml each). The organic phase was then dried over  $\text{MgSO}_4$  and solvent was removed. The residue was purified by column chromatography using hexane/ethyl acetate 24:1 as the eluent. A pale yellow oil was obtained in 87% yield.  $^1\text{H}$  NMR (400 MHz,  $\text{CDCl}_3$ ):  $\delta$  = 1.09-1.28 (m, 3H), 1.29-1.47 (m, 2H), 1.58-1.66 (m, 1H), 1.74-1.86 (m, 4H), 2.48-2.57 (m, 1H), 7.43-7.51 (m, 3H), 7.53-7.58 (m, 2H) ppm.  $^{13}\text{C}$  NMR (400 MHz,  $\text{CDCl}_3$ ):  $\delta$  = 24.17 (s), 25.49 (s), 25.63 (s), 25.79 (s), 26.47 (s), 63.33 (s), 125.18 (s), 129.06 (s), 131.07 (s), 142.14 (s) ppm. HRMS: Calculated for  $\text{C}_{12}\text{H}_{16}\text{OS}+\text{Na}$ : 231.0814, found: 231.0817.



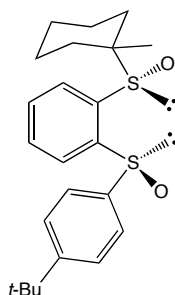
**Synthesis of ((S)-1-methyl-cyclohexylsulfinyl)benzene (21):** A solution of LDA (26.4 mmol) in 50ml THF was prepared in a 100ml schlenk flask at  $-78^\circ\text{C}$ . To this was added **22**, dropwise, *via* syringe at  $-78^\circ\text{C}$  with stirring. After addition, the reaction was left at this temperature for 30 minutes more and then 1.6ml MeI was added, dropwise, *via* syringe. The yellow solution was allowed to warm to room temperature over 30 minutes and then was quenched with distilled water. The aqueous layer was extracted three times with  $\text{CH}_2\text{Cl}_2$  (30ml each time) and the combined organic phases were dried over  $\text{MgSO}_4$ . Solvent was removed *in vacuo* and yellow residue remaining was purified by column chromatography, using  $\text{CH}_2\text{Cl}_2$ /ethyl acetate 24:1 as the eluent. A product was obtained as a pale yellow solid in 96% yield.  $^1\text{H}$  NMR (400 MHz,  $\text{CDCl}_3$ ):  $\delta$  = 0.96 (s, 3H), 1.35-1.86 (m, 11H), 7.42-7.44 (m, 3H), 7.52-7.54 (m, 2H) ppm.  $^{13}\text{C}$  NMR (400 MHz,  $\text{CDCl}_3$ ):  $\delta$  = 16.24 (s), 21.98 (s), 22.01 (s), 25.63 (s), 30.69 (s), 31.92 (s), 59.61 (s), 126.63 (s), 128.42 (s), 131.11 (s), 139.48 (s) ppm. HRMS: Calculated for  $\text{C}_{13}\text{H}_{18}\text{OS}+\text{Na}$ : 245.0971, found: 245.0972.

**General Procure for the Synthesis of **22** and **23**:** A 100ml Schlenk flask was charged with 500mg **21** (2.25 mmol) as a solution in 15ml dry THF. The solution was cooled to  $-78^\circ\text{C}$  and 1.0ml (2.5 mmol) of a 2.5M solution of *n*-BuLi in hexanes was added dropwise *via* syringe, with stirring. After 1 hour, a solution of the sulfinite (2.5

mmol) in 15ml dry THF was added to the reaction, dropwise, *via* a dropping funnel, at  $-78^{\circ}\text{C}$ . After the addition was complete, the reaction was stirred at  $-78^{\circ}\text{C}$  for another 30 minutes, and then allowed to warm to room temperature over 1 hour. The reaction was quenched with 15ml  $\text{H}_2\text{O}$  and 5 ml acetone, and extracted with  $\text{CH}_2\text{Cl}_2$  (3 x 20ml). The combined organic phases were dried over  $\text{MgSO}_4$  and volatiles were removed *in vacuo*. The residue was purified by column chromatography using  $\text{CH}_2\text{Cl}_2$ /ethyl acetate 4:1 as the eluent.

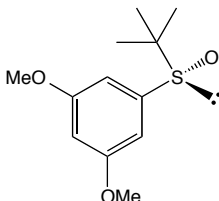


**1-((*S*)-1-methyl-cyclohexylsulfinyl)-2-((*S*)-*p*-tolylsulfinyl)benzene (22):** White solid, yield 44%.  $^1\text{H}$  NMR (400 MHz,  $\text{CDCl}_3$ ):  $\delta$  = 1.21 (s, 3H), 1.24-1.95 (m, 10H), 2.31 (s, 3H), 7.20-7.22 (d,  $J$  = 8 Hz, 2H), 7.53-7.55 (d,  $J$  = 8 Hz, 2H), 7.56-7.66 (m, 2H), 7.85-7.87 (d,  $J$  = 7.6 Hz, 1H), 8.08-8.09 (d,  $J$  = 7.7 Hz, 1H) ppm.  $^{13}\text{C}$  NMR (400 MHz,  $\text{CDCl}_3$ ):  $\delta$  = 16.23 (s), 21.61 (s), 22.06 (s), 22.28 (s), 25.55 (s), 30.56 (s), 31.94 (s), 63.04 (s), 123.81 (s), 125.41 (s), 127.31 (s), 130.47 (s), 131.38 (s), 132.80 (s), 136.28 (s), 137.88 (s), 141.55 (s), 142.39 (s) ppm. HRMS: Calculated for  $\text{C}_{20}\text{H}_{24}\text{O}_2\text{S}_2+\text{Na}$ : 383.1110, found: 383.1112.

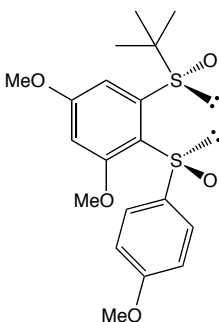


**1-((*S*)-1-methyl-cyclohexylsulfinyl)-2-((*S*)-*p*-*tert*-butyl-phenylsulfinyl)benzene (23):** White solid, yield 40%.  $^1\text{H}$  NMR (400 MHz,  $\text{CDCl}_3$ ):  $\delta$  = 1.21 (s, 3H), 1.25 (s, 9H), 1.40-1.96 (m, 10H), 7.41-7.43 (d,  $J$  = 8.3 Hz, 2H), 7.56-7.67 (m, 4H), 7.86-7.88 (d,  $J$  = 7.7 Hz, 1H), 8.12-8.14 (d,  $J$  = 7.7 Hz, 1H) ppm.  $^{13}\text{C}$  NMR (400 MHz,  $\text{CDCl}_3$ ):  $\delta$  = 16.23 (s), 22.07 (s), 22.28 (s), 25.55 (s), 30.55 (s), 31.28 (s), 31.93 (s), 35.19 (s),

63.07 (s), 123.79 (s), 125.35 (s), 126.88 (s), 127.28 (s), 131.38 (s), 132.80 (s), 137.80 (s), 141.30 (s), 146.65 (s), 155.45 (s) ppm. HRMS: Calculated for C<sub>23</sub>H<sub>30</sub>O<sub>2</sub>S<sub>2</sub>+Na: 425.1579, found: 425.1583.

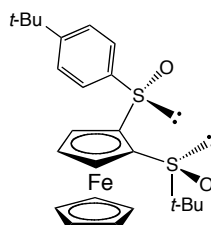


**1,3-dimethoxy-5-((*S*)-*tert*-butylsulfinyl)benzene (24):** A 250ml Schlenk flask was charged with 5g of 1-bromo-3,5-dimethoxybenzene (36.2 mmol) as a solution in 50ml dry THF. The solution was cooled to -78°C and 15.9ml (39.8 mmol) of a 2.5M solution of *n*-BuLi in hexanes was added dropwise *via* syringe, with stirring. After 1 hour, a solution of 7.74g of (*S*)-*tert*-butyl *tert*-butanethiosulfinate (39.8 mmol) in 50ml dry THF was added to the reaction, dropwise, *via* a dropping funnel, at -78°C. After the addition was complete, the reaction was stirred at -78°C for another 30 minutes, and then allowed to warm to room temperature over 1 hour. The reaction was quenched with 30ml H<sub>2</sub>O and 5 ml acetone, and extracted with CH<sub>2</sub>Cl<sub>2</sub> (3 x 40ml). The combined organic phases were dried over MgSO<sub>4</sub> and volatiles were removed *in vacuo*. The residue was purified by column chromatography using CH<sub>2</sub>Cl<sub>2</sub>/ethyl acetate 9:1 as the eluent. White solid, yield 86%. <sup>1</sup>H NMR (400 MHz, CDCl<sub>3</sub>): δ = 1.17 (s, 9H), 3.80 (s, 6H), 6.53 (s, 1H), 6.71 (d, *J* = 2.0 Hz, 2H) ppm. <sup>13</sup>C NMR (400 MHz, CDCl<sub>3</sub>): δ = 23.20 (s), 55.88 (s), 56.31 (s), 103.69 (s), 104.14 (s), 142.68 (s), 160.88 (s) ppm. HRMS: Calculated for C<sub>12</sub>H<sub>18</sub>O<sub>3</sub>S+Na: 265.0874, found: 265.0871.



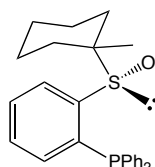
**Synthesis of 1,3-dimethoxy-4-((*S*)-*p*-methoxyphenylsulfinyl)-5-((*S*)-*tert*-butylsulfinyl)benzene (25):** A 100ml Schlenk flask was charged with 500mg of **24**

(2.06 mmol) as a solution in 15ml dry THF. The solution was cooled to  $-78^{\circ}\text{C}$  and 0.91ml (2.26 mmol) of a 2.5M solution of *n*-BuLi in hexanes was added dropwise *via* syringe, with stirring. After 1 hour, a solution of 702mg of (*S*)-menthyl 4-methoxyphenylsulfinate (2.26 mmol) in 15ml dry THF was added to the reaction, dropwise, *via* a dropping funnel, at  $-78^{\circ}\text{C}$ . After the addition was complete, the reaction was stirred at  $-78^{\circ}\text{C}$  for another 30 minutes, and then allowed to warm to room temperature over 1 hour. The reaction was quenched with 15ml  $\text{H}_2\text{O}$  and 5 ml acetone, and extracted with  $\text{CH}_2\text{Cl}_2$  (3 x 20ml). The combined organic phases were dried over  $\text{MgSO}_4$  and volatiles were removed *in vacuo*. The residue was purified by column chromatography using  $\text{CH}_2\text{Cl}_2$ /ethyl acetate 9:1 as the eluent. White solid, yield 18%.  $^1\text{H}$  NMR (400 MHz,  $\text{CDCl}_3$ ):  $\delta$  = 1.36 (s, 9H), 3.55 (s, 3H), 3.78 (s, 3H), 3.85 (s, 3H), 6.41 (d,  $J$  = 2.2 Hz, 1H), 6.88-6.90 (d,  $J$  = 8.8 Hz, 2H), 7.09 (d,  $J$  = 2.2 Hz, 1H), 7.45-7.47 (d,  $J$  = 8.8 Hz, 2H) ppm.  $^{13}\text{C}$  NMR (400 MHz,  $\text{CDCl}_3$ ):  $\delta$  = 23.84 (s), 55.63 (s), 56.16 (s), 59.14 (s), 101.69 (s), 103.26 (s), 114.10 (s), 124.30 (s), 126.34 (s), 134.76 (s), 146.25 (s), 160.99 (s), 161.20 (s), 164.22 (s) ppm. HRMS: Calculated for  $\text{C}_{19}\text{H}_{24}\text{O}_5\text{S}_2+\text{Na}$ : 419.0963, found: 419.0962.



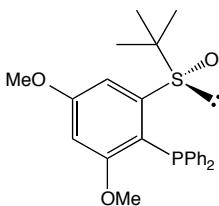
**Synthesis of 1-((*S*)-*tert*-butylsulfinyl)-2-(((*S*)-4-*tert*-butylphenylsulfinyl)ferrocene (26):** A 100ml Schlenk flask was charged with 865mg (2.98 mmol) (*S*)-*tert*-butylsulfinyl ferrocene as a solution in 25ml dry THF. This was cooled to  $-78^{\circ}\text{C}$  and 1.3ml (3.28 mmol) of a 2.5M solution of *n*-BuLi in hexanes was added dropwise by syringe. This was left stirring for 1 hour, after which time a solution of 1.1g (3.28 mmol) of (*S*)-menthyl 4-*tert*-butylphenylsulfinate in 25ml dry THF was added, dropwise, by dropping funnel. The reaction was left kept at  $-78^{\circ}\text{C}$  for another 30 minutes after addition was complete, and then allowed to warm to room temperature over 1 hour. The reaction was then quenched with 20ml distilled water and 5ml acetone. The aqueous phase was extracted with  $\text{CH}_2\text{Cl}_2$  (3 x 30ml) and the combined organic phases were dried over  $\text{MgSO}_4$ . The solvent was removed *in vacuo*, and the brown residue was purified by column chromatography, using hexane/ethyl acetate

1:2 as eluent. Yellow-brown solid, yield 95%.  $^1\text{H}$  NMR (400 MHz,  $\text{CDCl}_3$ ):  $\delta$  = 0.73 (s, 9H), 1.24 (s, 9H), 4.43 (s, 1H), 4.56 (s, 6H), 5.28 (s, 1H), 7.35-7.37 (d,  $J$  = 8.1 Hz, 2H), 7.66-7.68 (d,  $J$  = 8.0 Hz, 2H) ppm.  $^{13}\text{C}$  NMR (400 MHz,  $\text{CDCl}_3$ ):  $\delta$  = 22.87 (s), 23.79 (s), 31.48 (s), 35.12 (s), 67.16 (s), 69.80 (s), 70.27 (s), 71.10 (s), 72.21 (s), 125.90 (s), 127.18 (s), 154.82 (s) ppm. HRMS: Calculated for  $\text{C}_{24}\text{H}_{30}\text{FeO}_2\text{S}_2+\text{Na}$ : 493.0929, found: 493.0926.



**Synthesis of 1-((S)-1-methyl-cyclohexylsulfinyl)-2-(diphenylphosphine)benzene (27):** A 100ml Schlenk flask was charged with 500mg **21** (2.25 mmol) as a solution in 15ml dry THF. The solution was cooled to  $-78^\circ\text{C}$  and 1.0ml (2.5 mmol) of a 2.5M solution of *n*-BuLi in hexanes was added dropwise *via* syringe, with stirring. After 1 hour, 0.45ml (2.5 mmol)  $\text{PPh}_2\text{Cl}$  was added to the reaction, dropwise, *via* syringe, at  $-78^\circ\text{C}$ . After the addition was complete, the reaction was stirred at  $-78^\circ\text{C}$  for another 30 minutes, and then allowed to warm to room temperature over 1 hour. The reaction mixture was passed through a plug of celite and silica gel, and then solvent removed under reduced pressure. The residue was purified by column chromatography using hexane/ethyl acetate 1:1 as eluent. White solid, yield 52%.  $^1\text{H}$  NMR (400 MHz,  $\text{CDCl}_3$ ):  $\delta$  = 1.21 (s, 3H), 1.24-1.99 (m, 10H), 7.05-7.66 (m, 13H), 7.94-7.96 (dd,  $J$  = 7.9 Hz,  $J$  = 3.3 Hz, 1H) ppm.  $^{13}\text{C}$  NMR (400 MHz,  $\text{CDCl}_3$ ):  $\delta$  = 16.85 (d,  $J$  = 5.7 Hz), 22.09 (s), 22.42 (d, 2.9 Hz), 25.61 (s), 30.60 (s), 32.57 (d,  $J$  = 6.5 Hz), 62.63 (s), 127.14 (d,  $J$  = 86.3 Hz), 128.00 (d,  $J$  = 99.1 Hz), 128.82 (d,  $J$  = 3.4 Hz), 128.89 (d,  $J$  = 2.7 Hz), 129.11 (d,  $J$  = 1.7 Hz), 129.63 (s), 131.19 (s), 133.51 (d,  $J$  = 19.9 Hz), 134.00 (d,  $J$  = 19.7 Hz), 134.56 (d,  $J$  = 1.6 Hz), 136.01 (d,  $J$  = 15.4 Hz), 136.21 (d,  $J$  = 13.2 Hz), 138.80 (d,  $J$  = 19.4 Hz), 146.22 (d,  $J$  = 25.9 Hz) ppm.  $^{31}\text{P}$  NMR (400 MHz,  $\text{CDCl}_3$ ):  $\delta$  = -13.92 (s, 1P) ppm. HRMS: Calculated for  $\text{C}_{25}\text{H}_{27}\text{OPS}+\text{Na}$ : 429.1412, found: 429.1416.





**1,3-dimethoxy-4-((*S*)-*tert*-butylsulfinyl)-5-(diphenylphosphine)benzene (28):** A 100ml Schlenk flask was charged with 500mg **24** (2.06 mmol) as a solution in 15ml dry THF. The solution was cooled to -78°C and 0.91ml (2.26 mmol) of a 2.5M solution of *n*-BuLi in hexanes was added dropwise *via* syringe, with stirring. After 1 hour, 0.41ml (2.26 mmol) PPh<sub>2</sub>Cl was added to the reaction, dropwise, *via* syringe, at -78°C. After the addition was complete, the reaction was stirred at -78°C for another 30 minutes, and then allowed to warm to room temperature over 1 hour. The reaction mixture was passed through a plug of celite and silica gel, and then solvent removed under reduced pressure. The residue was purified by column chromatography using hexane/ethyl acetate 1:1 as eluent. White solid, yield 54%. <sup>1</sup>H NMR (400 MHz, CDCl<sub>3</sub>): δ = 1.21 (s, 9H), 3.28 (s, 3H), 3.88 (s, 3H), 6.42-6.43 (d, *J* = 2.1 Hz, 2H), 7.18-7.29 (m, 10H) ppm. <sup>13</sup>C NMR (400 MHz, CDCl<sub>3</sub>): δ = 2.26 (d, *J* = 16.0 Hz), 55.23 (s), 55.93 (s), 58.69 (s), 102.51 (s), 102.92 (s), 103.02 (s), 116.16 (d, *J* = 23.1), 127.81 (d, *J* = 7.0 Hz), 127.96 (d, *J* = 2.8 Hz), 128.00 (d, *J* = 6.3 Hz), 132.54 (d, *J* = 7.8 Hz), 132.73 (d, *J* = 6.5 Hz), 134.96 (d, *J* = 7.9 Hz), 138.00 (d, *J* = 11.2 Hz), 152.64 (d, *J* = 31.3 Hz), 163.26 (d, *J* = 2.1 Hz), 163.45 (d, *J* = 1.6 Hz) ppm. <sup>31</sup>P NMR (400 MHz, CDCl<sub>3</sub>): δ = -19.62 (s, 1P) ppm. HRMS: Calculated for C<sub>24</sub>H<sub>27</sub>O<sub>3</sub>PS+Na: 449.1311, found: 449.1317.

## 2.5. References

- <sup>1</sup> (a) Calligaris, M. *Coord. Chem. Rev.* **1996**, 153, 83; (b) Calligaris, M. *Coord. Chem. Rev.* **2004**, 248, 351
- <sup>2</sup> (a) Santana, S.A.A.; Carvalho Jr., V.P.; Lima-Neto, B.S. *J. Braz. Chem. Soc.* **2010**, 21, 279; (b) Riley, D.P. *Inorg. Chem.* **1983**, 22, 1965; (c) Srivastava, R.S.; Milani, B.; Alessio, E.; Mestoni, G. *Inorg. Chim. Acta* **1992**, 191, 15; (d) Haddad, Y.M.Y.; Henbest, H.B.; Husbands, J.; Mitchell, T.R.B. *Proc. Chem. Soc.* **1964**, 361; (e) Trocha-Grimshaw, J.; Henbest, H.B. *Chem. Commun.* **1967**, 544; (f) James, B.R.; Morris, R.H. *J. Chem. Soc., Chem. Commun.* **1978**, 929; (g) Chen, M.S.; White, M.C. *J. Am. Chem. Soc.* **2004**, 126, 1346; (h) Fraunhofer, K.J.; Bachovchin, D.A.; White, M.C. *Org. Lett.* **2005**, 7, 223; (i) Covell, D.J.; Vermeulen, N.A.; Labenz, N.A.; White, M.C. *Angew. Chem. Int. Ed.* **2006**, 45, 8217

- <sup>3</sup> (a) Hinsberg, O. *J. Prakt. Chem.* **1912**, 85, 344; (b) Bell, E.V.; Bennett, G.M. *J. Chem. Soc.* **1927**, 1798; (c) Greene Jr., J.L.; Shevlin, P.B. *J. Chem. Soc. D, Chem. Commun.* **1971**, 1092; (d) Svinning, T.; Mo, F.; Bruun, T. *Acta Cryst., Sect. B: Struct. Sci.* **1976**, 32, 759; (e) Kuneida, N.; Nokami, J.; Kinoshita, M. *Chem. Lett.* **1973**, 871; (f) Kuneida, N.; Nokami, J.; Kinoshita, M. *Bull. Chem. Soc. Jpn.* **1976**, 49, 256; (g) Maryanof, C.; Maryanof, B.; Tang, R.; Mislow, K. *J. Am. Chem. Soc.* **1973**, 95, 5839; (h) Madan, S.K.; Hull, C.M.; Herman, L.J. *Inorg. Chem.* **1968**, 7, 491; (i) Cattalini, L.; Michelon, G.; Marangoni, G.; Pelizzi, G. *J. Chem. Soc., Dalton Trans.* **1979**, 96; (j) Evans, D.R.; Huang, M.; Seganish, W.M.; Fettingner, J.C.; Williams, T.L. *Inorg. Chem. Commun.* **2003**, 6, 462; (k) Schaub, T.; Diskin-Poser, Y.; Radius, U.; Milstein, D. *Inorg. Chem.* **2008**, 47, 6502; (l) Mallorquin, R.M.; Chelli, S.; Brebion, F.; Fensterbank, L.; Goddard, J-P.; Malacria, M. *Tetrahedron: Asymmetry* **2010**, 21, 1695; (m) Khiar, N.; Fernandez, I.; Alcudia, F. *Tetrahedron Lett.* **1993**, 34, 123; (n) Aggarwal, V.K.; Drabowicz, J.; Grainger, R.S.; Gültekin, Z.; Lightowler, M.; Spargo, P.L. *J. Org. Chem.* **1995**, 60, 4962; (o) Pettinari, C.; Pellei, M.; Cavicchio, G.; Crucianelli, M.; Panzeri, W.; Colapietro, M.; Cassetta, A. *Organometallics* **1999**, 18, 555
- <sup>4</sup> (a) Chen, M.S.; Prabakaran, N.; Labenz, N.A.; White, M.C. *J. Am. Chem. Soc.* **2005**, 127, 6970; (b) Fraunhofer, K.J.; Prabakaran, N.; Sirois, L.E.; White, M.C. *J. Am. Chem. Soc.* **2006**, 128, 9032; (c) Fraunhofer, K.J.; White, M.C. *J. Am. Chem. Soc.* **2007**, 129, 7274
- <sup>5</sup> Fernandez, I.; Khiar, N. *Chem. Rev.* **2003**, 103, 3651
- <sup>6</sup> (a) Kowalski, P.; Mitka, K.; Ossowska, K.; Kolarska, Z. *Tetrahedron* **2005**, 61, 1933; (b) Kaczorowska, K.; Kolarska, Z.; Mitka, P.; Kowalska, P. *Tetrahedron* **2005**, 61, 8315
- <sup>7</sup> (a) Andersen, K.K. *Tetrahedron Lett.* **1962**, 3, 93; (b) Andersen, K.K.; Gaffield, W.; Papanikolaou, N.E.; Foley, J.W.; Perkins, R.I. *J. Am. Chem. Soc.* **1964**, 86, 5637
- <sup>8</sup> Gilman, H.; Robinson, J.; Beaber, N.J. *J. Am. Chem. Soc.* **1926**, 48, 2715
- <sup>9</sup> (a) Mislow, K.; Ternay, A.; Melillo, J.T. *J. Am. Chem. Soc.* **1963**, 85, 2329; (b) Alexrod, M.; Bickert, P.; Jacobus, J.; Green, M.; Mislow, K. *J. Am. Chem. Soc.* **1968**, 90, 4835
- <sup>10</sup> Solladié, G.; Hutt, J.; Girardin, A. *Synthesis* **1987**, 173
- <sup>11</sup> (a) Mioskowski, C.; Solladié, G. *Tetrahedron Lett.* **1975**, 16, 3341; (b) Mioskowski, C.; Solladié, G. *Tetrahedron* **1980**, 36, 227
- <sup>12</sup> (a) Klunder, J.M.; Sharpless, K.B. *J. Org. Chem.* **1987**, 52, 2598; (b) Pyne, S.G.; Hajipour, A.R.; Prabakaran, K. *Tetrahedron Lett.* **1994**, 35, 645; (c) Watanabe, Y.; Mase, N.; Tateyama, M.; Toru, T. *Tetrahedron: Asymmetry* **1999**, 10, 737
- <sup>13</sup> (a) Wudl, F.; Lee, T.B.K. *J. Am. Chem. Soc.* **1973**, 95, 6349; (b) Rebiere, F.; Kagan, H.B. *Tetrahedron Lett.* **1989**, 30, 3659; (c) Rebiere, F.; Samuel, O.; Ricard, L.; Kagan, H.B. *J. Org. Chem.* **1991**, 56, 5991; (d) Benson, S.C.; Snider, J.K. *Tetrahedron Lett.* **1991**, 32, 5885; (e) Han, Z.; Krishnamurphy, D.; Grover, P.; Fang, Q.K.; Senanayake, C.H. *J. Am. Chem. Soc.* **2002**, 124, 7880; (f) Cogan, D.A.; Liu, G.C.; Kim, K.J.; Backes, B.J.; Ellman, J.A. *J. Am. Chem. Soc.* **1998**, 120, 8011; (g) Weix, D.J.; Ellman, J.A. *Org. Lett.* **2003**, 5, 1317
- <sup>14</sup> (a) Fernandez, I.; Khiar, N.; Llera, J.M.; Alcudia, F. *J. Org. Chem.* **1992**, 57, 6789; (b) Khiar, N.; Fernandez, I.; Alcudia, F. *Tetrahedron Lett.* **1994**, 35, 5719
- <sup>15</sup> Mariz, R.; Luan, X.; Gatti, M.; Linden, A.; Dorta, R. *J. Am. Chem. Soc.* **2008**, 130, 2172

- 
- <sup>16</sup> Miashita, A.; Yasuda, A.; Takaya, H.; Toriumi, K.; Ito, T.; Souchi, T.; Noyori, R. *J. Am. Chem. Soc.* **1980**, *102*, 7933
- <sup>17</sup> (a) Bürgi, J.J.; Mariz, R.; Gatti, M.; Drinkel, E.; Luan, X.; Blumentritt, S.; Linden, A.; Dorta, R. *Angew. Chem. Int. Ed.* **2009**, *48*, 2768; (b) Mariz, R.; Poater, A.; Gatti, M.; Drinkel, E.; Bürgi, J.J.; Luan, X.; Blumentritt, S.; Linden, A.; Cavallo, L.; Dorta, R. *Chem. Eur. J.* **2010**, *16*, 14335
- <sup>18</sup> (a) Tokunoh, R.; Sodeoka, M.; Aoe, K.; Shibasaki, M. *Tetrahedron Lett.* **1995**, *36*, 8035; (b) Chen, J.; Chen, J.; Lang, F.; Zhang, X.; Cun, L.; Zhu, J.; Deng, J.; Liao, J. *J. Am. Chem. Soc.* **2010**, *132*, 4552
- <sup>19</sup> Liao, J.; Sun, X.; Cui, X.; Yu, K.; Zhu, J.; Deng, J. *Chem. Eur. J.* **2003**, *9*, 2611
- <sup>20</sup> Chen, J.; Li, D.; Ma, H.; Cun, L.; Zhu, J.; Deng, J.; Liao, J. *Tetrahedron Lett.*, **2008**, *49*, 6921
- <sup>21</sup> Priego, J.; Mancheno, O.G.; Cabrera, S.; Arrayas, R.G.; Llamas, T.; Carretero, J.C. *Chem. Commun.* **2002**, 2512
- <sup>22</sup> Hiroi, K.; Suzuki, Y.; Kawagishi, R. *Tetrahedron Lett.* **1999**, *40*, 715
- <sup>23</sup> Lang, F.; Li, D.; Chen, J.; Chen, J.; Li, L.; Cun, L.; Zhu, J.; Deng, J.; Liao, J. *Adv. Synth. Catal.* **2010**, *352*, 843

---

## Chapter 3

### Iridium-Catalysed Hydroamination

#### 3.1. Introduction

The abundance of nitrogen containing molecules in nature, especially in therapeutically active molecules, has meant that interest in finding selective methods of forming C-N bonds is high. Inter- and intramolecular hydroamination reactions of unactivated alkenes are becoming powerful tools for this, as they allow a wide range of structures to be formed. There are a few reports of iridium-catalysed intermolecular hydroamination with activated alkenes, such as the strained molecule norbornene. Probably the first example was from Milstein and co-workers,<sup>1</sup> later Togni and co-workers published an enantioselective version of this reaction, using the ferrocene based ligand Josiphos.<sup>2</sup> Finally, the most successful example of enantioselective hydroamination to norbornene was from Zhou and Hartwig, achieving high *e.e.*'s using phosphine ligands, such as (*R*)-DTBM-segphos (DTBM = 3,5-di-*tert*-butyl-4-methoxyphenyl), as shown in figure 1.<sup>3</sup>

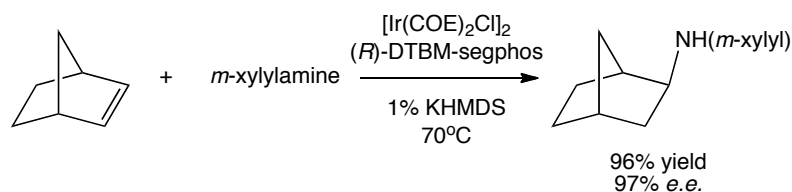


**Figure 1** Iridium-catalysed intermolecular hydroamination of norbornene

Until lately, there were no reports of iridium-catalysed intramolecular hydroamination reactions. These types of reactions have been catalysed by lanthanide,<sup>4</sup> early transition metal,<sup>5</sup> and late transition metal (including platinum,<sup>6</sup> rhodium,<sup>7</sup> gold<sup>8</sup> and copper<sup>9</sup>) complexes. In 2008, complexes of Rh and Ir with NHC pincer ligands were described as efficient catalysts for intramolecular hydroamination reactions, giving conversions up to 98%.<sup>10</sup> A year later, Stradiotto and co-workers

reported that the commercially available complex  $[\text{Ir}(\text{COD})\text{Cl}]_2$  (COD = cyclooctadiene) could also be used as a good precatalyst in the same reaction.<sup>11,12</sup>

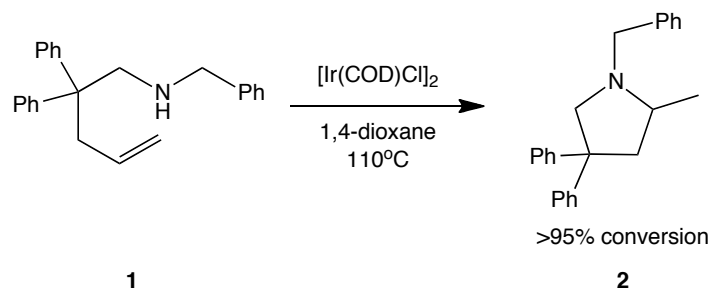


**Figure 2** Iridium catalysed intramolecular hydroamination with  $[\text{Ir}(\text{COD})\text{Cl}]_2$

The same group also developed iridium phosphino-phenolate complexes, which gave high conversions, but when a chiral version of the catalyst was made, no enantioselectivity was observed in the reaction.<sup>13</sup> The only example, to the best of our knowledge, of a late transition metal-catalysed asymmetric intramolecular hydroamination reactions is that of Buchwald, using mono-phosphine ligands with rhodium.<sup>7c</sup> However, there has so far been no iridium system catalysing the same reaction enantioselectively.

In the last 40 years there have been sporadic reports of bissulfoxide ligands being used in asymmetric catalysis,<sup>14</sup> sometimes with encouraging results. James and co-workers presented the first example in the 1970s.<sup>14a</sup> The ligand, **3** of figure 3, was based on the phosphine ligand diop, and was used in ruthenium-catalysed hydrogenation reactions, achieving enantioselectivities of up to 25% *e.e.* Following on from this Shibasaki and co-workers developed a method to synthesise **4**, and used the ligand in asymmetric palladium-catalysed allylic alkylations.<sup>14b</sup>

Our group then published bissulfoxide ligands **5** and **6**, based on the phosphine ligands BINAP (binaphthalene-2,2'-diyl-bis-diphenylphosphine) and BIPHEMP (dimethylbiphenyl-2,2'-diyl-bis(diphenylphosphine)). These ligands gave excellent results in enantioselective rhodium-catalysed 1,4-addition reactions of aryl boronic acids to enones.<sup>14c,f</sup> The latest contribution has been from Liao and co-workers with **7**. This ligand has also displayed outstanding results in rhodium-catalysed 1,4-additions.<sup>14e</sup> Another class of ligands that has appeared in the literature are chelating ligands binding through a sulfoxide and another heteroatom, where various applications were found in catalysis.<sup>15</sup>

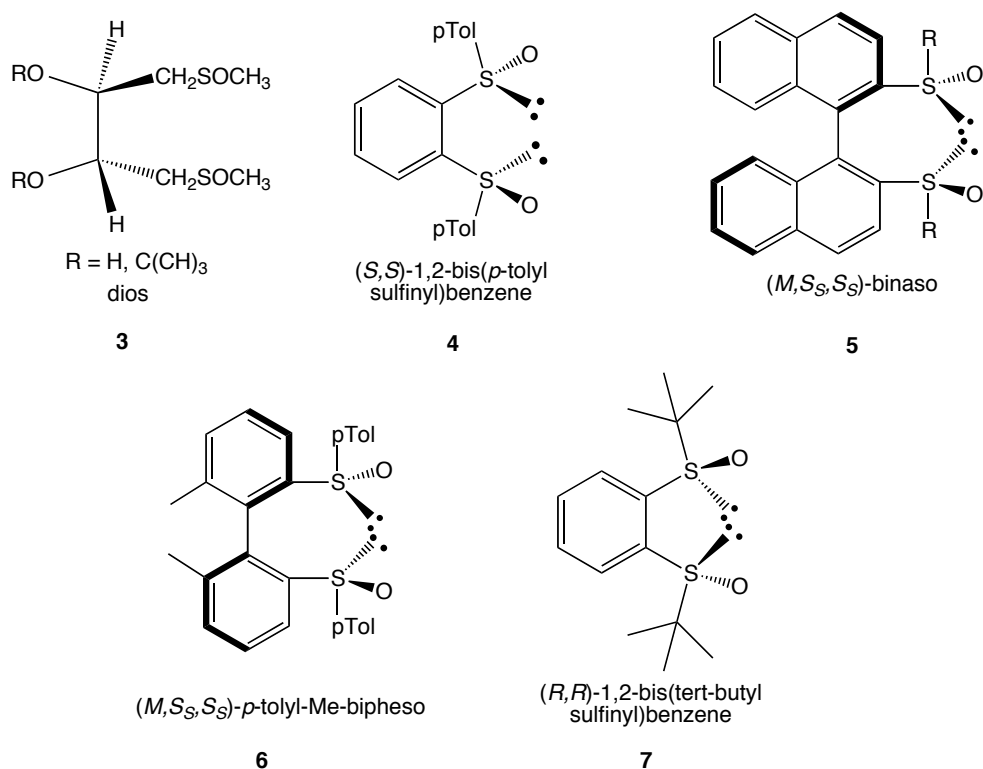


**Figure 3** Bissulfoxide ligands previously used in enantioselective catalysis

So far, there have been no reports of bissulfoxide ligands being used in catalysis with iridium. Within our group we have already tested bissulfoxide ligands in combination with rhodium, palladium and platinum.<sup>16</sup> A logical next step was to attempt to make iridium complexes with our bissulfoxide ligands and use these in catalysis.

### 3.2. Results and Discussion

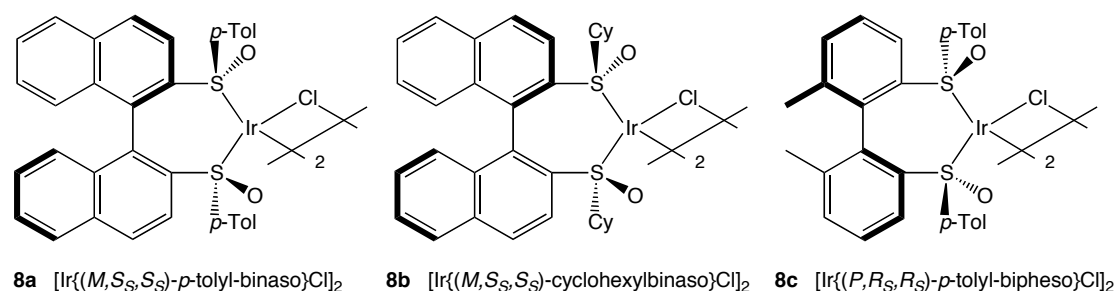


**Figure 4** Ir-bissulfoxide complexes previously synthesised in our lab

Our investigation into iridium catalysed intramolecular hydroamination reactions began with iridium-bissulfoxide complexes that had already been prepared in our lab (figure 4).<sup>17</sup> Unfortunately, **8a** gave only trace amounts of the hydroamination product. **8b** and **c** gave better yields, but disappointing selectivity (table 1).

**Table 1** Initial screening of catalysts for intramolecular hydroamination reaction

entry	catalyst	yield <sup>a</sup> %	<i>e.e.</i> <sup>b</sup> %
1	<b>8a</b>	trace	-
2	<b>8b</b>	31	6
3	<b>8c</b>	33	1
4	<b>9</b>	98	11
5	<b>10</b>	trace	-
6	<b>12</b>	84	22

<sup>a</sup> Isolated yield <sup>b</sup> Determined by HPLC, chiralcel OJ-H, see experimental section for more details

We decided to try other bissulfoxide ligands that have also been described previously. Ir complexes were made with **4** and **7**. [IrCl]<sub>2</sub> (**10**) could be made by reacting the ligand directly with [Ir(COE)<sub>2</sub>Cl]<sub>2</sub> at room temperature. However, [IrCl]<sub>2</sub> (**9**) had to be made *via* an Ir-ethylene intermediate by a method reported by Togni *et al.*<sup>2</sup> Only traces of hydroamination product were obtained when **10** was employed as a catalyst in the reaction. When **9** was used, good reactivity, but poor selectivity, was observed. In order to try and improve selectivity, a new hetero-bissulfoxide ligand was designed, based on **4** and **7**, with a <sup>t</sup>Bu-sulfoxide and a *p*-tolyl sulfoxide, **11** (figure 5). This ligand was synthesised in two steps from bromobenzene; in the first step, the bromobenzene was lithiated with *n*-BuLi and quenched with (*S*)-*tert*-butyl *tert*-butanethiosulfinate; in the second step the monosulfoxide was again lithiated and quenched with (-)-menthyl-(*S*)-*p*-tolyl sulfinate (see chapter 2 of this thesis for details). The Ir complex of this ligand was made by displacement of COE from [Ir(COE)<sub>2</sub>Cl]<sub>2</sub>.



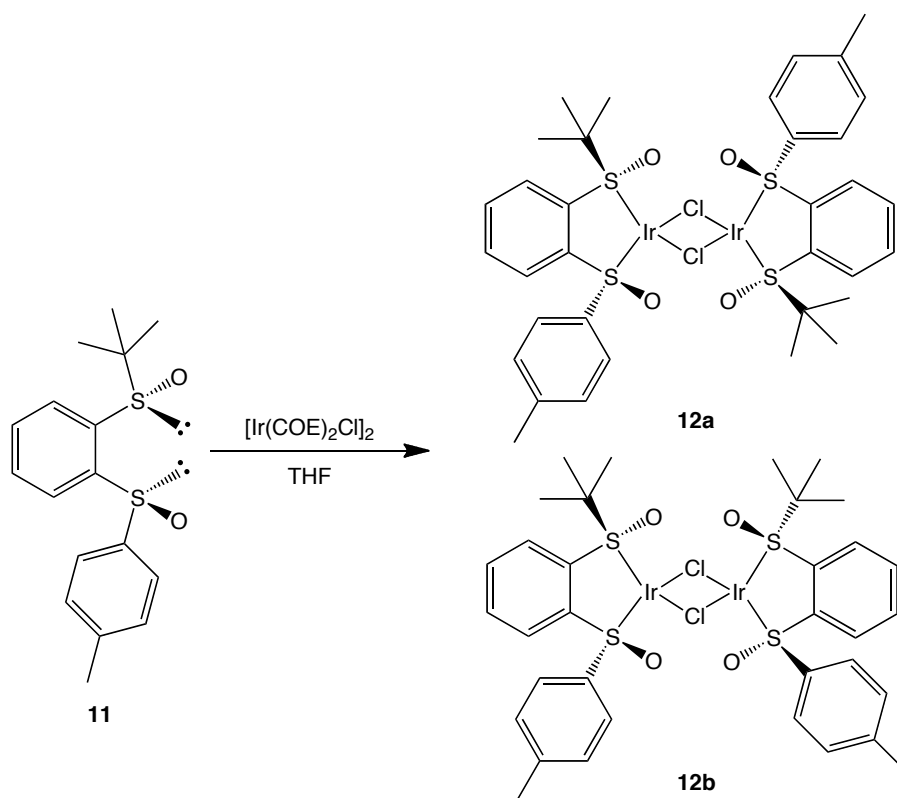


**Figure 5** Synthesis of  $[\text{Ir}(\mathbf{11})\text{Cl}]_2$ , **12**

NMR analysis of the complex formed revealed there to be two different compounds present. This was due to the  $C_1$ -symmetric nature of the ligand, and therefore there were two possible Ir-dimers that could form, **12a** and **b**. The mixture of these two complexes gave an improved result in the intramolecular hydroamination reaction, reaching a yield of 84% and an enantiomeric excess of 22%.

Encouraged by this result, a family of bis(sulfoxide) ligands were made with differently substituted sulfoxides (figure 6). The syntheses of these are described in the second chapter of this thesis. The chirality at sulfur for all these complexes was of (*S*)-configuration, except for **21**, which is the *meso* analogue of **11**.

Iridium chloro-bridged dimers analogous to **12** could be made with all the ligands by treating  $[\text{Ir}(\text{COE})_2\text{Cl}]_2$  directly with the ligand in a THF solution as shown in figure 5. As can be seen in table 2, the yields obtained in the formation of the iridium complexes were very high, except in the cases where the ligands were bulkier, *i.e.* ligands **19** and **20**. Interestingly a mixture of two isomers was observed in the  $^1\text{H}$  NMR spectra of all the complexes, except that made with ligand **20** (complex **33**). This is probably because the aryl substituent of this ligand is too sterically hindered, so only the isomer where these substituents are as far apart as possible forms.

Additionally, only one isomer was seen in the  $^1\text{H}$  NMR spectrum of complex **34**, although the reason for this is not clear.

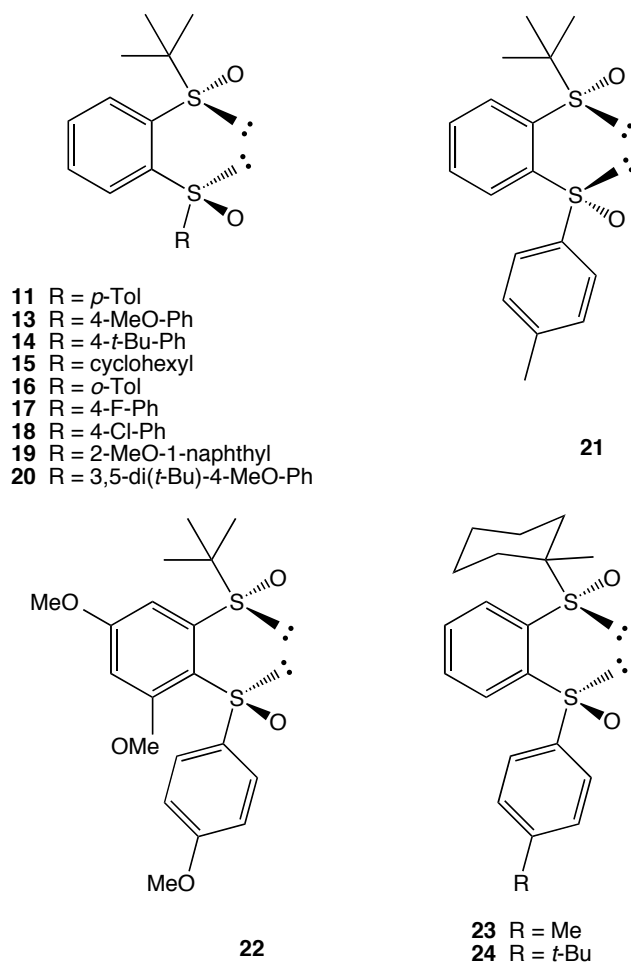


**Figure 6** Hetero-bissulfoxide ligands described in chapter 2 of this thesis

Ligand	Complex	Yield %
<b>11</b>	[Ir( <b>11</b> )Cl] <sub>2</sub> , <b>12</b>	93
<b>13</b>	[Ir( <b>13</b> )Cl] <sub>2</sub> , <b>26</b>	95
<b>14</b>	[Ir( <b>14</b> )Cl] <sub>2</sub> , <b>27</b>	98
<b>15</b>	[Ir( <b>15</b> )Cl] <sub>2</sub> , <b>28</b>	90
<b>16</b>	[Ir( <b>16</b> )Cl] <sub>2</sub> , <b>29</b>	90
<b>17</b>	[Ir( <b>17</b> )Cl] <sub>2</sub> , <b>30</b>	98
<b>18</b>	[Ir( <b>18</b> )Cl] <sub>2</sub> , <b>31</b>	98
<b>19</b>	[Ir( <b>19</b> )Cl] <sub>2</sub> , <b>32</b>	64
<b>20</b>	[Ir( <b>20</b> )Cl] <sub>2</sub> , <b>33</b>	76
<b>21</b>	[Ir( <b>21</b> )Cl] <sub>2</sub> , <b>34</b>	89
<b>22</b>	[Ir( <b>22</b> )Cl] <sub>2</sub> , <b>35</b>	94
<b>23</b>	[Ir( <b>23</b> )Cl] <sub>2</sub> , <b>36</b>	96
<b>24</b>	[Ir( <b>24</b> )Cl] <sub>2</sub> , <b>37</b>	95

**Table 2** Ligands and their corresponding Ir-complexes with yields from the complexation reaction

All of these complexes were then tested as catalysts in the intramolecular hydroamination reaction (table 3). As can be seen from entries 1-3, 6 and 7, varying the *para*-position of the aryl sulfoxide affected both reactivity and selectivity. Changing the *para*-substituent from methyl to the more bulky *tert*-butyl was favourable for both the yield and enantioselectivity. However, substituting for a methoxy group gave almost the same *e.e.* with a lower yield. Interestingly, when the *para*-position carried a halogen (entries 6 and 7) the selectivity was increased, but the reactivity was diminished. It is of note that we have previously observed that fluoro groups in bissulfoxide ligands give good selectivities in 1,4-addition reactions.<sup>18</sup>

**Table 3** Screening of ligands in intramolecular hydroamination

Reaction scheme: **1**  $\xrightarrow[\text{Toluene, 70}^\circ\text{C, 12h}]{\text{1 mol\% Ir cat.}}$  **2**

entry	catalyst	yield <sup>a</sup> %	<i>e.e.</i> <sup>b</sup> %
1	<b>12</b>	84	22
2	<b>26</b>	75	23
3	<b>27</b>	98	26
4	<b>28</b>	99	2
5	<b>29</b>	94	24
6	<b>30</b>	59	28
7	<b>31</b>	43	27
8	<b>32</b>	trace	n.d.
9	<b>33</b>	35	3
10	<b>34</b>	11	0
11	<b>35</b>	61	22
12	<b>36</b>	50	25
13	<b>37</b>	67	28

<sup>a</sup> Isolated yield <sup>b</sup> Determined by HPLC using chiralcel OJ-H column, see experimental section for more details.

Placing substituents on the *ortho*- and *meta*-positions of the aryl sulfoxide gave mixed results. An *o*-tolyl group on the sulfoxide (entry 5) improved both conversion and enantioselectivity when compared to the corresponding *p*-tolyl analogue (entry 1). Introducing *tert*-butyl groups onto the *meta*-positions of the aryl sulfoxide was

detrimental to both reactivity and selectivity (entry 9). Additionally, complex **32** with a 2-methoxy-naphthyl substituent gave almost no product. It is likely that the methoxy is also able to bind to iridium, deactivating the catalyst.

When the ligand contained two alkyl sulfoxide moieties (entry 4) the product **2** was obtained in excellent yield, but it was almost racemic. The (*R,S*)-bissulfoxide **21** also gave racemic product, and in very low yield (entry 10). It was thought that making the ligand more electron rich by putting methoxy substituents on the backbone might help the ligand form more stable complexes with iridium and improve the reactivity, unfortunately this didn't seem to be the case as can be seen by comparing entries 2 and 11. From the results obtained with complexes **12** and **26-35** (entries 1-11), we concluded that alterations to the aryl sulfoxide did not make drastic differences to the selectivity of the reaction. Therefore, the alkyl sulfoxide was substituted for a more bulky *ipso*-methylated cyclohexyl group to give ligands **23** and **24**. Disappointingly, these changes did not improve the selectivity of the hydroamination reaction greatly (entries 12 and 13). Indeed, the reactivity of the reaction was hampered by the inclusion of a more bulky alkyl sulfoxide.

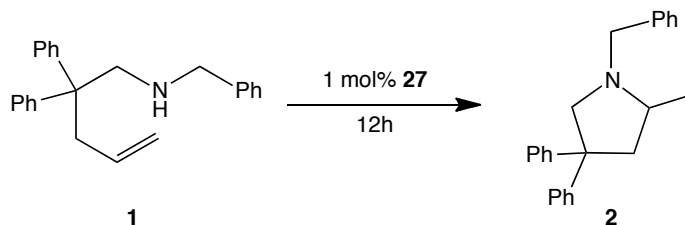
Following on from this, optimisation of the reaction was attempted using **27** as the precatalyst of choice. The reaction was attempted in different solvents and at different temperatures (table 4). Of the solvents tested, toluene was found to give the best compromise between reactivity and selectivity. Interestingly, when dichloromethane was used as the solvent, the selectivity was inverted (table 4, entry 4).

The neat reaction did not give much better selectivity, and led to diminished reactivity (entry 10). From the above results, it can be concluded that it does not seem possible to improve the enantioselectivity drastically by changing solvent alone. Polar solvents such as THF and EtOH seem to have a negative impact on the selectivity; possibly they bind to the metal and interfere with the reaction. The best result in terms of *e.e.* was achieved with pentane, the least polar solvent tested, although the yield was only moderate (entry 8).

It was seen that temperature affects both yield and selectivity during catalysis. The *e.e.* was increased by 14% by lowering the temperature by 30°C (entries 1 vs. 11). Unfortunately the reactivity was greatly sacrificed. Somewhat unexpectedly, increasing the temperature reduced not only the selectivity, but also diminished the

reactivity of the catalytic system (entry 13); we presume that the catalyst is destroyed over time at such high temperatures.

**Table 4** Screening of solvents and temperatures in intramolecular hydroamination reaction



entry	solvent	temp °C	yield <sup>a</sup> %	<i>e.e.</i> <sup>b</sup> %
1	toluene	70	98	26 ( <i>R</i> )
2	THF	70	82	11 ( <i>R</i> )
3	dioxane	70	83	23 ( <i>R</i> )
4	CH <sub>2</sub> Cl <sub>2</sub>	70	37	19 ( <i>S</i> )
5	EtOH	70	24	10 ( <i>R</i> )
6	hexane	70	37	30 ( <i>R</i> )
7	cyclohexane	70	65	27 ( <i>R</i> )
8	pentane	70	49	32 ( <i>R</i> )
9	heptane	70	23	30 ( <i>R</i> )
10	neat (no solvent)	70	40	28 ( <i>R</i> )
11	toluene	40	25	40 ( <i>R</i> )
12	toluene	50	27	32 ( <i>R</i> )
13	toluene	110	80	0

<sup>a</sup> Isolated yield. <sup>b</sup> Determined by HPLC, chiral OJ-H, see experimental section for details

Stradiotto and co-workers<sup>12</sup> reported that the use of 5 mol% HNEt<sub>3</sub>Cl was required as a co-catalyst in the [Ir(COD)Cl]<sub>2</sub> catalysed hydroamination of primary amino alkenes. Table 5 summarises results obtained in the standard reaction when additives were mixed in, and using 50°C as the reaction temperature. We tested 4 ammonium salts (entries 2-5) to investigate whether they increased the yield of **2** at 50°C in the reaction shown above (table 5). As can be seen in entry 2, NH<sub>4</sub>Cl increases the reactivity slightly, with no effect on the enantioselectivity of the reaction. HNEt<sub>3</sub>Cl and NBu<sub>4</sub>Br have a slight negative impact on both activity and selectivity (entries 3 and 4). It was thought that the ammonium salts could impede the reaction by competitively binding to the metal. Therefore, a bulky ammonium salt (entry 5) was

tested as co-catalyst; unfortunately the reactivity was still low. Addition of triflic acid to the reaction (entry 6) reduced the activity and led to racemic product.

**Table 5** Screening of additives in the intramolecular hydroamination reaction

1 2

entry	additive	yield <sup>a</sup> %	<i>e.e.</i> <sup>b</sup> %
1	-	27	32
2	NH <sub>4</sub> Cl	31	32
3	HNEt <sub>3</sub> Cl	18	29
4	NBu <sub>4</sub> Br	20	30
5		24	31
6	CF <sub>3</sub> SO <sub>3</sub> H	15	0
7	LiI	65	26
8	NaI	55	26
9	AgOTf	0	n.d.
10	AgBF <sub>4</sub>	0	n.d.
11	Ligand	0	n.d.

<sup>a</sup> Isolated yield. <sup>b</sup> Determined by HPLC, chiral OJ-H, see experimental section for details

The additives NaI and LiI (entries 7 and 8) increased the conversion of **1** to **2** considerably. The chlorides of the precatalyst are abstracted and replaced by iodide, which is a larger and more labile ligand, allowing the substrate to bind more easily to iridium. Conversely, adding AgOTf or AgBF<sub>4</sub> shuts down the reactivity (entries 9 and 10). It could be that the chloride is needed for catalysis, or the formed AgCl interferes with the reaction. An extra equivalent of ligand in the reaction also leads to no product; probably the ligand binds to the Ir, preventing the substrate from coordinating.

In the pursuit of higher yields and higher enantioselectivities we turned our attention to other iridium complexes with ligand **14**. A cationic iridium complex was made by

reacting ligand with  $[\text{Ir}(\text{COD})\text{Cl}]_2$  and then abstracting the chlorides with  $\text{NaBAr}_\text{F}$  (sodium tetrakis[(3,5-trifluoromethyl)phenyl] borate) in a manner similar to that used by Pfaltz *et al.*<sup>19</sup> The complex, **38**, could then be crystallised from ethanol to give bright red crystals suitable for X-ray analysis (figure 7).

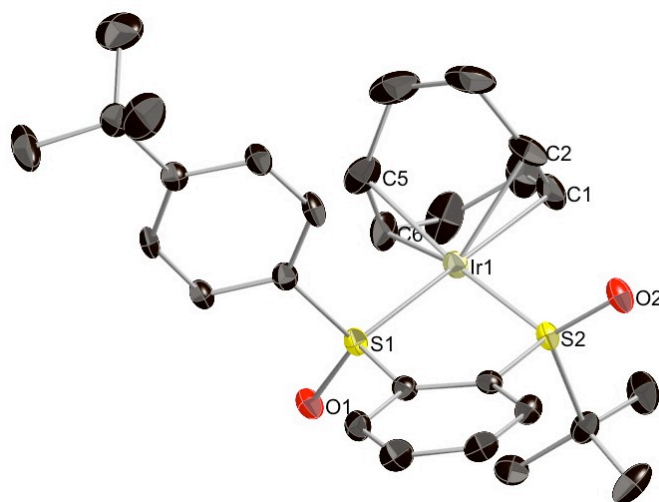


**Figure 7** Thermal ellipsoid drawing of **38**, at 50% probability. Hydrogen atoms and  $\text{BAr}_\text{F}^-$  are omitted for clarity. Selected bond lengths (Å) and angles (°): Ir1-S1, 2.264; Ir1-S2, 2.245; S1-O1, 1.464; S2-O2, 1.465; Ir1-C1, 2.220; Ir1-C2, 2.190; Ir1-C5, 2.247; Ir1-C6, 2.189; S1-Ir1-S2, 87.549; S1-Ir1-C2, 146.731; S2-Ir1-C6, 156.802; C1-Ir1-C2, 36.088; C5-Ir1-C6, 35.826; C1-Ir1-C6, 81.510; C2-Ir1-C5, 80.117.

Unfortunately the COD complex did not give any product when used as the precatalyst in the hydroamination reaction. Nevertheless, the crystal structure provides some useful information about the nature of ligation of the ligand to Ir. By looking at the bond lengths within the complex, it can be seen that the two sulfur atoms are not at equal distances from the iridium. The Ir-S2 bond is shorter by almost 0.02 Å, which is a significant difference in these types of compounds. This is as expected when the electronics of the two different sulfur atoms are considered. The *tert*-butyl group attached to S2 is more electron-donating than the aryl group attached to S1. This means that S2 is more electron rich than S1, so it is able to  $\sigma$ -donate more electron density to the metal centre, leading to a shorter, stronger bond. Upon close inspection of the structure, one can see that the COD ligand is tilted away from the *tert*-butyl attached to S2. This signifies that the steric bulk of this substituent does affect the binding of other ligands to the iridium. This might explain in part the observed enantioselectivity in catalysis when employing the neutral precatalysts described above.

### 3.3. Sulfinyl Phosphine Ligands

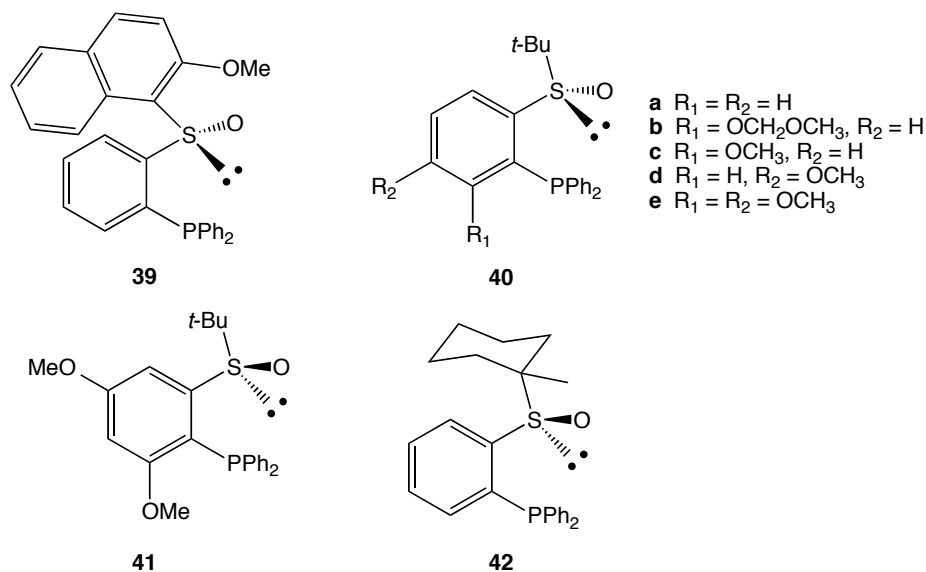


**Figure 8** Sulfinyl phosphine ligands

As well as bissulfoxide ligands, attempts were made to catalyse the hydroamination reaction with sulfinyl phosphine ligands of the type shown in figure 8. **39** was first published by Hiroi *et al.*<sup>20</sup> and was used as a ligand in palladium-catalysed allylic alkylation reactions. Ligand **40** was reported by Liao *et al.*<sup>21</sup> and used as a ligand in palladium-catalysed allylic alkylations, rhodium-catalysed 1,4-additions of boronic acids to enones and copper-catalysed additions of diethylzinc to diphenylphosphonyl imines. In many cases these ligands gave good yields and enantioselectivities in the aforementioned reactions. For the iridium-catalysed hydroamination reaction, the known ligand **40a** was tested, along with two new ligands, **41** and **42**.

The syntheses of iridium complexes with these ligands were attempted using both methods described (see experimental section). In each reaction, the <sup>1</sup>H NMR spectra of the isolated product revealed a complicated mixture of compounds. It was discovered, however, that these ligands could be used *in situ* in combination with [Ir(COE)<sub>2</sub>Cl]<sub>2</sub>. The catalytic mixture gave good yields and some selectivity; these results are shown in table 6. This was not the case for the bissulfoxide ligands, where the Ir complexes first had to be isolated and purified before they could be used in catalysis. Probably the sulfinylphosphine ligands bind more favourably with iridium, whereas the bissulfoxides compete with the amino alkene substrate. Contrary to what



was observed with the bissulfoxide ligands, the additional methoxy groups on the backbone of ligand **41** have a positive impact both on the reactivity and selectivity of the catalyst. Also, changing the *tert*-butyl substituent to a methylated cyclohexyl (ligand **42**) increased the reactivity, and slightly improved the enantioselectivity (entries 1 vs. 3).

**Table 6** Screening of sulfinylphosphine ligands in the intramolecular hydroamination reaction

entry	ligand	yield <sup>a</sup> %	<i>e.e.</i> <sup>b</sup> %
1	<b>40a</b>	80	18
2	<b>41</b>	85	25
3	<b>42</b>	88	19

<sup>a</sup> Isolated yield. <sup>b</sup> Determined by HPLC, chiral OJ-H, see experimental section for details

### 3.4. Summary

A range of novel bissulfoxide and sulfinylphosphine ligands have been presented and used in iridium-catalysed intramolecular hydroamination reactions. Good yields were obtained in these catalytic reactions, but the enantioselectivities were low. Different solvents, temperatures and additives were screened in an attempt to improve the selectivity of the catalytic reaction. Toluene was found to be the best solvent, with 70°C being the optimum temperature to keep reactivity high. From the screening of the catalysts, it was found that a bulky alkyl substituent on the sulfoxide was required to provide enantioselectivity in catalysis. A *tert*-butyl and a more bulky *ipso*-methylated cyclohexyl group were compared as the alkyl substituent. Although the bulkier group gave slightly higher enantioselectivity, the reactivity was lower. The *para* position of the aryl sulfoxide also affected the selectivity, but increasing steric bulk in the *meta* position did not improve selectivity. For the bissulfoxide ligands, making the ligand more electron-rich reduced reactivity and had no effect on selectivity. The best catalyst was **27**, [**1**-(*S*)-*tert*-butylsulfinyl]-2-(*S*)-4-*tert*-butyl-

phenylsulfinyl)benzene}IrCl]<sub>2</sub>, and this was used for screening the reaction conditions further.

For the bissulfoxide ligands, the iridium complex had to be formed and purified before it could be used in catalysis, but the sulfinylphosphine ligands could be used with [Ir(COE)<sub>2</sub>Cl]<sub>2</sub> to form the catalytic species *in situ*. In the case of the bissulfoxide ligands, it is possible that the ligand competes with the amino alkene starting material to bind to the metal, whereas the sulfinylphosphines are better ligands for iridium.

The results presented in this chapter are promising, but further work must be done towards improving the enantioselectivity of the reaction. More modifications to the ligand should be studied to better understand the relationship between the structure of the ligand and the activity. The reaction procedure can be varied further, for example, a greater range of additives can be screened. The substrate can be changed; the benzyl group could be substituted for a different moiety, or an internal alkene could be tested. Further insights into the mechanism of this transformation are needed in order to improve the catalytic behaviour.

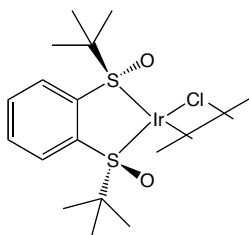
### 3.5. Experimental Section

All reactions were carried out using standard Schlenk or glovebox (Mecaplex or Innovative Technology) techniques under nitrogen. NMR spectra were collected on an AV2 400 MHz Bruker spectrometer. Solvents were purchased in the best quality available, degassed by purging thoroughly with nitrogen and dried over activated molecular sieves of appropriate size. Alternatively, they were purged with argon and passed through alumina columns in a solvent purification system (Innovative Technology). HPLC analysis was performed using JASCO series PU-2089/MD-2010 apparatus with chiralcel OJ-H column. Ligands were prepared according to previously described procedures.<sup>22</sup> [Ir(COE)<sub>2</sub>Cl]<sub>2</sub>, [Ir(COD)Cl]<sub>2</sub> and Benzyl(2,2-diphenyl-4-pentenyl)amine were prepared according to published procedures.<sup>23,24,6a</sup>

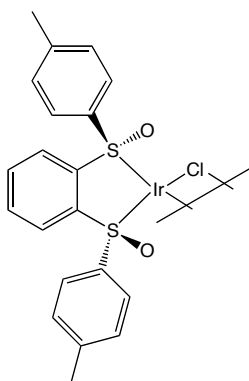
**General procedure for synthesis of iridium complexes (method 1):** A vial was charged with 80mg (0.089 mmol) [Ir(COE)<sub>2</sub>Cl]<sub>2</sub> and ligand (0.179 mmol). THF (3ml) was added to the solids, and the mixture was left stirring until the reaction became a clear, orange solution. The solvent was removed under high vacuum, and the orange

residue remaining was redissolved in CH<sub>2</sub>Cl<sub>2</sub> (1ml). The complex was precipitated as a yellow solid by adding pentane (20ml) slowly to the stirred solution. The vial was then centrifuged, so that the supernatant solvent could be decanted off by Pasteur pipette. The solid was washed twice with diethyl ether (2 x 5ml) and dried thoroughly under high vacuum. Solvents for NMR spectroscopy were degassed with nitrogen and dried over molecular sieves (4Å).

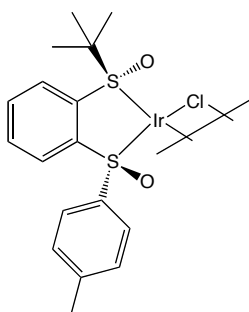
**General procedure for synthesis of iridium complexes (method 2):** A Schlenk tube was charged with 100mg (0.11 mmol) [Ir(COE)<sub>2</sub>Cl]<sub>2</sub> suspended in 10ml dry pentane. The suspension was cooled to 0°C and bubbled with ethylene gas for 10 minutes, after this time, the reaction changed appearance to a white suspension. This was subsequently cooled to -78°C, the ethylene bubbling stopped, and the nitrogen inlet opened. A solution of the ligand (0.056 mmol) was added dropwise, *via* dropping funnel, to the suspension below at -78°C. The reaction was allowed to slowly come to room temperature overnight. Solvent was removed *in vacuo* and the flask was taken inside the glovebox. The yellow residue was redissolved in 5ml CH<sub>2</sub>Cl<sub>2</sub> and transferred into a vial. To the stirred solution, 20ml diethyl ether was added dropwise by Pasteur pipette to precipitate a yellow solid. The vial was then centrifuged for ten minutes, so that the supernatant solvent could be removed by Pasteur pipette. The solid was washed twice more with diethyl ether (2 x 5ml) and dried thoroughly under high vacuum.



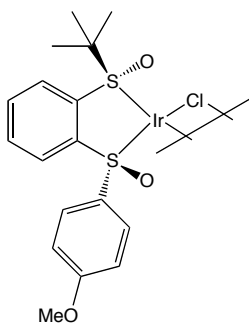
**[{(S,S)-1,2-bis(*tert*-butylsulfinyl)benzene}IrCl]<sub>2</sub> (9):** Made by method 2. Yellow solid, yield 76%. <sup>1</sup>H NMR (400 MHz, CDCl<sub>3</sub>): δ = 1.37 (s, 36H), 7.68-7.71 (m, 4H), 7.94-7.97 (m, 4H) ppm. <sup>13</sup>C NMR (400 MHz, CDCl<sub>3</sub>): δ = 25.29 (s), 71.28 (s), 125.55 (s), 132.43 (s), 143.04 (s) ppm. Elemental analysis: Calculated for Ir<sub>2</sub>C<sub>28</sub>H<sub>44</sub>O<sub>4</sub>S<sub>4</sub>Cl<sub>2</sub>·4CDCl<sub>3</sub>: C = 25.53%, H = 3.21%; Found: C = 25.48%, H = 3.43%.



**[(*S,S*)-1,2-bis(*p*-tolylsulfinyl)benzene]IrCl<sub>2</sub> (10):** Made by method 1. Yellow solid, yield 90%. <sup>1</sup>H NMR (400 MHz, CDCl<sub>3</sub>): δ = 2.39 (s, 12H), 7.26-7.28 (d, *J* = 8.0 Hz, 8H), 7.32-7.37 (m, 4H), 7.50-7.55 (m, 4H), 8.02-8.04 (d, *J* = 7.7 Hz, 8H) ppm. <sup>13</sup>C NMR (400 MHz, CDCl<sub>3</sub>): δ = 22.56 (s), 125.89 (s), 127.12 (s), 129.84 (s), 130.57 (s), 132.50 (s), 133.49 (s), 143.14 (s) ppm. Elemental analysis: Calculated for Ir<sub>2</sub>C<sub>40</sub>H<sub>36</sub>O<sub>4</sub>S<sub>4</sub>Cl<sub>2</sub>: C = 41.26%, H = 3.12%; Found: C = 41.31%, H = 3.35%.

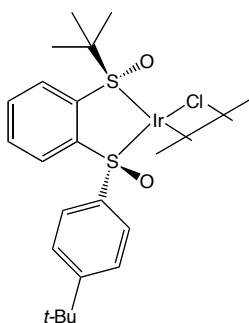


**[1-((*S*)-*tert*-butylsulfinyl)-2-((*S*)-*p*-tolylsulfinyl)benzene]IrCl<sub>2</sub> (12):** Made by method 1. Yellow solid, yield 93%. <sup>1</sup>H NMR (400 MHz, CDCl<sub>3</sub>): δ = 1.52 (s, 9H, 1<sup>st</sup> isomer), 1.57 (s, 9H, 2<sup>nd</sup> isomer), 2.38 (s, 3H), 7.22-7.26 (m, 3H), 7.40-7.54 (m, 3H), 7.87-7.96 (m, 2H) ppm. <sup>13</sup>C NMR (400 MHz, CDCl<sub>3</sub>): δ = 21.60 (s), 21.63 (s), 24.88 (s), 24.94 (s), 68.91 (s), 69.95 (s), 125.05 (s), 125.15 (s), 127.23 (s), 127.35 (s), 129.49 (s), 129.54 (s), 131.78 (s), 133.70 (s), 141.12 (s), 142.02 (s), 143.15 (s), 144.36 (s), 150.71 (s) ppm. Elemental analysis: Calculated for Ir<sub>2</sub>C<sub>34</sub>H<sub>40</sub>O<sub>4</sub>S<sub>4</sub>Cl<sub>2</sub>·2.2CDCl<sub>3</sub>: C = 31.99%, H = 3.13%; Found: C = 31.92%, H = 3.25%.



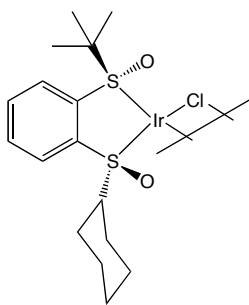
**[{1-((*S*)-*tert*-butylsulfinyl)-2-((*S*)-4-methoxy-phenylsulfinyl)benzene}IrCl]<sub>2</sub> (26):**

Made by method 1. Yellow solid, yield 95% <sup>1</sup>H NMR (400 MHz, CDCl<sub>3</sub>): δ = 1.52 (s, 9H, 1<sup>st</sup> isomer), 1.57 (s, 9H, 2<sup>nd</sup> isomer), 3.83 (s, 3H, 2<sup>nd</sup> isomer), 3.84 (s, 3H, 1<sup>st</sup> isomer), 6.91-6.97 (m, 2H), 7.42-7.51 (m, 3H), 7.86-7.90 (m, 1H), 8.01-8.07 (m, 2H) ppm. <sup>13</sup>C NMR (400 MHz, CDCl<sub>3</sub>): δ = 24.33 (s), 24.89 (s), 55.85 (s), 55.90 (s), 68.85 (s), 69.88 (s), 110.68 (s), 114.10 (s), 114.20 (s), 124.87 (s), 125.13 (s), 129.07 (s), 129.20 (s), 131.66 (s), 131.71 (s), 133.62 (s), 133.67 (s), 135.35 (s), 136.11 (s), 144.18 (s), 151.04 (s), 162.85 (s), 162.92 (s) ppm. Elemental analysis: Calculated for Ir<sub>2</sub>C<sub>34</sub>H<sub>40</sub>O<sub>6</sub>S<sub>4</sub>Cl<sub>2</sub>·2CDCl<sub>3</sub>: C = 31.63%, H = 3.10%; Found: C = 31.67%, H = 3.58%.

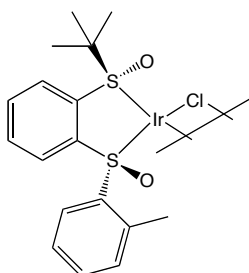


**[{1-((*S*)-*tert*-butylsulfinyl)-2-((*S*)-4-*tert*-butyl-phenylsulfinyl)benzene}IrCl]<sub>2</sub> (27):**

Made by method 1. Yellow solid, yield 98%. <sup>1</sup>H NMR (400 MHz, CDCl<sub>3</sub>): δ = 1.30 (s, 9H, 1<sup>st</sup> isomer), 1.32 (s, 9H, 2<sup>nd</sup> isomer), 1.53 (s, 3H, 2<sup>nd</sup> isomer), 1.58 (s, 3H, 1<sup>st</sup> isomer), 7.42-7.53 (m, 5H), 7.88-8.01 (m, 3H) ppm. <sup>13</sup>C NMR (400 MHz, CDCl<sub>3</sub>): δ = 24.91 (s), 24.95 (s), 29.92 (s), 31.41 (s), 35.24 (s), 68.91 (s), 70.00 (s), 125.16 (s), 125.82 (s), 125.96 (s), 127.02 (s), 127.22 (s), 131.67 (s), 131.77 (s), 133.65 (s), 133.73 (s), 141.01 (s), 141.92 (s), 143.87 (s), 144.39 (s), 150.67 (s), 151.04 (s), 155.86 (s), 156.05 (s) ppm. Elemental analysis: Calculated for Ir<sub>2</sub>C<sub>40</sub>H<sub>52</sub>O<sub>4</sub>S<sub>4</sub>Cl<sub>2</sub>·1.3C<sub>4</sub>H<sub>8</sub>O: C = 42.60%, H = 4.94%; Found: C = 42.79%, H = 4.88%.

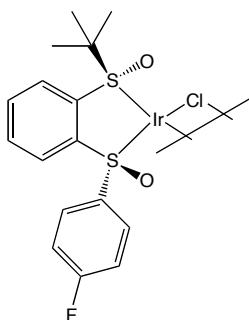


**[{1-((*S*)-*tert*-butylsulfinyl)-2-((*S*)-cyclohexylsulfinyl)benzene}IrCl]<sub>2</sub> (28):** Made by method 1. Yellow solid, yield 90%. <sup>1</sup>H NMR (400 MHz, CDCl<sub>3</sub>): δ = 1.08-1.94 (m, 9H), 1.39 (s, 9H, 1<sup>st</sup> isomer), 1.41 (s, 9H, 2<sup>nd</sup> isomer), 2.67-2.74 (m, 1H), 3.66-3.76 (m, 1H), 7.65-7.73 (m, 2H), 7.92-7.94 (d, *J* = 7.5 Hz, 1H), 7.98-8.02 (t, *J* = 8.1 Hz, 1H) ppm. <sup>13</sup>C NMR (400 MHz, CDCl<sub>3</sub>): δ = 24.98 (s), 25.04 (s), 25.71 (s), 25.75 (s), 25.77 (s), 25.87 (s), 26.03 (s), 27.33 (s), 28.01 (s), 28.07 (s), 70.02 (s), 70.13 (s), 74.02 (s), 74.07 (s), 124.35 (s), 124.39 (s), 125.28 (s), 125.37 (s), 132.37 (s), 132.39 (s), 133.65 (s), 133.68 (s), 144.44 (s), 145.43 (s), 145.47 (s) ppm. Elemental analysis: Calculated for Ir<sub>2</sub>C<sub>32</sub>H<sub>48</sub>O<sub>4</sub>S<sub>4</sub>Cl<sub>2</sub>·1.6CDCl<sub>3</sub>: C = 31.74%, H = 3.93%; Found: C = 31.66%, H = 4.10%.

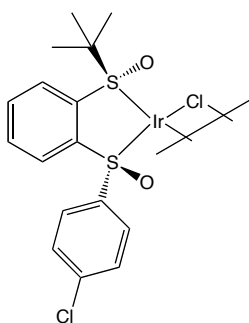


**[{1-((*S*)-*tert*-butylsulfinyl)-2-((*S*)-*o*-tolylsulfinyl)benzene}IrCl]<sub>2</sub> (29):** Made by method 1. Yellow solid, yield 90%. <sup>1</sup>H NMR (400 MHz, CDCl<sub>3</sub>): δ = 1.50 (s, 9H, 1<sup>st</sup> isomer), 1.61 (s, 9H, 2<sup>nd</sup> isomer), 2.37 (s, 3H, 1<sup>st</sup> isomer), 2.45 (s, 3H, 2<sup>nd</sup> isomer), 7.08-7.09 (d, *J* = 7.4 Hz, 1H, 1<sup>st</sup> isomer), 7.18-7.20 (d, *J* = 6.9 Hz, 1H, 2<sup>nd</sup> isomer), 7.28-7.47 (m, 4H), 7.55-7.59 (t, *J* = 7.6 Hz, 2H, 2<sup>nd</sup> isomer), 7.83-7.85 (d, *J* = 7.1 Hz, 1H, 2<sup>nd</sup> isomer), 7.94-7.97 (t, *J* = 7.4 Hz, 2H, 1<sup>st</sup> isomer), 8.19-8.21 (d, *J* = 6.7 Hz, 1H, 1<sup>st</sup> isomer) ppm. <sup>13</sup>C NMR (400 MHz, CDCl<sub>3</sub>): δ = 20.54 (s), 20.67 (s), 24.75 (s), 24.98 (s), 68.89 (s), 70.18 (s), 124.78 (s), 125.39 (s), 125.72 (s), 126.06 (s), 127.27 (s), 132.01 (s), 132.13 (s), 132.20 (s), 132.32 (s), 132.83 (s), 133.15 (s), 133.72 (s), 133.82 (s), 136.77 (s), 140.76 (s), 144.80 (s), 144.87 (s), 149.15 (s) ppm. Elemental

analysis: Calculated for  $\text{Ir}_2\text{C}_{34}\text{H}_{40}\text{O}_4\text{S}_4\text{Cl}_2 \cdot \text{CH}_2\text{Cl}_2$ : C = 35.59%, H = 3.58%; Found: C = 35.62%, H = 3.62%.

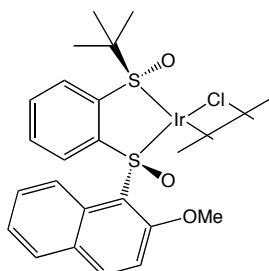


**[{1-((*S*)-*tert*-butylsulfinyl)-2-((*S*)-4-F-phenylsulfinyl)benzene}IrCl]<sub>2</sub> (30):** Made by method 1. Yellow solid, yield 98%. <sup>1</sup>H NMR (400 MHz, CDCl<sub>3</sub>): δ = 1.51 (s, 9H, 1<sup>st</sup> isomer), 1.56 (s, 9H, 2<sup>nd</sup> isomer), 7.11-7.17 (m, 2H), 7.39-7.56 (m, 3H), 7.89-7.92 (m, 1H), 8.06-8.11 (m, 2H) ppm. <sup>13</sup>C NMR (400 MHz, CDCl<sub>3</sub>): δ = 24.87 (s), 24.91 (s), 69.15 (s), 70.11 (s), 115.87 (s), 116.10 (s), 125.03 (s), 125.30 (s), 129.47 (s), 129.52 (s), 129.56 (s), 129.61 (s), 132.08 (s), 132.10 (s), 133.87 (s), 133.92 (s), 139.96 (s), 140.66 (s), 143.84 (s), 144.27 (s), 150.31 (s), 150.47 (s) ppm. <sup>19</sup>F NMR (400 MHz, CDCl<sub>3</sub>): δ = -107.04- -106.97 (m, 1F), -106.74- -106.67 (m, 1F) ppm. Elemental analysis: Calculated for  $\text{Ir}_2\text{C}_{32}\text{H}_{34}\text{F}_2\text{O}_4\text{S}_4\text{Cl}_2 \cdot 0.5\text{CDCl}_3$ : C = 33.53%, H = 2.99%; Found: C = 33.58%, H = 3.04%.



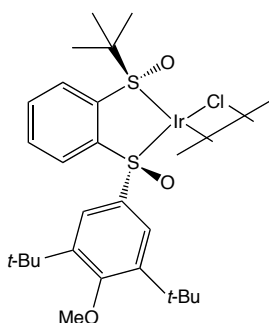
**[{1-((*S*)-*tert*-butylsulfinyl)-2-((*S*)-4-Cl-phenylsulfinyl)benzene}IrCl]<sub>2</sub> (31):** Made by method 1. Yellow solid, yield 98%. <sup>1</sup>H NMR (400 MHz, CDCl<sub>3</sub>): δ = 1.51 (s, 9H, 1<sup>st</sup> isomer), 1.56 (s, 9H, 2<sup>nd</sup> isomer), 7.38-7.58 (m, 5H), 7.89-7.92 (m, 1H), 7.98-8.01 (m, 2H) ppm. <sup>13</sup>C NMR (400 MHz, CDCl<sub>3</sub>): δ = 24.86 (s), 24.90 (s), 69.17 (s), 70.17 (s), 125.14 (s), 125.35 (s), 128.43 (s), 128.55 (s), 129.07 (s), 129.12 (s), 132.15 (s), 132.18 (s), 133.89 (s), 133.98 (s), 138.69 (s), 138.87 (s), 142.64 (s), 143.53 (s), 144.02 (s), 144.37 (s) ppm. Elemental analysis: Calculated for

$\text{Ir}_2\text{C}_{32}\text{H}_{34}\text{O}_4\text{S}_4\text{Cl}_4 \cdot 0.5\text{CDCl}_3$ : C = 32.61%, H = 2.91%; Found: C = 32.67%, H = 2.92%.



**[{1-((*S*)-*tert*-butylsulfinyl)-2-((*S*)-2-methoxynaphthyl-1-sulfinyl)benzene}IrCl]<sub>2</sub>**

**(32):** Made by method 1. Yellow solid, yield 64%. <sup>1</sup>H NMR (400 MHz, CDCl<sub>3</sub>): δ = 1.44 (s, 9H, 1<sup>st</sup> isomer), 1.67 (s, 9H, 2<sup>nd</sup> isomer), 4.00 (s, 3H, 1<sup>st</sup> isomer), 4.36 (s, 3H, 2<sup>nd</sup> isomer), 7.19-8.18 (m, 8H), 8.51-8.53 (d, *J* = 7.8 Hz, 1H, 2<sup>nd</sup> isomer), 8.63-8.65 (d, *J* = 7.9 Hz, 1H, 1<sup>st</sup> isomer), 8.82-8.88 (m, 1H) ppm. Elemental analysis: Calculated for  $\text{Ir}_2\text{C}_{42}\text{H}_{44}\text{O}_6\text{S}_4\text{Cl}_2 \cdot 0.4\text{CDCl}_3$ : C = 39.91%, H = 3.51%; Found: C = 39.82%, H = 3.25%.

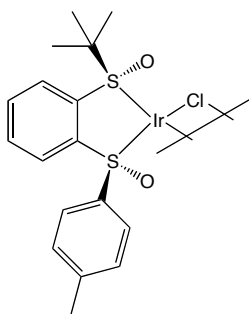


**[{1-((*S*)-*tert*-butylsulfinyl)-2-((*S*)-3,5-di-*tert*-butyl-4-methoxy-**

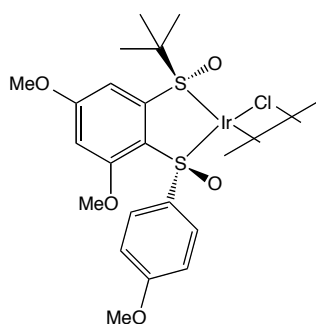
**phenylsulfinyl)benzene }IrCl]<sub>2</sub> (33):** Made by method 1. Yellow solid, yield 76%.

<sup>1</sup>H NMR (400 MHz, CDCl<sub>3</sub>): δ = 1.29 (s, 9H), 1.34 (s, 18H), 3.64 (s, 3H), 7.59-7.68 (m, 2H), 7.94-7.96 (d, *J* = 7.6 Hz, 1H), 8.07-8.09 (d, *J* = 7.7 Hz, 1H), 8.14 (s, 2H) ppm. <sup>13</sup>C NMR (400 MHz, CDCl<sub>3</sub>): δ = 25.06 (s), 32.00 (s), 36.54 (s), 64.75 (s), 68.76 (s), 125.59 (s), 125.90 (s), 126.48 (s), 132.42 (s), 133.46 (s), 140.00 (s), 144.71 (s), 145.48 (s), 150.34 (s), 162.84 (s) ppm. Elemental analysis: Calculated for  $\text{Ir}_2\text{C}_{50}\text{H}_{72}\text{O}_6\text{S}_4\text{Cl}_2 \cdot 0.5\text{CDCl}_3$ : C = 42.94%, H = 5.17%; Found: C = 42.91%, H = 5.14%.

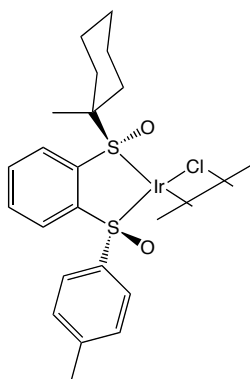




**[{1-((*S*)-*tert*-butylsulfinyl)-2-((*R*)-*p*-tolylsulfinyl)benzene}IrCl]<sub>2</sub> (34):** Made by method 1. Yellow solid, yield 89%. <sup>1</sup>H NMR (400 MHz, CDCl<sub>3</sub>): δ = 1.32 (s, 9H), 2.34 (s, 3H), 7.24-7.26 (d, *J* = 7.5 Hz, 2H), 7.61-7.69 (m, 2H), 7.96-7.98 (d, *J* = 7.7 Hz, 1H), 8.11-8.13 (d, *J* = 7.9, 1H), 8.14-8.16 (d, *J* = 8.2 Hz, 2H) ppm. Elemental analysis: Calculated for Ir<sub>2</sub>C<sub>34</sub>H<sub>40</sub>O<sub>4</sub>S<sub>4</sub>Cl<sub>2</sub>·1.2CDCl<sub>3</sub>: C = 34.11%, H = 3.35%; Found: C = 34.01%, H = 3.29%.

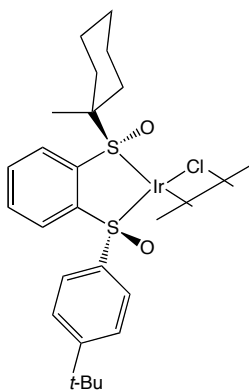


**[{1,3-dimethoxy-4-((*S*)-*p*-methoxy-phenylsulfinyl)-5-((*S*)-*tert*-butylsulfinyl)benzene }IrCl]<sub>2</sub> (35):** Made by method 1. Yellow solid, yield 94%. <sup>1</sup>H NMR (400 MHz, CDCl<sub>3</sub>): δ = 1.50 (s, 9H, 1<sup>st</sup> isomer), 1.57 (s, 9H, 2<sup>nd</sup> isomer), 3.47 (s, 3H, 1<sup>st</sup> isomer), 3.50 (s, 3H, 2<sup>nd</sup> isomer), 3.80 (s, 3H), 3.85 (s, 3H), 6.34 (s, 1H, 1<sup>st</sup> isomer), 6.36 (s, 1H, 2<sup>nd</sup> isomer), 6.83-6.89 (m, 3H), 7.89-7.91 (d, *J* = 8.6 Hz, 2H) ppm. <sup>13</sup>C NMR (400 MHz, CDCl<sub>3</sub>): δ = 24.93 (s), 25.08 (s), 55.74 (s), 55.85 (s), 56.08 (s), 56.13 (s), 56.50 (s), 56.54 (s), 68.84 (s), 70.14 (s), 100.96 (s), 103.53 (s), 113.04 (s), 113.10 (s), 128.49 (s), 129.14 (s), 129.37 (s), 136.98 (s), 149.50 (s), 150.02 (s), 156.51 (s), 156.93 (s), 162.00 (s), 164.93 (s) ppm. Elemental analysis: Calculated for Ir<sub>2</sub>C<sub>38</sub>H<sub>48</sub>O<sub>10</sub>S<sub>4</sub>Cl<sub>2</sub>·0.2CDCl<sub>3</sub>: C = 36.05%, H = 3.83%; Found: C = 36.12%, H = 3.74%.



**[{1-((*S*)-1-methyl-cyclohexylsulfinyl)-2-((*S*)-*p*-tolylsulfinyl)benzene }IrCl]<sub>2</sub> (36):**

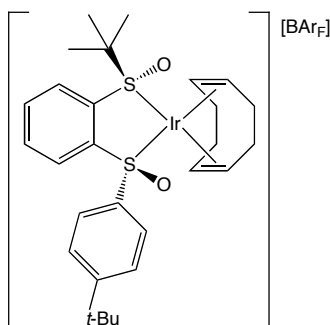
Made by method 1. Yellow solid, 96% yield. <sup>1</sup>H NMR (400 MHz, CDCl<sub>3</sub>): δ = 0.83-0.87 (m, 1H), 1.18-1.62 (m, 10H), 1.79-2.02 (m, 4H), 2.25-2.57 (m, 5H), 7.22-7.24 (d, *J* = 6.8 Hz, 2H), 7.36-7.51 (m, 3H), 7.85-7.86 (d, *J* = 7.7 Hz, 1H), 7.91-7.99 (m, 2H) ppm. <sup>13</sup>C NMR (400 MHz, CDCl<sub>3</sub>): δ = 17.95 (s), 21.61 (s), 22.68 (s), 22.91 (s), 25.52 (s), 30.96 (s), 32.95 (s), 125.11 (s), 125.48 (s), 127.27 (s), 129.47 (s), 131.61 (s), 133.50 (s), 142.03 (s), 143.12 (s), 143.94 (s), 152.12 (s) ppm. Elemental analysis: Calculated for Ir<sub>2</sub>C<sub>40</sub>H<sub>48</sub>O<sub>4</sub>S<sub>4</sub>Cl<sub>2</sub>·0.6CDCl<sub>3</sub>: C = 39.07%, H = 3.93%; Found: C = 39.15%, H = 3.85%.



**[{1-((*S*)-1-methyl-cyclohexylsulfinyl)-2-((*S*)-*p*-*tert*-butyl-phenylsulfinyl)benzene**

**}IrCl]<sub>2</sub> (37):** Made by method 1. Yellow solid, 95% yield. <sup>1</sup>H NMR (400 MHz, CDCl<sub>3</sub>): δ = 1.30 (s, 9H, major isomer), 1.32 (s, 9H, minor isomer), 1.36-1.63 (m, 4H), 1.44 (s, 3H), 1.78-2.02 (m, 4H), 2.24-2.53 (m, 2H), 7.40-7.51 (m, 5H), 7.84-7.88 (m, 1H), 7.94-8.02 (m, 2H) ppm. <sup>13</sup>C NMR (400 MHz, CDCl<sub>3</sub>): δ = 17.92 (s), 22.68 (s), 22.90 (s), 25.54 (s), 30.98 (s), 31.42 (s), 33.00 (s), 35.25 (s), 74.00 (s), 125.22 (s), 125.47 (s), 125.80 (s), 127.07 (s), 131.61 (s), 133.53 (s), 141.84 (s), 143.93 (s), 151.07 (s), 156.03 (s) ppm. Elemental analysis: Calculated for

Ir<sub>2</sub>C<sub>40</sub>H<sub>48</sub>O<sub>4</sub>S<sub>4</sub>Cl<sub>2</sub>.0.5C<sub>4</sub>H<sub>8</sub>O: C = 44.46%, H = 4.98%; Found: C = 44.46%, H = 4.90%.



**Procedure for Synthesis of [ $\{1-((S)\text{-tert-butylsulfinyl})\text{-}2-((S)\text{-}4\text{-tert-butylphenylsulfinyl})\text{benzene}\}\text{Ir}(\text{COD})\}\text{[BarF]}$  (25):** A 50 ml Schlenk tube was charged with 46.3 mg (0.07 mmol) [Ir(COD)Cl]<sub>2</sub> and 50 mg (0.14 mmol) 1-((*S*)-*tert*-butylsulfinyl)-2-((*S*)-4-*tert*-butylphenylsulfinyl)benzene. 4ml dry CH<sub>2</sub>Cl<sub>2</sub> was added to the flask, and the solution was heated to reflux for 1 hour, in which time the reaction became deep red. The solution was then allowed to cool to room temperature and 183.4 mg (0.21 mmol) NaBAR<sub>F</sub> was added as a solid, followed by 4ml deoxygenated H<sub>2</sub>O. The reaction was left stirring for 10 minutes and then the phases were separated. The aqueous phase was extracted three times with CH<sub>2</sub>Cl<sub>2</sub>; the combined organic phases were washed with H<sub>2</sub>O, and then dried over MgSO<sub>4</sub>. The solvent was removed and the red solid was redissolved in 1ml EtOH. Pentane was added to the solution and the complex began to crystallise. The crystallising solution was left in the fridge overnight, after which the red crystals were filtered giving 83% yield from the reaction. <sup>1</sup>H NMR (400 MHz, CDCl<sub>3</sub>): δ = 1.30 (s, 9H), 1.50 (s, 9H), 1.73-1.81 (m, 1H), 1.87-1.97 (m, 1H), 2.11-2.40 (m, 4H), 2.48-2.58 (m, 1H), 2.68-2.74 (m, 1H), 4.03-4.08 (m, 1H), 5.05-5.10 (m, 1H), 5.73-5.76 (m, 1H), 6.13-6.17 (m, 1H), 7.49 (s, 4H), 7.52-7.54 (d, *J* = 7.9 Hz, 1H), 7.60-7.64 (m, 4H), 7.68-7.72 (m, 9H), 7.77-7.81 (t, *J* = 7.5 Hz, 1H), 7.95-7.97 (d, *J* = 7.9 Hz, 1H) ppm. <sup>13</sup>C NMR (400 MHz, CDCl<sub>3</sub>): δ = 25.61 (s), 27.51 (s), 27.79 (s), 31.10 (s), 34.12 (s), 35.72 (s), 77.50 (s), 85.67 (s), 85.67 (s), 95.42 (s), 100.08 (s), 106.72 (s), 117.68 (q, *J* = 3.8 Hz), 120.7 (s), 123.42 (s), 125.50 (s), 126.13 (s), 126.47 (s), 127.66 (s), 128.38 (s), 128.83-129.33 (m), 135.02 (s), 135.50 (s), 137.12 (s), 137.15 (s), 138.85 (s), 145.32 (s), 159.42 (s), 161.93 (q, *J* = 49.1 Hz) ppm. <sup>19</sup>F NMR (400 MHz, CDCl<sub>3</sub>): δ = -62.39 (s)

ppm. Elemental analysis: Calculated for  $\text{IrC}_{60}\text{H}_{50}\text{O}_2\text{BF}_{24}\text{S}_2$ : C = 47.22%, H = 3.30%; Found: C = 47.34%, H = 3.42%.

**General Procedure for Catalytic Intramolecular Hydroamination Reactions:** A vial was charged with 81.9 mg (0.25 mmol) **1**, Ir complex (0.0025 mmol) and 1ml dry toluene inside the glovebox. A stirring bar was added and the vial was sealed with a cap with a PTFE septum. The vial was removed from the glovebox and placed into an oilbath at 70°C. After 12 hours, the vial was allowed to cool to room temperature and the reaction mixture was then transferred into a 100ml round bottomed flask with 1.5g silica gel and 30ml  $\text{CH}_2\text{Cl}_2$ . The solvent was removed *in vacuo* and the impregnated silica was applied to the top of a silica gel column. The product was eluted using 4% ethyl acetate in hexane. The product, **2**, was obtained as a white solid and was analysed by  $^1\text{H}$  NMR spectra, which were compared to literature.<sup>7</sup> The *e.e.* of **2** was analysed by chiral HPLC. HPLC conditions: chiralcel OJ-H column (hexane/*i*-PrOH, 99:1, 1 mlmin<sup>-1</sup>);  $t_R$  21.1 min (minor),  $t_R$  38.4 min (major).

**General Procedure for *in situ* Catalytic Intramolecular Hydroamination Reactions:** A vial was charged with 81.9 mg (0.25 mmol) **1**, 2.2 mg (0.0025 mmol)  $[\text{Ir}(\text{COE})_2\text{Cl}]_2$ , sulfinylphosphine ligand (0.005 mmol) and 1ml dry toluene inside the glovebox. A stirring bar was added and the vial was sealed with a cap with a PTFE septum. The vial was removed from the glovebox and placed into an oilbath at 70°C for 12 hours. The work-up and analysis of the reaction was carried out as above.

---

### 3.6. References

- <sup>1</sup> Casalnuovo, A.L.; Calabrese, J.C.; Milstein, D. *J. Am. Chem. Soc.* **1988**, *110*, 6738
- <sup>2</sup> Dorta, R.; Egli, P.; Zürcher, F.; Togni, A. *J. Am. Chem. Soc.* **1997**, *119*, 10857
- <sup>3</sup> Zhou, J.; Hartwig, J. *J. Am. Chem. Soc.* **2008**, *130*, 12220
- <sup>4</sup> (a) Hong, S.; Marks, T.J. *Acc. Chem. Res.* **2004**, *37*, 673; (b) Tobisch, S. *J. Am. Chem. Soc.* **2005**, *127*, 11979; (c) Gribkov, D.V.; Hultzs, K.C.; Hampel, F. *J. Am. Chem. Soc.* **2006**, *128*, 3748
- <sup>5</sup> (a) Tobisch, S. *Chem. Eur. J.* **2008**, *14*, 8590; (b) Zi, G.; Zhang, F.; Xiang, L.; Chen, Y.; Fang, W.; Song, H. *Dalton Trans.* **2010**, *39*, 4048
- <sup>6</sup> (a) Bender, C.F.; Widenhoefer, R.A. *J. Am. Chem. Soc.* **2005**, *127*, 1070; (b) Liu, C.; Bender, C.F.; Han, X.; Widenhoefer, R.A. *Chem. Commun.* **2007**, 3607; (c) Bender, C.F.; Hudson, W.B.; Widenhoefer, R.A. *Organometallics* **2008**, *27*, 2356

- <sup>7</sup> (a) Liu, Z.; Hartwig, J.F. *J. Am. Chem. Soc.* **2008**, *130*, 1570; (b) Julian, L.D.; Hartwig, J.F. *J. Am. Chem. Soc.* **2010**, *132*, 13813; (c) Shen, X.; Buchwald, S.L. *Angew. Chem. Int. Ed.* **2010**, *49*, 564
- <sup>8</sup> (a) Han, X.; Widenhoefer, R.A. *Angew. Chem. Int. Ed.* **2006**, *45*, 1747; (b) Bender, C.F.; Widenhoefer, R.A. *Chem. Commun.* **2006**, 4143; (c) Zhang, Z.; Bender, C.F.; Widenhoefer, R.A. *J. Am. Chem. Soc.* **2007**, *129*, 14148; (d) LaLonde, R.L.; Sherry, B.D.; Kang, E.J.; Toste, F.D. *J. Am. Chem. Soc.* **2007**, *129*, 2452; (e) Zhang, Z.; Bender, C.F.; Widenhoefer, R.A. *Org. Lett.* **2007**, *9*, 2887
- <sup>9</sup> Zeng, W.; Chemler, S.R. *J. Am. Chem. Soc.* **2007**, *129*, 12948
- <sup>10</sup> Bauer, E.B.; Andavan, G.T.S.; Hollis, T.K.; Rubio, R.J.; Cho, J.; Kuchenbeiser, G.R.; Helgert, T.R.; Letko, C.S.; Tham, F.S. *Org. Lett.* **2008**, *10*, 1175
- <sup>11</sup> Hesp, K.D.; Stradiotto, M. *Org. Lett.* **2009**, *11*, 1449
- <sup>12</sup> Hesp, K. D.; Tobisch, S.; Stradiotto, M. *J. Am. Chem. Soc.* **2010**, *132*, 413
- <sup>13</sup> Hesp, K.D.; McDonald, R.; Stradiotto, M. *Can. J. Chem.* **2010**, *88*, 700
- <sup>14</sup> (a) James, B.R.; McMillan, R.S. *Can. J. Chem.* **1977**, *55*, 3927; (b) Tokunoh, R.; Sodeoka, M.; Aoe, K.; Shibasaki, M. *Tetrahedron Lett.* **1995**, *36*, 8035; (c) Mariz, R.; Luan, X.; Gatti, M.; Linden, A.; Dorta, R. *J. Am. Chem. Soc.* **2008**, *130*, 2172; (d) Mariz, R.; Bürgi, J.J.; Gatti, M.; Drinkel, E.; Luan, X.; Dorta, R. *Chimia* **2009**, *63*, 508; (e) Chen, J.; Chen, J.; Lang, F.; Zhang, X.; Cun, L.; Zhu, J.; Deng, J.; Liao, J. *J. Am. Chem. Soc.* **2010**, *132*, 4552; (f) Bürgi, J.J.; Mariz, R.; Gatti, M.; Drinkel, E.; Luan, X.; Blumentritt, S.; Linden, A.; Dorta, R. *Angew. Chem. Int. Ed.* **2009**, *48*, 2768
- <sup>15</sup> (a) Allen, J.V.; Bower, J.F.; Williams, J.M.J. *Tetrahedron: Asymmetry* **1994**, *5*, 1895; (b) Hiroi, K.; Suzuki, Y.; Ikuko, A.; Hasegawa, Y.; Suzuki, K. *Tetrahedron: Asymmetry* **1998**, *9*, 3797; (c) Hiroi, K.; Suzuki, Y.; Abe, I.; Kawagishi, R. *Tetrahedron* **2000**, *56*, 4701; (d) Hiroi, K.; Izawa, I.; Takizawa, T.; Kawai, K. *Tetrahedron* **2004**, *60*, 2155; (e) Chen, J.; Li, D.; Ma, H.; Cun, L.; Zhu, J.; Deng, J.; Liao, J. *Tetrahedron Lett.* **2008**, *49*, 6921; (f) Han, F.; Chen, J.; Zhang, X.; Liu, J.; Cun, L.; Zhu, J.; Deng, J.; Liao, J. *Tetrahedron Lett.* **2011**, *52*, 830
- <sup>16</sup> *Unpublished Results*
- <sup>17</sup> Details regarding the preparation of these complexes are described in the master theses of M. Bigi and the doctoral thesis of R. Mariz.
- <sup>18</sup> Mariz, R.; Poater, A.; Gatti, M.; Drinkel, E.; Bürgi, J.J.; Luan, X.; Blumentritt, S.; Linden, A.; Cavallo, L.; Dorta, R. *Chem. Eur. J.* **2010**, *16*, 14335
- <sup>19</sup> Lightfoot, A.; Schnider, P.; Pfaltz, A. *Angew. Chem. Int. Ed.* **1998**, *37*, 2897
- <sup>20</sup> Hiroi, K.; Suzuki, Y.; Kawagishi, R. *Tetrahedron Lett.* **1999**, *40*, 715
- <sup>21</sup> (a) Chen, J.; Li, D.; Ma, H.; Cun, L.; Zhu, J.; Deng, J.; Liao, J. *Tetrahedron Lett.* **2008**, *49*, 6921; (b) Chen, J.; Lang, F.; Li, D.; Cun, L.; Zhu, J.; Deng, J.; Liao, J. *Tetrahedron: Asymmetry* **2009**, *20*, 1953; (c) Lang, F.; Li, D.; Chen, J.; Chen, J.; Li, L.; Cun, L.; Zhu, J.; Deng, J.; Liao, J. *Adv. Synth. Catal.* **2010**, *352*, 843
- <sup>22</sup> Synthesis of ligands is described in chapter 2
- <sup>23</sup> van der Ent, A.; Onderdelinden, A.L. *Inorg. Synth.* **1990**, *28*, 90
- <sup>24</sup> Herde, J.L.; Lambert, J.C.; Senoff, C.V.; Cushing, M.A. *Inorg. Synth.* **1974**, *15*, 18

---

## Chapter 4

### Synthesis, Structure and Catalytic Studies of Novel Palladium and Platinum Bissulfoxide Complexes

#### 4.1. Introduction

The binding of sulfoxides with transition metals has been of interest for many years,<sup>1</sup> and many complexes with sulfoxide ligands, particularly dimethylsulfoxide (DMSO), are known and well characterised. It was observed very early on that sulfoxides were ambidentate in nature,<sup>2</sup> and depending on the metal and the steric environment, could bind through S or O. Another interesting feature of sulfoxides is their chirality when dissymmetrically substituted. This makes them good candidates for the design of chiral ligands for enantioselective catalysis. The synthesis of enantiopure sulfoxides has been well studied,<sup>3</sup> and they are generally optically stable up to temperatures as high as 200°C. A few studies have demonstrated the use of chiral sulfoxide ligands in enantioselective catalysis, with excellent results in some cases.<sup>4,5</sup> Successful examples though, where the only chelating moieties are sulfoxides are still sporadic.<sup>5</sup>

Complexes of bissulfoxide ligands with palladium and platinum are known,<sup>5b,6</sup> but there are not many reports of them being used successfully in catalysis. The only examples reported are from the groups of Shibasaki<sup>5b</sup> and White,<sup>6c</sup> using palladium bissulfoxides. Following the success of bissulfoxide ligands developed in our lab in Rh catalysis,<sup>5c,f</sup> we decided to study complexes of these ligands with palladium and platinum, with the goal of using them in catalysis. In this chapter, these complexes are presented along with some preliminary catalytic results.

For several of the complexes, it was possible to grow crystals suitable for X-ray crystallographic analysis. From these analyses we were able to more thoroughly understand the nature of the binding of these types of ligands, and also to see how the presence of other ligands in the complex affects the binding of bissulfoxides to metals. We observed that *trans*-influences are important in determining the stability of

the complex. These effects have previously been studied in platinum DMSO complexes.<sup>7</sup>

The ligand used for most of the following studies was *p*-tolyl-binaso, **1**, previously developed in our lab, and based on the well-known diphosphine ligand binap developed by Noyori.<sup>8</sup> The synthesis of this ligand was carried out in a one-step procedure with commercially available starting materials, see figure 1.<sup>5c</sup>

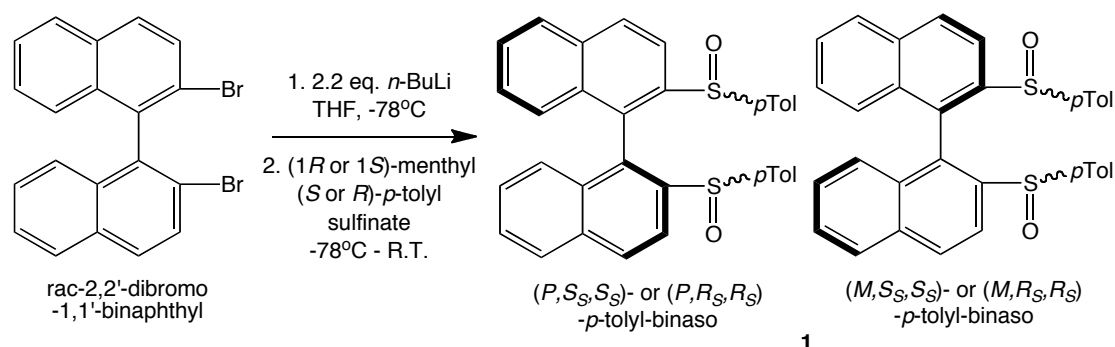


**Figure 1** Synthesis of *p*-tolyl-binaso

When enantiopure sulfinate was used, two diastereomers of the ligand were obtained, either (*P,S,S,S*)- and (*M,S,S,S*)-**1**, or (*P,R,S,S*)- and (*M,R,S,S*)-**1**. These could be separated by column chromatography. In the following work we used mainly the (*M,S,S,S*)- isomer.

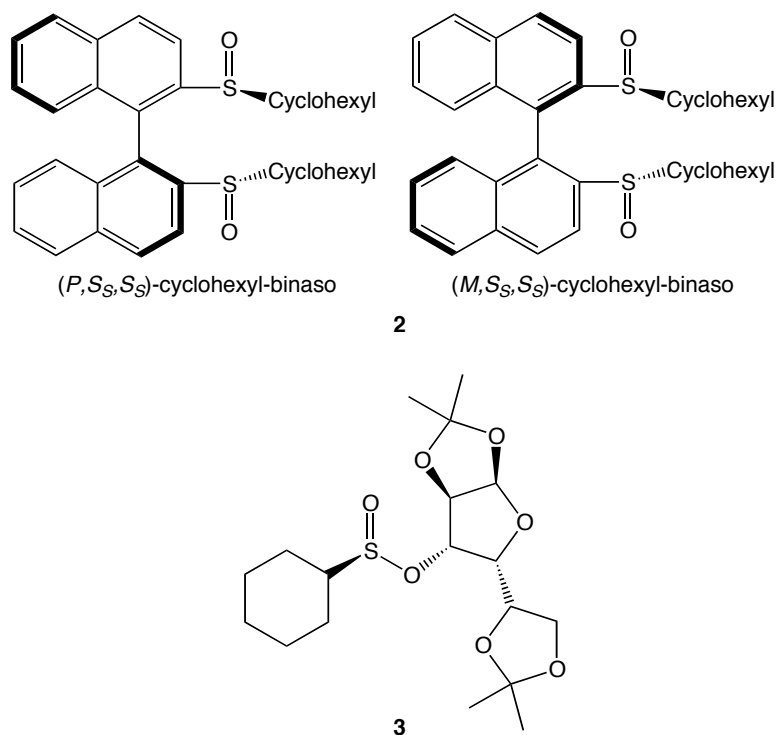


**Figure 2** Cyclohexyl-binaso and DAG-(*S*)-cyclohexylsulfinate



Another related ligand, (*M,S,S,S*)-cyclohexyl-binaso, was also used in studies with palladium and platinum reported here. This ligand was made by the same procedure, as shown in figure 1, except the sulfinate used was DAG-(*S*)-cyclohexylsulfinate **3** (DAG = 1,2:5,6-Di-*O*-isopropylidene- $\alpha$ -D-glucofuranosyl) to give two diastereoisomers of ligand **2** (Figure 2).<sup>9</sup>

## 4.2. Results and Discussion

Our studies into palladium and platinum complexes with bissulfoxide ligands began with the discovery that we could make the monomeric dichloride complexes with **1** from  $M(\text{PhCN})_2\text{Cl}_2$  (where  $M = \text{Pt}$  or  $\text{Pd}$ ). The benzonitrile ligands could be displaced by one equivalent of bissulfoxide ligand. The first results were achieved when the palladium complex,  $\text{Pd}(\text{PhCN})_2\text{Cl}_2$  (palladium(II) bis(benzonitrile)dichloride) was treated with a solution of the ligand in  $\text{CH}_2\text{Cl}_2$ . The solution changed colour from yellow to red. However when the solvent was removed, the  $^1\text{H}$  NMR spectrum of the resulting red solid was the same as that of the free ligand. Nevertheless, the elemental analysis matched that predicted for  $\text{Pd}\{(\text{M},\text{S}_\text{S},\text{S}_\text{S})\text{-}p\text{-tolyl-binaso}\}\text{Cl}_2$  (**4**), and no benzonitrile was observed in the  $^1\text{H}$  NMR spectrum. We postulate that in this case, the ligand forms very weak interactions with the palladium, but is not properly bound. This was also observed by White and co-workers, where a bissulfoxide ligand appeared to form a complex with  $\text{Pd}(\text{OAc})_2$ , but the  $^1\text{H}$  NMR of the ‘complex’ and the free ligand were the same.<sup>10</sup>

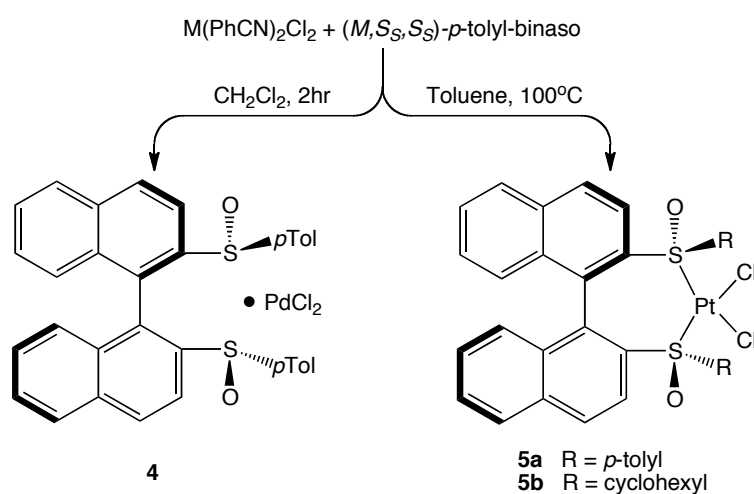


**Figure 3** Syntheses of  $\text{PdCl}_2 \cdot \text{binaso}$  and  $\text{Pt}(\text{binaso})\text{Cl}_2$

On the other hand,  $\text{Pt}\{(M,S_S,S_S)\text{-}p\text{-tolyl-binaso}\}\text{Cl}_2$  (**5a**) and  $\text{Pt}\{(M,S_S,S_S)\text{cyclohexyl-binaso}\}\text{Cl}_2$  (**5b**) were unequivocally formed. The ligand was heated with the Pt precursor in toluene, and a yellow solid precipitated out of solution. The  $^1\text{H}$  NMR spectra of this solid showed that the signals of the bound ligand were shifted compared to the free ligand. The complex was very stable under  $\text{N}_2$ , and can be kept for months without any decomposition being observed. For further confirmation that the complex had formed, an X-ray crystal structure of **5a** was obtained.

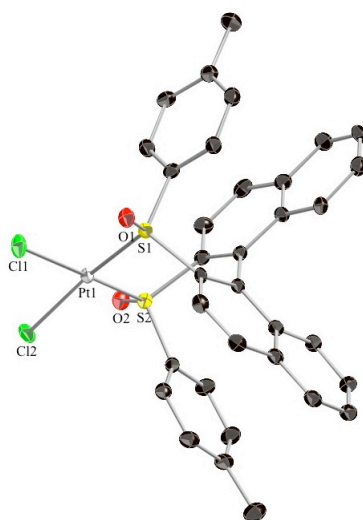


**Figure 4** Thermal ellipsoid drawing of  $\text{Pt}\{(M,S_S,S_S)\text{-}p\text{-tolylbinaso}\}\text{Cl}_2$ , **5a**, at 50% probability. Hydrogen atoms are omitted for clarity. Selected bond lengths (Å) and angles (°): Pt1-S1, 2.250; Pt1-S2, 2.253; Pt1-Cl1, 2.304; Pt1-Cl2, 2.315; S1-O1, 1.462; S2-O2, 1.467; Cl1-Pt1-Cl2, 88.725; S1-Pt1-S2, 98.463; Cl1-Pt1-S1, 88.626; Cl2-Pt1-S2, 85.477; S1-Pt1-Cl2, 169.412; S2-Pt1-Cl1, 170.214.

The crystal structure of **5a** revealed the bond distances between Pt and S to be 2.250 and 2.253 Å, and the distance between Pt and Cl to be 2.304 and 2.315 Å. The complex is almost square planar in geometry, the chlorides being 10.59° and 9.79° out of plane. It seems that the chlorides are pushed out of plane in order to accommodate the oxygens of the sulfoxides, as the rest of the bisulfonate ligand is too far away to create any steric hindrance. The angles between the bound ligands are not 90°. Indeed, the bite angle of the bisulfonate is 98.46°, which in turn means the chlorides are pushed closer together, giving an angle of 88.73° between them.

It was found that palladium complexes with *p*-tolyl-binaso, where the ligand was clearly bound, could be formed using  $\text{Pd}(\text{PhCN})_2\text{Cl}_2$  in combination with silver salts,  $\text{AgX}$ . The exchange of the chlorides for other binding ligands can help the ligand to interact better with the metal. When 2 equivalents of  $\text{AgTFA}$  (TFA = trifluoroacetate)

were added,  $\text{Pd}(p\text{-tolyl-binaso})\text{TFA}_2$  (**6**) was formed. The synthesis was possible with both diastereoisomers of the ligand. Crystals of complex **6**, with  $(P,S_S,S_S)$ - $p$ -tolyl-binaso were grown, and an X-ray analysis was performed (figure 6). The complex is almost square planar, with the trifluoroacetate ligands being pushed out of the plane by only  $4.29^\circ$ , possibly to avoid interactions between the sulfoxide oxygens and the TFA oxygens. The Pd-S bond distances were 2.242 and 2.243 Å. Overall, the trifluoroacetate ligands modulate the electronic environment at the metal in such a way as to allow binaso to bind relatively tightly to palladium.

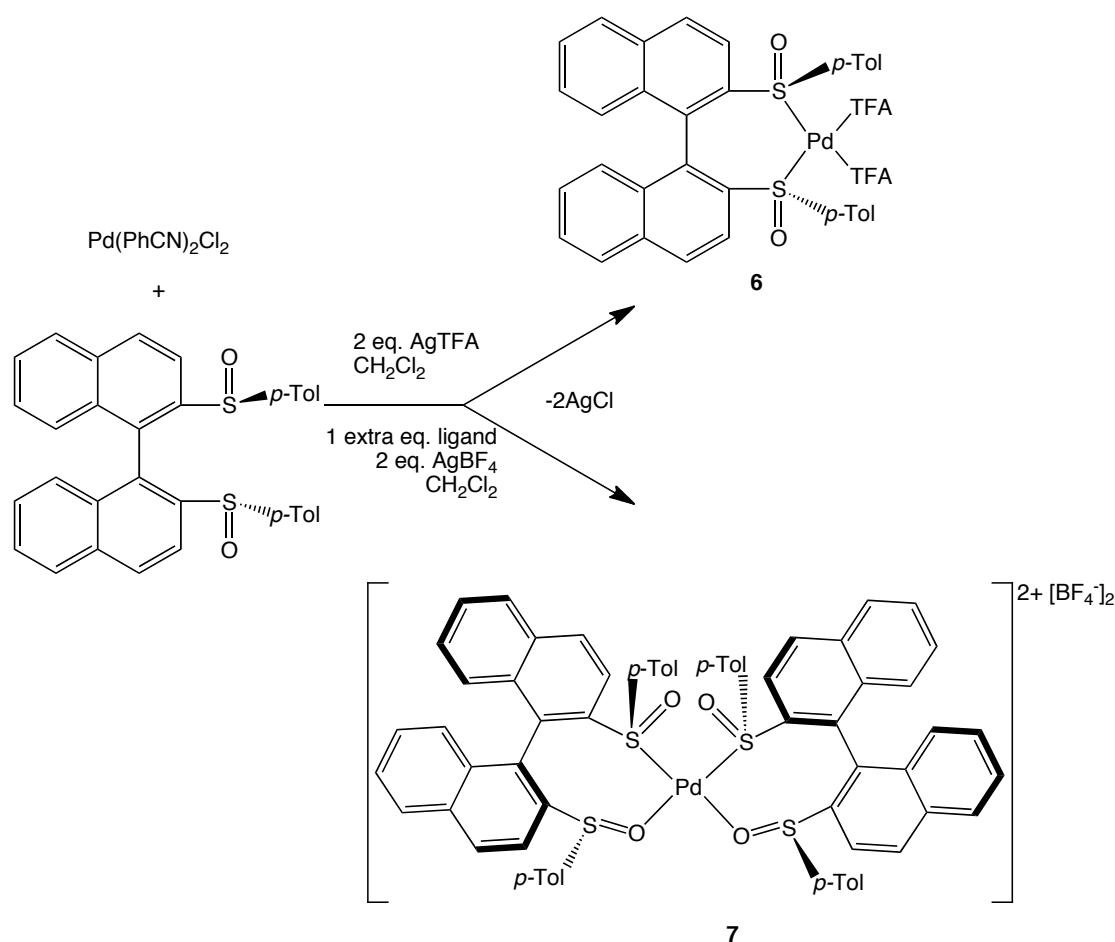


**Figure 5** Synthesis of palladium  $p$ -tolyl-binaso complexes *via* abstraction of chlorides

When  $\text{AgBF}_4$  was added to the reaction instead of  $\text{AgTFA}$ , an interesting transformation occurred. Initially the reaction was carried out with one equivalent of  $\text{Pd}(\text{PhCN})_2\text{Cl}_2$ , one equivalent of  $(P,S_S,S_S)$ - $p$ -tolyl-binaso and two equivalents of  $\text{AgBF}_4$ . It was observed that the quantity of white solid, at the time believed to be  $\text{AgCl}$ , precipitating out of the reaction was greater than expected. The solid was filtered off, and an  $^1\text{H}$  NMR analysis revealed it to be a mixture of  $\text{AgCl}$  and

$\text{Pd}(\text{PhCN})_4(\text{BF}_4)_2$ . The remaining red solution was also dried and was speculated to be  $\text{Pd}((P,S_S,S_S)\text{-}p\text{-tolyl-binaso})_2(\text{BF}_4)_2$  (**7**).  $^1\text{H}$  NMR spectra showed the ligand to be desymmetrised and supported this theory. The complex is fairly stable; when stored in the glovebox, no decomposition was observed after 1 year. Confirmation of the structure came from X-ray crystallographic analysis of crystals of the complex, grown by layering a concentrated  $\text{CH}_2\text{Cl}_2$  solution with pentane (figure 7). From each ligand, one sulfoxide is S-bound and the other is O-bound to the palladium. To the best of our knowledge, this is the first example of a bissulfoxide ligand chelating simultaneously through S and O with a late transition-metal. The Pd-S bond distances in **7** are 2.24 Å, which is slightly longer than in **6**, and the Pd-O bond distances are 2.09 Å. The O-bound sulfoxides are out of plane with the S-bound sulfoxides by  $6.74^\circ$ . *p*-tolyl-binaso forms an 8-membered metallocycle with the palladium, and this gives the ligands more flexibility to form the preferred  $90^\circ$  bite angles.

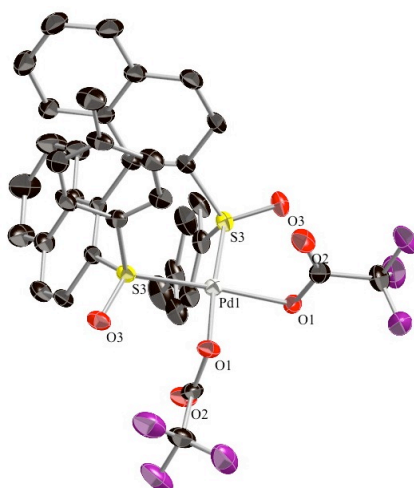


**Figure 6** Thermal ellipsoid drawing of  $\text{Pd}((P,S_S,S_S)\text{-}p\text{-tolyl-binaso})\text{TFA}_2$ , **6**, at 50% probability. Hydrogen atoms are omitted for clarity. Selected bond lengths (Å) and angles ( $^\circ$ ): Pd1-S3, 2.242; Pd1-S3, 2.243; Pd1-O1, 2.044; Pd1-O1, 2.046; S3-O3, 1.460; S3-O3, 1.460; S3-Pd1-S3,  $97.072^\circ$ ; O1-Pd1-O1,  $88.536^\circ$ ; S3-Pd1-O1,  $87.229^\circ$ ; S3-Pd1-O1,  $87.165^\circ$ .

$(P,S_S,S_S)\text{-}p\text{-tolyl-binaso}$  could only be used to make neutral complexes with palladium, no neutral platinum complexes were made cleanly with this ligand. In addition, only the  $(P,S_S,S_S)$ -ligand could be used to make complex **7**. When the reaction was carried out using one equivalent of  $\text{Pd}(\text{PhCN})_2\text{Cl}_2$ , one equivalent of  $(P,S_S,S_S)\text{-}p\text{-tolyl-binaso}$  and one equivalents of  $\text{AgBF}_4$ , a complicated mixture of products was seen in the  $^1\text{H}$  NMR spectrum. We had hoped that the chloro-bridged

dimer, with one ligand bound to each palladium, would form but this does not seem to be the case.

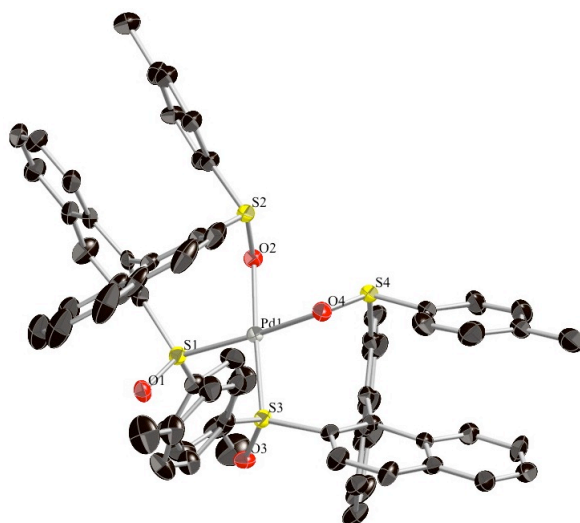


**Figure 7** Thermal ellipsoid drawing of  $[\text{Pd}((P,S,S,S)\text{-}p\text{-tol-binaso})_2][\text{BF}_4]_2$ , **7**, at 50% probability. Hydrogen atoms are omitted for clarity. Selected bond lengths (Å) and angles (°): Pd1-S1, 2.238; Pd1-S3, 2.237; Pd1-O2, 2.087; Pd1-O4, 2.088; S1-O1, 1.457; S2-O2, 1.548; S3-O3, 1.451; S4-O4, 1.551; S1-Pd1-S3, 89.631; O2-Pd1-O4, 90.064; S1-Pd1-O2, 90.366; S3-Pd1-O4, 90.730.

Returning to the investigation into the coordination of binaso to platinum, we were able to use complex **5a** as an entry point to a variety of other complexes (figure 8). The dichloride complex (**5a**) could be treated with AgTFA in  $\text{CH}_2\text{Cl}_2$  to abstract both chlorides resulting in complex **8**, which was very stable at room temperature inside the glovebox. Crystals suitable for X-ray analysis were grown by diffusion of THF into a  $\text{CH}_2\text{Cl}_2$  solution of the complex (figure 9). Upon close inspection of the crystal structure of **8**, it can be seen that the geometry about the platinum is not completely square planar and one of the TFA ligands fluctuates between two positions. This TFA ligand is pushed out of plane with the chelating ligand by  $16.12^\circ$ , and has a Pt-O bond distance of 2.062 Å. The other TFA ligand deviates from the plane by an angle of only  $10.37^\circ$ , and has a Pt-O bond distance of 2.041 Å. The bite angle of the bisulfonate is bigger than in the Pd analogue ( $99.03^\circ$  for **8**, compared with  $97.07^\circ$  for **6**) and the TFA ligands are pushed closer together ( $82.70^\circ$  for **8**, compared with  $88.54^\circ$  for **6**). This could lead to more steric interactions, and might be the reason why one TFA ligand is further from Pt and from the coordination plane. Differences can also be seen in the Pt-S bond distances, with that of the sulfonate *cis* to the most in-plane trifluoroacetate being 2.197 Å and the other being 2.239 Å. This is a difference of more than 0.04 Å, which is a significant value for these types of complexes.

When **5a** was treated with only one equivalent of AgTFA, only one chloride was abstracted and replaced by a TFA ligand to form complex **9**, which could be stored for months at room temperature under nitrogen. The  $^1\text{H}$  NMR spectrum of this complex shows that the binaso ligand is desymmetrised by this transformation, and we believe the structure to be that shown in figure 8. Complex **9** could be reacted with another equivalent of AgTFA to cleanly give **8**.

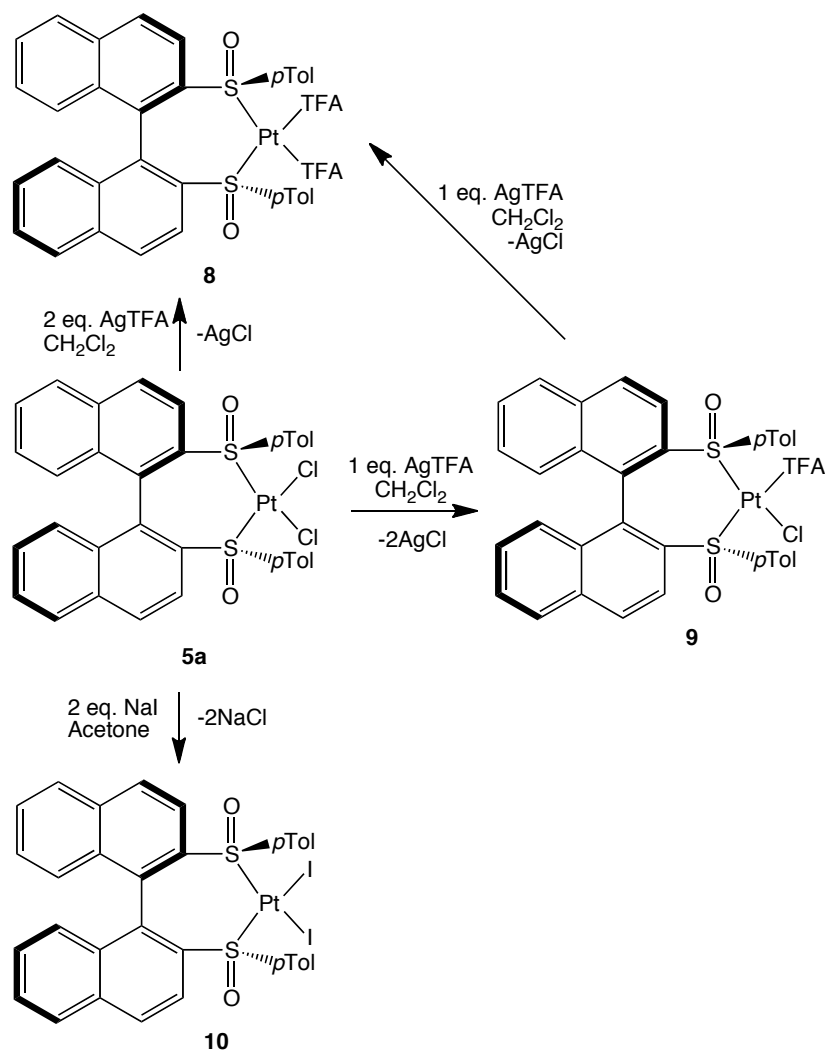


**Figure 8** Platinum complexes for which **5a** was a precursor

Reacting **5a** with NaI in an acetone solution substituted the chlorides for iodides, giving an orange precipitate in less than 10 minutes. The orange solid could be redissolved in  $\text{CH}_2\text{Cl}_2$  and layered with THF to give crystals of **10** suitable for X-ray analysis. Unlike complexes **8** and **9**, **10** decomposed in a matter of weeks if stored outside the fridge. The Pt-I bond distance in **10** is 2.59 Å; this is almost 0.3 Å longer than the Pt-Cl bonds in **5a** and almost 0.6 Å longer than the Pt-O bonds in **8**. The

geometry is quite distorted from square planar, with both iodides being pushed out of the plane by 17.09°. The rather long Pt-I bond distances, and the distortion from square planar geometry suggest that the interaction of the sulfoxide oxygens and the iodides is the reason for the destabilisation of the complex. The Pt-S bond distance is 2.261 Å. This is slightly longer than in the chloride and TFA complexes.

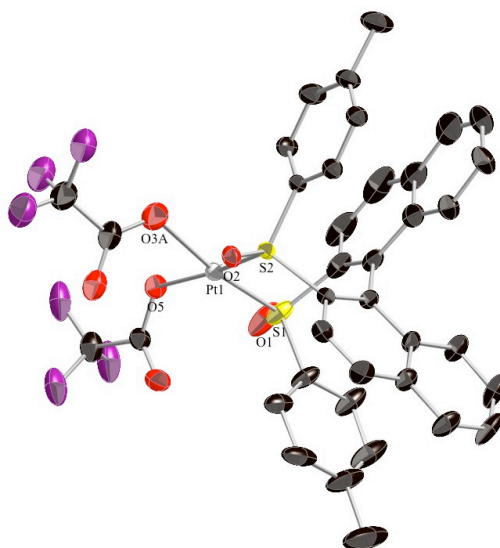


**Figure 9** Thermal ellipsoid drawings of Pt(*M,S<sub>S</sub>,S<sub>S</sub>*)-*p*-tol-binasoTFA<sub>2</sub>, **8**, at 50% probability. Hydrogen atoms are omitted for clarity. Selected bond lengths (Å) and angles (°): Pt-S1, 2.197; Pt-S2, 2.239; Pt-O3, 2.062; Pt-O5, 2.041; S1-O1, 1.464; S2-O2, 1.476; S1-Pt1-S2, 99.034; O3-Pt1-O5, 82.704; S1-Pt1-O5, 91.091; S2-Pt1-O3, 88.074.

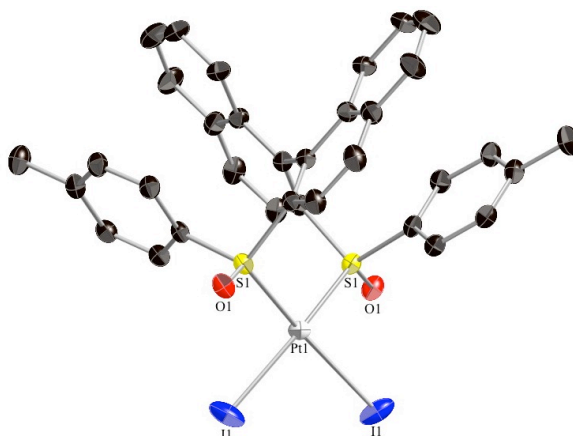


**Figure 10** Thermal ellipsoid drawings of Pt(*M,S<sub>S</sub>,S<sub>S</sub>*)-*p*-tol-binasoI<sub>2</sub>, **10**, at 50% probability. Hydrogen atoms are omitted for clarity. Selected bond lengths (Å) and angles (°): Pt-S1, 2.261; Pt-I1, 2.588; S1-O1, 1.466; S1-Pt1-S1, 97.786; I1-Pt1-I1, 88.752; S1-Pt1-I1, 89.085.

Starting from a different Pt precursor [Pt( $\mu$ -SMe<sub>2</sub>)Me<sub>2</sub>] the dimethyl complex could be formed with both ligands **1** and **2** as shown in figure 11.

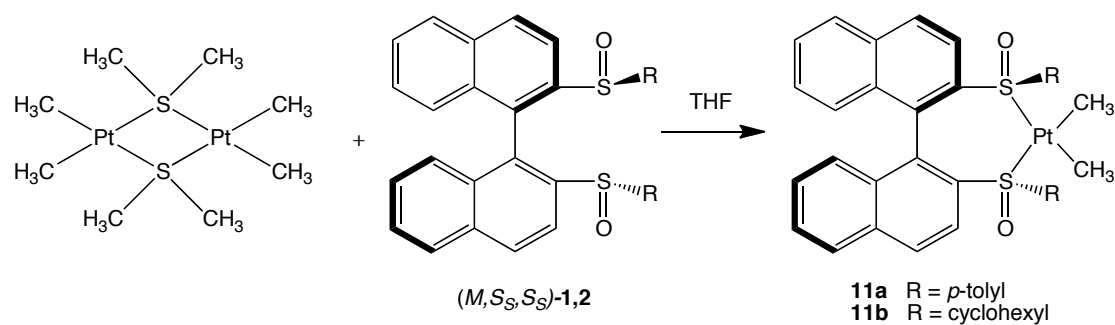


**Figure 11** Synthesis of complexes **11a** and **11b**

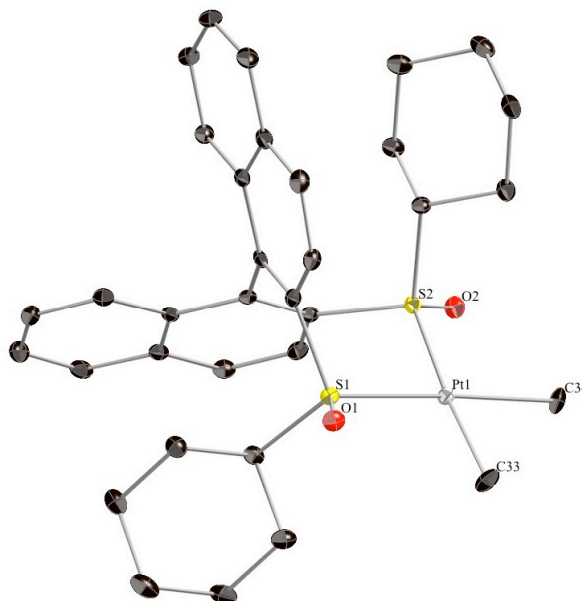
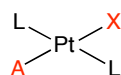
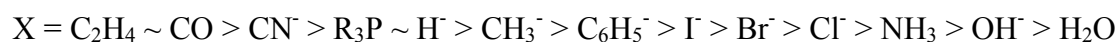


**Figure 12** Thermal ellipsoid drawing of Pt(*M,S<sub>S</sub>,S<sub>S</sub>*)-cyclohexyl-binaso, **11b**, at 50% probability; hydrogen atoms are omitted for clarity. Selected bond lengths (Å) and angles (°): Pt1-S1, 2.308; Pt1-S2, 2.311; Pt1-C33, 2.071; Pt1-C34, 2.067; S1-O1, 1.479; S2-O2, 1.481; S1-Pt1-S2, 97.410; C33-Pt1-C34, 84.380; S1-Pt1-C33, 88.774; S2-Pt1-C34, 89.528.

Crystals of the dimethyl complex **11b** were grown, and an X-ray analysis performed (figure 12). The crystal structure revealed bond distances of 2.308 and 2.311 Å between the Pt and S. These are the longest Pt-S bonds observed for any of the complexes described herein. Complex **11b** was also the least stable and had to be stored in the fridge, inside the glovebox, to avoid decomposition. The square planar geometry is distorted as the methyl groups are pushed out of the plane by the sulfoxide oxygens, by an angle of 6.96°.

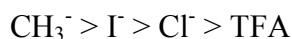
It has long been known that there are two phenomena at play in square planar Pt complexes, where a ligand X, *trans* to another ligand A, affects the stability of the Pt-A bond (*trans*-influence) or the ease of substitution of A (kinetic *trans*-effect).<sup>11</sup> It was verified experimentally that the labilising effect (kinetic *trans*-effect) decreases in the following order:





It is believed that  $\sigma$ - or  $\pi$ -interactions, or a combination of both, are important for ligands displaying a strong kinetic *trans*-effect. Good  $\sigma$ -bonding between the p-orbital of the ligand X and the 6p orbitals of Pt stabilises the transition state in the substitution of A for another ligand.<sup>11a</sup> Whereas, empty  $\pi^*$  orbitals on the ligand X may assist the substitution reaction by accommodating electron density built up on the metal centre coming from the entering ligand.

Studies of complexes of the general formula *trans*-PtCl<sub>2</sub>(L)(NH<sub>3</sub>), where L was various  $\sigma$ -bonding ligands, led to the conclusion that the *trans*-influence closely mirrors the kinetic *trans*-effect in most cases.<sup>11a</sup> Upon inspection of the Pt-S bond lengths (from X-ray crystal structures) and the S=O bond IR frequencies of the neutral Pt complexes described herein (table 1), we observed a *trans*-influence of the following order:<sup>12</sup>



Compound	<i>trans</i> Ligand	Av. Pt-S bond distance (Å)	$\nu(\text{S=O})$ (cm <sup>-1</sup> )
Free binaso	N/A	N/A	1055.84
<b>8</b>	-TFA	2.22	1177.33
<b>5a</b>	-Cl	2.25	1136.83
<b>10</b>	-I	2.26	1129.12
<b>11b</b>	-CH <sub>3</sub>	2.31	1093.44

**Table 1** Comparison of Pt-S bond lengths and IR frequency of S=O bond

This is in agreement with what is stated in literature for square planar Pt complexes<sup>11</sup> and our own observations as to the stability of these complexes. The *trans*-influence and kinetic *trans*-effect are important to bear in mind when designing new complexes to synthesise or predicting the behaviour of these complexes in catalysis. Ligands in the *trans* position to the sulfoxides with a strong *trans*-influence might labilise the bissulfoxide during catalysis. If this were the case, the chiral ligand might not be chelating to the metal throughout the catalytic cycle, and the desired enantioselectivity would not be observed.

Parallels can be drawn between the trends observed for the Pt complexes and those observed with the Pd complexes. Above we have seen that Cl appears to exert a stronger *trans*-influence on the bissulfoxide ligand than TFA in the neutral Pt complexes discussed. Similarly, we saw earlier that in the Pd-bissulfoxide dichloride complex (**4**) the binaso seemed to coordinate weakly, whereas the Pd-bissulfoxide TFA complex (**6**) was a stable, isolable compound.

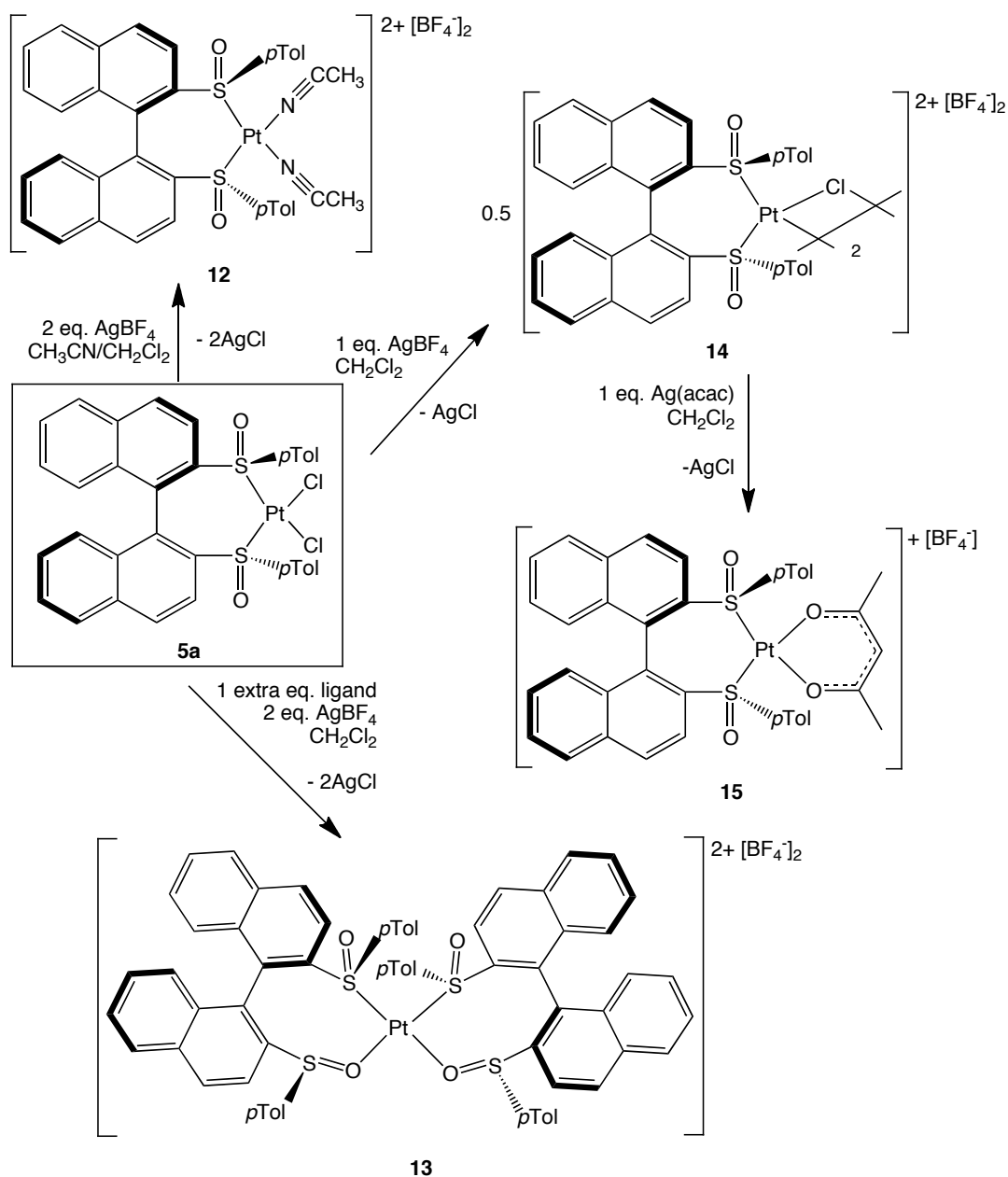


**Figure 13** Cationic platinum complexes made from **5a**

Various cationic Pt complexes could also be synthesised employing **5a** as the starting point. When **5a** was treated with 2 equivalents of  $\text{AgBF}_4$  in a solvent mixture of  $\text{CH}_2\text{Cl}_2$  and  $\text{CH}_3\text{CN}$ , the chlorides were abstracted and replaced by 2  $\text{CH}_3\text{CN}$

molecules to form complex **12**. The bound CH<sub>3</sub>CN could clearly be seen in the <sup>1</sup>H and <sup>13</sup>C NMR spectra. This complex was quite stable inside the glovebox and could be stored at room temperature. Similarly, complex **13** could be formed by again reacting **5a** with 2 equivalents of AgBF<sub>4</sub>, but also with 1 equivalent of *p*-tolyl-binaso in a CH<sub>2</sub>Cl<sub>2</sub> solution. We were not able to obtain a crystal of this complex to confirm the structure unambiguously, but we believe it is analogous to the Pd complex **7** (figure 13). The <sup>1</sup>H NMR spectrum of **13** shows the binaso ligand to be desymmetrised, which suggests formation of the proposed structure.

When **5a** was treated with only 1 equivalent of AgBF<sub>4</sub>, unlike in the Pd case, the stable complex **14** was formed. No crystals could be grown to confirm the structure, but the <sup>1</sup>H NMR spectrum of the complex shows the ligand is still symmetric. There is precedence for this type of chloro-bridged Pt dimers in the literature with phosphine ligands.<sup>13</sup> Pregosin *et al.* were able to obtain an X-ray crystal structure of a dimeric Pt complex with the ligand MeO-Biphep.<sup>14</sup> **14** could then react cleanly with 1 equivalent of Ag(acac) (acac = acetylacetonate) to give the monocationic complex **15**. This complex was stable at room temperature under nitrogen and <sup>1</sup>H and <sup>13</sup>C NMR spectra revealed both acac and binaso ligands to be bound.

Finally, another group of cationic platinum complexes were made from the precursor Pt(COD)Cl<sub>2</sub> (COD = cyclooctadiene). It was found that treating the precursor with one equivalent of ligand and two equivalents of AgBF<sub>4</sub>, the chlorides were abstracted and the ligand co-ordinated to Pt to produce the dicationic complexes **16a**, **b** and **c** (figure 14). <sup>1</sup>H NMR spectra confirmed that both the bissulfoxide ligand and cyclooctadiene were bound in each case.

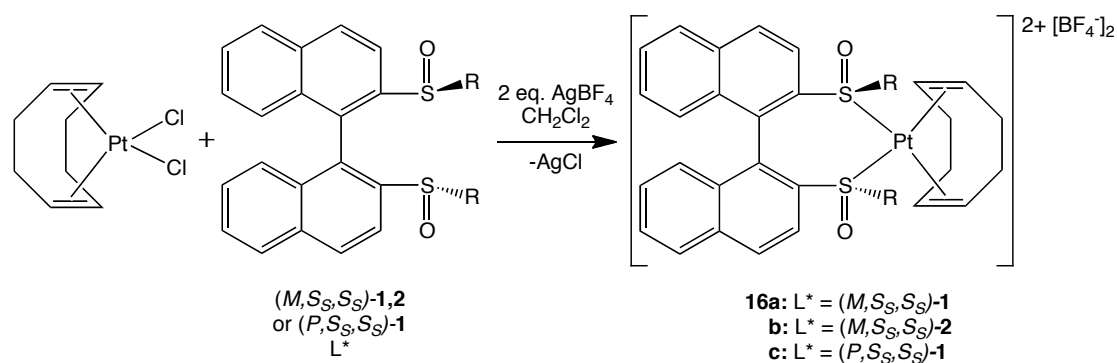
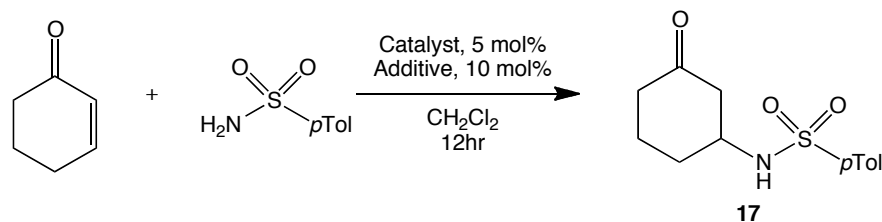


**Figure 14** Synthesis of [Pt(binaso)(COD)][BF<sub>4</sub>]<sub>2</sub> complexes, **16a**, **b** and **c**.

### 4.3. Intermolecular Hydroamination

**Table 2** Screening of platinum complexes in the intermolecular hydroamination reaction



Entry	Catalyst	Additive	Isolated Yield % <sup>a</sup>
1	<b>5a</b>	-	trace
2	<b>5a</b>	AgOTf	84
3	<b>5a</b>	AgBF <sub>4</sub>	60
4	<b>5a</b>	AgTFA	0
5 <sup>b</sup>	<b>5a</b>	AgOAc	4
6 <sup>b</sup>	<b>5a</b>	Ag(acac)	0
7	<b>7</b>	-	0
8	<b>8</b>	-	0
9	<b>10</b>	-	0
10	<b>11</b>	-	trace
11	<b>13</b>	-	0
12	<b>14</b>	-	0
13	-	AgOTf	80
14	-	AgBF <sub>4</sub>	40
15	-	TfOH	79

<sup>a</sup> Isolated yield. <sup>b</sup> Reaction performed at 80°C.

Following the work of Tilley *et al.*,<sup>15</sup> we decided to test the platinum complexes in intermolecular hydroamination reactions (table 2). In the first test, we used **5a** with no additive; no addition product was obtained even with heating up to 70°C. However, if the chlorides were abstracted before the substrates were added to the reaction, better results were achieved. The highest isolated yield, 84%, was reached when **5a** was first reacted with 2 equivalents of AgOTf (OTf = -OSO<sub>2</sub>CF<sub>3</sub>) in CH<sub>2</sub>Cl<sub>2</sub>. The catalyst solution was filtered over celite after 30 minutes, added to cyclohexenone and *p*-tolylsulfonamide, and the catalytic reaction was run at room temperature. Employing AgBF<sub>4</sub> in the same way also provided the product, but in lower yield. Other platinum

binaso complexes described above were tested in the hydroamination reaction, but no product or only trace amounts were recovered.

It was previously shown by Hartwig and co-workers that triflic acid (TfOH) by itself was capable of catalysing hydroamination reactions.<sup>16</sup> To test whether this was the case for our standard reaction, control experiments were carried out with 5 mol % AgOTf, AgBF<sub>4</sub> and triflic acid (entries 13-15). We observed product in all of these reactions, albeit in slightly lower yield than with the Pt complexes present. When triflic acid or AgOTf was applied as the catalyst, yields almost as high as that obtained with the **5a**/AgOTf mixture were achieved. HPLC analysis of the product obtained from these reactions showed it to be racemic in all cases. In light of this information it is difficult to say whether the Pt complex participates in the reaction. However, when AgBF<sub>4</sub> is used as the catalyst, the yield obtained is considerably lower than when **5a** is used in combination with AgBF<sub>4</sub>. So we can conclude that although the anion alone is capable of catalysing the hydroamination reaction presented, the platinum complex does seem to play some role.

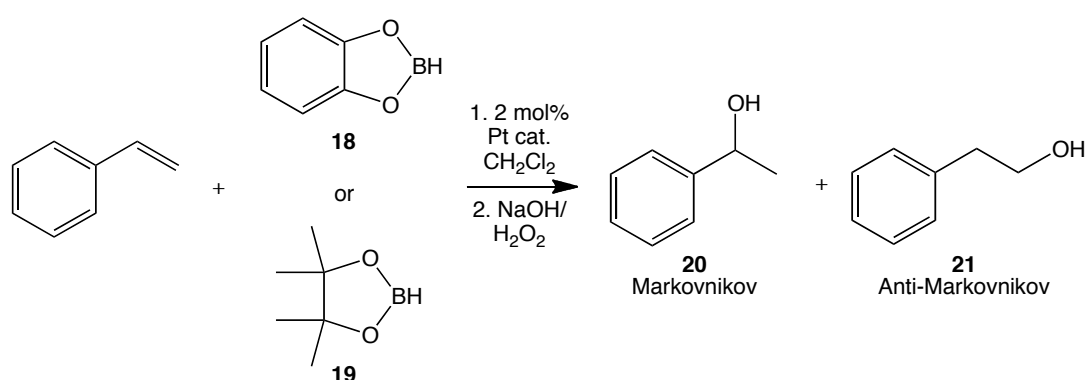
#### 4.4. Hydroboration

After the limited success of the hydroamination catalysis, we turned our attention to hydroboration reactions. Hydroboration reactions can be carried out non-catalytically, but the major product observed is the anti-Markovnikov addition product,<sup>17</sup> catalysts can be used to invert this selectivity. The catalytic version of this reaction has been most well-developed with rhodium catalysts.<sup>18,19</sup> There is very little in the current literature regarding the use of platinum in hydroboration reactions. There is only one example of catechol borane being used in the hydroboration of a terminal alkene with a platinum catalyst.<sup>20</sup> Other examples include the hydroboration of terminal alkenes with polyboranes,<sup>21</sup> and the hydroboration of allenes with pinacol borane.<sup>22</sup>

As can be seen from entry 1, when no catalyst is present there is no reaction. For this type of reaction the non-catalytic version usually requires heating to high temperatures to obtain any product.<sup>18a</sup> **5a** was the first platinum complex tested in the hydroboration of styrene with catechol borane, **18**, but only a trace of product was observed. Following the trends observed in the hydroamination reactions, we thought

that abstracting the chlorides in the complex with silver salt first would aid catalysis. As can be seen in entry 3 of table 3, this approach also failed to give the desired product. The cationic Pt complexes **16a**, **b** and **c** were then tested in the reaction. **16a** and **c** gave moderate yields at -25°C. Interestingly, when the temperature was raised to room temperature, only traces of product were obtained. **16a** gave the best selectivity observed in this study, with a 4:1 ratio of Markovnikov to anti-Markovnikov product being observed at 25°C (entry 4). **16b** did not give any product (entry 8).

**Table 3** Screening of Pt complexes in hydroboration reactions



Entry	Catalyst	Borane	Temp (°C)	Yield <sup>a</sup> %	Ratio <sup>b</sup> 20:21
1	-	18	-20	0	-
2	<b>5a</b>	18	-20	trace	-
3	<b>5a<sup>c</sup></b>	18	-20	0	-
4	<b>16a</b>	18	-25	55	4:1
5	<b>16c</b>	18	-25	38	2.6:1
6	<b>16a</b>	18	23	trace	-
7	<b>16c</b>	18	23	trace	-
8	<b>16b</b>	18	0	0	-
9	<b>16a</b>	19	23	90	1.2:1
10	<b>16c</b>	19	23	94	1.1:1
11	<b>16c</b>	19	-5	79	1:1
12	<b>16c<sup>d</sup></b>	19	23	39	0.9:1
13	<b>16c<sup>e</sup></b>	19	23	47	1.3:1
14	<b>16c<sup>f</sup></b>	19	23	82	0.8:1
15	<b>16c<sup>g</sup></b>	19	23	60	1.1:1

<sup>a</sup>Isolated yield; <sup>b</sup>Determined by GC; <sup>c</sup>Pt complex was reacted with 10 mol% AgOTf for 30 minutes and filtered prior to catalytic reaction; <sup>d</sup>Reaction carried out in THF; <sup>e</sup>Reaction carried out in ether; <sup>f</sup>Reaction carried out in acetone; <sup>g</sup>Reaction carried out in toluene.

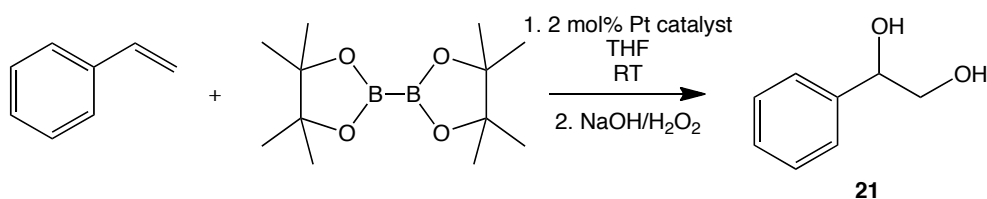
When the borane was changed to pinacol borane, the yields were dramatically improved and the reaction could be run at room temperature (entries 9 and 10), although the regioselectivity was also decreased. Running the reaction at lower temperatures did not improve the selectivity with pinacol borane, and the yield was lower (entry 11). The reaction was screened with different solvents (entries 12-15), and it was found that the solvent affects both the yield and the selectivity of the reaction. THF and acetone gave higher selectivity for the anti-Markovnikov product.

For each of the reactions yielding enough isolable product, the mixture of primary and secondary alcohol were analysed by GC to give the ratio of these two alcohols. The *e.e.* of the secondary alcohol was determined using a GC column with a chiral stationary phase (Lipodex E). In each case the secondary alcohol was found to be racemic.

#### 4.5. Diboration

Inspired by recent publications on Pt-catalysed diborations, we tested some of our Pt complexes in the diboration of styrene by  $B_2(\text{pin})_2$  (table 4).<sup>23</sup> Diborations have been well developed with transition metal catalysts.<sup>24</sup> They are useful transformations to introduce new functional groups into a molecule. Obviously if the reaction can be carried out enantioselectively, it is an efficient way to introduce chiral centres.

Most examples of diboration with platinum catalysts have been carried out with  $Pt(0)$ ,<sup>25</sup> although there are some examples using  $Pt(II)$ .<sup>26</sup> This reaction was more convenient than the hydroboration reaction, as it could be run at room temperature with good results. Interestingly, **16a** and **16c** were not successful as catalysts in this reaction. This might indicate that the diboration goes through a different mechanism than the hydroboration reaction. Baker and co-workers showed that  $PtCODCl_2$  was a good catalyst for diboration and proposed that the first step of the mechanism was reduction of  $Pt(II)$  to  $Pt(0)$  by the diborane, as they observed  $R_2B-Cl$  by  $^{11}B$  NMR. This could explain why **16a** and **16c** do not catalyse the reaction. Both these complexes do not have any ligand that can be removed by transmetallation to the boron.

**Table 4** Screening of Pt catalysts in the diboration reaction

entry	catalyst	Yield <sup>a</sup> %
<b>1</b>	<b>5a</b>	18
<b>2<sup>b</sup></b>	<b>5a</b>	39
<b>3</b>	<b>8</b>	65
<b>4</b>	<b>15</b>	74
<b>5</b>	<b>13</b>	45
<b>6</b>	<b>11a</b>	80
<b>7</b>	<b>16a</b>	0
<b>8</b>	<b>16c</b>	0

<sup>a</sup> Isolated yield after quenching with NaOH/H<sub>2</sub>O<sub>2</sub> <sup>b</sup> **5a** was first reacted with AgOTf in THF, then filtered and used in the catalytic reaction.

As can be seen in table 4, relatively good yields can be obtained with some of the platinum complexes in this reaction, particularly **15** and **11a**. We were hoping that the product would show some enantiomeric excess. Unfortunately, when analysed by HPLC using chiral stationary phases (chiralcel OD-H), the product turned out to be racemic.

#### 4.6. Summary

We have developed a family of new palladium and platinum complexes with the bissulfoxide ligands *p*-tolyl-binaso and cyclohexyl-binaso. These include a novel example of a bissulfoxide ligand binding simultaneously through S and O.

Through inspection of the X-ray crystal structures and IR spectra of the neutral Pt complexes, we were able to observe that other ligands in the complex can have a *trans*-influence on the Pt-S binding strength. This is important to bear in mind when designing Pt-binaso complexes to be used as catalysts. When the other ligands in the



complex have a *trans*-influence on the Pt-S bond, the chiral bissulfoxide ligand may be made labile and not fully chelating throughout the catalytic cycle. This could explain the lack of enantioselectivity we observed in the catalytic reactions tested. Extrapolating the trends seen for Pt to Pd it appears likely that binaso and other chelating bissulfoxide ligands will have to be electronically altered significantly in order for them to be bound tightly to the palladium centre.

It was also observed from the X-ray crystal structures that although the backbone and sulfoxide substituents are removed from the metal centre and have little influence on the geometry of the complexes, the sulfoxide oxygens are influential. For all the complexes studied, the square-planar geometry was distorted as the other ligands were pushed out of the plane and away from the sulfoxide oxygens. The observation that the S=O bond plays an important role in sulfoxide-metal complexes is not surprising, as we have seen similar results in rhodium complexes with bissulfoxide ligands.<sup>27</sup>

The platinum complexes were tested as catalysts for an intermolecular hydroamination reaction. Although the results initially appeared good, we could not be sure whether the platinum complex was truly the catalytic species, and to what extent the counterion played a role in catalysis. Selected Pt complexes were also tested in the hydroboration and diboration of styrene. **16a** gave selectivities of up to 4:1 of the Markovnikov product vs. the anti-Markovnikov product with catechol borane. Better yields were obtained with pinacol borane, but the selectivities were lower. In the diborations, **11a** was found to be the best catalyst, with **16a** and **16c** giving no product at all. Work is on-going to find new catalytic applications for these complexes, and to try to reach a more thorough understanding of the nature of the binding of these ligands to palladium and platinum.

#### 4.7. Experimental section

All reactions were carried out using standard Schlenk or glovebox (Mecaplex or Innovative Technology) techniques under nitrogen. NMR spectra were collected on an AV2 400 MHz Bruker spectrometer. Solvents were purchased in the best quality available, degassed by purging thoroughly with nitrogen and dried over activated molecular sieves of appropriate size. Alternatively, they were purged with argon and passed through alumina columns in a solvent purification system (Innovative

Technology).  $\text{Pt}(\text{PhCN})_2\text{Cl}_2$ <sup>28</sup>,  $[\text{Pt}(\mu\text{-SMe}_2)\text{Me}_2]_2$ <sup>29</sup>,  $\text{PtCODCl}_2$ <sup>30</sup> and the ligands<sup>9</sup> were prepared according to literature procedures.  $\text{Pd}(\text{PhCN})_2\text{Cl}_2$ , silver salts, boranes, diboranes, cyclohexenone and *p*-tolylsulfonamide were purchased from Aldrich or Strem and used as received. Styrene was purchased from Aldrich, distilled and stored in the fridge of the glovebox. Elemental analysis was performed at OCI or ETH, Zürich (hygroscopic compounds were corrected for water content).

**$\text{Pd}(\text{II})\text{Cl}_2\cdot(M,S_S,S_S)\text{-}p\text{-tolyl-binaso}$  (4):** A vial was charged with 49mg (0.188 mmol)  $\text{Pd}(\text{PhCN})_2\text{Cl}_2$  and 100mg (0.188 mmol)  $(M,S_S,S_S)\text{-}p\text{-tolyl-binaso}$ . 5ml  $\text{CH}_2\text{Cl}_2$  was added and the mixture was left stirring for 1 hour. The red solution was then concentrated to roughly 1ml volume, and diethyl ether (20ml) was slowly added with vigorous stirring. A red solid precipitated out of solution. The vial was centrifuged for 10 minutes, and then the supernatant solvent was decanted off *via* Pasteur pipette. The remaining solid was washed twice more with diethyl ether, and then dried thoroughly under high vacuum, to obtain 111mg (83% yield) of product. <sup>1</sup>H-NMR (400 MHz,  $\text{CD}_2\text{Cl}_2$ ):  $\delta$  = 2.09 (s, 6H), 6.20-6.22 (d,  $J$  = 8.5 Hz, 2H), 6.61-6.69 (m, 8H), 6.81-6.85 (t,  $J$  = 7.4 Hz, 2H), 7.40-7.43 (t,  $J$  = 7.6 Hz, 2H), 7.92-7.94 (d,  $J$  = 8.2 Hz, 2H), 8.30-8.32 (d,  $J$  = 8.8 Hz, 2H), 8.43-8.46 (d,  $J$  = 8.7 Hz, 2H) ppm. <sup>13</sup>C-NMR (400 MHz,  $\text{CD}_2\text{Cl}_2$ ):  $\delta$  = 21.46, 120.21, 126.23, 126.46, 127.65, 127.81, 128.85, 129.71, 129.84, 131.07, 131.55, 132.74, 132.83, 133.35, 134.81 ppm. Elemental analysis: Calculated for  $\text{PdC}_{34}\text{H}_{26}\text{Cl}_2\text{O}_2\text{S}_2$ : C = 57.67%, H = 3.70%; Found: C = 57.45%, H = 3.63%.

**$\text{Pt}(\text{II})(M,S_S,S_S)\text{-}p\text{-tolyl-binasoCl}_2$  (5a):** A 100ml Schlenk tube was charged with 533.8mg (1.13 mmol)  $\text{Pt}(\text{PhCN})_2\text{Cl}_2$  and 600mg (1.13 mmol)  $(M,S_S,S_S)\text{-}p\text{-tolyl-binaso}$ . 30ml dry toluene was added, and the yellow suspension was stirred at 100°C overnight. The reaction was then allowed to cool to room temperature; the Schlenk tube was then taken inside the glove box. Pentane was added to the stirred yellow suspension, the solid was allowed to settle, and the supernatant solvent was decanted off *via* Pasteur pipette. The remaining yellow solid was washed twice with toluene (2 x 5ml), and twice with pentane (2 x 5ml). The complex was then dried thoroughly under high vacuum to give 795mg (88% yield) of product. Yellow needle-like crystals, suitable for x-ray analysis, could be grown by diffusion of diethyl ether into a concentrated solution of the complex in  $\text{CH}_2\text{Cl}_2$ . <sup>1</sup>H-NMR (400 MHz,  $\text{CD}_2\text{Cl}_2$ ):  $\delta$  =

1.96 (s, 6H), 6.48-6.51 (d,  $J = 8.6$  Hz, 2H), 6.56-6.58 (d,  $J = 7.8$  Hz, 4H), 7.11-7.15 (t,  $J = 7.4$  Hz, 2H), 7.47-7.51 (m, 6H), 7.77-7.79 (d,  $J = 7.9$  Hz, 2H), 8.16-8.18 (d,  $J = 9.0$  Hz, 2H), 8.52-8.54 (d,  $J = 9.0$  Hz, 2H) ppm.  $^{13}\text{C}$ -NMR (400 MHz,  $\text{CD}_2\text{Cl}_2$ ):  $\delta = 21.54, 122.00, 127.68, 127.81, 128.54, 128.81, 129.04, 129.09, 129.56, 129.62, 129.75, 130.27, 132.06, 132.33, 135.70, 139.84, 145.03$  ppm. Elemental analysis: Calculated for  $\text{PtC}_{34}\text{H}_{26}\text{Cl}_2\text{O}_2\text{S}_2$ : C = 51.26%, H = 3.29%; Found: C = 51.32%, H = 3.43%.

**Pt(II)( $M,S_S,S_S$ )-cyclohexyl-binasoCl<sub>2</sub> (5b):** A 100ml Schlenk tube was charged with 92mg (0.194 mmol)  $\text{Pt}(\text{PhCN})_2\text{Cl}_2$  and 100mg (0.194 mmol) ( $M,S_S,S_S$ )-cyclohexyl-binaso. 10ml dry toluene was added, and the yellow suspension was stirred at 100°C overnight. The reaction was then allowed to cool to room temperature; the Schlenk tube was then taken inside the glove box. Pentane was added to the stirred yellow suspension, the solid was allowed to settle, and the supernatant solvent was decanted off *via* Pasteur pipette. The remaining yellow solid was washed twice with toluene (2 x 5ml), and twice with pentane (2 x 5ml). The complex was then dried thoroughly under high vacuum to give 129mg (85% yield) of product.  $^1\text{H}$ -NMR (400 MHz,  $\text{CDCl}_3$ ):  $\delta = -0.81$ -- $0.69$  (m, 1H),  $0.41$ - $0.51$  (m, 1H),  $0.76$ - $0.88$  (m, 3H),  $1.02$ - $1.37$  (m, 9H),  $1.53$ - $1.59$  (m, 2H),  $1.69$ - $1.81$  (m, 2H),  $2.53$ - $2.56$  (m, 1H),  $7.21$ - $7.23$  (d,  $J = 8.8$  Hz, 1H),  $7.43$ - $7.47$  (t,  $J = 7.7$  Hz, 1H),  $7.53$ - $7.57$  (t,  $J = 7.8$  Hz, 4H),  $7.71$ - $7.79$  (m, 6H),  $8.14$ - $8.16$  (d,  $J = 8.4$  Hz, 1H),  $8.42$ - $8.48$  (q,  $J = 3.8$  Hz,  $J = 12.9$  Hz, 2H) ppm.  $^{13}\text{C}$ -NMR (400 MHz,  $\text{CDCl}_3$ ):  $\delta = 23.85, 24.51, 24.73, 26.05, 28.30, 29.93, 65.00, 109.32, 117.02, 123.50, 127.13, 128.11, 129.11, 129.37, 129.69, 130.01, 132.08, 132.40, 133.99, 135.45, 135.52, 135.96$  ppm. Elemental analysis: Calculated for  $\text{PtC}_{32}\text{H}_{34}\text{O}_2\text{S}_2\text{Cl}_2 \cdot 2\text{CDCl}_3$ : C = 39.98%, H = 3.55%; Found: C = 40.06%, H = 3.07%.

**Pd(II)( $M,S_S,S_S$ )-*p*-tolyl-binaso(OC(O)CF<sub>3</sub>)<sub>2</sub> (6):** A vial was charged with 49mg (0.188 mmol)  $\text{Pd}(\text{PhCN})_2\text{Cl}_2$ , 100mg (0.188 mmol) ( $M,S_S,S_S$ )-*p*-tolyl-binaso and 83mg (0.376 mmol)  $\text{Ag}(\text{OC}(\text{O})\text{CF}_3)$ . 5ml  $\text{CH}_2\text{Cl}_2$  was added, the vial was covered, and the reaction was left stirring in the dark for three hours. After this time, the precipitated  $\text{AgCl}$  was filtered off over celite to leave a yellow solution. Solvent was removed to leave a volume of about 1ml, and diethyl ether (20ml) was added dropwise, with stirring, to precipitate a yellow solid. The vial was centrifuged for 5 minutes, so the

supernatant solvent could be decanted off *via* Pasteur pipette. The remaining yellow solid was washed twice more with diethyl ether (2 x 5ml), and then dried thoroughly under high vacuum, to give 140mg (86% yield) of the product. Crystals suitable for x-ray analysis could be grown by slow diffusion of diethyl ether into a concentrated solution of the complex in CH<sub>2</sub>Cl<sub>2</sub>. <sup>1</sup>H-NMR (400 MHz, CD<sub>2</sub>Cl<sub>2</sub>): δ = 1.99 (s, 6H), 6.43-6.46 (d, *J* = 8.6 Hz, 2H), 6.64-6.66 (d, *J* = 8.3 Hz, 2H), 7.13-7.17 (t, *J* = 7.4 Hz, 2H), 7.53-7.57 (t, *J* = 7.5 Hz, 2H), 7.75-7.77 (d, *J* = 7.0 Hz, 2H), 7.80-7.82 (d, *J* = 8.3 Hz, 2H), 8.22-8.24 (d, *J* = 9.0 Hz, 2H), 8.50-8.52 (d, *J* = 9.0 Hz, 2H) ppm. <sup>13</sup>C-NMR (400 MHz, CD<sub>2</sub>Cl<sub>2</sub>): δ = 21.50, 122.03, 127.37, 127.72, 128.78, 129.14, 129.71, 130.13, 130.63, 131.95, 132.75, 134.28, 135.94, 138.03, 145.69 ppm. <sup>19</sup>F-NMR (400 MHz, CD<sub>2</sub>Cl<sub>2</sub>): δ = -74.14 (s) ppm. Elemental Analysis: Calculated for PdC<sub>38</sub>H<sub>26</sub>F<sub>6</sub>O<sub>6</sub>S<sub>2</sub>·0.5H<sub>2</sub>O: C = 52.33%, H = 3.12%; Found: C = 52.22%, H = 3.51%.

**Pd(II)((*P,S,S,S*)-*p*-tolyl-binaso)<sub>2</sub>(BF<sub>4</sub>)<sub>2</sub> (7):** A vial was charged with 49mg (0.188 mmol) Pd(PhCN)<sub>2</sub>Cl<sub>2</sub>, 200mg (0.376 mmol) (*P,S,S,S*)-*p*-tolyl-binaso and 73mg (0.376 mmol) AgBF<sub>4</sub>. 5ml CH<sub>2</sub>Cl<sub>2</sub> was added, the vial was covered, and the reaction was left stirring in the dark for three hours. After this time, the precipitated AgCl was filtered off over celite to leave a deep red solution. Solvent was removed to leave a volume of about 1ml, and diethyl ether (20ml) was added dropwise, with stirring, to precipitate a red solid. The vial was centrifuged for 5 minutes, so the supernatant solvent could be decanted off *via* Pasteur pipette. The remaining red solid was washed twice more with diethyl ether (2 x 5ml), and then dried thoroughly under high vacuum, to give 214mg (85% yield) of the product. Crystals suitable for x-ray analysis could be grown by slow diffusion of a 1:1 pentane/diethyl ether mixture into a concentrated solution of the complex in CH<sub>2</sub>Cl<sub>2</sub>. <sup>1</sup>H-NMR (400 MHz, CD<sub>2</sub>Cl<sub>2</sub>): δ = 1.99 (s, 6H), 2.51 (s, 6H), 5.84-5.86 (d, *J* = 8.7 Hz, 2H), 6.59-6.71 (m, 12H), 6.82-6.86 (t, *J* = 7.8 Hz, 2H), 7.22-7.43 (m, 12H), 7.72-7.78 (m, 4H), 7.88-7.91 (d, *J* = 9.2 Hz, 2H), 8.37-8.39 (d, *J* = 8.4 Hz, 2H), 8.70-8.72 (d, *J* = 8.4 Hz, 2H), 8.94-8.96 (d, *J* = 8.5 Hz, 2H) ppm. <sup>13</sup>C-NMR (400 MHz, CD<sub>2</sub>Cl<sub>2</sub>): δ = 20.74, 21.95, 120.79, 123.44, 126.58, 126.82, 127.20, 127.41, 127.56, 128.26, 128.85, 128.93, 129.16, 129.45, 129.99, 130.29, 131.68, 132.59, 132.69, 133.76, 133.79, 134.9, 135.46, 136.41, 138.52, 139.50, 143.14, 147.35 ppm. <sup>19</sup>F-NMR (400 MHz, CD<sub>2</sub>Cl<sub>2</sub>): δ = -152.11 (s, 4F), -152.06 (s, 1F) ppm.

Elemental Analysis: Calculated for  $\text{PdC}_{68}\text{H}_{52}\text{B}_2\text{F}_8\text{O}_4\text{S}_4 \cdot 3\text{H}_2\text{O}$ : C = 58.53%, H = 4.18%; Found: C = 58.57%, H = 3.95%.

**Pt(II)(*M,S,S*)-*p*-tolyl-binaso(OC(O)CF<sub>3</sub>)<sub>2</sub> (8):** A vial was charged with 100mg (0.126 mmol) of **5** and 56mg (0.252 mmol) Ag(OC(O)CF<sub>3</sub>). 5ml CH<sub>2</sub>Cl<sub>2</sub> was added and the vial was covered. The reaction was left stirring in the dark for four hours, after this time it was filtered over celite to remove the precipitated AgCl. The resulting colourless solution was concentrated to a volume of about 1ml, and diethyl ether (20ml) was added dropwise to the stirred solution to precipitate a white solid. The vial was centrifuged for five minutes, so that the supernatant solvent could be decanted off *via* Pasteur pipette. The solid was washed twice with diethyl ether (2 x 5ml) and then dried thoroughly under high vacuum to give 97mg (81% yield) of the complex. Colourless crystals suitable for x-ray analysis could be grown by diffusion of THF into a concentrated solution of the complex in CH<sub>2</sub>Cl<sub>2</sub>. <sup>1</sup>H-NMR (400 MHz, CD<sub>2</sub>Cl<sub>2</sub>): δ = 1.96 (s, 6H), 6.44-6.46 (d, *J* = 8.6 Hz, 2H), 6.59-6.61 (d, *J* = 8.2 Hz, 4H), 7.12-7.16 (t, *J* = 7.7 Hz, 2H), 7.50-7.53 (t, *J* = 7.6, 2H), 7.65 (br s, 4H), 7.79-7.81 (d, *J* = 8.3 Hz, 2H), 8.21-8.23 (d, *J* = 9.0 Hz, 2H), 8.51-8.53 (d, *J* = 9.0 Hz, 2H) ppm. <sup>13</sup>C-NMR (400 MHz, CD<sub>2</sub>Cl<sub>2</sub>): δ = 21.40, 121.52, 127.55, 128.54, 129.06, 129.46, 129.91, 130.15, 131.75, 132.47, 134.70, 135.80, 137.64, 145.33, 145.34 ppm. <sup>19</sup>F-NMR (400 MHz, CD<sub>2</sub>Cl<sub>2</sub>): δ = -74.46 (s) ppm. Elemental Analysis: Calculated for PtC<sub>38</sub>H<sub>26</sub>F<sub>6</sub>O<sub>6</sub>S<sub>2</sub>: C = 47.95%, H = 2.75%; Found: C = 47.92%, H = 3.01%.

**Pt(II)(*M,S,S*)-*p*-tolyl-binaso(Me)<sub>2</sub> (9a):** A vial was charged with 100mg (0.174 mmol) [Pt(Me)<sub>2</sub>μ-S(Me)<sub>2</sub>]<sub>2</sub> and 185mg (0.348 mmol) (*M,S,S*)-*p*-tolyl-binaso. 4ml CH<sub>2</sub>Cl<sub>2</sub> was added, after 30 minutes a white precipitate began to appear. The mixture was left stirring overnight and then 10ml pentane was added to yield more precipitation of the white solid. The vial was centrifuged for five minutes, so the supernatant solvent could be decanted off *via* Pasteur pipette. The white solid was then redissolved in CH<sub>2</sub>Cl<sub>2</sub>, and filtered over celite. The complex was precipitated again by adding pentane to the colourless solution, and was centrifuged. The supernatant solvent was removed in the same way as before, and the solid was dried thoroughly under high vacuum to give 202mg (79% yield) of product. <sup>1</sup>H-NMR (400 MHz, CD<sub>2</sub>Cl<sub>2</sub>): δ = 0.91-1.11 (t, *J* = 41.0 Hz, 6H), 1.89 (s, 6H), 6.27-6.29 (d, *J* = 8.6

Hz, 2H), 6.43-6.45 (d,  $J = 8.2$  Hz, 4H), 6.92-6.96 (t,  $J = 7.8$  Hz, 2H), 7.29-7.31 (d,  $J = 7.7$  Hz, 4H), 7.34-7.38 (t,  $J = 7.5$  Hz, 2H), 7.67-7.69 (d,  $J = 8.1$  Hz, 2H), 8.06-8.08 (d,  $J = 8.8$  Hz, 2H), 8.52-8.55 (d,  $J = 8.9$  Hz, 2H) ppm.  $^{13}\text{C}$ -NMR (400 MHz,  $\text{CD}_2\text{Cl}_2$ ):  $\delta = -0.35, 21.29, 121.31, 126.39, 127.28, 127.51, 127.60, 128.09, 128.59, 129.19, 129.68, 129.73, 130.74, 132.64, 134.89, 139.10, 142.71, 143.99$  ppm. Elemental Analysis: Calculated for  $\text{PtC}_{36}\text{H}_{32}\text{S}_2\text{O}_2 \cdot 0.8(\text{C}_5\text{H}_{12})$ : C = 59.05%, H = 5.15%; Found: C = 59.06%, H = 4.96%.

**Pt(II)( $M,S_S,S_S$ )-cyclohexyl-binaso(Me) $_2$  (9b):** Made by the same method as described for **9a**, using 179mg (0.348 mmol) ( $M,S_S,S_S$ )-cyclohexyl-binaso. 165mg of the white solid product were obtained (64% yield). Colourless crystals were grown from a solution of the complex in a 10:1 hexane/ $\text{CH}_2\text{Cl}_2$  mixture, after being left at  $-20^\circ\text{C}$  for several weeks.  $^1\text{H}$ -NMR (400 MHz,  $\text{CD}_2\text{Cl}_2$ ):  $\delta = -0.57$ -- $0.50$  (m, 1H), 0.39-0.48 (m, 2H), 0.72-0.95 (m, 1H), 0.82 (t,  $J = 34.9$  Hz, 6H), 1.05-1.71 (m, 17H), 2.12-2.14 (m, 1H), 7.06-7.11 (m, 2H), 7.32-7.37 (m, 2H), 7.61-7.66 (m, 2H), 8.06-8.15 (m, 3H), 8.25-8.37 (m, 3H) ppm.  $^{13}\text{C}$ -NMR (400 MHz,  $\text{CDCl}_3$ ):  $\delta = 0.20, 22.04, 23.39, 24.89, 24.97, 25.25, 25.49, 25.94, 26.12, 26.18, 27.25, 27.94, 59.75, 61.56, 122.19, 123.28, 125.80, 127.12, 127.87, 127.93, 128.09, 128.13, 128.57, 129.11, 129.38, 129.77, 130.24, 130.95, 133.01, 133.14, 134.53, 134.78, 140.13, 140.49$  ppm. Elemental Analysis: Calculated for  $\text{PtC}_{34}\text{H}_{40}\text{S}_2\text{O}_2$ : C = 55.19%, H = 5.45%; Found: C = 55.23%, H = 5.34%.

**Pt(II)( $M,S_S,S_S$ )-*p*-tolyl-binaso(OC(O)CF $_3$ )Cl (10):** A vial was charged with 50mg (0.063 mmol) **5** and 14mg (0.063 mmol)  $\text{AgOC}(\text{O})\text{CF}_3$ . 3 ml  $\text{CH}_2\text{Cl}_2$  was added and the vial was covered. The reaction was left stirring in the dark for 4 hours and was then filtered over celite. The clear, colourless solution obtained was concentrated to a volume of about 1 ml and 20ml diethyl ether was added dropwise to the stirred solution so that a white precipitate appeared. The vial was centrifuged for 10 minutes, so the supernatant solvent could be removed by Pasteur pipette. The white solid was then dried thoroughly under high vacuum to give 45mg (82% yield).  $^1\text{H}$ -NMR (400 MHz,  $\text{CDCl}_3$ ):  $\delta = 1.91$  (s, 3H), 1.94 (s, 3H), 6.38-6.54 (m, 6H), 7.04-7.17 (m, 2H), 7.43-7.79 (m, 8H), 8.06-8.22 (m, 2H), 8.53-8.56 (m, 2H) ppm.  $^{13}\text{C}$ -NMR (400 MHz,

CDCl<sub>3</sub>):  $\delta$  = 21.33, 21.35, 21.39, 21.41, 66.07, 68.20, 121.50, 121.65, 121.73, 121.82, 127.18, 127.23, 127.28, 127.30, 127.52, 127.74, 127.86, 127.97, 128.00, 128.10, 128.21, 128.62, 128.65, 128.72, 128.77, 129.10, 129.13, 129.40, 129.59, 129.67, 129.77, 129.82, 130.06, 131.44, 131.47, 131.63, 131.70, 131.78, 131.85, 132.01, 132.10, 134.29, 134.63, 135.18, 135.24, 135.31, 135.42, 136.14, 137.81, 138.38, 139.10, 144.31, 144.65 ppm. Elemental Analysis: Calculated for PtC<sub>36</sub>H<sub>26</sub>O<sub>4</sub>F<sub>3</sub>S<sub>2</sub>Cl: C = 49.46%, H = 3.00%; Found: C = 49.16%, H = 3.14%.

**Pt(II)(*M,S<sub>S</sub>,S<sub>S</sub>*)-*p*-tolyl-binasol<sub>2</sub> (11):** A vial was charged with 100mg (0.126 mmol) **5** and 38mg (0.252 mmol) NaI. Acetone was added to the stirred mixture and the solution instantly became red. The reaction was left for 30 minutes, after which time an orange-red precipitate had appeared. The vial was centrifuged for 5 minutes and the supernatant solvent was decanted off, to leave the solid. The solid was redissolved in CH<sub>2</sub>Cl<sub>2</sub> (2ml) and filtered over celite, to give a clear red solution. Diethyl ether (20ml) was added dropwise to the solution to precipitate the complex. The vial was centrifuged and the supernatant solvent was decanted off *via* Pasteur pipette. The deep orange solid was washed twice more with diethyl ether (2 x 5ml) and dried thoroughly under high vacuum to give 91mg (74% yield) of the product. Crystals suitable for x-ray analysis were grown by slow diffusion of diethyl ether into a concentrated solution of the complex in CH<sub>2</sub>Cl<sub>2</sub>. <sup>1</sup>H-NMR (400 MHz, CD<sub>2</sub>Cl<sub>2</sub>):  $\delta$  = 1.95 (s, 6H), 6.46-6.49 (d, *J* = 9.0 Hz, 2H), 6.53-6.55 (d, *J* = 7.3 Hz, 4H), 7.08-7.12 (t, *J* = 7.7 Hz, 2H), 7.38 (br s, 4H), 7.47-7.51 (t, *J* = 7.1 Hz, 2H), 7.75-7.79 (d, *J* = 8.1 Hz, 2H), 8.12-8.16 (d, *J* = 9.1 Hz, 2H), 8.53-8.55 (d, *J* = 9 Hz, 2H) ppm. <sup>13</sup>C-NMR (400 MHz, CD<sub>2</sub>Cl<sub>2</sub>):  $\delta$  = 120.16, 122.31, 126.24, 126.45, 127.62, 128.32, 129.00, 129.48, 129.77, 131.39, 131.99, 132.08, 135.57, 136.26, 140.44, 144.53 ppm. Elemental Analysis: Calculated for PtC<sub>34</sub>H<sub>26</sub>I<sub>2</sub>S<sub>2</sub>O<sub>2</sub>·H<sub>2</sub>O·CH<sub>2</sub>Cl<sub>2</sub>: C = 38.83%, H = 2.79%, S = 5.93%; Found: C = 38.35%, H = 2.74%, S = 6.06%.

**Pt(II)((*M,S<sub>S</sub>,S<sub>S</sub>*)-*p*-tolyl-binaso)(CH<sub>3</sub>CN)<sub>2</sub>(BF<sub>4</sub>)<sub>2</sub> (12):** A vial was charged with 100mg (0.126 mmol) **5** and 49mg (0.252 mmol) AgBF<sub>4</sub>. 4ml of a 3:1 mixture of CH<sub>2</sub>Cl<sub>2</sub>/CH<sub>3</sub>CN was added and the vial was covered. The reaction was left stirring in the dark for 3 hours. After this time, the precipitated AgCl was filtered off over celite, to leave a clear, yellow solution. The solution was concentrated to a volume of about

1ml, and diethyl ether (20ml) was added slowly to the stirred solution to precipitate a yellow solid. The vial was centrifuged, so the supernatant solvent could be decanted off by Pasteur pipette. The complex was washed twice more with diethyl ether (2 x 5ml), and then dried thoroughly under high vacuum to give 101mg (82% yield) of product.  $^1\text{H}$ -NMR (400 MHz,  $\text{CDCl}_3$ ):  $\delta$  = 1.99 (s, 6H), 2.63 (s, 6H), 6.56-6.58 (d,  $J$  = 8.7 Hz, 2H), 6.62-6.83 (m, 4H), 7.22-7.25 (t,  $J$  = 7.7, Hz, 2H), 7.54-7.58 (t,  $J$  = 7.5, 6H), 7.80-7.82 (d,  $J$  = 8.3 Hz, 2H), 8.24-8.26 (d,  $J$  = 9.0 Hz, 2H), 8.55-8.57 (d,  $J$  = 9.0 Hz, 2H) ppm.  $^{13}\text{C}$ -NMR (400 MHz,  $\text{CD}_2\text{Cl}_2$ ):  $\delta$  = 4.05 (s), 21.51 (t,  $J$  = 80 Hz), 122.29, 127.21, 128.94, 129.13, 129.54, 130.35, 130.92, 131.41, 132.47, 133.24, 135.05, 135.95, 146.49 ppm.  $^{19}\text{F}$ -NMR (400 MHz,  $\text{CD}_2\text{Cl}_2$ ):  $\delta$  = -151.37 (s) ppm. Elemental analysis: Calculated for  $\text{PtC}_{38}\text{H}_{32}\text{B}_2\text{F}_8\text{N}_2\text{O}_2\text{S}_2\cdot\text{CH}_2\text{Cl}_2$ : C = 43.92, H = 3.21, N = 2.63; Found: C = 43.63, H = 3.25, N = 2.68.

**Pt(II)((*M,S,S,S*)-*p*-tolyl-binaso) $_2$ (BF $_4$ ) $_2$  (13):** A vial was charged with 50mg **5** (0.063 mmol), 33mg (0.063 mmol) (*M,S,S,S*)-*p*-tolyl-binaso) and 25mg (0.126 mmol) AgBF $_4$ . 3ml  $\text{CH}_2\text{Cl}_2$  was added and the vial was covered. The reaction was left stirring in the dark for 2 hours. It was then filtered over celite to remove precipitated AgCl. The clear yellow solution was then concentrated to a volume of around 1ml and diethyl ether was added dropwise. The complex precipitated as a yellow solid. The vial was centrifuged for 10 minutes, so the supernatant solvent could be removed by Pasteur pipette. The solid was washed twice more with diethyl ether and then thoroughly dried under high vacuum to give 77g (85% yield) of product.  $^1\text{H}$ -NMR (400 MHz,  $\text{CDCl}_3$ ):  $\delta$  = 2.10 (s, 3H), 2.28 (s, 3H), 6.42-6.44 (d,  $J$  = 8.6 Hz, 1H), 6.74-6.98 (br s, 2H), 7.14-7.17 (m, 6H), 7.43-7.59 (m, 5H), 7.86-7.88 (d,  $J$  = 8.2 Hz, 2H), 8.34 (s, 2H), 8.37-8.39 (d,  $J$  = 7.3 Hz, 1H), 8.48-8.50 (d,  $J$  = 9.0 Hz, 1H) ppm.  $^{13}\text{C}$ -NMR (400 MHz,  $\text{CDCl}_3$ ):  $\delta$  = 21.54, 21.75, 121.03, 121.18, 125.86, 126.79, 126.99, 128.91, 129.03, 129.54, 130.24, 130.56, 131.15, 131.38, 131.83, 132.26, 133.99, 135.30, 135.94, 147.55 ppm.  $^{19}\text{F}$ -NMR (400 MHz,  $\text{CDCl}_3$ ):  $\delta$  = -152.51 (s) ppm. Elemental Analysis: Calculated for  $\text{PtC}_{68}\text{H}_{52}\text{B}_2\text{F}_8\text{S}_4\text{O}_4\cdot 3\text{H}_2\text{O}$ : C = 55.70%, H = 3.85%; Found: C = 55.77%, H = 3.80%.



**Pt(II)((*M,S,S,S*)-*p*-tolyl-binaso)(acac)(BF<sub>4</sub>)<sub>2</sub> (14):** A vial was charged with 100mg (0.126 mmol) **5a** and 24mg (0.126 mmol) AgBF<sub>4</sub>. 2ml CH<sub>2</sub>Cl<sub>2</sub> was added, the vial was covered and the reaction was left stirring in the dark for 2 hours. After this time, the reaction was filtered over celite to remove AgCl. Solvent was then removed to leave a yellow residue in the vial, to this The remaining clear, yellow solution was concentrated to a volume of about 1ml, and diethyl ether was added in a dropwise manner to the stirred solution to precipitate a yellow solid. The vial was centrifuged so the supernatant solvent could be decanted off by Pasteur pipette. The yellow solid was washed twice more with ether and the dried completely under high vacuum to give 91mg (85% yield) of product. <sup>1</sup>H-NMR (400 MHz, CDCl<sub>3</sub>): δ = 1.99 (s, 6H), 2.21 (s, 6H), 5.90 (s, 1H), 6.48 (d, *J* = 8.7 Hz, 2H), 6.63-6.65 (d, *J* = 7.3 Hz, 4H), 7.18-7.22 (t, *J* = 7.1 Hz, 2H), 7.42-7.44 (d, *J* = 7.5 Hz, 4H), 7.52-7.56 (t, *J* = 7.2 Hz, 2H), 7.86-7.88 (d, *J* = 8.2 Hz, 2H), 8.31-8.34 (d, *J* = 9 Hz, 2H), 8.47-8.49 (d, *J* = 8.8 Hz, 2H) ppm. <sup>13</sup>C-NMR (400 MHz, CDCl<sub>3</sub>): δ = 21.56, 26.62, 104.20, 120.88, 126.94, 127.20, 128.94, 129.27, 129.53, 130.19, 130.48, 131.62, 133.15, 133.66, 135.71, 137.04, 146.06, 187.75 ppm. <sup>19</sup>F-NMR (400 MHz, CDCl<sub>3</sub>): δ = -152.00 (s, 3F), -151.95 (s, 1F) ppm. Elemental Analysis: Calculated for PtC<sub>39</sub>H<sub>33</sub>BF<sub>4</sub>O<sub>2</sub>S<sub>2</sub>: C = 51.38%, H = 3.65%; Found: C = 51.19, H = 3.54%.

**[Pt{(M,S,S,S)-*p*-tolyl-binaso}(COD)][BF<sub>4</sub>]<sub>2</sub> (15a):** A vial was charged with 35.2mg (0.094 mmol) PtCODCl<sub>2</sub>, 50mg (0.094 mmol) (*M,S,S,S*)-*p*-tolyl-binaso and 36.6mg (0.188 mmol) AgBF<sub>4</sub>. 2 ml CH<sub>2</sub>Cl<sub>2</sub> was added, the vial was covered and then the reaction was left stirring for 30 minutes. After this time the mixture was filtered over celite to remove precipitated AgCl. The solution was concentrated to about 1 ml and diethyl ether (20 ml) was added slowly, with stirring, to precipitate the complex as a white solid. The vial was centrifuged for 10 minutes and the supernatant solvent was removed by Pasteur pipette. The solid was washed twice more with diethyl ether (2 x 5 ml) and then thoroughly dried under high vacuum to give 92mg (97% yield) of product. <sup>1</sup>H-NMR (400 MHz, CDCl<sub>3</sub>): δ = 1.95-2.22 (m, 4H), 2.36 (s, 6H), 2.69-2.83 (m, 2H), 2.87-3.02 (m, 2H), 5.54-5.66 (m, 2H), 6.09-6.22 (m, 2H), 7.03-7.05 (d, *J* = 7.9 Hz, 2H), 7.26-7.41 (m, 8H), 7.47-7.50 (t, *J* = 7.5 Hz, 2H), 7.73-7.77 (t, *J* = 7.6 Hz, 2H), 7.81-7.83 (d, *J* = 8.8 Hz, 2H), 8.11-8.13 (d, *J* = 8.3 Hz, 2H), 8.38-8.40 (d, *J* = 8.8 Hz, 2H) ppm. <sup>13</sup>C-NMR (400 MHz, CDCl<sub>3</sub>): δ = 22.11, 30.68, 101.41, 122.16,

126.17, 127.36, 129.86, 130.12, 131.11, 131.89, 132.80, 134.79, 136.19, 137.07, 145.79 ppm.  $^{19}\text{F}$ -NMR (400 MHz,  $\text{CDCl}_3$ ):  $\delta$  = -151.82 (s, 3F), -151.77 (s, 1F) ppm. Elemental Analysis: Calculated for  $\text{PtC}_{42}\text{H}_{38}\text{B}_2\text{F}_8\text{O}_2\text{S}_2 \cdot 2\text{H}_2\text{O}$ : C = 48.33, H = 4.06; Found: C = 48.48, H = 3.90.

**[Pt{(M,S<sub>S</sub>,S<sub>S</sub>)-cyclohexyl-binaso}(COD)][BF<sub>4</sub>]<sub>2</sub> (15b):** Same procedure followed as in the synthesis of **15a**, except 50mg (0.097 mmol) (M,S<sub>S</sub>,S<sub>S</sub>)-cyclohexyl-binaso, 36.3mg (0.097 mmol) PtCODCl<sub>2</sub> and 37.8mg (0.194 mmol) AgBF<sub>4</sub> were used. 94 mg (98% yield) of a white solid was obtained.  $^1\text{H}$ -NMR (400 MHz,  $\text{CDCl}_3$ ):  $\delta$  = 0.45-0.53 (m, 2H), 0.98-1.52 (m, 16H), 1.77-1.79 (m, 2H), 1.95-2.16 (m, 6H), 2.82-2.91 (m, 2H), 2.99-3.05 (m, 2H), 3.69-3.81 (m, 2H), 5.48-5.65 (m, 2H), 5.97-6.13 (m, 2H), 7.15-7.18 (d,  $J$  = 8.6 Hz, 2H), 7.44-7.48 (t,  $J$  = 7.7 Hz, 2H), 7.72-7.76 (t,  $J$  = 7.6 Hz, 2H), 8.13-8.15 (d,  $J$  = 8.3 Hz, 2H), 8.32-8.34 (d,  $J$  = 8.9 Hz, 2H), 8.48-8.50 (d,  $J$  = 8.9 Hz, 2H) ppm.  $^{13}\text{C}$ -NMR (400 MHz,  $\text{CDCl}_3$ ):  $\delta$  = 24.56, 24.72, 24.77, 25.20, 27.06, 30.13, 30.56, 62.10, 101.41, 103.28, 121.93, 127.38, 129.07, 129.85, 130.68, 132.19, 133.68, 134.42, 136.02, 138.78 ppm.  $^{19}\text{F}$ -NMR (400 MHz,  $\text{CDCl}_3$ ):  $\delta$  = -151.60 (s, 3F), -151.55 (s, 1F) ppm. Elemental Analysis: Calculated for  $\text{PtC}_{40}\text{H}_{46}\text{B}_2\text{F}_8\text{O}_2\text{S}_2 \cdot 0.5\text{CH}_2\text{Cl}_2$ : C = 47.04, H = 4.58; Found: C = 47.16, H = 4.59.

**[Pt{(P,S<sub>S</sub>,S<sub>S</sub>)-p-tolyl-binaso}(COD)][BF<sub>4</sub>]<sub>2</sub> (15c):** Same procedure followed as in the synthesis of **15a**, except 50mg (0.094 mmol) (P,S<sub>S</sub>,S<sub>S</sub>)-p-tolyl-binaso was used. 94 mg (99% yield) of a white solid was obtained.  $^1\text{H}$ -NMR (400 MHz,  $\text{CDCl}_3$ ):  $\delta$  = 1.94-2.42 (m, 4H), 2.09 (s, 6H), 3.06-3.29 (m, 4H), 5.73-5.84 (m, 2H), 5.86-6.03 (m, 2H), 6.12-6.14 (d,  $J$  = 8.2 Hz, 2H), 6.58-6.73 (m, 8H), 6.78-6.82 (t,  $J$  = 7.4 Hz, 2H), 7.42-7.46 (t,  $J$  = 7.5 Hz, 2H), 7.90-7.92 (d,  $J$  = 8.2 Hz, 2H), 8.35-8.37 (d,  $J$  = 8.7 Hz, 2H), 8.61-8.63 (d,  $J$  = 7.4 Hz, 2H) ppm.  $^{13}\text{C}$ -NMR (400 MHz,  $\text{CDCl}_3$ ):  $\delta$  = 21.40, 29.74, 31.49, 102.34, 104.78, 124.66, 126.27, 127.40, 128.05, 128.71, 128.86, 130.08, 132.06, 133.35, 135.39, 143.21 ppm.  $^{19}\text{F}$ -NMR (400 MHz,  $\text{CDCl}_3$ ):  $\delta$  = -150.55 (s, 3F), -150.49 (s, 1F) ppm. Elemental analysis: Calculated for  $\text{PtC}_{42}\text{H}_{38}\text{B}_2\text{F}_8\text{O}_2\text{S}_2$ : C = 50.07, H = 3.80; Found: C = 49.69, H = 3.92.

**General Procedure for the Hydroamination of Cyclohexenone with p-tolyl sulfonamide:** A vial was charged inside the glovebox with Pt precatalyst (0.05 mmol)

and AgX (0.1 mmol), 2 ml CH<sub>2</sub>Cl<sub>2</sub> was added. The vial was covered and the reaction was left stirring in the dark for 30 minutes. After this time, the mixture was filtered over celite to remove solid AgCl. The clear yellow solution obtained was transferred to another vial containing the sulfonamide (171mg, 1 mmol). The vial was sealed with a cap with a PTFE septum, and removed from the glovebox. The cyclohexenone was deoxygenated and then added *via* syringe through the septum, the reaction was then stirred at room temperature for 12 hours. The reaction was quenched by adding water (20 ml) and extracted with diethyl ether (3 x 20 ml). The combined organic phases were dried over MgSO<sub>4</sub> and the solvent was removed to leave an off-white solid. The product was purified by column chromatography using 3:1 hexane/diethyl ether as the eluent. The e.e. of the pure product could be determined by HPLC using chiralcel OD-H column (4:1 Hexane/iPrOH, 0.5ml/min).

**General Procedure for the Hydroboration of Styrene:** A vial was charged with the Pt precatalyst (0.01 mmol), to this was added 2ml CH<sub>2</sub>Cl<sub>2</sub>. Low temperature reactions were charged in a special vial with a cooling jacket. To the stirred catalyst solution was added 57μl (0.5 mmol) styrene. The vial was then sealed with a cap containing a PTFE septum, and removed from the glovebox. For reactions at low temperature, the cooling jacket was connected to a cooling system so that cooled isopropanol flowed round the vial. The reaction was then left for 15 minutes for the temperature to equilibrate before the borane (0.6 mmol) was added through the septum *via* a syringe. After three hours, the reaction was diluted with diethyl ether (10ml) and transferred to a 100ml round bottom flask. 2ml NaOH was added with vigorous stirring, and the flask was cooled to 0°C with an ice bath. 2ml H<sub>2</sub>O<sub>2</sub> was added slowly via syringe, the reaction was left for 30 minutes with the neck open. After this time, the reaction was allowed to warm at room temperature; the flask was sealed with a rubber septum with a needle inside, so the system was not completely closed. The reaction was left for 6 hours like this and then diluted with more diethyl ether (20ml) and water (20ml). The phases were separated and the aqueous phase was extracted with diethyl ether (3 x 10ml). The combined organic phases were dried over MgSO<sub>4</sub> and the solvent was removed. The crude product was purified by column chromatography using hexane/ethyl acetate 24:1 as the eluent. A white solid was obtained which could be analysed by chiral GC (Lipodex E, 25m x 0.25 mm) to obtain the ratio of

Markovnikov and anti-Markovnikov product, and also the enantiomeric excess of the Markovnikov product.

**General Procedure for the Diboration of Styrene:** A vial was charged with the Pt precursor (0.01 mmol) and 152mg (0.6 mmol) B<sub>2</sub>(pin)<sub>2</sub>. 2ml CH<sub>2</sub>Cl<sub>2</sub> was added, and immediately after 57μl (0.5 mmol) styrene was added. The reaction was left stirring at room temperature for 1 hour and then removed from the glovebox. The solution was diluted with 10ml diethyl ether and quenched in the same way as the hydroboration reactions, except the quenching reaction was left overnight and then worked up. The crude product was purified by column chromatography using hexane/ethyl acetate 7:3 as the eluent. A white solid was obtained, which could be further analysed by chiral HPLC using chiralcel OD-H column (hexane/<sup>i</sup>PrOH, 95:5; 1ml/min) to determine its enantiomeric excess.

#### 4.8 References

- 
- <sup>1</sup> (a) Davies, J. A. *Adv. Inorg. Chem. Radiochem.* **1981**, 24, 11; (b) Calligaris, M.; Carugo, O. *Coord. Chem. Rev.* **1996**, 153, 83 (c) Calligaris, M. *Coord. Chem. Rev.* **2004**, 248, 351
- <sup>2</sup> Cotton, F.A.; Francis, R. *J. Am. Chem. Soc.* **1960**, 82, 2986
- <sup>3</sup> (a) Kagan, H.B.; Rebiere, F. *Synlett* **1990**, 643; (b) Rebiere, F.; Samuel, O.; Ricard, L.; Kagan, H.B. *J. Org. Chem.* **1991**, 56, 5991; (c) Fernandez, I.; Khiar, N.; Llera, J.M.; Alcudia, F. *J. Org. Chem.* **1992**, 57, 6789; (d) Khiar, N.; Araujo, C.S.; Alducia, F.; Fernandez, I. *J. Org. Chem.* **2002**, 67, 345; (e) Garcia Ruano, J.L.; Alemparte, C.; Aranda, M.T.; Zarzuelo, M.M. *Org. Lett.* **2003**, 5, 75; (f) Fernandez, I.; Khiar, N. *Chem. Rev.* **2003**, 103, 3651; (g) Han, Z.; Krishnamurphy, D.; Grover, P.; Fang, Q.K.; Su, X.; Wilkinson, H.S.; Lu, Z.; Magiera, D.; Senanayake, C. *Angew. Chem. Int. Ed.* **2003**, 42, 2032; (h) Han, Z.; Krishnamurphy, D.; Grover, P.; Wilkinson, H.S.; Fang, Q.K.; Su, X.; Lu, Z.; Magiera, D.; Senanayake, C. *Tetrahedron*, **2005**, 61, 6386; (i) Senanayake, C.; Krishnamurphy, D.; Lu, Z.; Han, Z.; Gallou, I. *Aldrichim. Acta* **2005**, 38, 93; (j) Wojaczynska, E.; Wojaczynska, J. *Chem. Rev.* **2010**, 110, 4303
- <sup>4</sup> (a) Allen, J.V.; Bower, J.F.; Williams, J.M.J. *Tetrahedron: Asymmetry* **1994**, 5, 1895; (b) Hiroi, K.; Suzuki, Y.; Ikuko, A.; Hasegawa, Y.; Suzuki, K. *Tetrahedron: Asymmetry* **1998**, 9, 3797; (c) Hiroi, K.; Suzuki, Y.; Abe, I.; Kawagishi, R. *Tetrahedron* **2000**, 56, 4701; (d) Hiroi, K.; Izawa, I.; Takizawa, T.; Kawai, K. *Tetrahedron* **2004**, 60, 2155; (e) Chen, J.; Li, D.; Ma, H.; Cun, L.; Zhu, J.; Deng, J.; Liao, J. *Tetrahedron Lett.* **2008**, 49, 6921; (f) Han, F.; Chen, J.; Zhang, X.; Liu, J.; Cun, L.; Zhu, J.; Deng, J.; Liao, J. *Tetrahedron Lett.* **2011**, 52, 830
- <sup>5</sup> (a) James, B.R.; McMillan, R.S. *Can. J. Chem.* **1977**, 55, 3927; (b) Tokunoh, R.; Sodeoka, M.; Aoe, K.; Shibasaki, M. *Tetrahedron Lett.* **1995**, 36, 8035; (c) Mariz,

- R.; Luan, X.; Gatti, M.; Linden, A.; Dorta, R. *J. Am. Chem. Soc.* **2008**, *130*, 2172;
- (d) Mariz, R.; Bürgi, J.J.; Gatti, M.; Drinkel, E.; Luan, X.; Dorta, R. *Chimia* **2009**, *63*, 508; (e) Chen, J.; Chen, J.; Lang, F.; Zhang, X.; Cun, L.; Zhu, J.; Deng J.; Liao J. *J. Am. Chem. Soc.* **2010**, *132*, 4552; (f) Bürgi, J.J.; Mariz, R.; Gatti, M.; Drinkel, E.; Luan, X.; Blumentritt, S.; Linden, A.; Dorta, R. *Angew. Chem. Int. Ed.* **2009**, *48*, 2768
- <sup>6</sup> (a) Cattalini, L.; Michelon, G.; Marangoni, G.; Pelizzi, G.; *J. Chem. Soc., Dalton Trans.* **1979**, 96; (b) Pettinari, C.; Pellei, M.; Cavicchio, G.; Crucianelli, M.; Panzeri, W.; Colapietro, M.; Cassetta, A. *Organometallics* **1999**, *18*, 555; (c) 6. Evans, D.R.; Huang, M.; Seganish, W.M.; Fetting, J.C.; Williams, T.L. *Inorg. Chem. Commun.* **2003**, *6*, 462; (d) Madec, D.; Mingoia, F.; Macovei, C.; Maitro, G.; Giambastiani, G.; Poli, G. *Eur. J. Org. Chem.* **2005**, 552; (e) Stang, E.M.; White, M.C. *Nat. Chem.* **2009**, *1*, 547 and references therein; (f) Mallorquin, R.M.; Chelli, S.; Brebion, F.; Fensterbank, L.; Goddard, J-P.; Malacria, M. *Tetrahedron: Asymmetry* **2010**, *21*, 1695
- <sup>7</sup> Kapoor, P.; Löqvist, K.; Oskarsson, A. *J. Mol. Struct.* **1998**, *470*, 39
- <sup>8</sup> Miashita, A.; Yasuda, A.; Takaya, H.; Toriumi, K.; Ito, T.; Souchi, T.; Noyori, R. *J. Am. Chem. Soc.* **1980**, *102*, 7933
- <sup>9</sup> Mariz, R.; Poater, A.; Gatti, M.; Drinkel, E.; Bürgi, J.J.; Luan, X.; Blumentritt, S.; Linden, A.; Cavallo, L.; Dorta, R. *Chem. Eur. J.* **2010**, *16*, 14335
- <sup>10</sup> Fraunhoffer, K.J.; White, M.C. *J. Am. Chem. Soc.* **2007**, *129*, 7274
- <sup>11</sup> (a) Zumdahl, S.S.; Drago, R.S. *J. Am. Chem. Soc.* **1968**, *90*, 6669; (b) Vanquickenborne, L.G.; Vranckx, J.; Görlner-Walrand, C. *J. Am. Chem. Soc.* **1974**, *96*, 4121
- <sup>12</sup> Increasing bond length indicates a weakening of the Pt-S bond. Increasing IR frequency of the S=O bond indicates increasing strength of the Pt-S bond: Davies, A.R.; Einstein, F.W.B.; Farrell, N.P.; James, B.R.; McMillan, R.S. *Inorg. Chem.* **1978**, *17*, 1965
- <sup>13</sup> Pignat, K.; Vallotto, J.; Pinna, F.; Strukul, G. *Organometallics*, **2000**, *19*, 5160
- <sup>14</sup> Schott, D.; Pregosin, P.S.; Albinati, A.; Rizzato, S. *Inorg. Chim. Acta.* **2007**, *360*, 3203
- <sup>15</sup> McBee, J.L.; Bell, A.T.; Tilley, T.D. *J. Am. Chem. Soc.* **2008**, *130*, 16562
- <sup>16</sup> Rosenfeld, D.C.; Shekhar, S.; Takemiya, A.; Utsunomiya, M.; Hartwig, J.F. *Org. Lett.* **2006**, *8*, 4179
- <sup>17</sup> Crudden, C.M.; Edwards, D. *Eur. J. Org. Chem.* **2003**, 4695
- <sup>18</sup> (a) Männig, D.; Nöth, H. *Angew. Chem. Int. Ed.* **1985**, *24*, 878; (b) Doucet, H.; Fernandez, E.; Layzell, T.P.; Brown, J.M. *Chem. Eur. J.* **1999**, *5*, 1320; (c) Edwards, D.R.; Hleba, Y.B.; Lata, C.J.; Calhoun, L.A.; Crudden, C.M. *Angew. Chem. Int. Ed.* **2007**, *46*, 7799; (d) Endo, K.; Hirokami, M.; Takeuchi, K.; Shibata, T. *Synlett* **2008**, *20*, 3231; (e) Endo, K.; Hirokami, M.; Shibata, T. *Organometallics* **2008**, *27*, 5390; (f) Kanas, D.A.; Geier, S.J.; Vogels, C.M.; Decken, A.; Westcott, S.A. *Inorg. Chem.* **2008**, *47*, 8727
- <sup>19</sup> (a) Burgess, K.; Ohlmeyer, M.J. *J. Org. Chem.* **1988**, *53*, 5179; (b) Sato, M.; Miyaura, N.; Suzuki, A. *Tetrahedron Lett.* **1990**, *31*, 231; (c) Hayashi, T.; Matsumoto, Y. *Tetrahedron: Asymmetry* **1991**, *2*, 601; (d) Burgess, K.; van der Donk, W.A.; Ohlmeyer, M.J. *Tetrahedron: Asymmetry* **1991**, *2*, 613; (e) Brunel, J.M.; Buono, G. *Tetrahedron Lett.* **1999**, *40*, 3561; (f) Crudden, C.M.; Hleba, Y.B.; Chen, A.C. *J. Am. Chem. Soc.* **2004**, *126*, 9200; (g) Fleming, W.J.; Müller-Bunz, H.;

- 
- Lillo, V.; Fernandez, E.; Guiry, P.J. *Org. Biomol. Chem.* **2009**, *7*, 2520; (h) Noh, D.; Chea, H.; Ju, J.; Yun, J. *Angew. Chem. Int. Ed.* **2009**, *48*, 6062
- <sup>20</sup> Lillo, V.; Mata, J.A.; Segara, A.M.; Peris, E.; Fernandez, E. *Chem. Commun.* **2007**, 2184
- <sup>21</sup> (a) Mazighi, K.; Carroll, P.J.; Sneddon, L.G. *Inorg. Chem.* **1993**, *32*, 1963; (b) Kadlec, D.E.; Carroll, P.J.; Sneddon, L.G. *J. Am. Chem. Soc.* **2000**, *122*, 10868; (c) Pender, M.J.; Carroll, P.J.; Sneddon, L.G. *J. Am. Chem. Soc.* **2001**, *123*, 12222
- <sup>22</sup> Yamamoto, Y.; Fujikawa, R.; Yamada, A.; Miyaura, N. *Chem. Lett.* **1999**, *10*, 1069
- <sup>23</sup> (a) Burks, H.E.; Kilman, L.T.; Morken, J.P. *J. Am. Chem. Soc.* **2009**, *131*, 9134; (b) Kilman, L.T.; Mlynarski, S.N.; Morken, J.P. *J. Am. Chem. Soc.* **2009**, *131*, 13210
- <sup>24</sup> (a) Burks, H.E.; Morken, J.P. *Chem. Commun.* **2007**, 4717; (b) Beletskaya, I.; Moberg, C. *Chem. Rev.* **2006**, *106*, 2320; (c) Marder, T.B.; Norman, N.C. *Top. Catal.* **1998**, *5*, 63
- <sup>25</sup> (a) Ishiyama, T.; Matsuda, N.; Miyaura, N.; Suzuki, A. *J. Am. Chem. Soc.* **1993**, *115*, 11018; (b) Ishiyama, T.; Matsuda, N.; Murata, M.; Ozawa, F.; Suzuki, A.; Miyaura, N. *Organometallics*, **1996**, *15*, 713; (c) Iverson, C.N.; Smith, M.R. *Organometallics*, **1997**, *16*, 2757; (d) Lawson, Y.G.; Lesley, M.J.G.; Marder, T.B.; Norman, N.C.; Rice, C.R. *Chem. Commun.* **1997**, 2051; (e) Bell, N.J.; Cox, A.J.; Cameron, N.R.; Evans, J.S.O.; Marder, T.B.; Duin, M.A.; Elsevier, C.J.; Baucherel, X.; Tulloch, A.A.D.; Tooze, R.P. *Chem. Commun.* **2004**, 1854; (f) Wang, M.; Cheng, L.; Wu, Z. *Organometallics*, **2008**, *27*, 6464
- <sup>26</sup> Mann, G.; John, K.D.; Baker, R.T. *Org. Lett.* **2000**, *2*, 2105
- <sup>27</sup> Poater, A.; Ragone, F.; Mariz, R.; Dorta, R.; Cavallo, L. *Chem. Eur. J.* **2010**, *16*, 14348
- <sup>28</sup> Braunstein, P.; Bender, R.; Jud, J. *Inorg. Synth.* **1989**, *26*, 341
- <sup>29</sup> Hill, G.S.; Irwin, M.J.; Levy, C.J.; Redina, L.M.; Puddephatt, R.J. *Inorg. Synth.* **1998**, *32*, 149
- <sup>30</sup> Drew, D.; Doyle, J.R.; Shaver, A.G. *Inorg. Synth.* **1990**, *28*, 346

## Chapter 5

### Hemilabile P-Alkene Ligands in Chiral Rh and Cu Complexes: Catalytic Asymmetric 1,4 Additions to Enones, Part 2<sup>1</sup>

#### Abstract

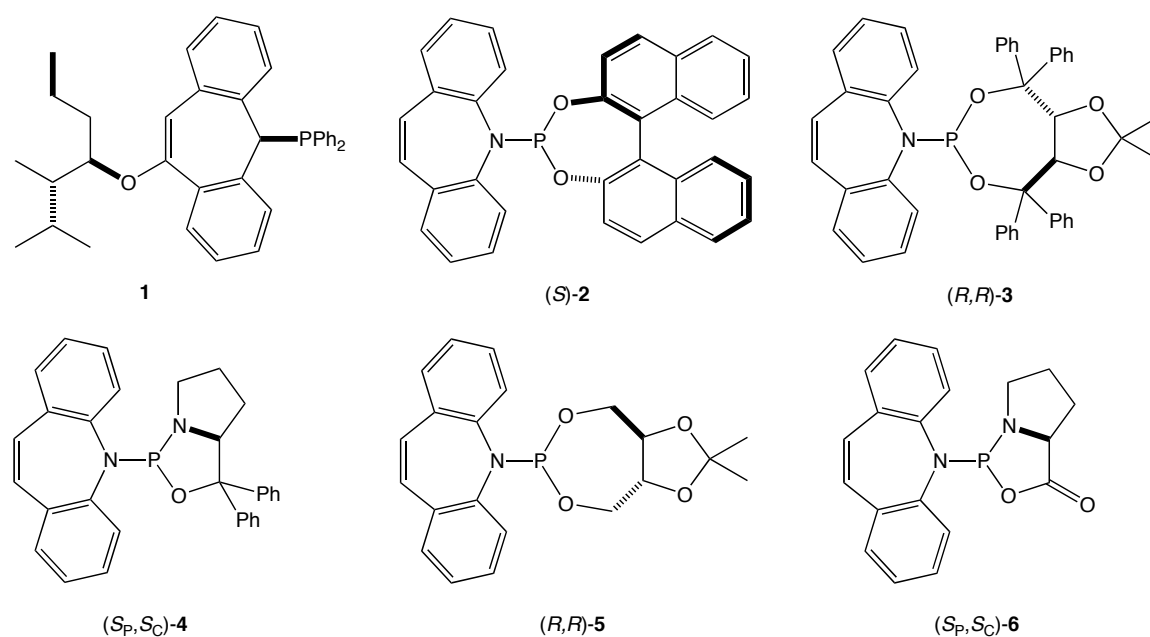
Two equivalents of chiral dibenz[b,f]azepine derived P-alkene ligands **2** – **6** per metal afforded mononuclear Rh(I) and Cu(I) complexes that were used as catalysts for the asymmetric conjugate addition reaction. Rh formed square planar neutral (**8** – **10**) and cationic complexes (**11**, **12**) of the general formulae  $[\text{RhCl}(\kappa^1\text{-P-alkene})(\kappa^2\text{-P-alkene})]$  and  $\text{cis-}[\text{Rh}(\kappa^2\text{-P-alkene})_2][\text{BF}_4]$ , respectively (P-alkene = **2**, **5**, **6**). In both cases reversible decoordination of the alkene function of the bidentate P-alkene ligands was observed in the presence of Lewis basic solvents, and model compounds of the mono- and bis-solvated species (**13**, **14**) were isolated. Cu formed trigonal planar neutral (**15** – **17**) and cationic complexes (**18**, **19**) of the general formulae  $[\text{CuI}(\kappa^1\text{-P-alkene})_2]$  and  $[\text{Cu}(\kappa^1\text{-P-alkene})_2\text{BF}_4]$ , respectively (P-alkene = **2**, **4**, **5**). The cationic Rh species **11** catalysed the 1,4-addition of arylboronic acids to cyclic and linear enones with high activities (TON = 62 at 40°C) and excellent enantiocontrol (up to 99% *e.e.*) for a wide range of substrates. The cationic Cu complex **18** catalysed the 1,4-addition of  $\text{Al}(\text{C}_2\text{H}_5)_3$  to 2-cyclohexenone with 39% *e.e.*

#### 5.1. Introduction

Chiral alkene ligands<sup>2</sup> and in particular chiral P-alkene ligands<sup>3</sup> with improved stability are evoking growing interest in the field of enantioselective catalysis. Grützmacher *et al.* introduced the highly effective tropylidene and dibenz[b,f]azepine molecules as alkene-bearing entities in P-alkene and N-alkene ligand systems, respectively.<sup>4</sup> Chiral variants of tropylidene (ligand **1**) and dibenz[b,f]azepine derivatives (ligands **2** – **6**) are depicted in Chart 1. The chiral phosphine-alkene ligand **1** yielded optically enriched amines with up to 86 % *e.e.* in Ir-catalysed asymmetric imine hydrogenations.<sup>5</sup> We have recently developed a general and facile method for

the preparation of dibenz[b,f]azepine-derived chiral P-alkene ligands, of which **2** – **6** are examples (note that ligands **4** and **6** possess stereogenic P atoms).<sup>1</sup> The alkene-phosphoramidite **2**<sup>6</sup> was used as a ligand in the Ir-catalysed enantioselective formation of allylic amines from allylic alcohols (70 % *e.e.*)<sup>7</sup> and for the Rh-catalysed conjugate addition (CA) of arylboronic acids to enones with up to 92 % *e.e.*<sup>1</sup>

**Chart 1.** Chiral P-alkene ligands based on the tropyliidene and dibenz[b,f]azepine motives



The enantioselective CA of carbon nucleophiles to enones is an important synthetic tool for the construction of stereogenic C-C bonds, and Rh and Cu based chiral complexes are among the most useful catalysts for this transformation. Rh-catalysed enantioselective CA reactions with boronic acid nucleophiles were very successfully achieved, *inter alia*,<sup>8</sup> with chiral phosphoramidites<sup>9</sup> and chiral dienes,<sup>10</sup> each on their own, and combined as chiral bidentate phosphine-olefin ligands<sup>11</sup> and phosphoramidite-alkene ligands such as **2** – **6**.<sup>1</sup> These latter ligands formed dinuclear chloro-bridged Rh complexes (of type **7**, see Scheme 1) and their bidentate coordination mode was authenticated by X-ray crystallography. The solid state structures of ligands and complexes revealed a hybridisation change of the dibenz[b,f]azepine N atom from  $\text{sp}^2$  in the free ligands to  $\text{sp}^3$  in the bidentate complexes, and we anticipated that this kind of spring-loaded coordination in



combination with the comparatively weak metal-alkene interaction might favour ligand hemilability.<sup>12</sup> Hemilabile ligands are important in catalysis because they stabilise resting states while freeing up coordination sites when they are needed, thus assuming the role of a coordinating solvent.<sup>13</sup> Recently, Mezzetti and co-workers pointed out that the classic Feringa type ‘monodentate’ phosphoramidites actually augment their hapticity through secondary, hemilabile interactions of their aryl functions with the metal centre,<sup>14</sup> and chiral hemilabile amido-phosphines were shown to be excellent ligands for the Rh-catalysed CAs of arylboronic acids.<sup>15</sup> In this context we note that Hayashi *et al.* postulated a solvent-stabilised 14 valence electron intermediate ( $[\text{Rh}(\text{OH})(\text{S})(\text{binap})]$ ,  $\text{S} = 1,4\text{-dioxane}$ ) in the catalytic cycle of the CA of phenylboronic acid to methyl vinyl ketone. The intermediate is supposed to form upon breakage of the hydroxo bridges of the complex  $[\text{Rh}(\mu\text{-OH})(\text{binap})]_2$ .<sup>16</sup> Analogously, having potentially hemilabile P-alkene ligands at hand, our working hypothesis is based on an alkene-stabilised mononuclear hydroxo complex  $[\text{Rh}(\text{OH})(\kappa^1\text{-P-alkene})(\kappa^2\text{-P-alkene})]$  representing the resting state of an active 14 electron species  $[\text{Rh}(\text{OH})(\kappa^1\text{-P-alkene})(\kappa^1\text{-P-alkene})]$ . Thus, catalyst precursors of the composition  $\text{Rh}(\text{P-alkene})_2\text{X}$  seemed to be a worthwhile synthetic goal.

Chiral Cu-phosphoramidite complexes represent the alternative of choice for CA reactions when dialkylzinc<sup>17</sup> and trialkylaluminium<sup>18</sup> nucleophiles are to be used. Chiral Cu phosphoramidite complexes are usually prepared *in situ* and the optimal ligand : Cu ratio was determined to be 2. However, due to dynamic processes in solution several species may form exhibiting varying Cu/ligand stoichiometries and coordination geometries.<sup>19</sup> Bis-phosphoramidite Cu-bromide complexes  $[\text{Cu}(\mu\text{-Br})(\text{L})_2]_2$  were shown to be dimeric in the crystal,<sup>20</sup> and although Feringa and coworkers were able to structurally characterise a monomeric phosphoramidite Cu complex of composition  $[\text{Cu}(\text{I})(\text{L})_3]$ ,<sup>17a</sup> it does not represent a catalytically relevant species in CA reactions due to its ligand/Cu stoichiometry of 3.<sup>17b</sup> We reasoned that the use of phosphoramidite-alkene ligands **2** – **6** may stabilise corresponding Cu(I) complexes of the correct stoichiometry through secondary interactions of the alkene function and thus lead to isolable and well defined systems.

In this paper we describe the synthesis of chiral mononuclear Rh(I) complexes of the composition  $\text{Rh}(\text{P-alkene})_2\text{X}$  bearing ligands **2**, **5**, and **6**, which are shown to be hemilabile. We also show that mononuclear Cu(I) complexes with the sought-after

L/Cu ratio of 2 are accessible with ligands **2**, **4**, and **5**. We then find that these mononuclear complexes catalyse the asymmetric 1,4-addition of carbon nucleophiles to enones with enantioselectivities of up to 99% *e.e.*

## 5.2. Results and discussion

**5.2.1. Complex Syntheses:** In the course of our studies on the formation of dinuclear chloro-bridged Rh(I) complexes of type **7** (see Scheme 1) with chiral P-alkene ligands starting from  $[\text{RhCl}(\text{COE})_2]_2$  (COE = cyclooctene) we sometimes observed the formation of by-products consisting of mononuclear species such as **8** when care was not taken to *slowly* add the ligand to the Rh precursor. Four equiv. of binaphthol derived ligand **2** cleanly reacted with  $[\text{RhCl}(\text{COE})_2]_2$  to form 2 equiv. of  $[\text{RhCl}(\textbf{2})_2]$  (**8**, Chart 2) on a gram scale in almost quantitative yield. This bright orange complex was only sparingly soluble in common solvents and its  $^{31}\text{P}\{^1\text{H}\}$  NMR spectrum suggested *cis* coordination of the P atoms: Two doublets of doublets are centred at 120 ppm and 179 ppm (P atom *trans* to Cl) with  $J_{\text{RhP}} = 286$  Hz,  $J_{\text{RhP}'} = 283$  Hz,  $J_{\text{PP}'} = 45$  Hz.

X-ray quality single crystals of **8** were obtained from  $\text{CH}_3\text{CN}$  and a diffraction study confirmed the expected *cis*-coordination of the phosphorous atoms in a pseudo square planar coordination environment (see Figure 1). This structure allowed us to directly compare the structural variations of the mono- and bidentate coordination modes of ligand **2** within the same metal complex: (1) The uncoordinated alkene arm displays a C27-C28 distance of 1.318(8) Å that is shorter than its coordinated counterpart (C7-C8: 1.405(9) Å). (2) While the N1 atom of the monodentate ligand is nearly planar with a deviation of only -0.062(6) Å with respect to the plane formed by its substituents P1/C21/C34 (similar to the value found in the free ligand **2**), the N2 atom in the bidentate ligand adopts a pyramidal geometry with a deviation of 0.423(6) Å in relation to the P2/C55/C68 plane. (3) The torsion angle along the P-N vector of ligand **2** is strongly dependent on its coordination mode (see Table 1). We measure this torsion angle by connecting the centroid of the alkene function of the dibenz[b,f]azepine moiety to its N atom, and by connecting the P atom to the centroid of the C-C bond joining the two naphthyl units, as illustrated by the red dotted lines in the drawing of Table 1. Structure **8** shows that ligand **2** in its bidentate ligand mode

adopts a nearly perfect (*i.e.*  $180^\circ$ ) *anti* conformation, with a torsion angle of  $172.29(11)^\circ$  along Cent1(C61-C62)-N2-P2-Cent2(C44-C45). In its monodentate mode, ligand **2** displays a *syn* conformation with a torsion angle of  $-51.309(24)$  along Cent1(C44-C45)-N1-P1-Cent2(C10-C11). This means that the uncoordinated alkene centroid is tilted away by *ca.*  $136^\circ$  in comparison to its coordinated counterpart. The torsional conformation of the free ligand **2** in the crystal lies between the values of mono- and bidentate **2**. The C1-C10-C11-C12 and C35-C44-C45-C46 torsion angles of the naphthyl groups are *ca.*  $52^\circ$  in both cases and fall into the usual range.

**Scheme 1**

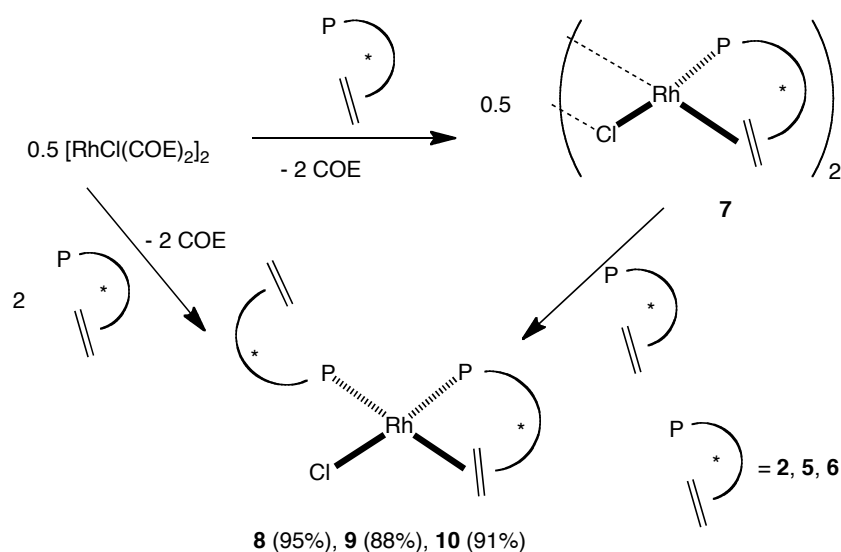
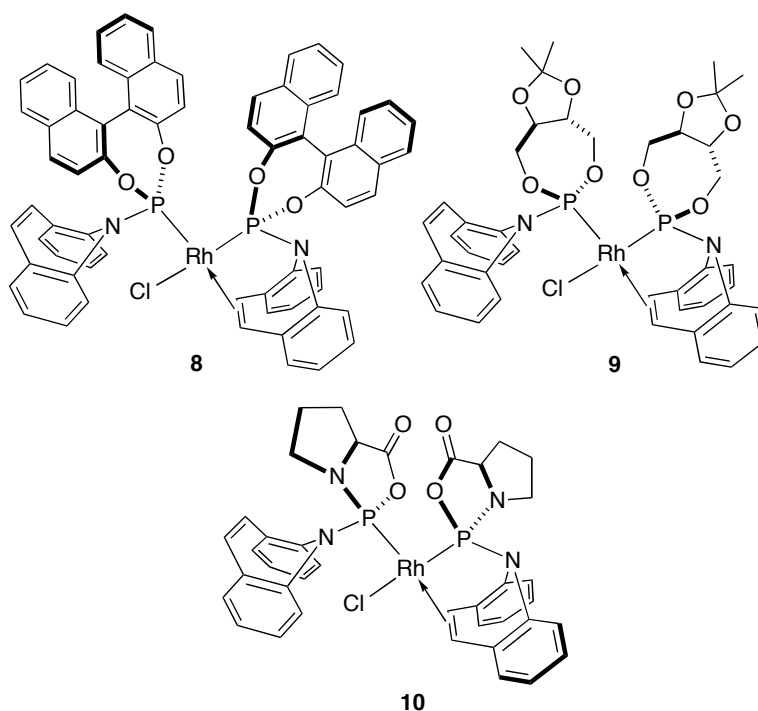


**Chart 2**



The taddol derived ligand **3** behaved quite differently and even large excesses of **3** in combination with either  $[\text{RhCl}(\text{COE})_2]_2$  or  $[\text{RhCl}(\text{COD})]_2$  (COD = 1,5 cyclooctadiene) did not lead to the formation of the sought after complex  $[\text{RhCl}(\mathbf{3})_2]$ , but only afforded the dimer  $[\text{RhCl}(\mathbf{3})_2]^1$  along with unreacted ligand. Similarly, the addition of 4 equiv. of diphenylprolinol derived ligand **4** to  $[\text{RhCl}(\text{COE})_2]_2$  only led to an inseparable mixture of the minor (27 % of total P integrals) expected complex  $[\text{RhCl}(\mathbf{4})_2]$  and a major fluxional species that was observed *in situ* by NMR spectroscopy. The reluctance of ligands **3** and **4** to co-ordinate in a 2:1 stoichiometry is possibly due to the steric bulk exerted by the phenyl groups present in both ligands. Indeed, complex **9** bearing the less bulky analogue of ligand **3** was obtained in good yield by adding 4 equiv. of ligand **5** to  $[\text{RhCl}(\text{COE})_2]_2$  and its  $^{31}\text{P}\{^1\text{H}\}$  NMR spectrum showed the characteristic pattern already observed with complex **8** indicative of *cis* coordination of the P atoms (two doublets of doublets centred at 121 ppm and 151 ppm with  $J_{\text{RhP}} = 275$  Hz,  $J_{\text{RhP}'} = 267$  Hz,  $J_{\text{PP}'} = 52$  Hz).

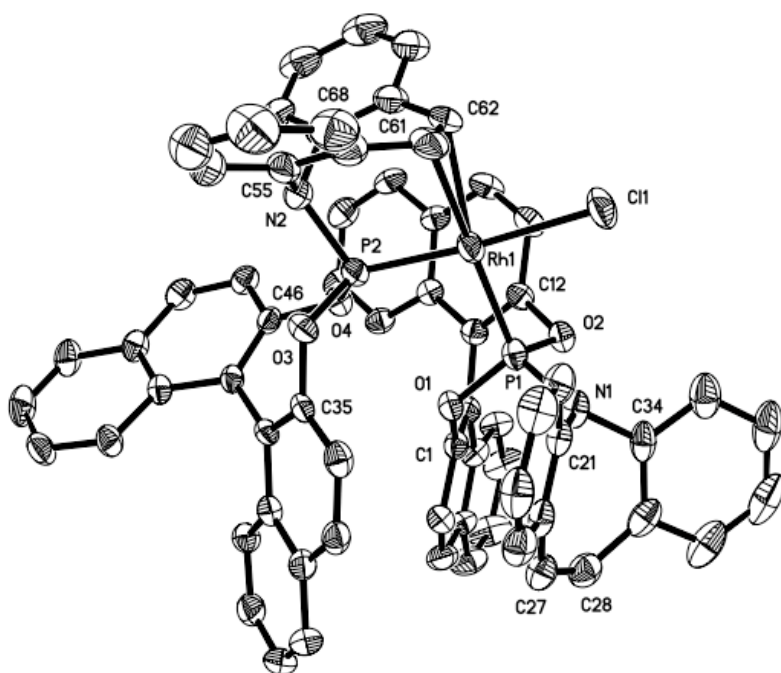
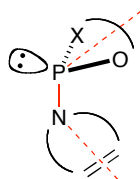


**Figure 1.** Structure of complex **8** in the crystal (30% ORTEP). Selected bond lengths (Å) and angles (°) are: Rh1-P1, 2.2421(16); Rh1-P2, 2.1464(16); Rh1-C61, 2.2296(6); Rh1-C62, 2.253(6); Rh1-Cl1, 2.4027(16); P1-N1, 1.661(5); P1-O1, 1.616(4); P1-O2, 1.614(4); P2-N2, 1.703(5); P2-O3, 1.624(4), P2-O4, 1.608(4); O1-C1, 1.391(6); O2-C12, 1.425(6); O3-C35, 1.398(6); O4-C46, 1.411(6); N1-C21, 1.430(7); N1-C34, 1.450(7); N2-C55, 1.440(7); N2-C68, 1.476(6); C27-C28, 1.318(8); C61-C62, 1.405(9); P1-Rh1-P2, 95.59(5); P1-Rh1-Cl1, 86.75(6); O2-P1-O1 101.76 (18); O2-P1-N1 99.0 (2); O1-P1-N1 108.8 (2); O4-P2-O3 103.63 (18); O4-P2-N2 103.5 (2); O3-P2-N2 95.5 (2); C21-N1-C34 115.7 (4); C21-N1-P1 118.4 (4); C34-N1-P1 125.4 (4); C55-N2-C68 111.8 (4); C55-N2-P2 113.2 (4); C68-N2-P2 113.1 (3).

**Table 1.** Torsion angles in **2** and **6** along their P-N bonds<sup>a</sup> as a function of coordination mode



Ligand	2 (X = O)	6 (X = N)
free	-116.68(2) <sup>b</sup>	-99.32(1) <sup>b</sup>
monodentate	-51.309(24) <sup>c</sup>	41.715(4) <sup>d</sup>
bidentate	172.29(11) <sup>c</sup>	176.97(2) <sup>d</sup>

<sup>a</sup> For definitions of centroids, see text. <sup>b</sup> Taken from ref. (1). <sup>c</sup> Complex **8**. <sup>d</sup> Complex **10**

Likewise, by lowering the steric pressure exerted by the diphenylprolinol auxiliary in ligand **4** and instead using the simple proline-derived analogue **6**, complex [RhCl(**6**)<sub>2</sub>] (**10**, see chart 2) formed in excellent yields from either [RhCl(COE)<sub>2</sub>]<sub>2</sub> or

from the more convenient starting material  $[\text{RhCl}(\text{COD})]_2$  by displacement of the COD molecule.<sup>21</sup> As for complexes **8** and **9**, the  $^{31}\text{P}\{^1\text{H}\}$  NMR spectrum **10** suggested *cis*-coordination of the P atoms with doublets of doublets at 135 ppm ( $J_{\text{RhP}} = 258$  Hz,  $J_{\text{PP}} = 59.5$  Hz) and at 176 ppm ( $J_{\text{RhP}} = 250$  Hz,  $J_{\text{PP}} = 59.5$  Hz). The precise molecular structure of complex **10** was revealed by a single crystal diffraction analysis and is depicted in Figure 2.

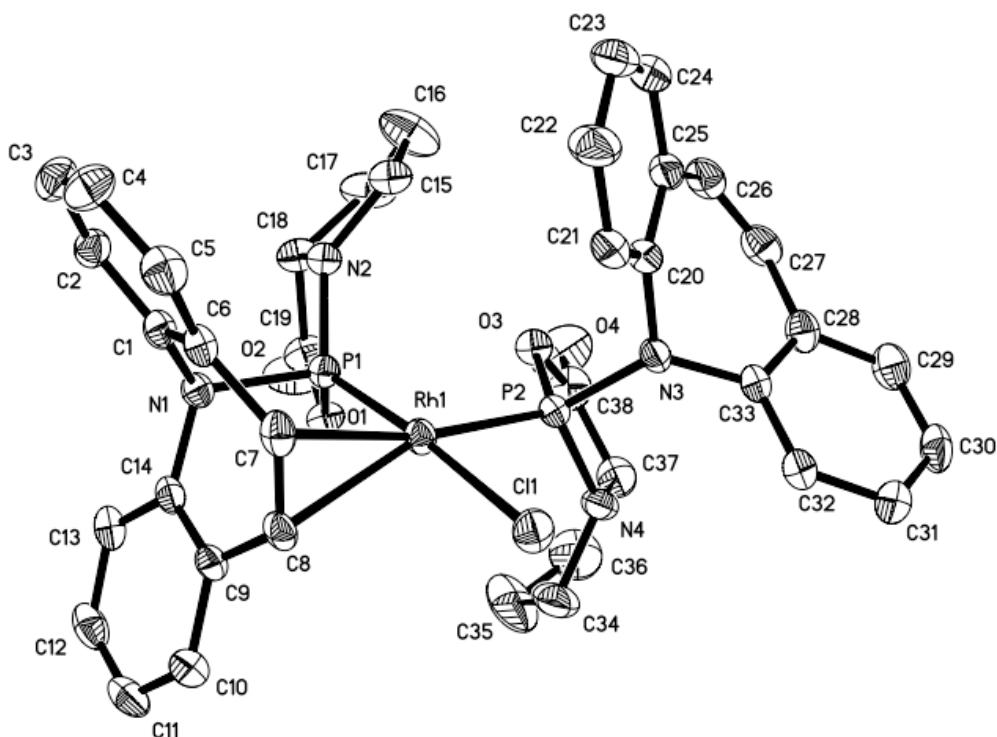
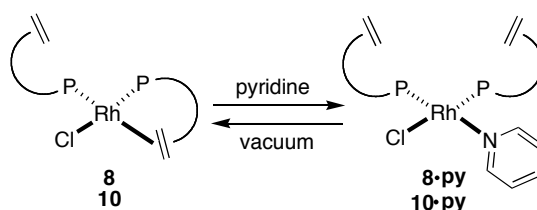


**Figure 2.** Structure of complex **10** in the crystal (30% ORTEP). Selected bond lengths (Å) and angles (°) are: Rh1-P1, 2.1385(14); Rh1-P2, 2.2107(14); Rh1-C7, 2.309(5); Rh1-C8, 2.286(4); Rh1-C11, 2.3957(14); P1-N1, 1.723(4); P1-N2, 1.638(4); P1-O1, 1.657(3); P2-N4, 1.658(4); P2-N3, 1.659(4); P2-O3, 1.681(4); O1-C19, 1.368(6); O2-C19, 1.195(6); O4-C8, 1.198(7); O3-C38, 1.376(7); N1-C1, 1.454(6); N1-C14, 1.451(6); N3-C20, 1.456(6); N3-C33, 1.435(6); C7-C8, 1.389(7); C26-C27, 1.337(8); P1-Rh1-P2, 92.94; P1-Rh1-C11, 175.47(6); C1-N1-C14, 114.6(4); C14-N1-P1, 113.1(3); C1-N1-P1, 109.7(3); C33-N3-C20, 116.2(4); C33-N3-P2, 122.7(3); C20-N3-P2, 119.4(3).

In analogy to the structure of **8**, complex **10** features *cis*-coordination of the P atoms in a pseudo square planar coordination environment. The distances of 1.337(8) Å for the uncoordinated C26-C27 alkene arm and of 1.389(7) Å for the coordinated C7-C8 counterpart are similar to those observed in compound **8**. The monodentate ligand **6** shows a *syn* conformation of the dibenz[b,f]azepine moiety and the proline ring with a torsion angle of 41.7° along the P1-N1 vector (defined in analogy to complex **8**, *i.e.*: Cent1(C26-C27)-N3-P2-Cent2(C37-C38, see Table 1). On the other hand, ligand **6** in bidentate coordination mode exhibits an almost perfect *anti*

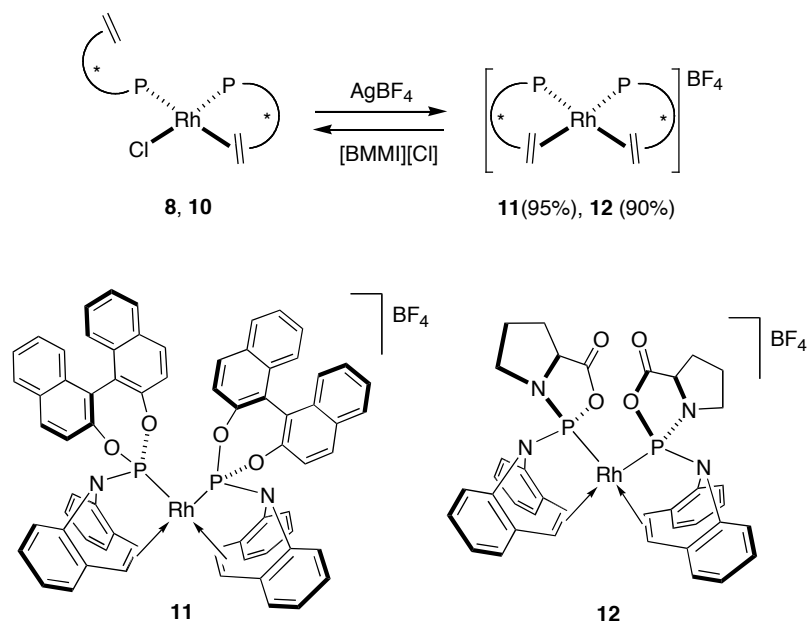
conformation with a torsion angle of  $177.0^\circ$ , along Cent1(C7-C8)-N1- P1-Cent2(C18-C19). Thus, the alkene centroid turns by *ca.*  $136^\circ$  between the mono- and bidentate coordination modes, the same amount as in complex **8** (see above). Again, the free ligand **6** in its crystalline state adopts a conformation that lies between the two coordination modes. The dihedral angles between the five-membered rings are  $118^\circ$  for the monodentate ligand and  $136^\circ$  for the bidentate ligand. As in structure **8**, the N3 atom of the monodentate ligand is nearly planar with a deviation of  $-0.113(5)$  Å with respect to the plane formed by the P2/C33/C20 atoms (similar to the value found in the free ligand **6**),<sup>1</sup> while the N1 atom in the bidentate ligand adopts a trigonal pyramidal geometry with a deviation of  $0.429(5)$  Å with respect to the P1/C1/C14 plane. We also note that the P-O and P-N distances contract slightly when compared to the distances in the free ligand **6**.

Equation 1



Complexes **8** – **10** were appreciably soluble in chlorinated solvents affording orange solutions, while in benzene, toluene, THF,  $\text{CH}_3\text{CN}$ , and  $\text{NEt}_3$  they were only sparingly soluble. In methanol decomposition of complex **10** took place at 333 K. On the other hand, **8** and **10** dissolved readily in pyridine- $d_5$  to give yellow solutions and their NMR spectra indicated the generation of solvated species (see eq 1): The  $^{31}\text{P}\{^1\text{H}\}$  NMR spectrum of solvated **8•py** showed a pair of broad doublets of doublets centred around 144 ppm and 150 ppm with  $J_{\text{RhP}} = 306$  Hz and  $J_{\text{RhP}'} = 264$  Hz, respectively ( $J_{\text{PP}'} = 57$  Hz), and **10•py** displayed a very similar pair of broad doublets of doublets at 149 ppm and 156 ppm with  $J_{\text{RhP}} = 279$  Hz and  $J_{\text{RhP}'} = 238$  Hz, respectively ( $J_{\text{PP}'} = 48$  Hz). The lemon yellow pyridine adduct **8•py** crystallised from its pyridine solution by exposure to  $\text{Et}_2\text{O}$  vapour.<sup>22</sup> However, this microcrystalline product slowly lost solvent when left open to the glove-box atmosphere, and vacuum treatment mostly yielded the orange starting complex **8** thus clearly indicating the reversibility of solvent coordination.<sup>23</sup>

Scheme 2



Complexes **8** and **10** were transformed to the respective tetrafluoroborate salts **11** and **12** in excellent yields according to Scheme 2.<sup>24</sup> While the starting chloride complexes in solution are orange or dark yellow, their cationic counterparts **11** and **12** form deep red solutions.<sup>25</sup> The  $^{31}\text{P}\{^1\text{H}\}$  NMR spectra of the cations are simplified to one characteristic sharp doublet resonating at 165.7 ppm ( $J_{\text{RhP}} = 280$  Hz) and at 161.5 ppm ( $J_{\text{RhP}} = 256$  Hz), respectively, indicative of the higher symmetry of the cations and pointing to a *cis* arrangement of the ligands. *Trans* coordination of the chiral ligands would lead to complexes of lower symmetry and correspondingly complex  $^{31}\text{P}\{^1\text{H}\}$  NMR spectra. In fact, similar complexes having having *trans* geometry and high symmetry (with the Rh atom lying on a centre of inversion) were described with achiral P-alkene ligands.<sup>4a</sup> The addition of 1 equiv. of the  $\text{CD}_2\text{Cl}_2$ -soluble 1-butyl-2,3-dimethylimidazolium chloride ( $[\text{BMMI}][\text{Cl}]$ ) to the red cationic complexes **11** and **12** regenerated within the time of mixing, and quantitatively, the neutral yellow species **8** and **10** (Scheme 2).

The X-ray crystal structure of complex **12** bearing the proline-derived ligand confirmed the *cis* orientation of the two ligands in a pseudo square-planar coordination environment and the pseudo  $C_2$  point symmetry of the cation (see Figure 3). The distances of the coordinated alkene functions C12-C13 and C31-C32 are 1.391(16) Å and 1.383(14) Å, respectively, and are statistically equal to those observed in the neutral complexes **8** and **10**. Likewise, both nitrogen atoms N2 and N4 of the dibenz[b,f]azepine moieties adopt a pyramidal geometry with deviations of



-0.431(8) and -0.442(9) Å in relation to the P1/C6/C19 and P2/C25/C38 planes, respectively.

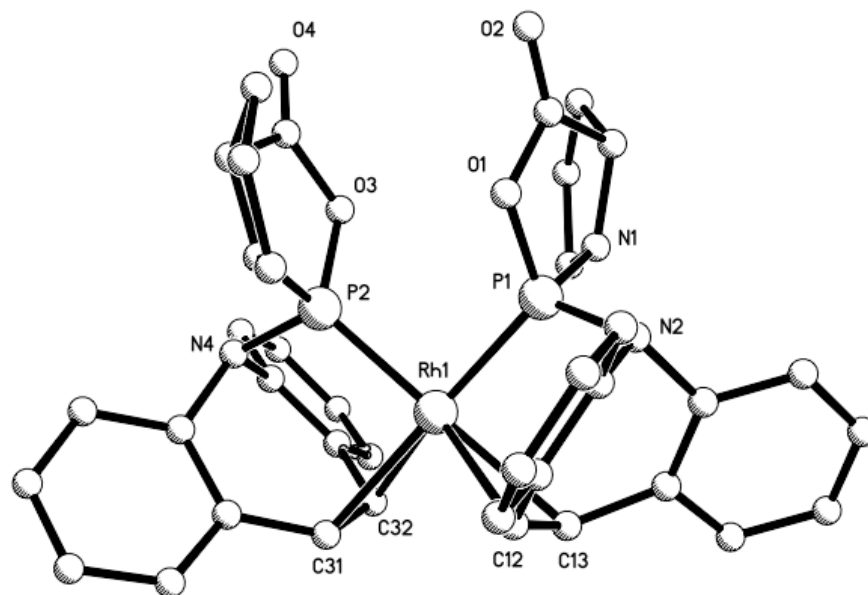
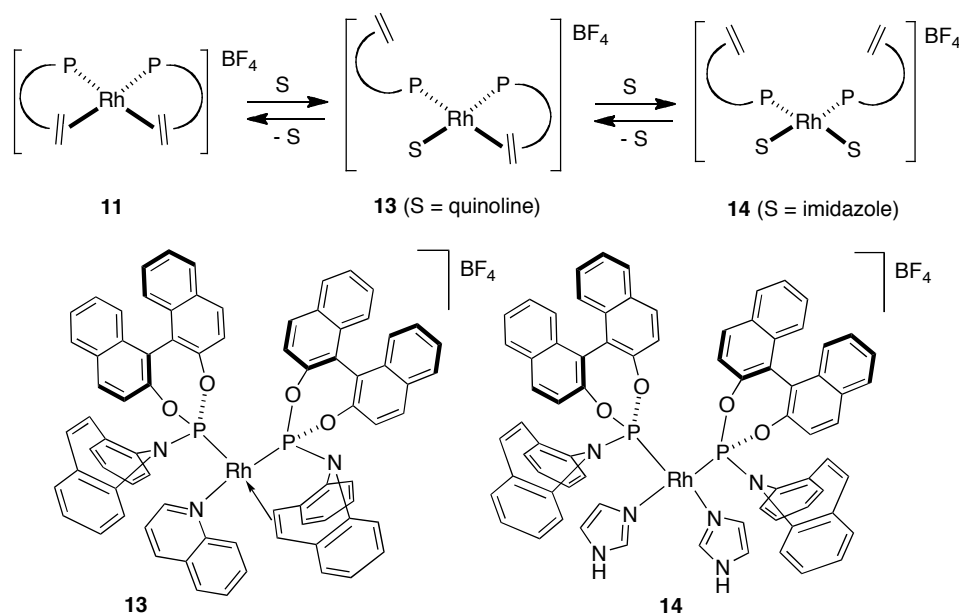


**Figure 3.** Structure of the cation of **12** in the crystal (ball and stick representation for clarity). Selected bond lengths (Å) and angles (°) are: Rh1-P1, 2.185(2); Rh1-P2, 2.184(2); Rh1-C12, 2.320(8); Rh1-C13, 2.385(7); Rh1-C31, 2.359(8); Rh1-C32, 2.3852(9); P1-N1, 1.640(8); P1-N2, 1.703(7); P1-O1, 1.656(6); P2-N3, 1.638(9); P2-N4, 1.715(8); P2-O3, 1.641(6); N2-C6, 1.460(10); N2-C19, 1.449(11); N4-C25, 1.447(12); N4-C38, 1.477(14); C12-C13, 1.391(16); C31-C32, 1.383(14); P1-Rh1-P2, 92.52(9); C6-N2-P1, 111.4(5); C19-N2-P1, 112.5(5); C19-N2-C6, 113.2(7); C25-N4-C38, 114.5(8); C25-N4-P2, 109.5(7), C38-N4-P2, 112.2(6).

Similarly to the addition of Cl<sup>-</sup> to the cations **11** and **12** (scheme 2), excess amounts of pyridine, CH<sub>3</sub>CN, or DMSO to the blood-red solutions of **11** and **12** led to lemon yellow solutions by the time of mixing. Even though these cationic solvento complexes (analogues of **14**, see Scheme 3) were more stable than the corresponding neutral chlorides **8•py** and **10•py** described above, they were not readily amenable to isolation.

**Scheme 3.** Solvation equilibria of **11** with S = pyridine, CH<sub>3</sub>CN, DMSO and their isolated analogues **13** and **14**



These adducts did not withstand vacuum drying, or washings with pentane or Et<sub>2</sub>O, thereby successively losing the coordinated solvent molecules and reverting first to the monosolvento complex **13** (observed *in situ* by <sup>31</sup>P{<sup>1</sup>H} NMR) and finally to the starting, dark red Rh cation **11** according to Scheme 3. However, the heavier and bulkier pyridine analogue quinoline readily coordinated to **11**, allowing the isolation and characterisation of the orange monosolvento complex **13**. This high yielding reaction was completely selective for the 1:1 adduct, and even at a ten-fold excess of quinoline, no bis-solvento analogue was observed. Neither under high vacuum nor on washing **13** with alkanes or ether did we observe decoordination of the quinoline molecule. Its <sup>31</sup>P{<sup>1</sup>H} NMR spectrum indicated lowered symmetry with respect to **11** showing a pair of doublets of doublets centred at 116 ppm (*J*<sub>RhP</sub> = 299 Hz, *J*<sub>PP'</sub> = 59 Hz) and 182 ppm (*J*<sub>RhP'</sub> = 246 Hz, *J*<sub>PP'</sub> = 59 Hz), reminiscent of the spectrum of the chloride complex **8**. Similarly, in an attempt to model the bis-solvento complex we opted for imidazole to mimic pyridine due to its lower volatility and improved crystallinity. Indeed, addition of 2 equiv of imidazole to **11** in CH<sub>2</sub>Cl<sub>2</sub> solution yielded the bis-imidazole adduct **14** almost quantitatively as a lemon yellow, microcrystalline powder. As expected, the <sup>31</sup>P{<sup>1</sup>H} NMR spectrum indicated higher symmetry featuring a sole broadened doublet at 148 ppm (*J*<sub>RhP</sub> = 273 Hz), similar to the spectrum of **11**, and the imidazole protons were characterised by a broad singlet at 11.6 ppm in the <sup>1</sup>H NMR spectrum. However, electron spray ionization of **13** and **14** in a CH<sub>3</sub>CN matrix only gave the molecular peak of the cation of **11** in both cases.

Additions of other nucleophiles to cations **11** and **12** that are relevant to CA catalysis such as hydroxides and arylboronic acids only led to inseparable mixtures.

The neutral Cu(I) iodide complexes **15** – **17** were prepared on gram scales by adding benzene to CuI and 2 equiv. of ligands **2**, **4**, and **5**, respectively (see eq. 2).  $^{31}\text{P}\{^1\text{H}\}$  NMR spectra of all three complexes showed broad singlets ( $\nu_{1/2} \approx 80$  Hz). When only 1 equiv. of ligand **2** was reacted slowly with CuI in benzene solution, the 1 : 2 adduct **15** formed along with 0.5 equiv. of unreacted CuI.<sup>26</sup>  $^1\text{H}$  NMR spectra of compounds **15** – **17** did not indicate coordination of the olefin functions of ligands **2**, **4**, and **5** to the Cu centre, and the monodentate coordination mode was confirmed by X-ray single crystal diffraction experiments on complexes **15** and **16** (see Figures 4 and 5). Both complexes are monomeric with a trigonal planar coordination around the Cu atom.<sup>27</sup>

The asymmetrical unit of **15** contains one half of the neutral complex that displays  $C_2$  symmetry along the Cu-I vector. The N atom of the dibenzazepine moiety adopts a trigonal planar conformation with a deviation of  $-0.078(9)$  Å in relation to the P1/C34/C21 plane. The dibenzazepine unit was found disordered over two sets of positions (see crystal determination section). The torsion angle of the naphthyl groups along C1-C10-C11-C12 is *ca.*  $50^\circ$ . In contrast, the asymmetrical unit of **16** contains a complete molecular unit that also exhibits a pseudo  $C_2$  symmetry around the Cu-I bond. Similar planar conformations of N2 and N4 are observed with distances of  $0.149(8)$  Å and  $0.067(8)$  Å from to the P1/C18/C31 and P2/C49/C62 planes, respectively.

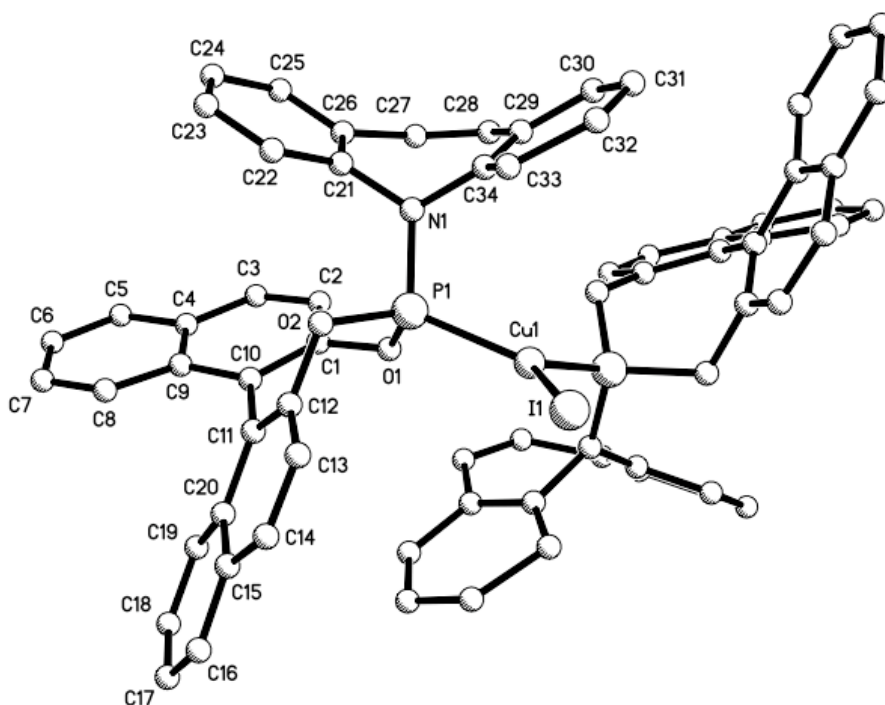


**Figure 4.** Ball and stick representation of complex **15** in the crystal showing its  $C_2$ -symmetry around the Cu-I vector. Selected bond lengths (Å) and angles (°) are: I1-Cu1, 2.4983(12); Cu1-P1, 2.2294(18); N1-C34, 1.391(8); N1-C21, 1.443(8); N1-P1, 1.661(6); P1-O1, 1.619(4); P1-O2, 1.637(4); O1-C1, 1.391(7); O2-C12, 1.412(7); C27-C28, 1.317(5); P1-Cu1-P1<sup>i</sup>, 109.18(9); P1-Cu1-I1, 125.41(4); P1<sup>i</sup>-Cu1-I1, 125.41(4); C34-N1-P1, 117.8(9); C21-N1-P1, 122.3(6); C34-N1-C21, 119.0(10); Symmetry code: (i)  $-x+2, -y+2, z$ .

In order to assess the coordinating ability of the olefinic part of the ligands in complexes **15** and **16**, the iodide was abstracted with  $\text{AgBF}_4$  in THF solution to afford two new complexes **18** and **19**, respectively, in excellent yields. Their  $^{31}\text{P}\{^1\text{H}\}$  NMR spectra showed small low field frequency shifts compared to the iodides, while the  $^1\text{H}$  NMR spectra did not provide evidence for olefin coordination to the Cu centres. Large single crystals of **18** were grown from a saturated and filtered toluene solution. Unfortunately, attempts to solve the crystal structure were hampered by serious disorder.<sup>28</sup> At least two comments about the structure may be made at this stage: First, the alkene functions of the two ligands do not coordinate the Cu centre, and second, the coordination sphere around Cu is trigonal planar. We believe that the third coordination site is occupied by the  $\text{BF}_4$  counteranion as depicted in the proposed structure<sup>29</sup> in eq. 2. However, THF instead of anion coordination cannot be ruled out on the basis of the available diffraction data.

### Equation 2

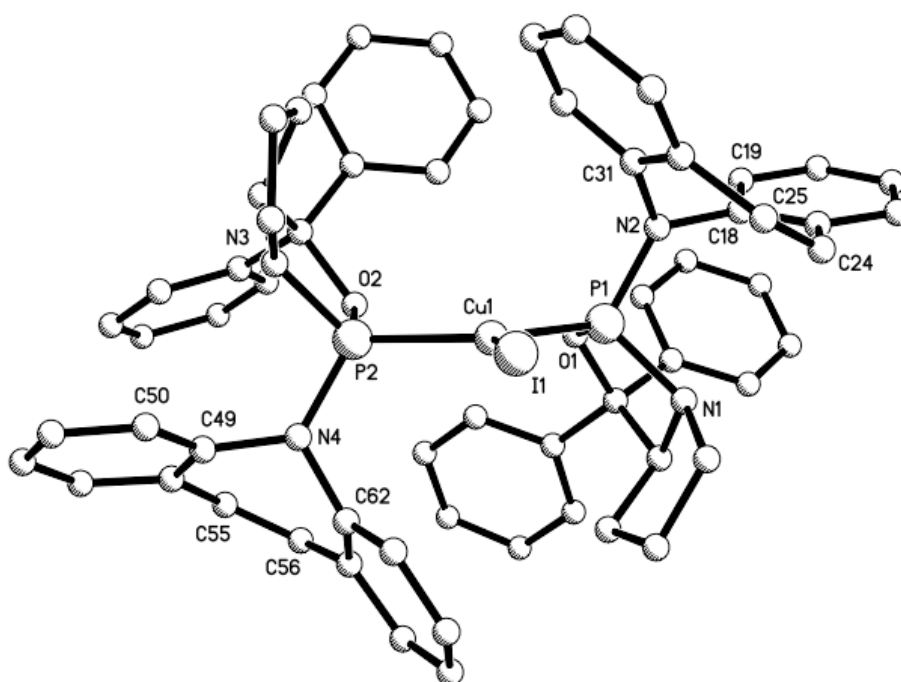
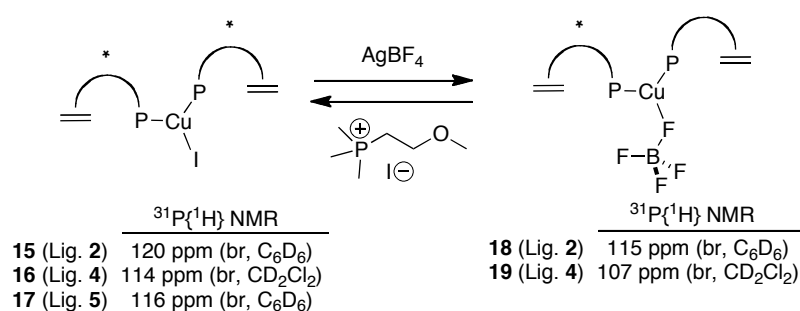
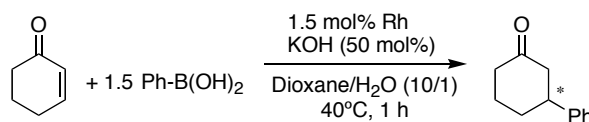


**Figure 5.** Structure of complex **16** in the crystal (ball and stick representation for clarity). Selected bond lengths (Å) and angles (°) are: Cu1-I1, 2.5354(13); Cu1-P1, 2.246(2); Cu1-P2, 2.255(2); P1-N1, 1.698(6); P1-N2, 1.663(7); P1-O1, 1.627(5); P2-N3, 1.682(7); P2-N4, 1.672(7); P2-O2, 1.617(5); N1-C2, 1.470(10); N1-C5, 1.481(10); N2-C18, 1.439(10); N2-C31, 1.443(9); N3-C33, 1.442(10); N3-C36, 1.471(11); N4-C49, 1.461(11); N4-C62, 1.454(10); C55-C56, 1.345(15); C24-C25, 1.339(14); P1-Cu1-P2, 120.82(9); P1-Cu1-I1, 120.90(7); O1-P1-N1, 93.2(3); O1-P1-N2, 107.7(3); N2-P1-N1, 104.9(3); O2-P2-N3, 93.2(3); O2-P2-N4, 110.4(3); N4-P2-N3, 102.7(3); C18-N2-P1, 125.4(5); C31-N2-P1, 118.5 (6); C18-N2-C31, 113.2 (6); C62-N4-C49, 112.7(6); C62-N4-P2, 120.2(5); C49-N4-P2, 126.5(6).

The most obvious difference in the coordination modes of the P-alkene ligands on comparison of the Rh(I) and Cu(I) complexes is the absence of alkene binding to Cu(I), to the extent where the weakly coordinating anion  $\text{BF}_4^-$  appears to be the preferred ligand. This could be explained with a preference of the P-alkene ligands for smaller bite-angles in square planar complexes and a stronger alkene-Rh(I) interaction due to efficient metal-alkene backbonding.

**5.2.2. Catalysis:** Preliminary trials showed the neutral Rh-chloride complexes **8** and **9** to be the far more active catalysts for the CA of arylboronic acid nucleophiles to enones than the corresponding recently reported chloro-bridged dimeric Rh complexes of type **7** (*vide supra*).<sup>1</sup> For example, in the benchmark reaction of phenylboronic acid with cyclohexenone at 80°C in a dioxane/H<sub>2</sub>O/KOH mixture dimer [Rh( $\mu$ -Cl)(**2**)<sub>2</sub>] yielded 90% of 3-phenylhexanone after 1 h reaction time, while the analogous monomer **8** gave quantitative yields in 0.5 h with similar selectivity. We therefore chose a reaction temperature of 40 °C to compare the performance of complexes **8** – **14** and the results are summarised in Table 2.

**Table 2.** Screening of Complexes **8** – **14** for the Catalytic 1,4-Addition



Catalyst	<b>8</b>	<b>9</b>	<b>10</b>	<b>11</b>	<b>12</b>	<b>13</b>	<b>14</b>
Yield (%) <sup>a</sup>	33	83	38	93	trace	trace	33
ee (%) <sup>b</sup>	89	2	32	92	nd	nd	92
Configuration <sup>c</sup>	( <i>R</i> )	( <i>R</i> )	( <i>R</i> )	( <i>R</i> )	nd	nd	( <i>R</i> )

<sup>a</sup> Isolated yields of 3-phenylcyclohexanone. <sup>b</sup> Determined by HPLC analysis with chiral column Daicel Chiralcel OD-H (for details see experimental). <sup>c</sup> Configuration determined by comparison with reported data. nd = not determined.

Complex **8** turned out to be quite an enantioselective catalyst, while **9** bearing the less bulky taddol derived ligand was very active. The neutral complex **10** and cationic **12** bearing the proline derived ligand **6** fared poorly. Apparently the ester function present in ligand **6** is incompatible with the phenylboronic acid substrate, which may also explain the formation of a black precipitate during catalysis. On the other hand, cation **11** combined excellent activity with high enantioselectivity and thus was used in the subsequent substrate screening (see Table 3). The high activity of **11** in comparison to its neutral analogue **8** could be explained by swifter arylation and/or hydroxylation of the cationic Rh centre during catalysis. Since the quinoline and imidazole complexes **13** and **14** already contain bases they were also tested in the absence of KOH, however, no reaction was observed. Likewise, quinoline adduct **13**

in the presence of KOH did not exhibit any noticeable activity, while the imidazole complex **14** behaved like the neutral chloride analogue **8**.

**Table 3.** Substrate Screening with Complex **11**

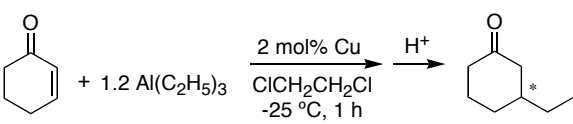
$\text{20A-G}^a + 1.5 \text{ Ar-B(OH)}_2^b \xrightarrow[\text{Dioxane/H}_2\text{O (10/1), 60 }^\circ\text{C, 1 h}]{1.5 \text{ mol\% (S)-11, KOH (50 mol\%)}} \text{22}$

Entry	Enone	Boronic Acid	Yield of <b>22</b> (%) <sup>c</sup>	ee (%) <sup>d,e</sup>
1	<b>20A</b>	<b>21a</b>	98 ( <b>22Aa</b> )	88
2	<b>20A</b>	<b>21b</b>	98 ( <b>22Ab</b> )	99
3	<b>20A</b>	<b>21c</b>	99 ( <b>22Ac</b> )	99
4	<b>20A</b>	<b>21d</b>	98 ( <b>22Ad</b> )	99
5	<b>20A</b>	<b>21e</b>	68 ( <b>22Ae</b> )	99
6	<b>20A</b>	<b>21f</b>	55 ( <b>22Af</b> )	85
7	<b>20A</b>	<b>21g</b>	75 ( <b>22Ag</b> )	90
8	<b>20A</b>	<b>21h</b>	99 ( <b>22Ah</b> )	95
9	<b>20B</b>	<b>21a</b>	90 ( <b>22Ba</b> )	60
10	<b>20C</b>	<b>21a</b>	95 ( <b>22Ca</b> )	95
12	<b>20E</b>	<b>21a</b>	97 ( <b>22Ea</b> )	99
13	<b>20F</b>	<b>21a</b>	99 ( <b>22Fa</b> )	98
14	<b>20G</b>	<b>21a</b>	60 ( <b>22Ga</b> )	65

<sup>a</sup> **20A** = 2-cyclohexenone, **20B** = 2-cyclopentenone, **20C** = 3-penten-2-one, **20D** = 3-hepten-2-one, **20E** = 3-octen-2-one, **20F** = 3-nonen-2-one, **20G** = 5-methyl-3-hexen-2-one. <sup>b</sup> Ar = Ph (**21a**), 3-CH<sub>3</sub>C<sub>6</sub>H<sub>4</sub> (**21b**), 4-CH<sub>3</sub>C<sub>6</sub>H<sub>4</sub> (**21c**), 3-CH<sub>3</sub>OC<sub>6</sub>H<sub>4</sub> (**21d**), 4-FC<sub>6</sub>H<sub>4</sub> (**21e**), 3-ClC<sub>6</sub>H<sub>4</sub> (**21f**), 4-ClC<sub>6</sub>H<sub>4</sub> (**21g**), 1-naphthyl (**21h**). <sup>c</sup> Isolated yields. <sup>d</sup> Determined by HPLC (chiral columns: Daicel Chiralcel OD-H, OJ-H, and OB. See Experimental Part). <sup>e</sup> Major enantiomers all have (*R*) configuration.

The substrate screening reactions were performed at a slightly higher temperature of 60 °C for it did not affect selectivities significantly (see entry 1, Table 3). The addition of a variety of arylboronic acids to cyclic and linear enones proceeded with very high activities and reaction times of less than 1 hour. More importantly, enantioselectivities of the products are high and, at times, total stereocontrol was observed in the reaction employing complex **11** as the catalyst (entries 2-5, 11, 12). Furthermore, all substrates were used from commercial suppliers as received without further purification, in order to test the robustness of the catalyst precursors toward common impurities.

**Table 4.** Screening of Complexes **15** – **19** for the Catalytic 1,4-Addition

						
Catalyst	-	<b>15</b>	<b>16</b>	<b>17</b>	<b>18</b>	<b>19</b>
Yield (%) <sup>a</sup>	64	52	24	47	98	98
ee (%) <sup>b</sup>	0	2	0	0	39	24
Configuration <sup>c</sup>	-	( <i>S</i> )	-	-	( <i>S</i> )	( <i>S</i> )

<sup>a</sup> GC yields of 3-ethylcyclohexanone. <sup>b</sup> Determined by GC using a chiral Lipodex E column (for details see experimental part). <sup>c</sup> Configuration determined by comparison with reported data.

The neutral Cu complexes **15** – **17** did not catalyse the ethylation of cyclohexenone with AlEt<sub>3</sub> in 1,2 dichloroethane solvent at -25 °C (see Table 4). It is noteworthy that the blank reaction afforded the 1,4 addition product in higher yield (64%) than in the presence of the Cu-iodo complexes **16** – **18**.<sup>30</sup> On the other hand, the corresponding cationic species **18** and **19** were active catalysts and in the case of complex **18** showed promising levels of enantioselectivity. The addition of AlEt<sub>3</sub> to the  $\beta$ -substituted enone 3-methyl-2-cyclohexenone was catalysed by **18** at -25 °C and over 4 h to afford the quaternary ketone in 83% isolated yield and 9% *e.e.* The optimization of this reaction is the subject of ongoing efforts in our laboratories.

### 5.3. Conclusions

Ligands **2**, **5**, and **6** were shown to act as hemilabile monodentate and bidentate ligands in mononuclear complexes of composition [RhX(L)<sub>2</sub>] (X = Cl, BF<sub>4</sub>). The hemilabile nature of the alkene function in these ligands is in part due to a flexible hybridisation state of the dibenz[b,f]azepine N atom, varying from quasi trigonal planar in the free and monodentate structures, to tetrahedral in bidentate structures with diminished P-alkene bite angles. The mononuclear complexes described here showed activities and selectivities for the CA of arylboronic acids to enones higher than those for the previously reported analogous neutral dimeric chloro-bridged



complexes. In particular, the cationic mononuclear complex **11**, turned out to be highly active and enantioselective, leading, in various cases, to optically pure cyclic and linear ketones in quantitative yields. These results highlight an often forgotten aspect in chiral catalyst development: optimisation of catalyst performance may well be achieved by tuning the coordination sphere of the metal catalyst, rather than by the usually less cost-effective strategy of ligand modification. Here we demonstrated a dramatic improvement of catalyst performance (using the same ligand!) simply by modifying the coordination chemistry of Rh(I) from dimeric neutral to mononuclear cationic. Finally, ligands **2**, **4**, and **5** formed isolable complexes with CuI in a stoichiometry of 2 : 1 that is relevant to CA catalysis. Structural analyses only revealed monodentate P-coordination. The corresponding cationic species were active catalysts for the moderately enantioselective addition of AlEt<sub>3</sub> to cyclohexenone.

#### 5.4. Experimental Part

All reactions were carried out under anaerobic and anhydrous conditions, using standard Schlenk and glove box techniques unless otherwise stated. THF, Et<sub>2</sub>O, benzene were distilled from purple Na/Ph<sub>2</sub>CO solutions, toluene from Na, pentane, C<sub>6</sub>D<sub>6</sub>, and THF-D<sub>8</sub> from Na/K alloy, CH<sub>3</sub>CN, CH<sub>2</sub>Cl<sub>2</sub>, CD<sub>2</sub>Cl<sub>2</sub> from CaH<sub>2</sub>, NEt<sub>3</sub> and 1,4-dioxane from K. CDCl<sub>3</sub> was degassed with three freeze-pump-thaw cycles and then kept over activated molecular sieves (4 Å) in a glove box. Quinoline (Merck) was distilled from a dark red Na solution. NMR spectra were recorded on a Jeol 400 MHz spectrometer. Ligands **2** – **6**,<sup>6</sup> [RhCl(COD)], and [RhCl(COE)<sub>2</sub>]<sub>2</sub><sup>31</sup> were prepared according to published procedures. Only freshly precipitated, snow-white CuI was used for complex synthesis. Only crystalline, *white* AgBF<sub>4</sub> was used (98 %, Aldrich Corp.), and reactions involving Ag were carried out in the dark. Elemental analyses were performed at IVIC or OCI and samples were handled in air (hygroscopic compounds are corrected for water content).

**[RhCl((S)-2)<sub>2</sub>] (8).** Method A: A solution of **2** (1441.9 mg, 2.8071 mmol) in dioxane (30 mL) was added dropwise over 10 min to a vigorously stirred orange slurry of [RhCl(COE)<sub>2</sub>]<sub>2</sub> (503.5 mg, 0.7071 mmol) in dioxane (30 mL) to afford a clear red solution that was stirred for 2 h. Then the volatiles were removed in vacuo and the

solid washed with hexane (2 x 40 mL). HV drying afforded 1.66 g (97%) of a fine orange powder. Elemental analysis found: C 71.21, H 4.03, N 2.18. Calculated for  $\text{RhClC}_{68}\text{H}_{44}\text{N}_2\text{O}_4\text{P}_2 \cdot 1/3\text{C}_6\text{H}_{14}$ : C 71.12, H 4.15, N 2.37.  $^1\text{H}$  NMR (400 MHz,  $\text{CDCl}_3$ )  $\delta$  4.84 (ABX,  $J = 56$  Hz, 9 Hz, 2H), 6.10-6.20 (m, 2H), 6.40-7.75 (m, 35H), 7.80-7.85 (m, 1H), 7.90-8.10 (m, 2H), 8.25-8.30 (m, 1H), 8.80-8.85 (m, 1H). The spectrum indicates the presence of ca. 0.3 equiv of co-crystallized hexane.  $^{31}\text{P}\{^1\text{H}\}$  NMR (162 MHz,  $\text{CD}_2\text{Cl}_2$ )  $\delta$  119.5 (dd,  $J_{\text{RhP}} = 286$  Hz,  $J_{\text{PP}'} = 45$  Hz), 179.0 (dd,  $J_{\text{RhP}'} = 283$  Hz,  $J_{\text{PP}'} = 45$  Hz). Method B: A solution of **2** (261 mg, 0.514 mmol) in dioxane (5 ml) was added dropwise over 5 min to a vigorously stirred light yellow-orange solution of  $[\text{RhCl}(\text{C}_2\text{H}_4)_2]_2$  (50.0 mg, 0.119 mmol) in dioxane (4 ml) affording a clear orange solution. The solution was kept stirring for 2 h and then dried in HV to give a bright orange crystalline solid. The solid was slurried in pentane (10 mL) for 1 h, decanted, and washed with additional pentane (2 x 5 ml). Drying *in vacuo* yielded 277 mg (94 %) of a finely divided orange powder. Spectroscopic data corresponded.

**$[\text{RhCl}((R,R)\text{-5})_2]$  (9).** Benzene (1.6 g) was added to thoroughly mixed  $[\text{RhCl}(\text{COE})_2]_2$  (101.0 mg, 0.1408 mmol) and *(R,R)*-**5** (216.3 mg, 0.5642 mmol) and the resulting deep red solution was stirred overnight. The solution was evaporated to a red solid that was washed pentane (2 x 6 mL) and then dried in HV to afford an orange powder (225 mg, 88 %). Elemental analysis found: C 56.51, H 4.91, N 3.01. Calculated for  $\text{C}_{42}\text{H}_{44}\text{ClN}_2\text{O}_8\text{P}_2\text{Rh} \cdot 2/5\text{C}_5\text{H}_{12}$ : C 56.58, H 5.27, N 3.00.  $^1\text{H}$  NMR (400 MHz,  $\text{CDCl}_3$ )  $\delta$  1.30 (s, 6H), 1.46 (s, 3H), 1.55 (s, 3H), 3.45-4.05 (m, 5H), 4.05-4.40 (m, 6H), 4.85-5.00 (m, 1H), 6.11 (s br, 2H), 6.62 (ABX,  $J = 35$  Hz, 12 Hz, 2H), 6.95-7.50 (m, 14H), 7.55-7.75 (m, 2H). The spectrum indicates the presence of ca. 0.4 equiv of co-crystallized pentane.  $^{31}\text{P}\{^1\text{H}\}$  NMR (162 MHz, toluene- $\text{D}_8$ )  $\delta$  121.9 (dd,  $J_{\text{RhP}} = 268$  Hz,  $J_{\text{PP}'} = 53.4$  Hz), 152.9 (dd,  $J_{\text{RhP}'} = 278$  Hz,  $J_{\text{PP}'} = 53.4$  Hz).  $^{13}\text{C}$  NMR (101 MHz,  $\text{CDCl}_3$ )  $\delta$  14.1, 22.4, 26.7, 26.8, 27.0, 27.1, 64.6, 65.7, 65.9, 66.3, 68.0, 68.1, 78.3, 78.8, 79.5, 89.1, 89.9, 111.0, 112.2, 126.6, 127.4, 127.5, 127.7, 128.1, 128.6, 128.8, 129.0, 130.0, 130.4, 130.8, 131.0, 136.1, 136.3, 139.6, 140.5-142.0 (m).

**$[\text{RhCl}((S,S)\text{-6})_2]$  (10).** A solution of *(S,S)*-**6** (694.4 mg, 2.065 mmol) in benzene (4 g) was added dropwise over 10 min to a vigorously stirred orange slurry of  $[\text{RhCl}(\text{COD})]_2$  (254.5 mg, 0.5161 mmol) in benzene (2 g) to afford first a clear deep

orange solution. Within minutes under stirring copious amounts of a bright orange solid started to precipitate and this mixture was stirred overnight. The solid was separated by filtration (glass fibre GF/B), dried in vacuo, slurried and washed with pentane (12 mL), and dried under HV. Yield: 762 mg (91%), orange powder. Elemental analysis found: C 54.70, H 4.35, N 6.84. Calculated for  $\text{N}_4\text{O}_4\text{P}_2\text{RhClC}_{38}\text{H}_{34}\cdot\text{H}_2\text{O}$ : C 55.05 H 4.38 N 6.76.  $^1\text{H}$  NMR (400 MHz,  $\text{CDCl}_3$ )  $\delta$  1.20-1.35 (m, 1H), 1.40-1.55 (m, 2H), 1.65-2.20 (m, 7H), 2.75-2.85 (m, 1H), 2.95-3.10 (m, 1H), 4.05-4.15 (m, 1H), 4.35-4.50 (m, 1H), 6.40-6.50 (m, 1H), 6.60-6.80 (m, 2H), 7.03 (d, 1H), 7.10-7.15 (m, 6H), 7.15-7.40 (m, 6H), 7.45-7.60 (m, 3H), 8.40 (d, 1H).  $^{31}\text{P}\{^1\text{H}\}$  NMR (162 MHz,  $\text{C}_6\text{D}_6$ )  $\delta$  135.2 ( $J_{\text{RhP}} = 258$  Hz,  $J_{\text{PP}} = 60$  Hz), 175.7 ( $J_{\text{RhP}} = 250$  Hz,  $J_{\text{PP}} = 59.5$  Hz).  $^{13}\text{C}$  NMR (101 MHz,  $\text{CDCl}_3$ )  $\delta$  26.0, 26.5, 28.7, 30.2, 47.7, 47.8, 51.8, 52.0, 60.6, 61.5, 93.2, 93.5, 100.7, 100.8, 127.1, 127.4, 127.8, 127.9, 128.0, 128.4, 129.0, 129.2, 129.4, 129.5, 129.6, 130.1, 130.4, 130.7, 130.8, 131.2, 131.6, 135.8, 137.7, 138.5, 139.7, 140.7, 140.8, 141.3, 141.5, 142.7, 172.1, 172.6. Single crystals suitable for X-ray diffraction were obtained by not disturbing the clear reaction solution that forms immediately after completed addition of the ligand.

**[Rh((S)-2)<sub>2</sub>][BF<sub>4</sub> (11).** A solution of  $\text{AgBF}_4$  (195.8 mg, 1.006 mmol) in THF (10 g) was added dropwise over 15 min to a vigorously stirred orange slurry of **8** (1217.2 mg, 1.0032 mmol) in THF (15 g) resulting in a deep red mixture which was stirred for 4 h. The volatiles were then evaporated *in vacuo* and the product was extracted with  $\text{CH}_2\text{Cl}_2$  (13 g) by GF/B glass fibre filtration. The clear blood red solution was evaporated to dryness and slurried in  $\text{Et}_2\text{O}$  (8 g) overnight. The solid was separated by filtration and dried in HV to yield 392 mg (95 %) of a red powder. Elemental analysis found: C 67.69, H 3.64, N 2.36. Calculated for  $\text{RhBF}_4\text{C}_{68}\text{H}_{44}\text{N}_2\text{O}_4\text{P}_2$ : C 67.79, H 3.68, N 2.33.  $^1\text{H}$  NMR (400 MHz,  $\text{CD}_2\text{Cl}_2$ )  $\delta$  5.51 (d, 9 Hz, 2H), 6.38 (d, 8 Hz, 2H), 6.52 (d, 10 Hz, 2H), 6.62 (d, 9 Hz, 2H), 6.65-6.75 (m, 2H), 6.82 (d, 8 Hz, 2H), 6.85-6.95 (m, 2H), 6.95-7.05 (m, 2H), 7.15 (d, 9 Hz, 2H), 7.15-7.25 (m, 2H), 7.25-7.40 (m, 8H), 7.40-7.45 (m, 2H), 7.65-7.95 (m, 12H), 7.95-8.05 (m, 2H).  $^{31}\text{P}\{^1\text{H}\}$  NMR (162 MHz,  $\text{CD}_2\text{Cl}_2$ )  $\delta$  165.7 (d,  $J_{\text{RhP}} = 280$  Hz). Quantitative  $^{13}\text{C}$  NMR (101 MHz,  $\text{CDCl}_3$ )  $\delta$  100.5 (br, 2C), 107.8 (br, 2C), 119.2 (2C), 120.3 (m, 4C), 122.7 (2C), 125.4 (2C), 125.5-126.8 (m, 10C), 128.1 (2C), 128.5 (2C), 128.7 (2C), 129.2-130.2 (m, 12C),

130.9 (m, 4C), 131.7 (m, 8C), 132.8 (2C), 136.6 (2C), 139.4 (m, 2C), 140.0 (m, 4C), 145.3 (2C), 147.2 (m, 2C).

**[Rh((*S,S*)-6)<sub>2</sub>][BF<sub>4</sub> (12).** A solution of AgBF<sub>4</sub> (50.2 mg, 0.258 mmol) in toluene (3 g) was added dropwise over 10 min to a vigorously stirred slurry of **10** (208.8 mg, 0.2575 mmol) in toluene (8 g) immediately forming a large amount of a brick-red flocculating solid and a colourless supernatant solution. The solid was separated by filtration (GF/B), dried *in vacuo*, after which CH<sub>2</sub>Cl<sub>2</sub> (4 g) was added to afford a blood-red solution and a fine white precipitate. Separation by filtration (GF/B), evaporation of the red solution, and washing of the resultant red solid by slurring in hexane (3 g) for 4 h yielded 208 mg (90 %) of a dark red solid. Elemental analysis found: C 48.54, H 3.94, N 5.60. Calculated for RhBF<sub>4</sub>C<sub>38</sub>H<sub>34</sub>N<sub>4</sub>P<sub>2</sub>O<sub>4</sub>•CH<sub>2</sub>Cl<sub>2</sub>•H<sub>2</sub>O: C 48.53, H 3.97, N 5.80. <sup>1</sup>H NMR (400 MHz, CDCl<sub>3</sub>) δ 1.30-1.55 (m, 4H), 1.75-1.95 (m, 2H), 1.95-2.10 (m, 2H), 2.10-2.25 (m, 2H), 2.60-2.80 (m, 2H), 3.90-4.10 (m, 2H), 6.75-6.95 (m, 4H), 7.00-7.35 (m, 6H), 7.35-7.55 (m, 4H), 7.55-7.70 (m, 2H), 7.70-7.85 (m, 2H), 7.85- 8.00 (m, 2H). The spectrum indicates the presence of CH<sub>2</sub>Cl<sub>2</sub>. <sup>31</sup>P{<sup>1</sup>H} NMR (162 MHz, CDCl<sub>3</sub>) δ 161.5 (d, J<sub>RhP</sub> = 256 Hz). <sup>13</sup>C NMR (101 MHz, CDCl<sub>3</sub>) δ 25.8, 28.8, 48.9, 61.1, 104.3, 111.3, 128.7, 129.2, 129.8, 129.9, 130.7, 130.8, 131.3, 131.9, 137.7, 138.2, 138.7, 140.7.

**[Rh((*S,S*)-2)<sub>2</sub>(quinoline)][BF<sub>4</sub> (13).** A solution of quinoline (79 mg, 0.61 mmol) in CH<sub>2</sub>Cl<sub>2</sub> (5 g) was added dropwise at ca. 270 K over 10 min to a vigorously stirred, blood red solution of [Rh((*S,S*)-2)<sub>2</sub>][BF<sub>4</sub>•2/5Et<sub>2</sub>O (**11**, 289.0 mg, 0.2341 mmol) in CH<sub>2</sub>Cl<sub>2</sub> (5 g) to afford an orange solution that was stirred during 2 h and then evaporated to dryness. This left a microcrystalline, free-flowing orange red powder that was washed with Et<sub>2</sub>O (12 mL). Separation by filtration and drying *in vacuo* afforded 290 mg (92%) of an orange powder. Elemental analysis found: C 68.99, H 3.95, N 3.06. Calculated for RhBF<sub>4</sub>C<sub>77</sub>H<sub>51</sub>P<sub>2</sub>O<sub>4</sub>N<sub>3</sub>: C 69.33, H 3.85, N 3.15. <sup>1</sup>H NMR (400 MHz, CDCl<sub>3</sub>) δ 4.30-4.40 (m, 1H), 4.55-4.65 (m, 2H), 4.65-4.75 (m, 1H), 5.25-5.30 (m, 1H), 5.55-5.65 (m, 1H), 5.95-6.10 (m, 2H), 6.35-6.45 (m, 1H), 6.45-6.65 (m, 3H), 6.65-6.75 (m, 2H), 6.80-6.90 (m, 3H), 6.95-7.15 (m, 8H), 7.20-7.90 (m, 16H), 8.05-8.25 (m, 5H), 8.30-8.40 (m, 2H), 8.50-8.60 (m, 1H), 8.85-8.95 (m, 1H), 9.35-9.45 (m, 1H). <sup>31</sup>P{<sup>1</sup>H} NMR (162 MHz, CD<sub>2</sub>Cl<sub>2</sub>) δ 115.7 (dd, J<sub>RhP</sub> = 299 Hz, J<sub>PP'</sub> = 59

Hz ), 182.1 (dd,  $J_{\text{RhP}} = 246$  Hz,  $J_{\text{PP}} = 59$  Hz ).  $^{13}\text{C}$  NMR (101 MHz,  $\text{CDCl}_3$ )  $\delta$  88.9 (m), 96.9, 118.7, 120.6, 121.2, 122.0-123.0 (m), 125.0-132.5 (m), 136.3, 137.7, 138.1 (m), 139.0 (m), 139.3, 140.5-141.0 (m), 147.0-148.5 (m), 150.7, 156.0.

**[Rh((*S,S*)-2)<sub>2</sub>(imidazole)<sub>2</sub>]BF<sub>4</sub>•3/5Et<sub>2</sub>O (14).** A solution of imidazole (35.4 mg, 0.520 mmol) in  $\text{CH}_2\text{Cl}_2$  (5 g) was added dropwise at ca. 270 K over 10 min to a vigorously stirred, blood red solution of [Rh((*S,S*)-2)<sub>2</sub>]BF<sub>4</sub>•2/5Et<sub>2</sub>O (**12**, 301.5 mg, 0.2478 mmol) in  $\text{CH}_2\text{Cl}_2$  (5 g) to afford a bright yellow solution that was stirred during 2 h and then evaporated to dryness. This left a microcrystalline, free-flowing lemon yellow solid that was washed with Et<sub>2</sub>O (2 x 7 mL). Separation by filtration and drying *in vacuo* afforded 325 mg (95%) of a yellow fine powder. Elemental analysis found: C 65.24, H 4.28, N 6.00. Calculated for  $\text{RhBF}_4\text{C}_{74}\text{H}_{52}\text{P}_2\text{O}_4\text{N}_6\cdot 3/5\text{Et}_2\text{O}\cdot \text{H}_2\text{O}$ : C 65.39, H 4.31, N 5.99.  $^1\text{H}$  NMR (400 MHz,  $\text{CD}_2\text{Cl}_2$ )  $\delta$  5.18 (br, 2H), 5.43 (br, 2H), 5.60 (br, 2H), 6.14 (br, 1H), 6.16 (br, 1H), 6.25-6.40 (m, 4H), 6.55-6.70 (m, 4H), 6.70-6.80 (m, 2H), 6.95-7.15 (m, 7H), 7.15-7.30 (m, 6H), 7.30-7.40 (m, 2H), 7.40-7.50 (m, 2H), 7.60-7.85 (m, 13H), 7.90-7.95 (m, 2H), 11.63 (br, 2H). The spectrum indicates the presence of ca. 0.6 equiv Et<sub>2</sub>O.  $^{31}\text{P}\{^1\text{H}\}$  NMR (162 MHz,  $\text{CDCl}_3$ )  $\delta$  147.8 (d,  $J_{\text{RhP}} = 273$  Hz).  $^{13}\text{C}$  NMR (101 MHz,  $\text{CDCl}_3$ )  $\delta$  120.6, 121.5, 122.1, 124.8, 125.0, 125.2, 125.8, 126.0, 126.2, 126.5-131.5 (m), 131.7, 132.2, 132.9, 134.9, 135.9, 138.3 (m), 141.3, 142.2 (m), 147.7, 149.1. The spectrum indicates the presence of Et<sub>2</sub>O.

**[CuI((*S*)-2)<sub>2</sub>] (15).** Benzene (16 g) was rapidly added to CuI (616.2 mg, 3.235 mmol) and (*S*)-2 (3322 mg, 6.472 mmol) and the resulting mixture was stirred for 24 h affording a white precipitate and a yellow supernatant solution. The solid was separated by filtration (GF/B) and dried *in vacuo* to yield 3.76 g (93 %) of a white powder. Elemental analysis found: C 68.50, H 3.63, N 2.25. Calculated for  $\text{N}_2\text{O}_4\text{P}_2\text{CuC}_{68}\text{H}_{44}\text{I}\cdot 1/2\text{C}_6\text{H}_6$ : C 68.52, H 3.81, N 2.25.  $^1\text{H}$  NMR (400 MHz,  $\text{C}_6\text{D}_6$ )  $\delta$  5.74 (br, 1H), 6.17 (m, 2H), 6.30 (br, 1H), 6.42 (m, 2H), 6.55-6.75 (m, 8H), 6.90-7.00 (m, 4H), 7.00-7.20 (m, 10H), 7.30-7.45 (m, 8H), 7.60 (m, 2H), 7.69 (m, 2H), 7.80 (m, 2H), 8.43 (br, 2H). The spectrum indicated the presence of ca. 0.5 equiv of co-crystallized benzene.  $^{31}\text{P}\{^1\text{H}\}$  NMR (162 MHz,  $\text{C}_6\text{D}_6$ )  $\delta$  120 (br). Single crystals

suitable for an X-ray diffraction analysis were obtained by dissolving the complex (78 mg) in boiling benzene (1.2 g) and slowly cooling the solution to RT.

**[CuI((*S,S*)-4)<sub>2</sub>] (16).** Benzene (20 mL) was rapidly added to a mixture of CuI (382.8 mg, 2.010 mmol) and (*S,S*)-4 (1.908 g, 4.021 mmol) under vigorous stirring and the resulting clear pale yellow solution was stirred for 8 h. Evaporation of the volatiles afforded an off-white solid which is pure enough for most applications. The product was recrystallized by dissolving it in hot toluene (20 mL), followed by filtration over glassfibre (GF/B), and cooling to 250 K for 2 d. The resulting white crystals were separated from the mother liquor by decanting and were dried *in vacuo* (1.16 g, 51 %). This batch afforded single crystals suitable for an X-ray diffraction analysis. The mother liquor was concentrated to *ca.* 10 mL, Et<sub>2</sub>O (15 mL) was added, and the mixture kept at 250 K for 2 d to afford another crop of white microcrystals (0.75 g, 33 %). Elemental analysis found: C 64.87, H 4.53, N 4.86. Calculated for CuIn<sub>4</sub>O<sub>2</sub>P<sub>2</sub>C<sub>62</sub>H<sub>54</sub>•1/2H<sub>2</sub>O: C 64.84, H 4.83, N 4.88. <sup>1</sup>H NMR (400 MHz, C<sub>6</sub>D<sub>6</sub>) δ 0.90-1.05 (m, 2H), 1.20-1.45 (m, 6H), 2.85-2.95 (m, 2H), 3.45-3.55 (m, 2H), 3.55-3.75 (br, 2H), 6.55-6.70 (m, 6H), 6.80-7.40 (m, 28H), 7.40-7.55 (m, 6H). <sup>31</sup>P{<sup>1</sup>H} NMR (162 MHz) δ 116 (br, C<sub>6</sub>D<sub>6</sub>); 114 (br, CD<sub>2</sub>Cl<sub>2</sub>). Quantitative <sup>13</sup>C NMR (101 MHz, CD<sub>2</sub>Cl<sub>2</sub>) δ 27.1 (s, 2C), 29.1 (s, 2C), 46.0 (s, 2C), 68.7 (s, 2C), 94.3 (s, 2C), 126.0-129.0 (m, 34C), 129.4 (s, 2C), 130.0 (s, 4C), 132.3 (s, 2C), 137.0 (s, 2C), 137.8 (s, 2C), 140.4 (s, 2C), 142.2 (s, 2C), 144.0 (s, 2C), 145.6 (s, 2C).

**[CuI((*R,R*)-5)<sub>2</sub>] (17).** Benzene (3 g) was added to CuI (93.5 mg, 0.491 mmol) and (*R,R*)-5 (376 mg, 0.982 mmol) and the resulting mixture was stirred forming a clear pale yellow solution within 5 min. The solution was stirred overnight and then the volatiles were evaporated affording a white solid which was slurried in pentane (8 mL) for 12 h and then separated by filtration. HV drying afforded 378 mg (80 %) of a fine white solid. Elemental analysis found: C 51.80, H 4.50, N 2.84. Calculated for CuIn<sub>2</sub>O<sub>8</sub>P<sub>2</sub>C<sub>42</sub>H<sub>44</sub>•H<sub>2</sub>O: C 51.73, H 4.75, N 2.87. <sup>1</sup>H NMR (400 MHz, C<sub>6</sub>D<sub>6</sub>) δ 1.21 (s, 6H), 1.33 (s, 6H), 3.50-3.65 (m, 2H), 3.75-3.85 (m, 2H), 3.90-4.10 (m, 6H), 6.60-6.70 (m, 4H), 6.85-7.05 (m, 8H), 7.05-7.20 (m, 4H), 7.60-7.70 (m, 4H). <sup>31</sup>P{<sup>1</sup>H} NMR (162 MHz, C<sub>6</sub>D<sub>6</sub>) δ 116 (s, br). <sup>13</sup>C NMR (101 MHz, C<sub>6</sub>D<sub>6</sub>) δ 26.8 (d, 28Hz),

65.0 (d, 11Hz), 78.9, 79.6, 110.9, 126.6 (d, 5Hz), 128.8, 129.1, 129.3, 129.4, 131.0, 131.6, 136.3 (d, 7Hz), 142.1, 142.6 (d, 11Hz).

**Cu((S)-2)<sub>2</sub>(BF<sub>4</sub>) (18).** A solution of AgBF<sub>4</sub> (156.2 mg, 0.8023 mmol) in THF (10 g) was added dropwise over 10 min to a vigorously stirred clear, colourless solution of **15** (1011 mg, 0.7985 mmol) in THF (12 g) to afford a greenish white precipitate with a colourless supernatant. The mixture was stirred for 24 h, the precipitate separated by centrifugation (4000 rpm, 60 min), and the clear supernatant solution was evaporated to dryness and the white solid dried in HV (915 mg, 98 %). Elemental analysis found: C 67.28, H 3.78, N 2.15. Calculated for C<sub>68</sub>H<sub>44</sub>CuP<sub>2</sub>N<sub>2</sub>O<sub>4</sub>BF<sub>4</sub>•2.5H<sub>2</sub>O: C 67.48, H 4.08, N 2.31. <sup>1</sup>H NMR (400 MHz, CD<sub>2</sub>Cl<sub>2</sub>) δ 5.10-5.25 (m br, 2H), 6.20-6.30 (m, 2H), 6.35-6.55 (m, 4H), 6.60-6.80 (m, 4H), 6.85-7.05 (m, 8H), 7.05-7.45 (m, 12H), 7.50-7.60 (m, 4H), 7.75-7.85 (m, 2H), 7.90-8.00 (m, 2H), 8.05-8.15 (m, 2H), 8.20-8.30 (m, 2H). <sup>31</sup>P{<sup>1</sup>H} NMR (162 MHz, CD<sub>2</sub>Cl<sub>2</sub>) δ 114 (s, br). <sup>13</sup>C NMR (101 MHz, CD<sub>2</sub>Cl<sub>2</sub>) δ 120.4, 120.7, 122.4, 122.8, 125.3, 125.6, 126.2, 126.4 (m, br), 126.5, 126.8, 127.0 (br), 128.2, 128.5, 128.6, 129.0, 129.2, 129.3, 129.6, 129.7, 130.8, 131.2, 131.4, 131.8, 132.3, 132.8, 135.0, 136.1, 139.7, 140.4 (m) 147.2, 147.6 (m). Large single crystals grew from a filtered (cotton plug plus Celite) warm solution of the compound (120 mg) in toluene (4.5 g).

**Cu(BF<sub>4</sub>)((R,R)-4)<sub>2</sub>•THF (19).** A solution of AgBF<sub>4</sub> (87.1 mg, 0.447 mmol) in THF (6 g) was added dropwise over 10 min to a vigorously stirred clear, colourless solution of **16** (508.5 mg, 0.4462 mmol) in THF (6 g) to afford a greenish white precipitate with a colourless supernatant. The mixture was stirred for 8 h. The solid was separated by filtration, dried *in vacuo*, and then extracted with CH<sub>2</sub>Cl<sub>2</sub> (16 g) by filtration (GF/B glass fibre). The clear mother liquor was evaporated to an off-white solid that was slurried in THF (5 mL) for 30 min, separated by filtration, and finally dried in HV to afford 382 mg (73 %) of a snow white powder. This material is usually 95 % isomerically pure (the impurity is characterised by a pair of doublets in the <sup>31</sup>P{<sup>1</sup>H} NMR spectrum, see below). The impurity is removed by successive washings in benzene. Elemental analysis found: C 65.72, H 5.03, N, 4.68. Calculated for CuBF<sub>4</sub>N<sub>4</sub>O<sub>2</sub>P<sub>2</sub>C<sub>62</sub>H<sub>54</sub>•C<sub>4</sub>H<sub>8</sub>O•1/2CH<sub>2</sub>Cl<sub>2</sub>: C 65.79, H 5.23, N 4.62. <sup>31</sup>P{<sup>1</sup>H} NMR (162 MHz, C<sub>6</sub>D<sub>6</sub>) δ 106 (s, br), isomeric impurity (5-8 %): 116 (d, J<sub>PP'</sub> = 53 Hz), 121

(d,  $J_{\text{PP}} = 53$  Hz).  $^1\text{H}$  NMR (400 MHz,  $\text{C}_6\text{D}_6$ )  $\delta$  1.10-1.25 (m, 2H), 1.50-1.60 (m, 2H), 1.60-1.80 (m, 6H), 1.85-1.95 (m, 2H), 2.85-3.00 (m, 4H), 3.00-3.10 (m, 2H), 3.35-3.50 (m, 4H), 6.45-6.50 (m, 2H), 6.65-6.75 (m, 2H), 6.85-6.95 (m, 2H), 6.95-7.05 (m, 2H), 7.05-7.45 (m, 24H), 7.45-7.60 (m, 8H). The spectrum indicates the presence of *ca.* 0.5 equiv of  $\text{CH}_2\text{Cl}_2$  of co-crystallization.  $^{13}\text{C}$  NMR (101 MHz,  $\text{CD}_2\text{Cl}_2$ )  $\delta$  25.6 (THF), 27.3, 28.6, 44.9 (m), 69.3 (THF), 70.8, 95.6, 126.7, 127.1, 127.3, 127.8, 127.9, 128.0, 128.2, 128.26, 128.31, 129.0, 129.8, 129.9, 130.3, 130.6, 131.3, 136.2, 136.9, 139.4, 140.9, 143.7.

**Crystal structure determinations.** Intensity data were recorded at room temperature on a Rigaku AFC-7S diffractometer using monochromated  $\text{Mo}(\text{K}\alpha)$  radiation ( $\lambda = 0.71073$  Å). Experimental details on unit cell and intensity measurements can be found in the CIF files deposited with the Cambridge Crystallographic Data Centre under deposition numbers CCDC 770993 – 770997 corresponding to complexes **8**, **10**, **12**, **15**, and **16**, respectively. An empirical absorption correction (multi-scan) was applied to all the data using the CrystalClear crystallographic software package.<sup>32</sup> The structures were solved by Direct Methods and refined by full-matrix least-squares on  $F^2$ . The H-atoms on C were placed in calculated positions using a riding atom model with fixed C-H distances [0.93 Å for  $\text{C}(\text{sp}^2)$ , 0.96 Å for  $\text{C}(\text{sp}^3, \text{CH}_3)$  and 0.97 Å for  $\text{C}(\text{sp}^3, \text{CH}_2)$ ]. All the H atoms were refined with isotropic displacement parameters set to  $1.2 \times U_{\text{eq}}$  for  $\text{C}(\text{sp}^2)$  and 1.5 for  $\text{C}(\text{sp}^3)$  of the attached atom. In structure **8**, two acetonitrile molecules were found, of which one was found disordered over two sets of positions. The occupational parameters were refined to 46:54. In structure **12** either a  $\text{BF}_4^-$  anion or a dichloromethane molecule were found disordered. For each molecule the disorder was modelled over two orientations with restraints in the B-F, C-Cl and Cl...Cl distances and with complementary occupancies of 73:27 and 48:52 for the anion and dichloromethane, respectively. In structure **15** the dibenz[b,f]azepine unit was found disordered over two sets of positions, which were included by constraining the aromatic rings to a regular hexagon. The occupational parameters were refined to 59:41. Also, either benzene or water molecules were found disordered. For each molecule the disorder was modelled over two orientations. The benzene ring was refined by constraint to a regular hexagon, obtaining complementary occupancies of 50:50. The water molecule was refined with isotropic



displacement parameters only. All the refinement calculations were made using SHELXTL-NT.<sup>33</sup>

**General procedure for the 1,4-addition of boronic acids to enones:** Inside the glovebox a 20 ml vial was charged with Rh-precatalyst (0.0075 mmol), boronic acid (0.6 mmol) and a stirring bar. Dioxane was added (1 ml) and the vial was sealed with a PTFE cap and removed from the glovebox. Degassed enone (0.5 mmol) and degassed KOH solution (2.5M in H<sub>2</sub>O, 0.1 ml, 0.25 mmol) were added *via* syringe. The mixture was stirred at 40 or 60°C for 1 hour. After this time, it was diluted with Et<sub>2</sub>O (10 mL) and washed with water (2 x 10 mL). The organic phase was dried over MgSO<sub>4</sub> and the solvent evaporated. The product was purified by flash chromatography (silica gel G60, 9:1 hexane/ Et<sub>2</sub>O eluent) and analysed by NMR and HPLC. Compounds **22Aa-h**, **22Ba**, and **22Ea** have been previously reported.<sup>1</sup>

**(R)-4-phenylpentan-2-one (22Ca)**<sup>34</sup>: Eluted with hexane/ether (50:1), obtained as a yellow oil. HPLC conditions: Chiralcel OJ-H column (hexane:*i*-PrOH 98:2, 0.7ml/min); *t*<sub>R</sub> 23.0 min (minor), 25.1 min (major). <sup>1</sup>H NMR (400MHz, CDCl<sub>3</sub>): δ 1.25 (d, *J* = 6.9 Hz, 3H), 2.04 (s, 3H), 2.61-2.77 (m, 2H), 3.24-3.33 (m, 1H), 7.17-7.20 (m, 3H), 7.26-7.29 (m, 2H). <sup>13</sup>C NMR (100MHz, CDCl<sub>3</sub>) δ 22.31 (s), 30.88 (s), 35.77 (s), 52.32 (s), 126.62 (s), 127.07 (s), 128.86 (s), 146.49 (s), 208.12 (s).

**(R)-4-phenylheptan-2-one (22Da)**<sup>35</sup>: Eluted with hexane/ether (50:1), obtained as a colourless oil. HPLC conditions: chiralcel OJ-H column (hexane:*i*-PrOH 99.5:0.5, 0.5ml/min); *t*<sub>R</sub> 24.2 min (minor), 26.1 min (major). <sup>1</sup>H NMR (400MHz, CDCl<sub>3</sub>): δ 0.90 (t, *J* = 7.3 Hz, 3H), 1.26-1.29 (m, 2H), 1.56-1.70 (m, 2H), 2.07 (s, 3H), 2.71-2.82 (dd, *J* = 7.2 Hz and *J* = 3.3 Hz, 2H), 3.15-3.22 (m, 1H), 7.22-7.26 (m, 3H), 7.32-7.36 (m, 2H). <sup>13</sup>C NMR (100MHz, CDCl<sub>3</sub>): δ 14.26 (s), 20.82 (s), 30.95 (s), 39.00 (s), 41.38 (s), 51.24 (s), 126.61 (s), 127.78 (s), 128.75 (s), 144.88 (s), 208.31 (s).

**(R)-4-phenylnonan-2-one (22Fa)**<sup>36</sup>: Eluted with hexane/ether (50:1), obtained as a colourless oil. HPLC conditions: chiralcel OJ-H column (hexane:*i*-PrOH 98:2, 0.5ml/min); *t*<sub>R</sub> 12.5 min (major), 14.2 min (minor). <sup>1</sup>H NMR (400MHz, CDCl<sub>3</sub>): δ 0.80 (t, *J* = 6.9 Hz, 3H), 1.09-1.24 (m, 6H), 1.53-1.64 (m, 2H), 1.99 (s, 3H), 2.69 (dd,

$J = 7.2$  and  $J = 2.2$ ), 3.07-3.11 (m, 1H), 7.14-7.18 (m, 3H), 7.24-7.28 (m, 2H).  $^{13}\text{C}$  NMR (100MHz,  $\text{CDCl}_3$ ):  $\delta$  14.27 (s), 22.75 (s), 27.30 (s), 30.90 (s), 31.99 (s), 36.70 (s), 41.59 (s), 51.23 (s), 126.56 (s), 126.56 (s), 127.73 (s), 128.71 (s), 144.90 (s), 208.27 (s).

**(*R*)-4-phenyl-5-methylhexan-2-one (22Ga)**<sup>36</sup>: Eluted with hexane/ether (50:1), obtained as a colourless oil. HPLC conditions: chiralcel OJ-H column (hexane/iPrOH, 99:1, 1ml/min);  $t_R$  9.7 min (major),  $t_R$  11.6 min (minor).  $^1\text{H}$  NMR (400MHz,  $\text{CDCl}_3$ ):  $\delta$  0.75 (d,  $J = 6.7$  Hz, 3H), 0.93 (d,  $J = 6.6$  Hz, 3H), 1.79-1.87 (m, 1H), 1.97 (s, 3H), 2.78-2.80 (m, 2H), 2.89-2.94 (m, 1H), 7.12-7.20 (m, 3H), 7.24-7.28 (m, 2H).  $^{13}\text{C}$  NMR (100MHz,  $\text{CHCl}_3$ )  $\delta$ : 20.60 (s), 20.99 (s), 30.86 (s), 33.58 (s), 47.95 (s), 48.38 (s), 126.55 (s), 128.45 (s), 128.54 (s), 143.51 (s), 208.5 (s).

**General procedure for the 1,4-addition of  $\text{AlEt}_3$  to enones:** Inside the glovebox a 20ml vial was charged with Cu precatalyst (0.01 mmol for **16** – **20**) as a solution in 1,2-dichloroethane (2 ml) and a stirring bar. The vial was sealed with a PTFE cap, and taken outside the glovebox. Degassed enone (0.5 mmol) and degassed dodecane (0.5 mmol, as internal standard) were then added *via* syringe. The vial was cooled to  $-25^\circ\text{C}$  and  $\text{AlEt}_3$  was added dropwise via syringe, so not to increase the temperature. The reaction was analysed by GC (chiral column Lipodex E, 25m x 0.25mm) to obtain values for conversion and enantiomeric excess. The product was isolated and confirmed by comparison with literature values.<sup>18b</sup>

## Acknowledgments

We thank FONACIT (Projects S1-2001000851 and LAB-97000821) for financial support, Ms. Noelani Cigüela for technical assistance (NMR laboratory, USB), and Prof. Giuseppe Agrifoglio for helpful discussions.

## References

- <sup>1</sup> Part 1: Mariz, R.; Briceño, A.; Dorta, R.; Dorta, R. *Organometallics* **2008**, 27, 6605
- <sup>2</sup> For a review, see: Defieber, C.; Grützmacher, H.; Carreira, E. *Angew. Chem. Int. Ed.* **2008**, 47, 4482.

- <sup>3</sup> (a) Shintani, R.; Duan, W.-L.; Nagano, T.; Okada, A.; Hayashi, T. *Angew. Chem. Int. Ed.* **2005**, *44*, 4611; (b) Duan, W.-L.; Iwamura, H.; Shintani, R.; Hayashi, T. *J. Am. Chem. Soc.* **2007**, *129*, 2130; (c) Shintani, R.; Duan, W.-L.; Okamoto, K.; Hayashi, T. *Tetrahedron: Asymmetry* **2005**, *16*, 3400; (d) Kasák, P.; Arion, V. B.; Widhalm, M. *Tetrahedron: Asymmetry* **2006**, *17*, 3084.
- <sup>4</sup> (a) Schönberg, H.; Boulmaâz, S.; Wörle, M.; Liesum, L.; Schweiger, A.; Grützmacher, H. *Angew. Chem. Int. Ed.* **1998**, *37*, 1423; (b) Boulmaâz, S.; Mlakar, M.; Loss, S.; Schönberg, H.; Deblon, S.; Wörle, M.; Nesper, R.; Grützmacher, H. *Chem. Commun.* **1998**, 2623; (c) Büttner, T.; Breher, F.; Grütcher, H. *Chem. Commun.* **2004**, 2820; (d) Maire, P.; Büttner, T.; Breher, F.; LeFloch, P.; Grützmacher, H. *Angew. Chem. Int. Ed.* **2005**, *44*, 6318; (e) Büttner, T.; Geier, J.; Frison, G.; Harmer, J.; Calle, C.; Schweiger, A.; Schönberg, H.; Grützmacher, H. *Science* **2005**, *307*, 235. For additional examples of chiral tropylidene and achiral dibenzazepine derived ligands, see: Deblon, S.; Grützmacher, H.; Maire, P.; Schönberg, H. *WO 03/048175 A1*.
- <sup>5</sup> Maire, P.; Deblon, S.; Breher, F.; Geier, J.; Böhler, C.; Rüegger, H.; Schönberg, H.; Grützmacher, H. *Chem. Eur. J.* **2004**, *10*, 4198.
- <sup>6</sup> Briceño, A.; Dorta, R.; *Acta Cryst.* **2007**, *E63*, m1718.
- <sup>7</sup> Defieber, C.; Ariger, M. A.; Moriel, P.; Carreira, E. M. *Angew. Chem. Int. Ed.* **2007**, *47*, 3139.
- <sup>8</sup> (a) Takaya, Y.; Ogasawara, M.; Hayashi, T.; Sakai, M.; Miyaura, M. *J. Am. Chem. Soc.* **1998**, *120*, 5579; (b) Takaya, Y.; Ogasawara, M.; Hayashi, T. *Chirality* **2000**, *12*, 469; (c) Reetz, M. T.; Moulin, D.; Gosberg, A. *Org. Lett.* **2001**, *3*, 4083; (d) Mariz, R.; Luan, X.; Gatti, M.; Linden, A.; Dorta, R. *J. Am. Chem. Soc.* **2008**, *130*, 2172; (e) Burgi, J. J.; Mariz, R.; Gatti, M.; Drinkel, E.; Luan, X. J.; Blumentritt, S.; Linden, A.; Dorta, R. *Angew. Chem., Int. Ed.* **2009**, *48*, 2768; (f) Chen, J.; Chen, J.; Lang, F.; Zhang, X.; Cun, L.; Zhu, J.; Deng, J.; Liao, J. *J. Am. Chem. Soc.* **2010**, DOI:10.1021/ja1005477.
- <sup>9</sup> (a) Boiteau, J.-G.; Imbos, R.; Minnaard, A. J.; Feringa, B. L. *Org. Lett.* **2003**, *5*, 681; (b) Boiteau, J.-G.; Imbos, R.; Minnaard, A. J.; Feringa, B. L. *J. Org. Chem.* **2003**, *68*, 9481; (c) Kurihara, K.; Sugishita, N.; Oshita, K.; Piao, D.; Yamamoto, Y.; Miyaura, N. *J. Organomet. Chem.* **2007**, *692*, 428.
- <sup>10</sup> (a) Hayashi, T.; Ueyama, K.; Tokunaga, N.; Yoshida, K. *J. Am. Chem. Soc.* **2003**, *125*, 11508. (b) Tokunaga, N.; Otomaru, Y.; Okamoto, K.; Ueyama, K.; Shintani, R.; Hayashi, T. *J. Am. Chem. Soc.* **2004**, *126*, 13584; (b) Defieber, C.; Paquin, J.-F.; Serna, S.; Carreira, E. M. *Org. Lett.* **2004**, *6*, 3873. (c) Shintani, R.; Okamoto, K.; Otomaru, Y.; Ueyama, K.; Hayashi, T. *J. Am. Chem. Soc.* **2005**, *127*, 54; (d) Paquin, J. F.; Stephenson, C. R. J.; Defieber, C.; Carreira, E. M. *Org. Lett.* **2005**, *7*, 3821. (e) Paquin, J.-F.; Defieber, C.; Stephenson, C. R. J.; Carreira, E. M. *J. Am. Chem. Soc.* **2005**, *127*, 10850; (f) Otomaru, Y.; Kina, A.; Shintani, R.; Hayashi, T. *Tetrahedron: Asymmetry* **2005**, *16*, 1673; (g) Otomaru, Y.; Okamoto, K.; Shintani, R.; Hayashi, T. *J. Org. Chem.* **2005**, *70*, 2503.
- <sup>11</sup> Duan, W.-L.; Iwamura, H.; Shintani, R.; Hayashi, T. *J. Am. Chem. Soc.* **2007**, *129*, 2130.
- <sup>12</sup> In related studies we observed that the alkene function of **2** – **6** does not coordinate to Pd(II) (unpublished results and ref. 6).
- <sup>13</sup> Jeffrey, J. C.; Rauchfuss, T. B. *Inorg. Chem.* **1979**, *18*, 2658. For uses of hemilabile ligands in industrial catalysis, see: (a) Parshall, G. W.; Ittel, S. D. *Homogeneous Catalysis: The Applications and Chemistry of Catalysis by Soluble Transition Metal*

- Complexes*, 2nd ed.; Wiley Interscience: New York, **1992**; pp 70-72, (b) Keim, W. *Angew. Chem. Int. Ed.* **1990**, *29*, 235.
- <sup>14</sup> Mikhel, I. S.; Rüegger, H.; Butti, P.; Camponovo, F.; Huber, D.; Mezzetti, A. *Organometallics* **2008**, *27*, 2937.
- <sup>15</sup> (a) Kuriyama, M.; Tomioka, K. *Tetrahedron Lett.* **2001**, *42*, 921. (b) Kuriyama, M.; Nagai, K.; Yamada, K.-I.; Miwa, Y.; Taga, T.; Tomioka, K. *J. Am. Chem. Soc.* **2002**, *124*, 8932.
- <sup>16</sup> Kina, A.; Iwamura, H.; Hayashi, T. *J. Am. Chem. Soc.* **2006**, *128*, 3904.
- <sup>17</sup> (a) De Vries, A. H.; Meetsma, A.; Feringa, B. L. *Angew. Chem.* **1996**, *108*, 2526; (b) Alexakis, A.; Benhaim, C.; Rosset, S.; Humam, M. *J. Am. Chem. Soc.* **2002**, *124*, 5262.
- <sup>18</sup> (a) D'Augustin, M.; Palais, L.; Alexakis, A. *Angew. Chem. Int. Ed.* **2005**, *44*, 1376; (b) Alexakis, A.; Albrow, V.; Biswas, K.; D'Augustin, M.; Prieto, O.; Woodward, S. *Chem. Commun.* **2005**, 2843.
- <sup>19</sup> Zhang, H.; Gschwind, R. M. *Angew. Chem. Int. Ed.* **2006**, *45*, 6391.
- <sup>20</sup> Shi, W.-J.; Wang, L.-X.; Fu, Y.; Zhu, S.-F.; Zhou, Q.-L. *Tetrahedron: Asymmetry* **2003**, *14*, 3867.
- <sup>21</sup> The originally targeted complex [Rh(**6**)Cl(COD)] was never isolated in pure form, the main contaminant being the 1 : 2 complex **10** even when the [RhCl(COD)]<sub>2</sub> : **6** stoichiometry was strictly kept 1:1 and the ligand was added slowly to the Rh precursor.
- <sup>22</sup> Elemental analysis: Found C, 70.00, H 3.98, N 3.37; Calculated for **8**•py•H<sub>2</sub>O (hygroscopic!) C 70.11, H 4.11, N 3.36.
- <sup>23</sup> The quantification of these equilibria is the subject of ongoing studies. Heating a solution of complex **9** in a 'non-coordinating' solvent such as toluene-d<sub>8</sub> at 373 K caused the dd at 122 ppm in the <sup>31</sup>P{<sup>1</sup>H} NMR spectrum that corresponds to the P atom *trans* to the alkene to broaden to a considerably larger extent than the signal of the P atom *trans* to the chloride ligand. This observation suggests a hemilabile alkene coordination stabilising a 14 electron species.
- <sup>24</sup> **12** also formed quantitatively by disproportionation when AgBF<sub>4</sub> was added to a mixture of 0.5 equiv of [RhCl(COD)]<sub>2</sub> and **2** in an attempt to synthesise [Rh(**2**)(COD)]BF<sub>4</sub>.
- <sup>25</sup> The reaction of **10** with 1 equiv AgBF<sub>4</sub> in THF solution yields a light-stable and isolable brick-red Ag-adduct (only in CH<sub>2</sub>Cl<sub>2</sub> AgCl precipitates out to liberate the silver free complex **12**, see experimental part). We speculate that in THF AgCl is complexed by the two carbonyl teeth of the proline moiety (see X-ray structure, work in progress).
- <sup>26</sup> 3 equiv of ligand **6** reacted with CuI to form a complex displaying a broad singlet at around 122 ppm in the <sup>31</sup>P{<sup>1</sup>H} NMR spectrum.
- <sup>27</sup> For an example of a structurally characterised chiral monomeric Cu diphosphine complex used in CAs of Grignard nucleophiles, see: López, F.; Harutyunyan, S. R.; Meetsma, A.; Minnaard, A.; Feringa, B. L. *Angew. Chem. Int. Ed.* **2005**, *44*, 2752.
- <sup>28</sup> Briceño, A.; Dorta, R., unpublished data.
- <sup>29</sup> For structurally characterised η<sup>1</sup>-coordination of BF<sub>4</sub><sup>-</sup> to Cu(I), see for example: Gandhi, B. A.; Green, O.; Burstyn, J. N. *Inorg. Chem.* **2007**, *46*, 3816.
- <sup>30</sup> Ashby, E. C.; Noding, S. A. *J. Org. Chem.* **1979**, *44*, 4792.
- <sup>31</sup> Van der Ent, A.; Onderlinden, A. L.; Schunn, R. A. *Inorg. Synth.* **1990**, *28*, 90.
- <sup>32</sup> Rigaku/MSc, Inc., CRYSTALCLEAR, Software Users Guide, version 1.3.6, The Woodlands, TX, USA, 2000.

- 
- <sup>33</sup> Bruker (1998). SHELXTL-NT. Version 5.1 Bruker AXS Inc., Madison, Wisconsin, USA.
- <sup>34</sup> Shintani, R.; Kimura, T.; Hayashi, T. *Chem. Commun.* **2005**, 3213
- <sup>35</sup> Feng, C.; Wang, Z.; Shao, C.; Xu, M.; Lin, G. *Org. Lett.* **2008**, *10*, 4101
- <sup>36</sup> Okamoto, K.; Hayashi, T.; Rawal, V. H. *Org. Lett.* **2008**, *10*, 4387.



## Chapter 6

### Conclusions

In this thesis, was presented a range of sulfoxide and hemilabile P-alkene ligands. These ligands have been used in the preparation of transition metal complexes, which were well characterised. The complexes were then tested in catalytic reactions, the results of which have been presented

In the second chapter, the synthesis of a range of hetero-bissulfoxide ligands was described. Some novel sulfinylphosphine ligands were also synthesised. Electronic and steric variations were made to the ligands in order to provide a better understanding of the structure-activity relationship of this type of ligand in transition metal catalysis. The hetero-bissulfoxide ligands discussed mostly incorporated one alkyl sulfoxide and one aryl sulfoxide, with a phenyl backbone. In order to extend this work more variations can be made to these ligands, the simplest way is to vary the aryl sulfoxide, but more variations could be made to the backbone or the alkyl substituent. Also, the sulfinyl phosphine ligands could be modified, for example, the diphenylphosphine could be replaced by a more electron rich or electron poor phosphine. The phosphine could be replaced by another heteroatom, e.g. nitrogen.

In the third chapter, the ligands presented in the second chapter were used to make iridium complexes. These complexes were subsequently used in iridium catalysed hydroamination reactions. It was demonstrated that these catalysts could provide high reactivities and some enantioselectivity. Efforts were made to understand how the structure of the ligand affected the selectivity in the reaction, with the aim to enhance it. It was observed that a bulky alkyl substituent on one sulfoxide is important for selectivity. Also, the *para* substituent of the aryl group on the other sulfoxide could be varied to increase selectivity. Making the sulfoxides more electron rich had no effect on the enantioselectivity, but slightly reduced the reactivity in the bissulfoxide ligands. However, including electron-donating substituents on the backbone of the sulfinylphosphine ligands increased reactivity and selectivity.

In order to use the bissulfoxide ligands in intramolecular hydroamination reactions, the iridium complex had to be formed and isolated prior to the reaction. Using these ligands *in situ* with an Ir precursor led to no catalytic product. However, when complexation was attempted with the sulfinylphosphine ligands, no clean, characterisable complex was ever obtained. It was found that these ligands could be used *in situ* with an Ir precursor in the catalytic reaction, and good yields could be obtained. It is possible that the bissulfoxide ligands compete with the amino alkene starting material in binding to the metal, whereas the sulfinylphosphine is a better ligand.

Although the activity of some of these iridium complexes in the catalytic intramolecular hydroamination reaction is good, the enantioselectivity can still be improved. Other reaction conditions can be tested, for example, different additives and different solvents. As mentioned above, more variations can also be made to the sulfoxide ligands, as well as the amino alkene starting material.

In the fourth chapter, the syntheses of a family of palladium and platinum complexes with the ligand *p*-tolyl-binaso and cyclohexyl-binaso were presented. Crystal structures of some of these complexes were obtained, and from these a better understanding of the nature of ligation was achieved. It was noticed that the *trans*-influence of other ligands in the Pd- and Pt-bissulfoxide complexes were important in determining the stability of the complex. It was also observed from the crystal structures that the backbone and *p*-tolyl groups of the bissulfoxide ligand do not create a lot of steric bulk around the metal centre. Therefore, we conclude that enantioselectivity observed in catalysis with these ligands is mostly due to electronic factors, rather than steric factors.

Some of the platinum complexes were tested in catalysis. Firstly, hydroamination reactions were attempted with  $\text{Pt}\{(M,S_S,S_S)\text{-}p\text{-tolyl-binaso}\}\text{OTf}_2$ . The reactivity of the catalyst was high, but no enantioselectivity was observed. Therefore it was hard to say for sure if the complex was indeed the catalytic species, as triflic acid (TfOH) has been reported to catalyse such hydroamination reactions. Also attempted were hydroboration and diboration reactions of boranes and diboranes to styrene.  $[\text{Pt}(p\text{-tolyl-binaso})(\text{COD})][\text{BF}_4]_2$  gave 4:1 selectivity of the Markovnikov over the



anti-Markovnikov product, but the yield was quite low. Changing the borane from catechol borane to pinacol borane increased the yield, but reduced the regioselectivity. In order to find further catalytic applications for these complexes, the nature of ligation must be better understood. Studies should be carried out to see if the ligand remains bound to the metal throughout the catalytic reaction.

In the final chapter, catalytic results of copper and rhodium catalysed 1,4-addition reactions to enones with hemilabile P-alkene ligands were presented. These hemilabile P-alkene ligands had previously be shown to form chloro-bridged Rh dimeric complexes, which gave good reactivities and selectivities in conjugate addition reactions. Here, it was demonstrated that these ligands could also form monomeric Rh complexes of the form  $\text{RhX}(\text{L})_2$  ( $\text{X} = \text{Cl}, \text{BF}_4$ ). The monomeric complexes gave superior activities and enantioselectivities in conjugate addition reactions of boronic acids to cyclic and linear enones, when compared to the dimeric complexes. These ligands could also form complexes with CuI in a 2:1 ratio. The copper complexes were active catalysts for the conjugate addition of  $\text{AlEt}_3$  to cyclohexenone, giving moderate enantioselectivity.



# Curriculum Vitae

Surname: DRINKEL

First Names: Emma Elizabeth

Date of Birth: 10.06.1985

Nationality: British

## Education:

- |                 |  |
|-----------------|--|
| 09.2007-09.2011 | Ph.D studies in organic chemistry at the University of Zürich  |
| 09.2003-07.2007 | Undergraduate studies in chemistry at the University of Durham, UK   |
| 07.2006-07.2007 | Master in industry at Johnson Matthey Catalysts, UK<br>Thesis title: <i>Development of Non-Toxic Catalysts for the Polymerisation of Lactide to Produce Biodegradable Polymers</i> |
| 09.1999-07.2003 | King Edward VI Grammar School, Louth, UK<br>A levels obtained at A grade (E to A) in chemistry, maths and biology. AS levels obtained at A grade in further maths and art          |

## Grants obtained during PhD:

1 year sponsorship from the Roche Research Foundation

SCNAT/SCS 2011 Travel Award to attend OMCOS 16

## Publications:

- 1. Room Temperature Synthesis of Tetra-ortho-Substituted Biaryls by NHC-Catalyzed Suzuki-Miyaura Couplings**, Wu, L.; Drinkel, E.; Gaggia, F.; Capolicchio, S.; Linden, A.; Falivene, L.; Cavallo, L.; Dorta, R. *Chem. Eur. J.* **2011**, *17*, 12886
- 2. Hemilabile P-Alkene Ligands in Chiral Rhodium and Copper Complexes: Catalytic Asymmetric 1,4-Additions to Enones.** **2**, Drinkel, E.; Briceno, A.; Dorta, R.; Dorta, R. *Organometallics*, **2010**, *29*, 2503.

3. **Efficient Ring-Closing Metathesis of Alkenyl Bromides: The Importance of Protecting the Catalyst during the Olefin Approach**, Gatti, M.; Drinkel, E.; Wu, L.; Pusterla, I.; Gaggia, F.; Dorta, R. *J. Am. Chem. Soc.* **2010**, *132*, 15179.
4. **Highly chemo- and enantioselective synthesis of 3-allyl-3-aryl oxindoles via the direct palladium-catalyzed alpha-arylation of amides**, Luan, X.; Wu, L.; Drinkel, E.; Mariz, R.; Gatti, M.; Dorta, R. *Org. Lett.* **2010**, *12*, 1912.
5. **C2-Symmetric Chiral Disulfoxide Ligands in Rhodium-Catalysed 1,4-Addition: From Ligand Synthesis to Enantioselection Pathway**, Mariz, R.; Poater, A.; Gatti, M.; Drinkel, E.; Bürgi, J.J.; Luan, X.; Blumentritt, S.; Linden, A.; Cavallo, L.; Dorta, R., *Chem. Eur. J.* **2010**, *16*, 14335
6. **Disulfoxide Ligands in Rhodium Catalyzed Asymmetric 1,4-Addition: First Studies and Future Directions**, Mariz, R.; Bürgi, J.; Gatti, M.; Drinkel, E.; Luan, X.; Dorta, R. *CHIMIA* **2009**, *63*, 508-511.
7. **Impact of NHC Ligand Conformation and Solvent Concentration on the Ruthenium-Catalyzed Ring-Closing Metathesis Reaction**, Gatti, M.; Vieille-Petit, L.; Luan, X.; Mariz, R.; Drinkel, E.; Linden, A.; Dorta, R. *J. Am. Chem. Soc.* **2009**, *131*, 9498-9499.
8. **Unprecedented Selectivity via Electronic Substrate Recognition in the 1,4-Addition to Cyclic Olefins Using a Chiral Disulfoxide Rhodium Catalyst**, Bürgi, J.; Mariz, R.; Gatti, M.; Drinkel, E.; Luan, X.; Blumentritt, S.; Linden, A.; Dorta, R. *Angew. Chem. Int. Ed* **2009**, *48*, 2768-2771.

Conferences Attended:

**The 16th IUPAC International Symposium on Organometallic Chemistry Directed Towards Organic Synthesis**, Shanghai, China

Poster Presentation: *Synthesis, Structure and Initial Catalytic Studies of Novel Palladium and Platinum Complexes with Bissulfoxide Ligands.*

**2010 Fall Meeting of the Swiss Chemical Society**, ETH Hönggerberg, Zürich, Switzerland

Oral Presentation: *Interactions of chiral bis-sulfoxides with precious metals: synthesis, characterisation and possible catalytic applications.*